PTB Wissenschaftliche Veröffentlichungen
PTB-Bericht

PTB-CP-3
Braunschweig, Januar 2009

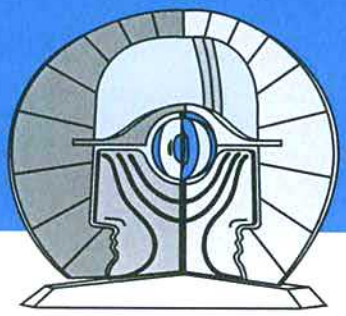

S. Herrmann, H.-J. Kretzschmar, V. Teske,
E. Vogel, P. Ulbig, R. Span, D. P. Gatley

Berechnung der thermodynamischen Zustandsgrößen und Transporteigenschaften von feuchter Luft für energietechnische Prozessmodellierungen

Determination of Thermodynamic and Transport Properties of Humid Air for Power-Cycle Calculations

ISSN 1614-953X
ISBN 978-3-86509-917-4

Physikalisch-Technische Bundesanstalt

Chemische Physik
PTB-CP-3
Braunschweig, Januar 2009

S. Herrmann, H.-J. Kretzschmar, V. Teske, E. Vogel, P. Ulbig, R. Span, D. P. Gatley

Berechnung der thermodynamischen Zustandsgrößen und Transporteigenschaften von feuchter Luft für energietechnische Prozessmodellierungen

Determination of Thermodynamic and Transport Properties of Humid Air for Power-Cycle Calculations

ISSN 1614-953X
ISBN 978-3-86509-917-4

PTB-Bericht

Berechnung der thermodynamischen Zustandsgrößen und Transporteigenschaften von feuchter Luft für energietechnische Prozessmodellierungen

Determination of Thermodynamic and Transport Properties of Humid Air for Power-Cycle Calculations

By S. Herrmann[1,2,3], H.-J. Kretzschmar[1,4], V. Teske[2,5], E. Vogel[2], P. Ulbig[6], R. Span[7], D.P. Gatley[8]

January 2009

[1] Department of Technical Thermodynamics, Zittau/Goerlitz University of Applied Sciences, D-02763 Zittau, Germany.
[2] Institute of Chemistry, University of Rostock, D-18059 Rostock, Germany.
[3] Chair of Technical Thermodynamics, University of Rostock, D-18059 Rostock, Germany.
[4] To whom correspondence should be addressed. E-mail: hj.kretzschmar@hs-zigr.de.
[5] Olefins & Polyolefins, CMAI Europe GmbH, D-40212 Düsseldorf, Germany.
[6] Legal Metrology and Technology Transfer, Physikalisch-Technische Bundesanstalt, D-38116 Braunschweig, Germany.
[7] Lehrstuhl für Thermodynamik, Ruhr-Universität Bochum, D-44780 Bochum, Germany.
[8] Gatley & Associates, Inc., Atlanta GA 30305, USA.

Abstract

This work has been carried out within the European Advanced Adiabatic Compressed Air Energy Storage (AA-CAES) project funded by the European Commission. Work package 4 of this project deals with the thermophysical properties of dry and humid air. Altogether eight institutions worked on this topic to determine the corresponding thermodynamic and transport properties.

In the beginning a literature search was carried out to collect all publications dealing with thermophysical properties of dry air, humid air, and humid air-like gas mixtures. For humid air, only seven publications concerned with experimental data existed before the project started. For this reason the determination of thermodynamic and transport properties of dry and humid air was included within this work package.

As one important result of this project all experimental data and the corresponding literature were collected and set up into a database.

In addition, it was intended to find existing models or correlations for the description of the thermophysical properties and to test them, especially for humid air. The most favourable models for the description of the thermodynamic properties and transport properties were included in the test. Using the database consisting of the experimental data from the literature and also of the newly measured data, the models were investigated.

The result of all investigations is a recommendation of one model for the thermodynamic and a second model for the transport properties. Both represent models taken from the literature, but modified within this work due to the comparisons with experimental data. For thermodynamic properties, the recommended model corresponds to the ideal mixture of the real fluids dry air and steam and includes the poynting correction calculated from the virial equation of state by Nelson and Sauer. For transport properties, an improved modification of the Vesovic-Wakeham model was developed.

In this report, the considered models are described in detail, and the results of all comparisons to experimental data are presented. In addition, the working equations of both recommended models were used to develop a corresponding new property library. This library establishes an useful tool for the design of humid air power cycles and represents the state-of-the-art models for the thermodynamic and transport properties of humid air, such as enthalpies, densities, saturation properties, viscosities, and thermal conductivities. In addition, this property library contains algorithms to calculate the thermodynamic and transport properties in the case of liquid fog and of ice fog. The application is possible for wide ranges of temperature ($T = 243.15$ K … 2000 K) and pressure ($p = 611.2$ Pa … 100 MPa) with some small restrictions concerning the calculation of transport properties.

The property library is commercially available from the authors at Zittau/Goerlitz University of Applied Sciences and the University of Rostock, respectively.

Table of Contents

Preface

In 2002, the European Commission and ALSTOM Ltd. founded the Advanced Adiabatic Compressed Air Energy Storage (AA-CAES) project to investigate and develop the power cycle for a power plant storing heat in an adiabatic way by the use of compressed humid air. Work Package 4 of the AA-CAES project dealt with the generation of experimental data on thermodynamic and transport properties for humid air, the development of a property database, the acquisition of all available data from the literature into the database, and the test of suitable models describing these properties. Based on experimental data newly measured within the AA-CAES project and supplemented by some data sets available from the literature, different models for thermodynamic and transport properties were assessed.

The following models for the calculation of thermodynamic properties were investigated regarding their accuracy in comparison with available experimental data:

- Ideal mixture of ideal gases
- Ideal mixture of the real fluids dry air and water
- Ideal mixture of the real fluids N_2, O_2, Ar, and water
- Modified Redlich-Kwong equation of state for the mixture proposed by Yan and co-workers
- Virial equation for the mixture proposed by Rabinovich and Beketov
- Virial equation for the mixture proposed by Hyland and Wexler
- Virial equation for the mixture proposed by Nelson and Sauer.

The models using an ideal mixture and a virial equation were programmed and partly updated by the working group of Zittau/Goerlitz University of Applied Sciences. The model of Yan *et al.* was developed and prepared by the working group of Kungl Tekniska Högskolan, Stockholm, Sweden. The numerical details were available from the literature or from these two universities. The calculated results were compared with the available experimental data for dry and humid air from previous studies and the new data measured within the AA-CAES project. We also compared the different models to each other.

For the transport properties, four models were identified and investigated:

- Multiparameter model proposed by Chung *et al.*
- Ideal mixture of the real fluids dry air and water
- Rigid-sphere model proposed by Vesovic and Wakeham
- Three-parameter corresponding states model proposed by Scalabrin *et al.*

The models were compared with the small number of available experimental data. In addition, comparison calculations were carried out between the different models.

Finally, based on all results, the most suitable models were identified and afterwards partly modified to obtain the smallest deviations in comparison with experimental data.

For the convenience of industrial users, a new property library containing these models for the calculation of the thermodynamic properties of humid air was generated including algorithms for the transport properties developed at the University of Rostock. The property library was also configured for ease of use in Excel®, MATLAB®, and Mathcad®.

Part A

Thermodynamic Properties

1 Nomenclature

Symbols

Variable	Description
a	Molar Helmholtz free energy, thermal diffusivity, coefficient, parameter
A	Parameter
b	Coefficient, parameter
B	Second virial coefficient, temperature dependent virial coefficient, parameter
c	Coefficient, parameter
C	Third virial coefficient, temperature dependent virial coefficient, parameter
c_p	Molar isobaric heat capacity
c_v	Molar isochoric heat capacity
D	Coefficient, parameter
E	Coefficient, parameter
f	Saturated steam-pressure enhancement factor, free energy
F	Parameter
g	Molar Gibbs free energy
g_w	Saturated water-concentration enhancement factor
G	Parameter
h	Molar enthalpy
I	Coefficient, sum of i serial numbers
J	Coefficient, functional
M	Molar mass, molar mass of the mixture
n	Coefficient, parameter
N	Parameter
p	Pressure
Q	Coefficient
R	Universal molar gas constant
s	Molar entropy
T	Temperature
u	Molar internal energy
v	Molar volume
w	Speed of sound
X	Reciprocal temperature

x_{w}	Humidity ratio, absolute humidity; **Note:** In Part B x_{w} is used as mole fraction of water.
z	Any property
$\tilde{z}$	Specific property
Z	Compressibility factor (real gas factor)
α	Reduced Helmholtz free energy, parameter
β	Reduced pressure, parameter
β_{H}	Henry's law constant
γ	Reduced Gibbs free energy, volume fraction, parameter
δ	Reduced density
$\Delta c_{p,\mathrm{dis}}$	Dissociation part of molar isobaric heat capacity
Δh_{dis}	Dissociation part of molar enthalpy
Δs_{dis}	Dissociation part of molar entropy
θ	Reduced temperature
ϑ	Temperature, parameter
κ	Isentropic exponent
κ_T	Isothermal compressibility
ν	Kinematic viscosity
ξ	Mass fraction
π	Reduced pressure
ρ	Molar density
$\tilde{\rho}$	Mass density
τ	Reciprocal reduced temperature
ϕ	Fugacity coefficient
ψ	Mole fraction
Ψ	Vector of mole fractions

Superscripts

E	Excess contribution
Lem	Value taken from Lemmon *et al.*
o	Ideal-gas contribution
r	Residual contribution
95	Value taken from the IAPWS-95 formulation
'	Saturated liquid
"	Saturated vapour
~	Specific property (mass related)

Subscripts

0	Reference state
a	Dry air
c	Critical
cal	Calculated
con	Condensed phase
exp	Experimental
i	Component, serial number
i	Ice phase
irr	Irreversible
j	Region of IAPWS-IF97, serial number
j	Maxcondentherm
k	Serial number
liq	Liquid phase
N_2	Nitrogen
O_2	Oxygen
r	Reducing quantity
s	Saturated state
t	Triple point
T	Contribution dependent on temperature
v	Vapour phase
w	Water (water vapour, liquid water, ice)
δ	Partial derivative with respect to reduced density
π	Partial derivative with respect to reduced pressure
τ	Partial derivative with respect to reciprocal reduced temperature

Abbreviations

Abbreviation	Description
AA-CAES	Advanced Adiabatic Compressed Air Energy Storage, Project in the Fifth Framework Programme by the European Commission, Contract-No. ENK6-CT-2002-00611; www.cordis.lu.
BOKU	Universität für Bodenkultur, Department für Materialwissenschaften und Prozesstechnik, Institut für Verfahrens- und Energietechnik, Prof. Dr. M. Wendland, Wien, Austria.
FHZI	Zittau/Goerlitz University of Applied Sciences, Department of Technical Thermodynamics, Prof. Dr. H.-J. Kretzschmar, Zittau, Germany.

HuAir	Ideal mixture of the real fluids dry air and water from FHZI; Software: LibHuAir from FHZI.
HuGas	Ideal mixture of the real fluids N_2, O_2, Ar, and water, from FHZI; Software: LibHuGas from FHZI.
HyW	Virial equation of state for the mixture from Hyland and Wexler; Software: LibHyW83 from this work.
IAPWS-IF97	Release on the IAPWS Industrial Formulation 1997 for the Thermodynamic Properties of Water and Steam IAPWS-IF97.
IAPWS-95	Release on the IAPWS Formulation 1995 for the Thermodynamic Properties of Ordinary Water Substance for General and Scientific Use.
ICSTM	Imperial College of Science, Technology and Medicine, Department of Chemical Engineering, Prof. Dr. J. P. M. Trusler, London, Great Britain.
IdGas	Ideal mixture of ideal gases, from FHZI; Software: LibIdGas from FHZI.
KTH	Modified Redlich-Kwong equation of state for the mixture proposed by Kungl Tekniska Högskolan of Stockholm, Sweden.
Lib	Shortcut for 'Library'; corresponds to a property library, e.g., LibHuAir which includes functions for the calculation of humid air.
NEL	Virial equation of state for the mixture from Nelson and Sauer; Software: LibNEL02 from this work.
PTB	Physikalisch-Technische Bundesanstalt, Department of Analytical Measuring Techniques and Pressure, Dr. P. Ulbig, Braunschweig, Germany.
RB	Virial equation of state for the mixture from Rabinovich and Beketov; Software: LibRB95 from this work.
RUB	Ruhr-Universität Bochum, Lehrstuhl für Thermodynamik, Bochum, Germany.
SKU	Ideal mixture of the real fluids dry air and water for the thermodynamic properties of humid air, proposed by Span, Kretzschmar, Ulbig, and Herrmann; Software: LibSKU from this work.

2 Overview on Data from the Literature and Newly Measured Data

An overview on available data for dry air, humid air, and aqueous mixtures similar to humid air is presented in the following sections. Section 2.1 comprises data available from the literature. Section 2.2 contains newly measured data for dry and humid air prepared by co-workers within the project "Advanced Adiabatic Compressed Air Energy Storage" (AA-CAES).

2.1 Data from the Literature

2.1.1 Dry Air

The database (for further information see Part D) comprises altogether 52 sources including experimental data for thermodynamic properties of dry air. Experimental data are available for the following thermodynamic properties:

- Critical temperature and pressure (T_c and p_c)
- Saturated liquid and vapour pressure (p' and p'')
- Saturated liquid and vapour density (ρ' and ρ'')
- $p\rho T$ data
- Isobaric heat capacity in the ideal gas state and isobaric heat capacity (c_p^o and c_p)
- Isochoric heat capacity (c_v)
- Enthalpy (h)
- Speed of sound (w).

There exists a hyperlink to a *p-T* diagram for each property in the sheet "Data Points" of the database. The *p-T* diagrams give an overview about the distribution of data points in the *p-T* range and characterise the corresponding sources. A comprehensive analysis of the existing experimental data for dry air was given by Lemmon *et al.* [1].

2.1.2 Humid Air

The database contains altogether 6 sources including experimental data for the thermodynamic properties of humid air. Figure 2.1 to Figure 2.3 illustrate the *p-T* ranges of these data. Only experimental data for the following three thermodynamic properties were available, before the EU project AA-CAES started:

- Mole fraction of saturated steam $\psi_{w,s}$ (Figure 2.1)
- Steam-pressure enhancement factor $f_{w,s}$ derived from mole fraction of saturated steam (Figure 2.2)
- $p\rho T$ data (Figure 2.3).

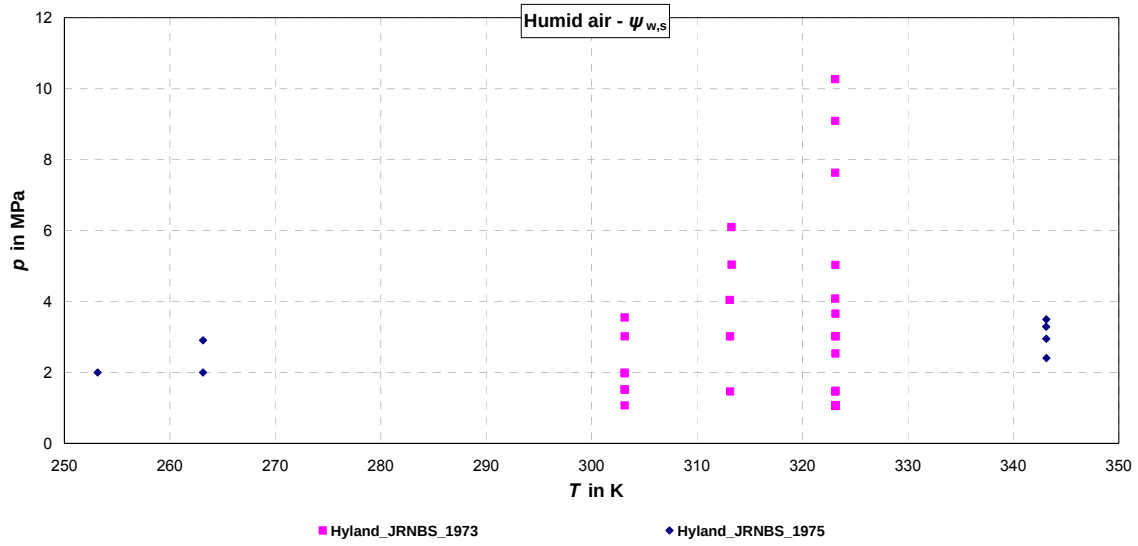

Figure 2.1: Pressure-temperature diagram with data points for the mole fraction of saturated steam of humid air given by Hyland and Wexler (1973) [2] as well as Hyland (1975) [3].

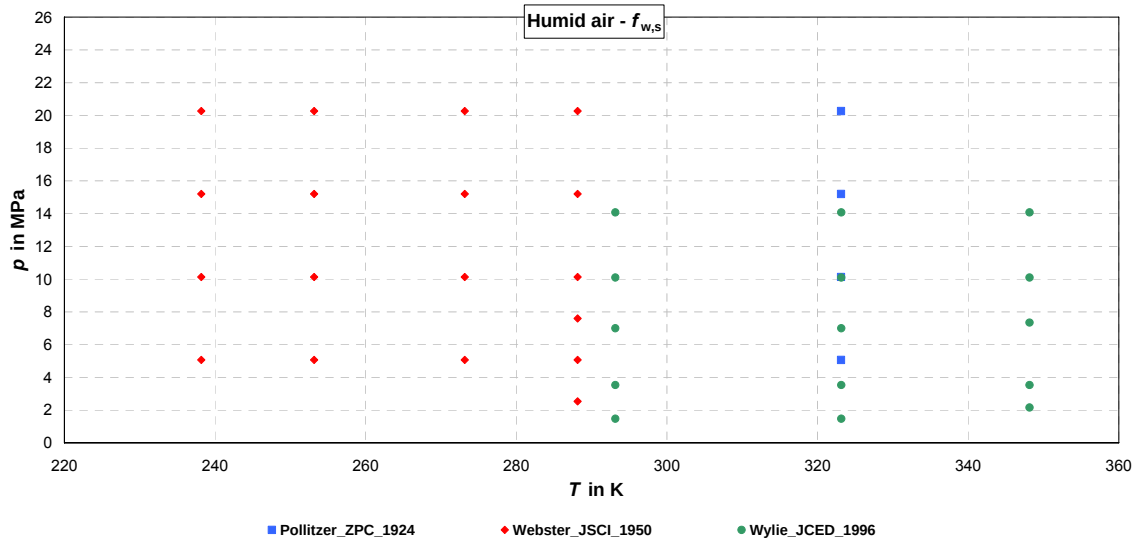

Figure 2.2: Pressure-temperature diagram with data points for the enhancement factor of humid air given by Pollitzer and Strebel (1924) [4], Webster (1950) [5], and Wylie and Fisher (1996) [6].

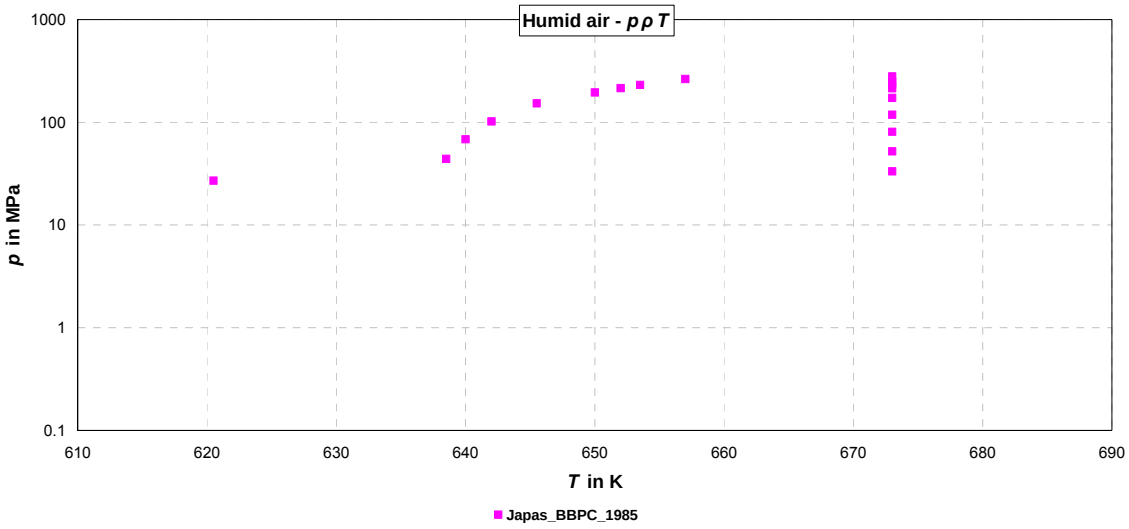

Figure 2.3: Pressure-temperature diagram with data points for $p\rho T$ measurements of humid air given by Japas and Franck (1985) [7].

2.1.3 Aqueous Mixtures

The database contains also sources including experimental data for thermodynamic properties of further aqueous mixtures. Experimental data were reported for the following thermodynamic properties of the nitrogen-water mixture ($N_2 + H_2O$):

- Critical temperature and pressure (T_c and p_c)
- Liquid and vapour mole fraction (ψ' and ψ'')
- $p\rho T$ data
- Compressibility factor Z
- Excess enthalpy h^E.

Figure 2.4 illustrates the p-T range of the $p\rho T$ data for the nitrogen-water mixture. The data set given by Fenghour and Wakeham (1993) [8] is used for comparison calculations in Section 4.2.4.

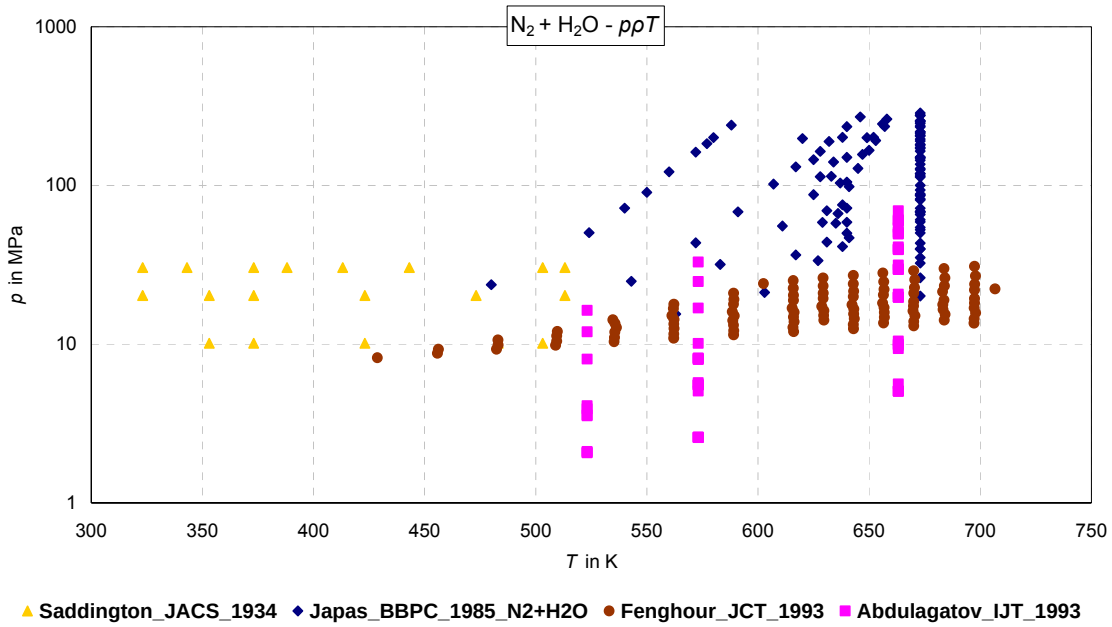

Figure 2.4: Pressure-temperature diagram with data points for $p\rho T$ measurements of nitrogen-water mixture given by Saddington and Krase (1934) [9], Japas and Franck (1985) [7], Fenghour and Wakeham (1993) [8], and Abdulagatov *et al.* (1993) [10].

In addition, experimental $p\rho T$ data and critical values for the oxygen-water mixture ($O_2 + H_2O$) are included in the database.

2.2 Newly Measured Data

2.2.1 Dry Air

Four data sets of new experimental data for thermodynamic properties of dry air measured in the project AA-CAES were included in the database. The density of dry air was measured at Physikalisch-Technische Bundesanstalt Braunschweig (PTB), at Imperial College of Science, Technology and Medicine London (ICSTM), and at Ruhr-Universität Bochum (RUB). Measurements of the speed of sound of dry air were performed at ICSTM. The range of these data is demonstrated in Figure 2.5 and Figure 2.6.

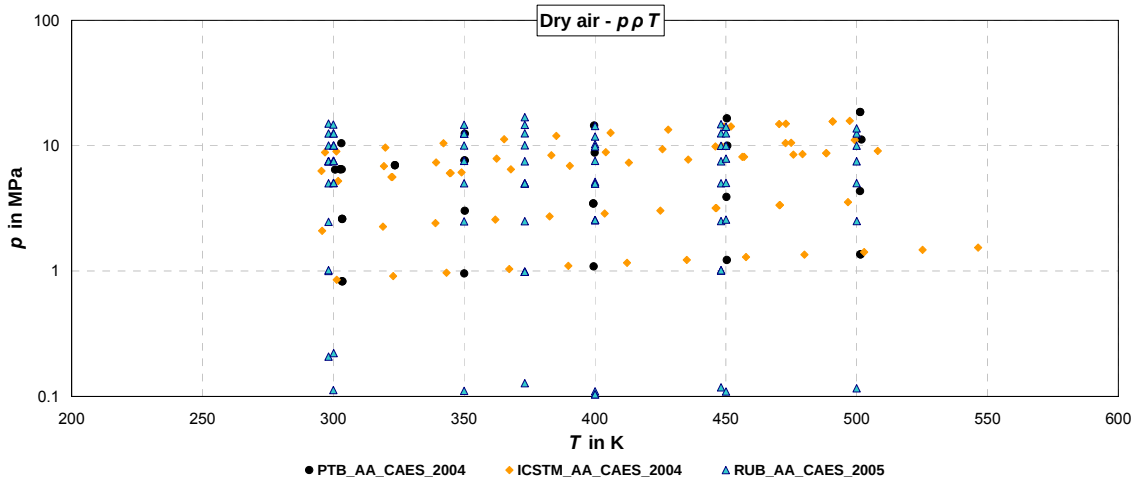

Figure 2.5: Pressure-temperature diagram with data points for the density of dry air measured in the project by Klingenberg and Ulbig (PTB, 2004/2007) [11], Trusler (ICSTM, 2004) [12], and Wöll (RUB, 2005) [13].

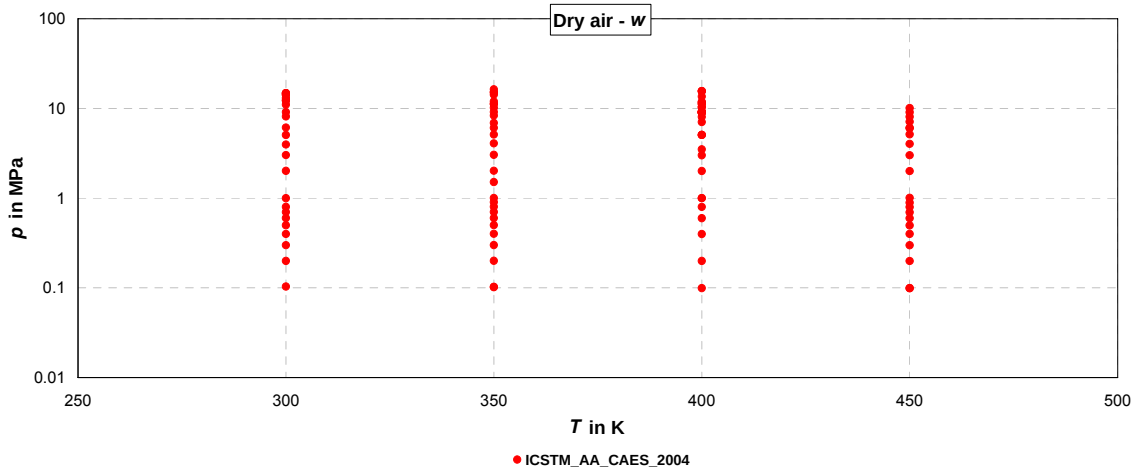

Figure 2.6: Pressure-temperature diagram with data points for the speed of sound of dry air measured in the project by Trusler (ICSTM, 2004) [12].

2.2.2 Humid Air

New experimental data for thermodynamic properties of humid air were measured within the AA-CAES project. The density of humid air was measured at Physikalisch-Technische Bundesanstalt Braunschweig (PTB), at Imperial College of Science, Technology and Medicine London (ICSTM), and at Ruhr-Universität Bochum (RUB). The water-concentration enhancement factor was measured at the Universität für Bodenkultur Wien (BOKU). The ranges of these data are demonstrated in Figure 2.7 and Figure 2.8.

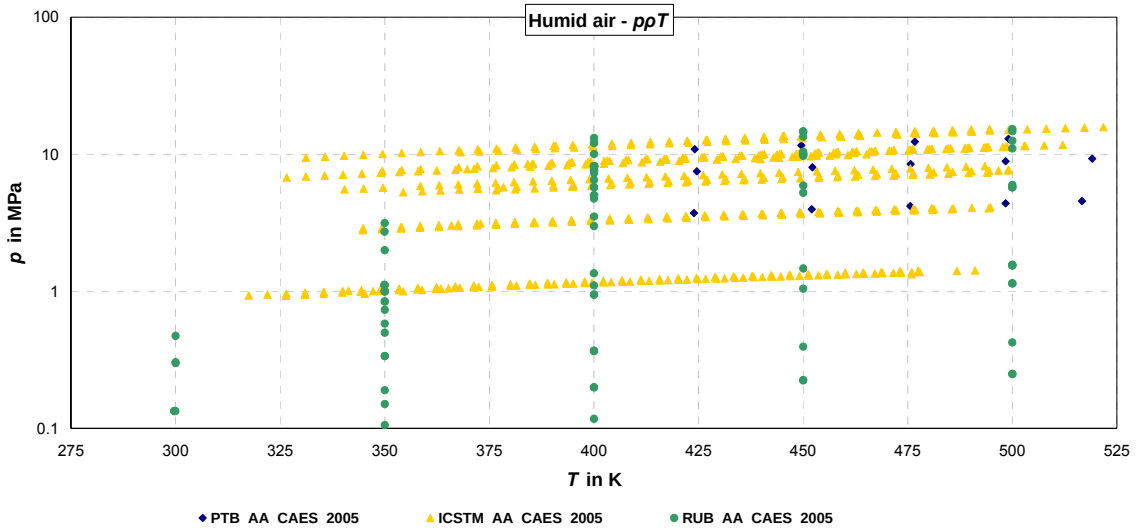

Figure 2.7: Pressure-temperature diagram with data points for the density of humid air measured in the project by Wöll (RUB, 2005) [13], Trusler (ICSTM, 2005) [14], and Klingenberg and Ulbig (PTB, 2005/2007) [11].

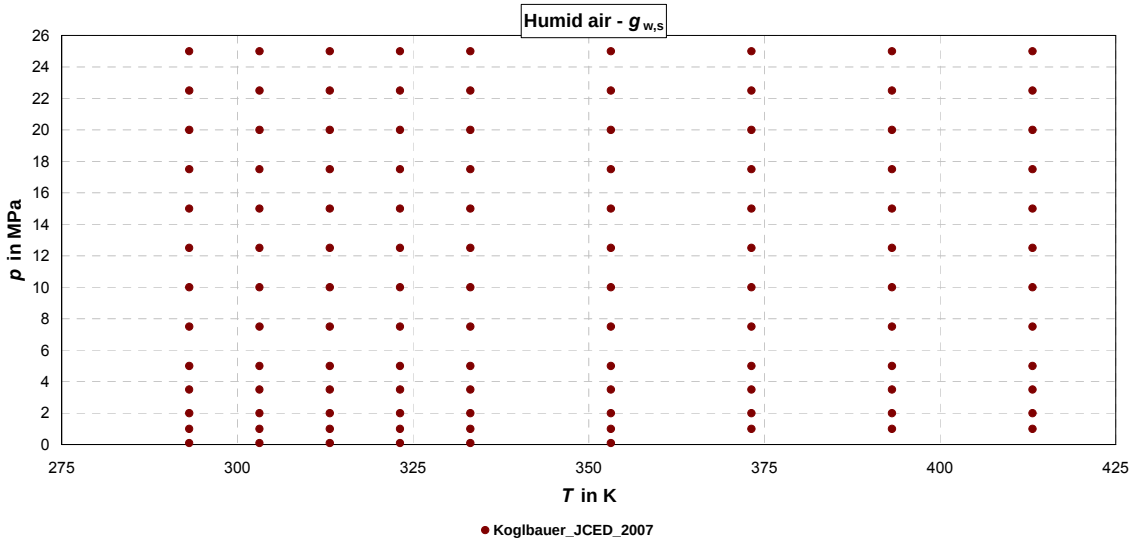

Figure 2.8: Pressure-temperature diagram with data points for the water-concentration enhancement factor of humid air measured in the AA-CAES project by Koglbauer and Wendland (BOKU, 2007) [15].

3 Description of Models for Thermodynamic Properties

Humid air is a mixture of nitrogen, oxygen, argon, carbon dioxide, water vapour (steam), and other trace elements. Dry air is often simplified in engineering to be a mixture of nitrogen, oxygen, and argon. The corresponding mole fractions from Lemmon *et al.* [1] are 0.7812, 0.2096, 0.0092, and from VDI [16] are 0.781109, 0.209548, 0.009342. In previous studies, it was stated that the solubility of argon in water is similar to that of oxygen [6]. Meanwhile, this assumption simplifies obviously the calculation within an uncertainty acceptable in engineering. Therefore, dry air can also be assumed to be a mixture of nitrogen and oxygen with the mole fractions of 0.7812 and 0.2188 [17]. Synthetic dry air with the mole fractions of 0.7820, 0.2090, and 0.0090 [11] was used for the experiments performed in this project.

3.1 Thermodynamic Properties of Dry Air and Pure Water

Hence humid air is a mixture of dry air and steam, liquid water, or ice, the latter cases referring to the supersaturated state (e.g., fog) of humid air. The following subsections present some of the existing models for the calculation of the thermodynamic properties for the components of humid air, dry air and water.

3.1.1 Dry Air

Lemmon *et al.* [1] proposed two models for dry air. Either dry air can be treated as a pseudo pure component, or it can be calculated as a mixture of the three components nitrogen, oxygen, and argon.

3.1.1.1 Dry Air as Pseudo Pure Component

The thermodynamic properties of dry air as a pseudo pure component are calculated using the NIST standard of Lemmon *et al.* [1]. It consists of a fundamental equation for the molar Helmholtz free energy a as a function of density ρ and temperature T. The dimensionless form reads

$$\frac{a(\tilde{\rho},T)}{RT} = \alpha(\delta,\tau) = \alpha^{\mathrm{o}}(\delta,\tau) + \alpha^{\mathrm{r}}(\delta,\tau) \tag{3.1}$$

where

$\alpha^{\mathrm{o}}(\delta,\tau)$ is the ideal-gas contribution,

$\alpha^{\mathrm{r}}(\delta,\tau)$ is the residual contribution,

with

$\delta = \dfrac{\tilde{\rho}}{\tilde{\rho}_{\mathrm{j}}}$ is the reduced density,

$\tau = \dfrac{T_{\mathrm{j}}}{T}$ is the reciprocal reduced temperature,

$\tilde{\rho}_\mathrm{j} = 302.5508\ \mathrm{kg\ m^{-3}}$ is the mass density at maxcondentherm,

$T_\mathrm{j} = 132.6312\ \mathrm{K}$ is the temperature at maxcondentherm,

and $R = 8.31451\ \mathrm{kJ\ kmol^{-1}\ K^{-1}}$ is the molar gas constant.

This fundamental equation allows calculating all thermodynamic properties from the equation itself and from its first, second, and mixed derivatives with respect to reduced density and reciprocal reduced temperature:

$$\alpha_\delta = \left(\frac{\partial\alpha}{\partial\delta}\right)_\tau,\ \alpha_{\delta\delta} = \left(\frac{\partial^2\alpha}{\partial\delta^2}\right)_\tau,\ \alpha_\tau = \left(\frac{\partial\alpha}{\partial\tau}\right)_\delta,\ \alpha_{\tau\tau} = \left(\frac{\partial^2\alpha}{\partial\tau^2}\right)_\delta,\ \alpha_{\delta\tau} = \left(\frac{\partial^2\alpha}{\partial\delta\,\partial\tau}\right). \quad (3.2)$$

The most important properties are:

Molar volume

$$v(p,T) = \frac{RT}{p}\left(1+\delta\,\alpha_\delta^\mathrm{r}\right). \quad (3.3)$$

Molar enthalpy

$$h(p,T) = RT\left[\tau\left(\alpha_\tau^\mathrm{o}+\alpha_\tau^\mathrm{r}\right)+\delta\,\alpha_\delta^\mathrm{r}+1\right]. \quad (3.4)$$

Molar isobaric heat capacity

$$c_p(p,T) = R\left[-\tau^2\left(\alpha_{\tau\tau}^\mathrm{o}+\alpha_{\tau\tau}^\mathrm{r}\right)+\frac{\left(1+\delta\,\alpha_\delta^\mathrm{r}-\delta\,\tau\,\alpha_{\delta\tau}^\mathrm{r}\right)^2}{1+2\,\delta\,\alpha_\delta^\mathrm{r}+\delta^2\,\alpha_{\delta\delta}^\mathrm{r}}\right]. \quad (3.5)$$

Molar entropy

$$s(p,T) = R\left[\tau\left(\alpha_\tau^\mathrm{o}+\alpha_\tau^\mathrm{r}\right)-\alpha^\mathrm{o}-\alpha^\mathrm{r}\right]. \quad (3.6)$$

3.1.1.2 Dry Air as Mixture of Nitrogen, Oxygen, and Argon

In addition, Lemmon *et al.* [1] used the multi-fluid model for calculating thermodynamic properties of dry air as mixture of the components nitrogen (N_2), oxygen (O_2), and argon (Ar). The dimensionless Helmholtz free-energy equation for the mixture reads

$$\alpha = \alpha^\mathrm{o}+\alpha^\mathrm{r}+\alpha^\mathrm{E} \quad (3.7)$$

where

α^o is the ideal-gas mixing contribution

$$\alpha^\mathrm{o} = \sum_i \psi_i\left[\alpha_i^\mathrm{o}(\delta_i,\tau_i)+\ln\psi_i\right]$$

for $i = \mathrm{N_2}, \mathrm{O_2}, \mathrm{Ar}$

with $\delta_i = \dfrac{\tilde{\rho}}{\tilde{\rho}_{\mathrm{c},i}}$, $\tau_i = \dfrac{T_{\mathrm{c},i}}{T}$.

α^{r} is the residual mixing contribution

$$\alpha^{\mathrm{r}} = \sum_i \psi_i \, \alpha_i^{\mathrm{r}}(\delta_{\mathrm{r},i}, \tau_{\mathrm{r},i})$$

for $i = \mathrm{N_2}$, $\mathrm{O_2}$, Ar

with $\delta_{\mathrm{r},i} = \dfrac{\tilde{\rho}}{\tilde{\rho}_{\mathrm{r},i}}$, $\tau_{\mathrm{r},i} = \dfrac{T_{\mathrm{r},i}}{T}$.

The reducing values $\tilde{\rho}_{\mathrm{r},i}$ and $T_{\mathrm{r},i}$ are calculated by algorithms given in [1] for reduced density and temperature lines.

α^{E} is the excess contribution

$$\alpha^{\mathrm{E}} = \alpha^{\mathrm{E}}(\delta_{\mathrm{r},i}, \tau_{\mathrm{r},i}, \Psi),$$

ψ_i is the mole fraction of the component i, $i = \mathrm{N_2}$, $\mathrm{O_2}$, Ar, and

Ψ is the vector of the mole fractions.

All thermodynamic properties of the mixture can be derived from the α equation itself and from its first, second, and mixed derivatives of density and temperature.

3.1.2 Steam, Liquid Water, and Ice

To calculate the thermodynamic properties of steam and water, the international standard for scientific and general use IAPWS-95 [18], [19] can be applied. This standard contains an equation for the dimensionless Helmholtz free energy α as a function of reduced density δ and reciprocal reduced temperature τ. The equation is formulated in analogy to the Helmholtz equation for dry air:

$$\alpha(\delta, \tau) = \alpha^{\mathrm{o}}(\delta, \tau) + \alpha^{\mathrm{r}}(\delta, \tau) \tag{3.8}$$

where

$\alpha^{\mathrm{o}}(\delta, \tau)$ is the ideal-gas contribution,

$\alpha^{\mathrm{r}}(\delta, \tau)$ is the residual contribution,

with

$\delta = \dfrac{\tilde{\rho}}{\tilde{\rho}_{\mathrm{c}}}$ is the reduced density, $\tau = \dfrac{T_{\mathrm{c}}}{T}$ is the reciprocal reduced temperature,

$\tilde{\rho}_{\mathrm{c}} = 322 \text{ kg m}^{-3}$ is the mass density at the critical point, and

$T_{\mathrm{c}} = 647.096 \text{ K}$ is the temperature at the critical point.

All thermodynamic properties are calculated from density and temperature using Eq. (3.8).

In addition, the industrial formulation IAPWS-IF97 for water and steam [20], [21] can be used for practical calculations. The range of validity of the IAPWS-IF97 is divided into five regions as shown in Figure 3.1. The liquid region 1 is described by an equation for the molar Gibbs free energy g as a function of pressure p and temperature T. The dimensionless form reads

$$\frac{g_1(p,T)}{\tilde{R}T} = \gamma_1(\pi,\tau) \tag{3.9}$$

where

$\pi = \dfrac{p}{p_{\mathrm{r},1}}$ and $\tau = \dfrac{T_{\mathrm{r},1}}{T}$,

$p_{\mathrm{r},1}$ and $T_{\mathrm{r},1}$ are special reducing parameters, and

$\tilde{R} = 0.461526\ \mathrm{kJ\ kg^{-1}\ K^{-1}}$ is the specific gas constant.

The thermodynamic properties in the vapour region 2 and the high-temperature gas region 5 are calculated by dimensionless Gibbs free-energy equations in the form:

$$\gamma_j(\pi,\tau) = \gamma_j^{\mathrm{o}}(\pi,\tau) + \gamma_j^{\mathrm{r}}(\pi,\tau) \tag{3.10}$$

where

$\gamma_j^{\mathrm{o}}(\pi,\tau)$ is the ideal-gas contribution,

$\gamma_j^{\mathrm{r}}(\pi,\tau)$ is the residual contribution,

with

$\pi = \dfrac{p}{p_{\mathrm{r},j}}$ is the reduced pressure,

$\tau = \dfrac{T_{\mathrm{r},j}}{T}$ is the reciprocal reduced temperature,

for $j = 2$ (region 2) and $j = 5$ (region 5),

$p_{\mathrm{r},j}$ and $T_{\mathrm{r},j}$ are special reducing values.

The numbers in Figure 3.1 have the following meanings. The Gibbs equations of regions 1, 2, and 5 allow calculating all thermodynamic properties from the equations themselves and from their first, second, and mixed derivatives with respect to the reduced pressure π and reciprocal reduced temperature τ:

$$\gamma_\pi = \left(\frac{\partial\gamma}{\partial\pi}\right)_\tau,\quad \gamma_{\pi\pi} = \left(\frac{\partial^2\gamma}{\partial\pi^2}\right)_\tau,\quad \gamma_\tau = \left(\frac{\partial\gamma}{\partial\tau}\right)_\pi,\quad \gamma_{\tau\tau} = \left(\frac{\partial^2\gamma}{\partial\tau^2}\right)_\pi,\quad \gamma_{\pi\tau} = \left(\frac{\partial\gamma}{\partial\pi\,\delta\tau}\right). \tag{3.11}$$

The critical and supercritical region (region 3) is covered by an equation for the dimensionless Helmholtz free energy α as a function of reduced density δ and reciprocal reduced temperature τ. The equation reads

$$\frac{a_3(\rho,T)}{\tilde{R}T} = \alpha_3(\delta,\tau) \tag{3.12}$$

where

$\delta = \dfrac{\tilde{\rho}}{\tilde{\rho}_c}$ is the reduced density,

$\tau = \dfrac{T_c}{T}$ is the reciprocal reduced temperature,

$\tilde{\rho}_c = 322 \text{ kg m}^{-3}$ is the mass density at the critical point,

$T_c = 647.096 \text{ K}$ is the temperature at the critical point, and

$\tilde{R} = 0.461526 \text{ kJ kg}^{-1} \text{K}^{-1}$ is the specific gas constant.

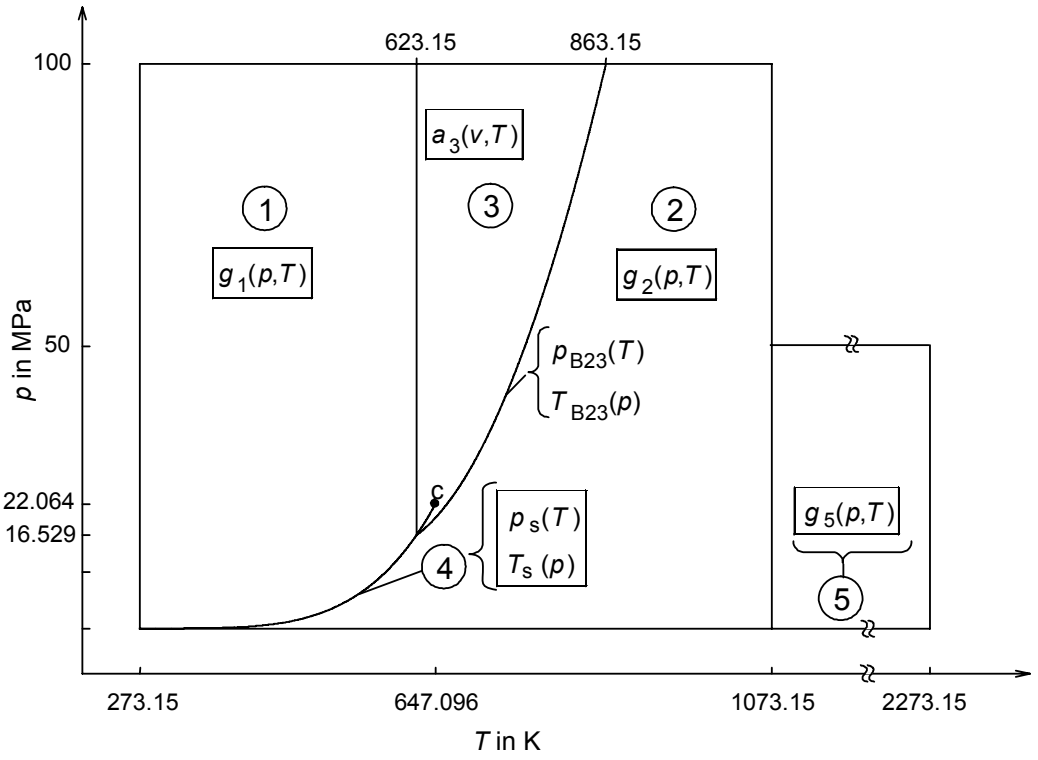

Figure 3.1: Range of validity and the assignment of the basic equations to the five regions of IAPWS-IF97 plotted in a pressure-temperature diagram. 1 – Compressed liquid, 2 – Superheated to 1073.15 K, 3 – Critical and supercritical, 4 – Two phase from 273.15 K to 647.096 K, 5 – Very high temperature superheated region > 1073.15 K, c – Critical point.

A vapour-pressure equation for the two-phase region (region 4) in the form

$$p_s = p_s(T) \tag{3.13}$$

is available. This equation can be solved explicitly for the temperature. Using the vapour-pressure equation, it is not necessary to solve the Maxwell criterion in the calculation of the phase equilibrium liquid-vapour.

The equation of state from Hyland and Wexler [22] can be used for calculating the thermodynamic properties of the ice crystals in ice fog.

The most important properties are:

Molar volume

$$v(T) = a_1 + a_2 T + a_3 T \,. \tag{3.14}$$

Molar enthalpy

$$h(p,T) = \sum_{i=0}^{3} D_i T^i + D_4 p \,. \tag{3.15}$$

Molar isobaric heat capacity

$$c_p = \left(\frac{\partial h(p,T)}{\partial T} \right)_p \,. \tag{3.16}$$

Molar entropy

$$s(p,T) = \sum_{i=0}^{2} E_i T^i + E_3 \ln\left(T\right) + \left(E_4 + E_5 T\right)\left(0.101325 - p/\mathrm{MPa}\right) \,. \tag{3.17}$$

3.2 Thermal and Caloric Properties for the Gas Phase of Humid Air

Three general models for calculating thermal and caloric properties will be discussed:

- Ideal mixture of ideal gases (ideal-gas model)
- Ideal mixture of real fluids (ideal-mixing models)
- Real mixture of real fluids (real models).

3.2.1 Ideal Mixture of Ideal Gases

For calculating thermodynamic properties of humid air as an ideal mixture of ideal gases (ideal-gas model), the VDI-Guideline 4670 [16], [23] or the NASA standard [24] can be applied. The important properties of unsaturated and saturated humid air are calculated as follows:

Mass density

$$\tilde{\rho} = \frac{p\,M}{R\,T} \tag{3.18}$$

where $M = \sum_i \psi_i M_i$ is the molar mass of the mixture, ψ_i is the mole fraction, and M_i the molar mass of one of the components N_2, O_2, Ar, and steam.

Molar volume

$$v = \frac{RT}{p}. \tag{3.19}$$

Molar isobaric heat capacity

$$c_p^{\mathrm{o}} = \sum_i \psi_i \, c_{p,i}^{\mathrm{o}}(T) + \Delta c_{p,\mathrm{dis}} \tag{3.20}$$

where

$c_{p,i}^{\mathrm{o}}(T)$ is the polynomial of the component *i* and

ψ_i is the mole fraction of the component *i*.

Molar enthalpy

$$h^{\mathrm{o}} = \sum_i \psi_i \, h_i^{\mathrm{o}}(T) + \Delta h_{\mathrm{dis}} \tag{3.21}$$

where $h_i^{\mathrm{o}}(T) = h_{i,0}^{\mathrm{o}} + \int_{T_{i,0}}^{T} c_{p,i}^{\mathrm{o}}(T)\mathrm{d}T$ for the component *i*.

Molar entropy

$$s^{\mathrm{o}} = \sum_i \psi_i \, s_i^{\mathrm{o}}(p,T) - R\sum_i \psi_i \ln \psi_i + \Delta s_{\mathrm{dis}} \tag{3.22}$$

where $s_i^{\mathrm{o}}(p,T) = s_{i,0}^{\mathrm{o}} + \int_{T_{i,0}}^{T} \frac{c_{p,i}^{\mathrm{o}}(T)}{T}\,\mathrm{d}T - R\ln\frac{p}{p_{i,0}}$ for the component *i*.

Isentropic exponent

$$\kappa^{\mathrm{o}} = \frac{c_p^{\mathrm{o}}}{c_p^{\mathrm{o}} - R}. \tag{3.23}$$

Speed of sound

$$w^{\mathrm{o}} = \sqrt{\frac{R}{M}\kappa^{\mathrm{o}} T}\,. \tag{3.24}$$

Dissociation

The terms $\Delta c_{p,\mathrm{dis}}$, Δh_{dis}, and Δs_{dis} consider the influence of the dissociation at temperatures greater than 1200 K and mole fractions of oxygen greater than or equal to 1%. The algorithms of the VDI-Guideline 4670 contain a simplified model for dissociation at high temperatures described in [16], [23]:

$$\Delta c_{p,\mathrm{dis}} = \Delta c_{p,\mathrm{dis}}(p,T,\Psi) \tag{3.25}$$

$$\Delta h_{\mathrm{dis}} = \Delta h_{\mathrm{dis}}(p,T,\Psi) \tag{3.26}$$

$$\Delta s_{\mathrm{dis}} = \Delta s_{\mathrm{dis}}(p,T,\Psi) \tag{3.27}$$

where Ψ is the vector of the mole fractions of the components.

Property libraries

The property library LibIdGas [25] contains these algorithms of the VDI-Guideline 4670 for the calculation of ideal-gas mixtures. In addition, the property library LibIdAir [26] was developed particularly for humid air where dry air is calculated from the VDI-Guideline 4670. This library allows calculating properties not only for unsaturated and saturated humid air but also for liquid fog and ice fog. The properties of the liquid droplets are calculated from the industrial formulation of water [20], [21]. For calculating the properties of ice, the equation of state from Hyland and Wexler [22] is used.

3.2.2 Ideal Mixture of Real Fluids

The calculation of humid air as an ideal mixture of real fluids can be realized in two ways:

- Ideal mixture of the components nitrogen, oxygen, argon, and steam (and liquid water or ice in case of fog)
- Ideal mixture of dry air and steam (and liquid water or ice in case of fog).

3.2.2.1 Ideal Mixture of Nitrogen, Oxygen, Argon, and Water

The important properties of unsaturated and saturated humid air are calculated as follows:

Mass density

$$\tilde{\rho} = \tilde{\rho}_{\mathrm{a}}(p_{\mathrm{a}},T) + \tilde{\rho}_{\mathrm{w}}(p_{\mathrm{w}},T) \tag{3.28}$$

where

the partial density of dry air $\tilde{\rho}_{\mathrm{a}}(p_{\mathrm{a}},T)$ is calculated iteratively for an ideal mixture using the reduced Helmholtz free-energy equations $\alpha_i(\delta,\tau) = \alpha_i^{\mathrm{o}}(\delta_i,\tau_i) + \alpha_i^{\mathrm{r}}(\delta_i,\tau_i)$ of

- Span *et al.* [27] for nitrogen N_2
- de Reuck, Wagner, and Schmidt [28], [29] for oxygen O_2
- Tegeler *et al.* [30] for argon Ar

via $$p_{\mathrm{a}} = \tilde{\rho}_{\mathrm{a}}\, T \frac{R}{M_{\mathrm{a}}}\left[1 + \sum_i \frac{\psi_i}{\psi_{\mathrm{a}}} \delta_i\, \alpha^{\mathrm{r}}_{\delta,i}(\delta_i,\tau_i)\right] \tag{3.29}$$

where

$p_{\mathrm{a}} = \psi_{\mathrm{a}}\, p$ is the partial pressure of the mixture dry air

with $\psi_{\mathrm{a}} = \psi_{\mathrm{N_2}} + \psi_{\mathrm{O_2}} + \psi_{\mathrm{Ar}}$ the mole fraction of dry air,

M_a is the molar mass of dry air $M_\mathrm{a} = \sum_i \psi_i M_i$,

$\delta_i = \dfrac{\tilde{\rho}_\mathrm{a}}{\tilde{\rho}_{\mathrm{c},i}},\ \tau_i = \dfrac{T_{\mathrm{c},i}}{T}$

for $i = \mathrm{N_2}, \mathrm{O_2}, \mathrm{Ar}$.

the partial density of steam $\tilde{\rho}_\mathrm{w}(p_\mathrm{w}, T)$ is calculated iteratively from the reduced Helmholtz free-energy equation $\alpha_\mathrm{w}(\delta,\tau) = \alpha_\mathrm{w}^\mathrm{o}(\delta_\mathrm{w},\tau_\mathrm{w}) + \alpha_\mathrm{w}^\mathrm{r}(\delta_\mathrm{w},\tau_\mathrm{w})$ of the scientific formulation of water IAPWS-95 [18], [19], Eq. (3.8),

via $p_\mathrm{w} = \tilde{\rho}_\mathrm{w}\, T\, R_\mathrm{w}\left[1 + \delta_\mathrm{w}\, \alpha_{\delta,\mathrm{w}}^\mathrm{r}(\delta_\mathrm{w},\tau_\mathrm{w})\right]$ (3.30)

where $p_\mathrm{w} = \psi_\mathrm{w}\, p,\ \delta_\mathrm{w} = \dfrac{\tilde{\rho}_\mathrm{w}}{\tilde{\rho}_{\mathrm{c,w}}},\ \tau_\mathrm{w} = \dfrac{T_{\mathrm{c,w}}}{T}$,

$\tilde{\rho}_{\mathrm{c,w}} = 322\ \mathrm{kg\ m^{-3}}$, $T_{\mathrm{c,w}} = 647.096\ \mathrm{K}$, and $\tilde{R}_\mathrm{w} = 0.46151805\ \mathrm{kJ\ kg^{-1}\ K^{-1}}$.

Molar volume

$$v = \frac{M}{\tilde{\rho}} \tag{3.31}$$

where $\tilde{\rho}$ results from Eq. (3.28) and $M = \psi_\mathrm{a}\, M_\mathrm{a} + \psi_\mathrm{w}\, M_\mathrm{w}$.

Molar isobaric heat capacity

$$c_p = \psi_\mathrm{a}\, c_{p,\mathrm{a}}(\tilde{\rho}_\mathrm{a}, T) + \psi_\mathrm{w}\, c_{p,\mathrm{w}}(\tilde{\rho}_\mathrm{w}, T) + \Delta c_{p,\mathrm{dis}}(p, T, \Psi) \tag{3.32}$$

Dry air:

$$c_{p,\mathrm{a}}(\tilde{\rho}_\mathrm{a}, T) = R\left[\sum_i -\frac{\psi_i}{\psi_\mathrm{a}}\tau_i^2\left(\alpha_{\tau\tau,i}^\mathrm{o} + \alpha_{\tau\tau,i}^\mathrm{r}\right) + \frac{\left(1 + \sum_i \frac{\psi_i}{\psi_\mathrm{a}}\delta_i\, \alpha_{\delta,i}^\mathrm{r} - \sum_i \frac{\psi_i}{\psi_\mathrm{a}}\delta_i\, \tau_i\, \alpha_{\delta\tau,i}^\mathrm{r}\right)^2}{1 + 2\sum_i \frac{\psi_i}{\psi_\mathrm{a}}\delta_i\, \alpha_{\delta,i}^\mathrm{r} + \sum_i \frac{\psi_i}{\psi_\mathrm{a}}\delta_i^2\, \alpha_{\delta\delta,i}^\mathrm{r}}\right] \tag{3.33}$$

where

$\tilde{\rho}_\mathrm{a}$ is calculated iteratively from Eq. (3.29) and

$\delta_i = \dfrac{\tilde{\rho}_\mathrm{a}}{\tilde{\rho}_{\mathrm{c},i}},\ \tau_i = \dfrac{T_{\mathrm{c},i}}{T}$ with $i = \mathrm{N_2}, \mathrm{O_2}, \mathrm{Ar}$.

Steam:

$$c_{p,\mathrm{w}}(\tilde{\rho}_\mathrm{w}, T) = R\left[-\tau_\mathrm{w}^2\left(\alpha_{\tau\tau,\mathrm{w}}^0 + \alpha_{\tau\tau,\mathrm{w}}^\mathrm{r}\right) + \frac{\left(1 + \delta_\mathrm{w}\, \alpha_{\delta,\mathrm{w}}^\mathrm{r} - \delta_\mathrm{w}\tau_\mathrm{w}\, \alpha_{\delta\tau,\mathrm{w}}^\mathrm{r}\right)^2}{1 + 2\,\delta_\mathrm{w}\, \alpha_{\delta,\mathrm{w}}^\mathrm{r} + \delta_\mathrm{w}^2\, \alpha_{\delta\delta,\mathrm{w}}^\mathrm{r}}\right] \tag{3.34}$$

where

$\tilde{\rho}_\mathrm{w}$ is calculated iteratively from Eq. (3.30)

and $\delta_\mathrm{w} = \dfrac{\tilde{\rho}_\mathrm{w}}{\tilde{\rho}_\mathrm{c,w}}$, $\tau_\mathrm{w} = \dfrac{T_\mathrm{c,w}}{T}$.

$\Delta c_{p,\mathrm{dis}}(p,T,\Psi)$ from Eq. (3.25).

Molar isochoric heat capacity

$$c_v = \psi_\mathrm{a}\, c_{v,\mathrm{a}}(\tilde{\rho}_\mathrm{a},T) + \psi_\mathrm{w}\, c_{v,\mathrm{w}}(\tilde{\rho}_\mathrm{w},T) + \Delta c_{p,\mathrm{dis}}(p,T,\Psi) \tag{3.35}$$

Dry air:

$$c_{v,\mathrm{a}}(\tilde{\rho}_\mathrm{a},T) = R\left[\sum_i -\frac{\psi_i}{\psi_\mathrm{a}}\tau_i^2\left(\alpha^\mathrm{o}_{\tau\tau,i} + \alpha^\mathrm{r}_{\tau\tau,i}\right)\right] \tag{3.36}$$

where

$\tilde{\rho}_\mathrm{a}$ is calculated iteratively from Eq. (3.29) and

$\delta_i = \dfrac{\tilde{\rho}_\mathrm{a}}{\tilde{\rho}_{\mathrm{c},i}}$, $\tau_i = \dfrac{T_{\mathrm{c},i}}{T}$ with $i = \mathrm{N_2}, \mathrm{O_2}, \mathrm{Ar}$.

Steam:

$$c_{v,\mathrm{w}}(\tilde{\rho}_\mathrm{w},T) = -R\,\tau_\mathrm{w}^2\left(\alpha^\mathrm{o}_{\tau\tau,\mathrm{w}} + \alpha^\mathrm{r}_{\tau\tau,\mathrm{w}}\right) \tag{3.37}$$

where

$\tilde{\rho}_\mathrm{w}$ is calculated iteratively from Eq. (3.30)

and $\delta_\mathrm{w} = \dfrac{\tilde{\rho}_\mathrm{w}}{\tilde{\rho}_\mathrm{c,w}}$, $\tau_\mathrm{w} = \dfrac{T_\mathrm{c,w}}{T}$.

$\Delta c_{p,\mathrm{dis}}(p,T,\Psi)$ from Eq. (3.25).

Molar enthalpy

$$h = \psi_\mathrm{a}\, h_\mathrm{a}(\tilde{\rho}_\mathrm{a},T) + \psi_\mathrm{w}\, h_\mathrm{w}(\tilde{\rho}_\mathrm{w},T) + \Delta h_\mathrm{dis}(p,T,\Psi) \tag{3.38}$$

Dry air:

$$h_\mathrm{a}(\tilde{\rho}_\mathrm{a},T) = RT\left[1 + \sum_i \frac{\psi_i}{\psi_\mathrm{a}}\tau_i\left(\alpha^\mathrm{o}_{\tau,i} + \alpha^\mathrm{r}_{\tau,i}\right) + \sum_i \frac{\psi_i}{\psi_\mathrm{a}}\delta_i\,\alpha^\mathrm{r}_{\delta,i}\right] \tag{3.39}$$

where

$\tilde{\rho}_\mathrm{a}$ is calculated iteratively from Eq. (3.29) and

$\delta_i = \dfrac{\tilde{\rho}_\mathrm{a}}{\tilde{\rho}_{\mathrm{c},i}}$, $\tau_i = \dfrac{T_{\mathrm{c},i}}{T}$ with $i = \mathrm{N_2}, \mathrm{O_2}, \mathrm{Ar}$.

Steam:

$$h_{\mathrm{w}}\left(\tilde{\rho}_{\mathrm{w}},T\right)=RT\left[1+\tau_{\mathrm{w}}\left(\alpha_{\tau,\mathrm{w}}^{\mathrm{o}}+\alpha_{\tau}^{\mathrm{r}}\right)+\delta_{\mathrm{w}}\,\alpha_{\delta}^{\mathrm{r}}\right] \tag{3.40}$$

where

$\tilde{\rho}_{\mathrm{w}}$ is calculated iteratively from Eq. (3.30)

and $\delta_{\mathrm{w}}=\dfrac{\tilde{\rho}_{\mathrm{w}}}{\tilde{\rho}_{\mathrm{c,w}}},\ \tau_{\mathrm{w}}=\dfrac{T_{\mathrm{c,w}}}{T}$.

$\Delta h_{\mathrm{dis}}(p,T,\Psi)$ from Eq. (3.26).

Molar entropy

$$s=\psi_{\mathrm{a}}\,s_{\mathrm{a}}(\tilde{\rho}_{\mathrm{a}},T)+\psi_{\mathrm{w}}\,s_{\mathrm{w}}(\tilde{\rho}_{\mathrm{w}},T)+\Delta s_{\mathrm{dis}}(p,T,\Psi) \tag{3.41}$$

Dry air:

$$s_{\mathrm{a}}(\tilde{\rho}_{\mathrm{a}},T)=R\left[\sum_i\frac{\psi_i}{\psi_{\mathrm{a}}}\tau_i\left(\alpha_{\tau,i}^{\mathrm{o}}+\alpha_{\tau,i}^{\mathrm{r}}\right)-\sum_i\frac{\psi_i}{\psi_{\mathrm{a}}}\alpha^{\mathrm{o}}-\sum_i\frac{\psi_i}{\psi_{\mathrm{a}}}\alpha^{\mathrm{r}}-\sum_i\frac{\psi_i}{\psi_{\mathrm{a}}}\ln\left(\frac{\psi_i}{\psi_{\mathrm{a}}}\right)\right] \tag{3.42}$$

where

$\tilde{\rho}_{\mathrm{a}}$ is calculated iteratively from Eq. (3.29) and

$\delta_i=\dfrac{\tilde{\rho}_{\mathrm{a}}}{\tilde{\rho}_{\mathrm{c},i}},\ \tau_i=\dfrac{T_{\mathrm{c},i}}{T}$ with $i=\mathrm{N_2},\mathrm{O_2},\mathrm{Ar}$.

Steam:

$$s_{\mathrm{w}}(\tilde{\rho}_{\mathrm{w}},T)=R\left[\tau_{\mathrm{w}}\left(\alpha_{\tau,\mathrm{w}}^{\mathrm{o}}+\alpha_{\tau,\mathrm{w}}^{\mathrm{r}}\right)-\alpha_{\mathrm{w}}^{\mathrm{o}}-\alpha_{\mathrm{w}}^{\mathrm{r}}\right] \tag{3.43}$$

where

$\tilde{\rho}_{\mathrm{w}}$ is calculated iteratively from Eq. (3.30)

and $\delta_{\mathrm{w}}=\dfrac{\tilde{\rho}_{\mathrm{w}}}{\tilde{\rho}_{\mathrm{c,w}}},\ \tau_{\mathrm{w}}=\dfrac{T_{\mathrm{c,w}}}{T}$.

$\Delta s_{\mathrm{dis}}(p,T,\Psi)$ from Eq. (3.27).

Speed of sound

$$w=\sqrt{-\frac{v^2}{M}\frac{c_p}{c_v}\left(\frac{\partial p}{\partial v}\right)_T} \tag{3.44}$$

where

$$\left(\frac{\partial p}{\partial v}\right)_T=\frac{1}{\psi_{\mathrm{a}}\left(\dfrac{\partial v}{\partial p}\right)_{T,\mathrm{a}}}+\frac{1}{\psi_{\mathrm{w}}\left(\dfrac{\partial v}{\partial p}\right)_{T,\mathrm{w}}} \tag{3.45}$$

Dry air:

$$\left(\frac{\partial v}{\partial p}\right)_{T,\mathrm{a}} = -\frac{v_\mathrm{a}^2}{RT\left(1+2\sum_i \frac{\psi_i}{\psi_\mathrm{a}}\delta_i\,\alpha^\mathrm{r}_{\delta,i}+\sum_i \frac{\psi_i}{\psi_\mathrm{a}}\delta_i^2\,\alpha^\mathrm{r}_{\delta\delta,i}\right)} \tag{3.46}$$

where

$v_\mathrm{a} = \frac{M_\mathrm{a}}{\tilde{\rho}_\mathrm{a}}$, $\tilde{\rho}_\mathrm{a}$ is calculated iteratively from Eq. (3.29),

$\delta_i = \frac{\tilde{\rho}_\mathrm{a}}{\tilde{\rho}_{\mathrm{c},i}}$, $\tau_i = \frac{T_{\mathrm{c},i}}{T}$ with $i = \mathrm{N_2}, \mathrm{O_2}, \mathrm{Ar}$.

Steam:

$$\left(\frac{\partial v}{\partial p}\right)_{T,\mathrm{w}} = -\frac{v_\mathrm{w}^2}{RT\left(1+2\,\delta_\mathrm{w}\,\alpha^\mathrm{r}_{\delta,\mathrm{w}}+\delta_\mathrm{w}^2\,\alpha^\mathrm{r}_{\delta\delta,\mathrm{w}}\right)} \tag{3.47}$$

where

$v_\mathrm{w} = \frac{M_\mathrm{w}}{\tilde{\rho}_\mathrm{w}}$, $\tilde{\rho}_\mathrm{w}$ is calculated iteratively from Eq. (3.30),

$\delta_\mathrm{w} = \frac{\tilde{\rho}_\mathrm{w}}{\tilde{\rho}_{\mathrm{c,w}}}$, $\tau_\mathrm{w} = \frac{T_{\mathrm{c,w}}}{T}$.

Isentropic exponent

$$\kappa = \frac{w^2\,\tilde{\rho}}{p}. \tag{3.48}$$

Property library

The property library LibHuGas [31] contains the algorithms to calculate properties of unsaturated and saturated humid air and of liquid and ice fog. The calculation of liquid fog and ice fog is described in [32].

3.2.2.2 Ideal Mixture of the Real Gases Dry Air and Water Vapour

The properties of dry air can be calculated by a very accurate fundamental equation of Lemmon *et al.* [1]. For the calculation of water, the scientific formulation IAPWS-95 [18], [19] and the industrial formulation IAPWS-IF97 [20], [21] are available.

The thermodynamic properties of humid air can be calculated by the model of an ideal mixture of the real fluids dry air and water. Such approach has been used for the property library LibHuAir [33], in which dry air (a) is calculated from Lemmon *et al.* and water (w) from IAPWS-IF97.

The following algorithms are implemented for unsaturated humid air, e.g., dry air plus superheated water vapour:

Mass density

$$\tilde{\rho} = \tilde{\rho}_{\mathrm{a}}(p_{\mathrm{a}}, T) + \tilde{\rho}_{\mathrm{w}}(p_{\mathrm{w}}, T) \tag{3.49}$$

where

the partial density of dry air $\tilde{\rho}_{\mathrm{a}}$ is calculated iteratively from

$$p_{\mathrm{a}} = \tilde{\rho}_{\mathrm{a}}\, T \frac{R}{M_{\mathrm{a}}}\left[1 + \delta_{\mathrm{a}}\, \alpha^{\mathrm{r}}_{\delta,\mathrm{a}}(\delta_{\mathrm{a}}, \tau_{\mathrm{a}})\right] \tag{3.50}$$

with

$p_{\mathrm{a}} = \psi_{\mathrm{a}}\, p$

and $\delta_{\mathrm{a}} = \dfrac{\tilde{\rho}_{\mathrm{a}}}{\tilde{\rho}_{\mathrm{c,a}}}$, $\tau_{\mathrm{a}} = \dfrac{T_{\mathrm{c,a}}}{T}$.

Using IAPWS-IF97 [20], [21] the partial density of steam $\tilde{\rho}_{\mathrm{w}}$ is directly calculated from

$$\tilde{\rho}_{\mathrm{w}} = \frac{p_{\mathrm{w}}}{T}\frac{M_{\mathrm{w}}}{R}\frac{1}{\gamma^{\mathrm{o}}_{\pi,j}(\pi_j, \tau_j) + \gamma^{\mathrm{r}}_{\pi,j}(\pi_j, \tau_j)} \tag{3.51}$$

with

$p_{\mathrm{w}} = \psi_{\mathrm{w}}\, p$

and $\pi_j = \dfrac{p_{\mathrm{w}}}{p_{\mathrm{r},j}}$, $\tau_j = \dfrac{T_{\mathrm{r},j}}{T}$, $j = 2, 5$ for the regions 2 and 5 of IAPWS-IF97.

Molar volume

$$v = \frac{M}{\tilde{\rho}} \tag{3.52}$$

where $\tilde{\rho}$ is calculated from Eq. (3.49) and $M = \psi_{\mathrm{a}}\, M_{\mathrm{a}} + \psi_{\mathrm{w}}\, M_{\mathrm{w}}$.

Molar isobaric heat capacity

$$c_p = \psi_{\mathrm{a}}\, c_{p,\mathrm{a}}(\tilde{\rho}_{\mathrm{a}}, T) + \psi_{\mathrm{w}}\, c_{p,\mathrm{w}}(p_{\mathrm{w}}, T) + \Delta c_{p,\mathrm{dis}}(p, T, \Psi) \tag{3.53}$$

where:

Dry air contribution from [1]

$$c_{p,\mathrm{a}}\left(\tilde{\rho}_{\mathrm{a}}, T\right) = R\left[-\tau_{\mathrm{a}}^2\left(\alpha^{\mathrm{o}}_{\tau\tau,\mathrm{a}} + \alpha^{\mathrm{r}}_{\tau\tau,\mathrm{a}}\right) + \frac{\left(1 + \delta_{\mathrm{a}}\, \alpha^{\mathrm{r}}_{\delta,\mathrm{a}} - \delta_{\mathrm{a}}\, \tau_{\mathrm{a}}\, \alpha^{\mathrm{r}}_{\delta\tau,\mathrm{a}}\right)^2}{1 + 2\,\delta_{\mathrm{a}}\, \alpha^{\mathrm{r}}_{\delta,\mathrm{a}} + \delta_{\mathrm{a}}^2\, \alpha^{\mathrm{r}}_{\delta\delta,\mathrm{a}}}\right] \tag{3.54}$$

where $\tilde{\rho}_{\mathrm{a}}$ is calculated iteratively from Eq. (3.50) and $\delta_{\mathrm{a}} = \dfrac{\tilde{\rho}_{\mathrm{a}}}{\tilde{\rho}_{\mathrm{c,a}}}$, $\tau_{\mathrm{a}} = \dfrac{T_{\mathrm{c,a}}}{T}$.

Water vapour respectively steam contribution from IAPWS-IF97 [20], [21]

$$c_{p,\mathrm{w}}\left(p_\mathrm{w},T\right)=-R\,\tau_\mathrm{w}^2\left(\gamma^\mathrm{o}_{\tau\tau,j}+\gamma^\mathrm{r}_{\tau\tau,j}\right) \tag{3.55}$$

with

$p_\mathrm{w}=\psi_\mathrm{w}\,p$

and $\pi_j=\dfrac{p_\mathrm{w}}{p_{\mathrm{r},j}}$, $\tau_j=\dfrac{T_{\mathrm{r},j}}{T}$, $j=2, 5$ for regions 2 and 5 of IAPWS-IF97.

$\Delta c_{p,\mathrm{dis}}(p,T,\Psi)$ from Eq. (3.25).

Molar isochoric heat capacity

$$c_v=\psi_\mathrm{a}\,c_{v,\mathrm{a}}\left(\tilde{\rho}_\mathrm{a},T\right)+\psi_\mathrm{w}\,c_{v,\mathrm{w}}\left(p_\mathrm{w},T\right)+\Delta c_{p,\mathrm{dis}}(p,T,\Psi) \tag{3.56}$$

where:

Dry air contribution from [1]

$$c_{v,\mathrm{a}}(\tilde{\rho}_\mathrm{a},T)=-R\,\tau_\mathrm{a}^2\left(\alpha^\mathrm{o}_{\tau\tau,\mathrm{a}}+\alpha^\mathrm{r}_{\tau\tau,\mathrm{a}}\right) \tag{3.57}$$

where $\tilde{\rho}_\mathrm{a}$ is calculated iteratively from Eq. (3.50) and $\delta_\mathrm{a}=\dfrac{\tilde{\rho}_\mathrm{a}}{\tilde{\rho}_{\mathrm{c,a}}}$, $\tau_\mathrm{a}=\dfrac{T_{\mathrm{c,a}}}{T}$.

Water vapour respectively steam contribution from IAPWS-IF97 [20], [21]

$$c_{v,\mathrm{w}}(p_\mathrm{w},T)=-R\left(\gamma^\mathrm{o}_{\tau\tau,j}+\gamma^\mathrm{r}_{\tau\tau,j}\right)+\frac{\left(1+\pi_j\,\gamma^\mathrm{r}_{\pi,j}-\tau_j\,\pi_j\,\gamma^\mathrm{r}_{\pi\tau,j}\right)^2}{1-\pi_j^2\,\gamma^\mathrm{r}_{\pi\pi,j}} \tag{3.58}$$

with

$p_\mathrm{w}=\psi_\mathrm{w}\,p$

and $\pi_j=\dfrac{p_\mathrm{w}}{p_{\mathrm{r},j}}$, $\tau_j=\dfrac{T_{\mathrm{r},j}}{T}$, $j=2, 5$ for regions 2 and 5 of IAPWS-IF97.

$\Delta c_{p,\mathrm{dis}}(p,T,\Psi)$ from Eq. (3.25).

Molar enthalpy

$$h=\psi_\mathrm{a}\,h_\mathrm{a}\left(\tilde{\rho}_\mathrm{a},T\right)+\psi_\mathrm{w}\,h_\mathrm{w}\left(p_\mathrm{w},T\right)+\Delta h_{\mathrm{dis}}(p,T,\Psi) \tag{3.59}$$

where:

Dry air contribution from [1]

$$h_\mathrm{a}\left(\tilde{\rho}_\mathrm{a},T\right)=R\,T\left[1+\tau_\mathrm{a}\left(\alpha^\mathrm{o}_{\tau,\mathrm{a}}+\alpha^\mathrm{r}_{\tau}\right)+\delta_\mathrm{a}\,\alpha^\mathrm{r}_{\delta}\right] \tag{3.60}$$

where $\tilde{\rho}_\mathrm{a}$ is calculated iteratively from Eq. (3.50) and $\delta_\mathrm{a}=\dfrac{\tilde{\rho}_\mathrm{a}}{\tilde{\rho}_{\mathrm{c,a}}}$, $\tau_\mathrm{a}=\dfrac{T_{\mathrm{c,a}}}{T}$.

Water vapour respectively steam contribution from IAPWS-IF97 [20], [21]

$$h_\mathrm{w}\left(p_\mathrm{w},T\right)=R\,T\left(\gamma^\mathrm{o}_{\tau,j}+\gamma^\mathrm{r}_{\tau,j}\right) \tag{3.61}$$

with

$$p_\mathrm{w} = \psi_\mathrm{w}\, p$$

and $\pi_j = \dfrac{p_\mathrm{w}}{p_{\mathrm{r},j}}$, $\tau_j = \dfrac{T_{\mathrm{r},j}}{T}$, $j = 2, 5$ for regions 2 and 5 of IAPWS-IF97.

$\Delta h_\mathrm{dis}(p, T, \Psi)$ from Eq. (3.26).

Molar entropy

$$s = \psi_\mathrm{a}\, s_\mathrm{a}\left(\tilde{\rho}_\mathrm{a}, T\right) + \psi_\mathrm{w}\, s_\mathrm{w}\left(p_\mathrm{w}, T\right) + \Delta s_\mathrm{dis}(p, T, \Psi) \tag{3.62}$$

where:

Dry air contribution from [1]

$$s_\mathrm{a}\left(\tilde{\rho}_\mathrm{a}, T\right) = R\left[\tau_\mathrm{a}\left(\alpha^\mathrm{o}_{\tau,\mathrm{a}} + \alpha^\mathrm{r}_{\tau,\mathrm{a}}\right) - \alpha^\mathrm{o}_\mathrm{a} - \alpha^\mathrm{r}_\mathrm{a}\right] + \Delta s_\mathrm{irr,a} \tag{3.63}$$

where $\tilde{\rho}_\mathrm{a}$ is calculated iteratively from Eq. (3.50) and $\delta_\mathrm{a} = \dfrac{\tilde{\rho}_\mathrm{a}}{\tilde{\rho}_\mathrm{c,a}}$, $\tau_\mathrm{a} = \dfrac{T_\mathrm{c,a}}{T}$.

Water vapour respectively steam contribution from IAPWS-IF97 [20], [21]

$$s_\mathrm{w}\left(p_\mathrm{w}, T\right) = R\left[\tau_\mathrm{w}\left(\gamma^\mathrm{o}_{\tau,j} + \gamma^\mathrm{r}_{\tau,j}\right) - \left(\gamma^\mathrm{o}_j + \gamma^\mathrm{r}_j\right)\right] \tag{3.64}$$

with

$$p_\mathrm{w} = \psi_\mathrm{w}\, p$$

and $\pi_j = \dfrac{p_\mathrm{w}}{p_{\mathrm{r},j}}$, $\tau_j = \dfrac{T_{\mathrm{r},j}}{T}$, $j = 2, 5$ for regions 2 and 5 of IAPWS-IF97.

$\Delta s_\mathrm{dis}(p, T, \Psi)$ from Eq. (3.27).

Speed of sound

$$w = \sqrt{-\frac{v^2}{M}\frac{c_p}{c_v}\left(\frac{\partial p}{\partial v}\right)_T} \tag{3.65}$$

where

$$\left(\frac{\partial p}{\partial v}\right)_T = \frac{1}{\psi_\mathrm{a}\left(\dfrac{\partial v}{\partial p}\right)_{T,\mathrm{a}}} + \frac{1}{\psi_\mathrm{w}\left(\dfrac{\partial v}{\partial p}\right)_{T,\mathrm{w}}}.$$

Dry air from [1]

$$\left(\frac{\partial v}{\partial p}\right)_{T,\mathrm{a}}(\tilde{\rho}_\mathrm{a}, T) = -\frac{v_\mathrm{a}^2}{R\,T\left(1 + 2\,\delta_\mathrm{a}\,\alpha^\mathrm{r}_{\delta,\mathrm{a}} + \delta_\mathrm{a}^2\,\alpha^\mathrm{r}_{\delta\delta,\mathrm{a}}\right)} \tag{3.66}$$

where $v_\mathrm{a} = \frac{M_\mathrm{a}}{\tilde{\rho}_\mathrm{a}}$, $\tilde{\rho}_\mathrm{a}$ is calculated iteratively from Eq. (3.50), and $\delta_\mathrm{a} = \frac{\tilde{\rho}_\mathrm{a}}{\tilde{\rho}_\mathrm{c,a}}$, $\tau_\mathrm{a} = \frac{T_\mathrm{c,a}}{T}$.

Water vapour respectively steam contribution from IAPWS-IF97 [20], [21]

$$\left(\frac{\partial v}{\partial p}\right)_{T,\mathrm{w}}(p_\mathrm{w},T) = \frac{RT}{p_\mathrm{w}^2}\,{\pi_j}^2\,\gamma_{\pi\pi,j} \tag{3.67}$$

with

$p_\mathrm{w} = \psi_\mathrm{w}\,p$

and $\pi_j = \frac{p_\mathrm{w}}{p_{\mathrm{r},j}}$, $\tau_j = \frac{T_{\mathrm{r},j}}{T}$, $j = 2, 5$ for regions 2 and 5 of IAPWS-IF97.

Isentropic exponent

$$\kappa = \frac{w^2\,\tilde{\rho}}{p}. \tag{3.68}$$

Property library

The property library LibHuAir [33] allows calculating properties of unsaturated and saturated humid air as well as of liquid and ice fog. The calculation of liquid fog and ice fog is described in [34].

3.2.3 Real Mixture of Real Fluids

Both, the ideal gas model and the ideal mixing model, correspond to a calculation as an ideal mixture. That means, the mixing effects are not considered. In the model "Real mixture of real fluids" (real model), these mixing effects are considered in the excess term (E). The calculation of any molar property (z) except molar entropy (s) by means of the real model is:

$$z = \psi_\mathrm{a}\,z_\mathrm{a}(p_\mathrm{a},T) + \psi_\mathrm{w}\,z_\mathrm{w}(p_\mathrm{w},T) + z^\mathrm{E}(p,T). \tag{3.69}$$

The calculation of the molar entropy s is:

$$s = \psi_\mathrm{a}\,s_\mathrm{a}(p_\mathrm{a},T) + \psi_\mathrm{w}\,s_\mathrm{w}(p_\mathrm{w},T) - R\ln\left(\frac{p}{p_0}\right) + s^\mathrm{E}(p,T). \tag{3.70}$$

3.2.3.1 Virial Equation Proposed by Rabinovich and Beketov

The virial equation of Rabinovich and Beketov [35] for the mixture reads:

$$Z = \frac{p\,v}{RT} = 1 + \frac{B(T,\psi_\mathrm{w})}{v} + \frac{C(T,\psi_\mathrm{w})}{v^2}, \tag{3.71}$$

where p is the mixture pressure, v is the molar volume of the mixture at specific p, T, and ψ_w, R is the universal gas constant with $R = 8.31441\,\mathrm{kJ\,kmol^{-1}\,K^{-1}}$, and T is the mixture temperature. The second virial coefficient $B(T,\psi_w)$ and the third virial coefficient $C(T,\psi_w)$ of humid air are functions of mixture temperature T and the mole fraction of water vapour ψ_w, given as:

$$B = B_{aa} + 2\left(B_{aw} - B_{aa}\right)\psi_w + \left(B_{aa} - 2B_{aw} + B_{ww}\right)\psi_w^2 \tag{3.72}$$

$$C = C_{aaa} + 3\left(C_{aaw} - C_{aaa}\right)\psi_w + 3\left(C_{aaa} - 2C_{aaw}\right)\psi_w^2 + \left(3C_{aaw} - C_{aaa}\right)\psi_w^3 \tag{3.73}$$

with

$$B_{aa} = b_1 + b_2\,\theta^{-1} + b_3\,\theta^{-2} + b_4\,\theta^{-4} + b_5\,\theta^{-5} \tag{3.74}$$

$$C_{aaa} = c_1 + c_2\,\theta^{-2} + c_3\,\theta^{-4} \tag{3.75}$$

where $\theta = \dfrac{T}{100\ \mathrm{K}}$, $b_1 ... b_5$ and $c_1 ... c_3$ are coefficients,

$$B_{ww} = b_1\,\theta^{-1} + b_2\,\theta^{-2} + b_3\,\theta^{-5} + b_4\,\theta^{-6} + b_5\,\theta^{-7} \tag{3.76}$$

where $\theta = \dfrac{T}{T_{c,w}}$ and $b_1 ... b_5$ are coefficients,

$$B_{aw} = b_1 + b_2\,\theta^{-1} + b_3\,\theta^{-2} + b_4\,\theta^{-3} + b_5\,\theta^{-5} \tag{3.77}$$

$$C_{aaw} = c_1 + c_2\,\theta^{-2} + c_3\,\theta^{-3} + c_4\,\theta^{-5} \tag{3.78}$$

where $\theta = \dfrac{T}{100\ \mathrm{K}}$, $b_1 ... b_5$ and $c_1 ... c_4$ are coefficients, and

ψ_w is the mole fraction of water vapour and ranges from 0 to $\psi_{s,w}(p,T)$, which is the saturated composition of water vapour in humid air at specific p and T.

The coefficients b_i and c_i used in the Eqs. (3.74) to (3.78) were taken from the book by Rabinovich and Beketov [35].

Molar volume

The molar volume $v(p,T,\psi_w)$ is calculated iteratively from the expression

$$p(v,T,\psi_w) = \frac{RT}{v}\left(1 + \frac{B(T,\psi_w)}{v} + \frac{C(T,\psi_w)}{v^2}\right). \tag{3.79}$$

Mass density

$$\tilde{\rho} = \frac{M}{v} \tag{3.80}$$

where v is calculated iteratively from Eq. (3.79) and $M = \psi_a\,M_a + \psi_w\,M_w$.

Molar isobaric heat capacity

$$c_p(p,T,\psi_\mathrm{w}) = \psi_\mathrm{a}\, c^\mathrm{o}_{p,\mathrm{a}}(T) + \psi_\mathrm{w}\, c^\mathrm{o}_{p,\mathrm{w}}(T) - R - \frac{RT}{v}\left(2\frac{\mathrm{d}B}{\mathrm{d}T} + T\frac{\mathrm{d}^2B}{\mathrm{d}T^2}\right) - \frac{RT}{2v^2}\left(2\frac{\mathrm{d}C}{\mathrm{d}T} + T\frac{\mathrm{d}^2C}{\mathrm{d}T^2}\right) + \frac{R\left(1+\frac{B}{v}+\frac{C}{v^2}+\frac{T}{v}\frac{\mathrm{d}B}{\mathrm{d}T}+\frac{T}{v^2}\frac{\mathrm{d}C}{\mathrm{d}T}\right)^2}{1+\frac{2B}{v}+\frac{3C}{v^2}} \tag{3.81}$$

where $c^\mathrm{o}_{p,\mathrm{a}}(T)$ and $c^\mathrm{o}_{p,\mathrm{w}}(T)$ are the functions for the isobaric heat capacity of the ideal gases dry air and steam given in the book.

Molar isochoric heat capacity

$$c_v(p,T,\psi_\mathrm{w}) = c_p\, T \frac{\left(\frac{\partial p}{\partial T}\right)^2_{v,\psi_\mathrm{w}}}{\left(\frac{\partial p}{\partial v}\right)_{T,\psi_\mathrm{w}}} \tag{3.82}$$

with

$$\left(\frac{\partial p}{\partial v}\right)_{T,\psi_\mathrm{w}}(p,T,\psi_\mathrm{w}) = -\frac{RT}{v^2}\left(1+\frac{2B}{v}+\frac{3C}{v^2}\right) \text{ and} \tag{3.83}$$

$$\left(\frac{\partial p}{\partial T}\right)_{v,\psi_\mathrm{w}}(p,T,\psi_\mathrm{w}) = \frac{R}{v}\left[1+\frac{1}{v}\left(B+T\frac{\mathrm{d}B}{\mathrm{d}T}\right)+\frac{1}{v^2}\left(C+T\frac{\mathrm{d}C}{\mathrm{d}T}\right)\right]. \tag{3.84}$$

Molar enthalpy

$$h(p,T,\psi_\mathrm{w}) = \psi_\mathrm{a}\, h^\mathrm{o}_\mathrm{a}(T) + \psi_\mathrm{w}\, h^\mathrm{o}_\mathrm{w}(T) + \frac{RT}{v}\left(B - T\frac{\mathrm{d}B}{\mathrm{d}T}\right) + \frac{RT}{2v^2}\left(2C - T\frac{\mathrm{d}C}{\mathrm{d}T}\right) \tag{3.85}$$

where $h^\mathrm{o}_\mathrm{a}(T) = h^\mathrm{o}_{0,\mathrm{a}}(T) + \int_{T_{0,\mathrm{a}}}^{T} c^\mathrm{o}_{p,\mathrm{a}}(T)\mathrm{d}T$ and $h^\mathrm{o}_\mathrm{w}(T) = h^\mathrm{o}_{0,\mathrm{w}}(T) + \int_{T_{0,\mathrm{w}}}^{T} c^\mathrm{o}_{p,\mathrm{w}}(T)\mathrm{d}T$.

Molar entropy

$$s(p,T,\psi_\mathrm{w}) = \psi_\mathrm{a}\, s^\mathrm{o}_{\mathrm{T},\mathrm{a}}(T) + \psi_\mathrm{w}\, s^\mathrm{o}_{\mathrm{T},\mathrm{w}}(T) - R\left(\psi_\mathrm{a}\ln\psi_\mathrm{a} + \psi_\mathrm{w}\ln\psi_\mathrm{w}\right) + R\ln\frac{p_0 v}{RT} - \frac{R}{v}\left(B+T\frac{\mathrm{d}B}{\mathrm{d}T}\right) - \frac{R}{2v^2}\left(C+T\frac{\mathrm{d}C}{\mathrm{d}T}\right) \tag{3.86}$$

where

$$s^\mathrm{o}_{\mathrm{T},\mathrm{a}}(T) = s^\mathrm{o}_{0,\mathrm{a}}(T) + \int_{T_{0,\mathrm{a}}}^{T}\frac{c^\mathrm{o}_{p,\mathrm{a}}(T)}{T}\mathrm{d}T,\ s^\mathrm{o}_{\mathrm{T},\mathrm{w}}(T) = s^\mathrm{o}_{0,\mathrm{w}}(T) + \int_{T_{0,\mathrm{a}}}^{T}\frac{c^\mathrm{o}_{p,\mathrm{w}}(T)}{T}\mathrm{d}T, \text{ and}$$

p_0 is the standard pressure with $p_0 = 0.101325$ MPa .

Speed of sound

$$w(v,T,\psi_{\mathrm{w}}) = \sqrt{-\frac{v^2}{M}\frac{c_p}{c_v}\left(\frac{\partial p}{\partial v}\right)_{T,\psi_{\mathrm{w}}}} \,. \tag{3.87}$$

Isentropic exponent

$$\kappa(p,T,\psi_{\mathrm{w}}) = \frac{w^2\,\tilde{\rho}}{p} \,. \tag{3.88}$$

Property library

The property library LibRB95 [36] allows calculating properties of unsaturated and saturated humid air from the model by Rabinovich and Beketov [35].

3.2.3.2 Virial Equation Proposed by Hyland and Wexler and the Modification Proposed by Nelson and Sauer

The virial equation of Hyland and Wexler [22], [37] for the mixture reads

$$Z = \frac{p\,v}{R\,T} = 1 + \frac{B(T,\psi_{\mathrm{w}})}{v} + \frac{C(T,\psi_{\mathrm{w}})}{v^2} \,. \tag{3.89}$$

The model of Hyland and Wexler differs from that of Rabinovich and Beketov [35] with regard to the determination of the virial coefficients. In 2002, Nelson and Sauer [38], [39] modified the algorithm again. The mixture virial coefficients $B(T,\psi_{\mathrm{w}})$ and $C(T,\psi_{\mathrm{w}})$ are calculated as follows:

$$B = \psi_{\mathrm{a}}^2\,B_{\mathrm{aa}} + 2\psi_{\mathrm{a}}\,\psi_{\mathrm{w}}\,B_{\mathrm{aw}} + \psi_{\mathrm{w}}^2\,B_{\mathrm{ww}} \tag{3.90}$$

$$C = \psi_{\mathrm{a}}^3\,C_{\mathrm{aaa}} + 3\psi_{\mathrm{a}}^2\,\psi_{\mathrm{w}}\,C_{\mathrm{aaw}} + 3\psi_{\mathrm{a}}\,\psi_{\mathrm{w}}^2\,C_{\mathrm{aww}} + \psi_{\mathrm{w}}^3\,C_{\mathrm{www}} \,, \tag{3.91}$$

where

the temperature-dependent virial coefficients proposed by Hyland and Wexler are given as:

$$B_{\mathrm{aa}} = \sum_{k=1}^{4} b_k\,T^{(1-k)} \tag{3.92}$$

where $b_1 ... b_4$ are coefficients,

$$C_{\mathrm{aaa}} = \sum_{k=1}^{3} c_k\,T^{(1-k)} \tag{3.93}$$

where $c_1 ... c_3$ are coefficients,

$$B_{\mathrm{ww}} = \sum_{k=1}^{11} b_k \, T^{(1-k)} \tag{3.94}$$

where $b_1 ... b_{11}$ are coefficients,

$$C_{\mathrm{www}} = -10^{-6} \exp\left\{ \sum_{k=1}^{7} c_k \, T^{(k-1)} \right\} \tag{3.95}$$

where $c_1 ... c_7$ are coefficients,

$$B_{\mathrm{aw}} = b_1 + b_2 \, T^{-1} + b_3 \, T^{-2} + b_4 \, T^{-4} \tag{3.96}$$

where $b_1 ... b_4$ are coefficients,

$$C_{\mathrm{aaw}} = \sum_{k=1}^{5} c_k \, T^{(1-k)} \tag{3.97}$$

where $c_1 ... c_5$ are coefficients,

$$C_{\mathrm{aww}} = -10^{-6} \exp\left\{ \sum_{k=1}^{4} c_k \, T^{(1-k)} \right\} \tag{3.98}$$

where $c_1 ... c_4$ are coefficients.

The temperature-dependent virial coefficients proposed by Nelson and Sauer are as follows:

$$B_{\mathrm{aa}} = \sum_{k=1}^{7} b_k \, T^{(1-k)} \tag{3.99}$$

where $b_1 ... b_7$ are coefficients,

$$C_{\mathrm{aaa}} = \sum_{k=1}^{7} c_k \, T^{(1-k)} \tag{3.100}$$

where $c_1 ... c_7$ are coefficients,

$$B_{\mathrm{ww}} = \sum_{k=1}^{11} b_k \, T^{(1-k)} \tag{3.101}$$

where $b_1 ... b_{11}$ are coefficients,

$$C_{\mathrm{www}} = -10^{-6} \exp\left\{ \sum_{k=1}^{7} c_k \, T^{(k-1)} \right\} \tag{3.102}$$

where $c_1 ... c_7$ are coefficients,

$$B_{\mathrm{aw}} = b_1 + b_2 \, T^{-1} + b_3 \, T^{-2} + b_4 \, T^{-4} \tag{3.103}$$

where $b_1 ... b_4$ are coefficients,

$$C_{\mathrm{aaw}} = \sum_{k=1}^{5} c_k \, T^{(1-k)} \tag{3.104}$$

where $c_1 ... c_5$ are coefficients,

$$C_{\mathrm{aww}} = -10^{-6} \exp\left\{ \sum_{k=1}^{4} c_k \, T^{(1-k)} \right\} \tag{3.105}$$

where $c_1 ... c_4$ are coefficients.

The coefficients b_k and c_k used in the Eqs. (3.92) to (3.98) are taken from Hyland and Wexler [37] and the coefficients b_k and c_k used in the Eqs. (3.99) to (3.105) are taken from Nelson and Sauer [38], [39]. The universal gas constant R in Eq. (3.89) has the value $R = 8.31441\,\mathrm{kJ\,kmol^{-1}\,K^{-1}}$ proposed by Hyland and Wexler whereas Nelson and Sauer used a value of $R = 8.3144\,\mathrm{kJ\,kmol^{-1}\,K^{-1}}$.

Molar volume

The molar volume $v(p,T,\psi_{\mathrm{w}})$ is calculated iteratively from

$$p(v,T,\psi_{\mathrm{w}}) = \frac{RT}{v}\left(1 + \frac{B(T,\psi_{\mathrm{w}})}{v} + \frac{C(T,\psi_{\mathrm{w}})}{v^2}\right). \tag{3.106}$$

Mass density

$$\tilde{\rho} = \frac{M}{v} \tag{3.107}$$

where v is calculated iteratively from Eq.(3.106) and $M = \psi_{\mathrm{a}} M_{\mathrm{a}} + \psi_{\mathrm{w}} M_{\mathrm{w}}$.

Molar enthalpy

$$h(p,T,\psi_{\mathrm{w}}) = \psi_{\mathrm{a}} \, h_{\mathrm{a}}^{\mathrm{o}}(T) + \psi_{\mathrm{w}} \, h_{\mathrm{w}}^{\mathrm{o}}(T) + RT\left[\left(B - T\frac{\mathrm{d}B}{\mathrm{d}T}\right)\frac{1}{v} + \left(C - \frac{T}{2}\frac{\mathrm{d}C}{\mathrm{d}T}\right)\frac{1}{v^2}\right] \tag{3.108}$$

where

$$h_{\mathrm{a}}^{\mathrm{o}}(T) = a_1 + a_2\,(T - T_{0,\mathrm{a}}) + \frac{a_3}{2}(T^2 - T_{0,\mathrm{a}}^2) + \frac{a_4}{3}(T^3 - T_{0,\mathrm{a}}^3) + \frac{a_5}{4}(T^4 - T_{0,\mathrm{a}}^4) + \frac{a_6}{5}(T^5 - T_{0,\mathrm{a}}^5)$$

with $a_1 ... a_6$ are coefficients, $T_{0,\mathrm{a}} = 273.15\,\mathrm{K}$, and

$h_{\mathrm{w}}^{\mathrm{o}}(T) = RT\,\tau\,\gamma_{\tau}^{\mathrm{o}}(\tau)$ from IAPWS-IF97 [20], [21].

Molar entropy

$$s(p,T,\psi_{\mathrm{w}}) = \psi_{\mathrm{a}} \, s_{\mathrm{T,a}}^{\mathrm{o}}(T) + \psi_{\mathrm{w}} \, s_{\mathrm{w}}^{\mathrm{o}}(p,T) + R\left\{\begin{array}{l} -\ln\dfrac{p}{p_0} + \psi_{\mathrm{a}} \ln\dfrac{pv}{\psi_{\mathrm{a}} RT} + \psi_{\mathrm{w}} \ln\dfrac{pv}{\psi_{\mathrm{w}} RT} \\ -\left[\left(B + T\dfrac{\mathrm{d}B}{\mathrm{d}T}\right)\dfrac{1}{v} + \left(C + T\dfrac{\mathrm{d}C}{\mathrm{d}T}\right)\dfrac{1}{2v^2}\right] \end{array}\right\} \tag{3.109}$$

where

p_0 is the standard pressure with $p_0 = 0.101325\,\text{MPa}$,

$$s^{\text{o}}_{\text{T,a}}(T) = a_1 + a_2 \ln\left(\frac{T}{T_{0,\text{a}}}\right) + a_3 (T - T_{0,\text{a}}) + \frac{a_4}{2}(T^2 - T^2_{0,\text{a}}) + \frac{a_5}{3}(T^3 - T^3_{0,\text{a}}) + \frac{a_6}{4}(T^4 - T^4_{0,\text{a}})$$

with $a_1 ... a_6$ are coefficients, $T_{0,\text{a}} = 273.15\,\text{K}$, and

$s^{\text{o}}_{\text{W}}(p,T) = R\left[\tau\,\gamma^{\text{o}}_{\tau}(\tau) - \gamma^{\text{o}}(\pi,\tau)\right]$ from IAPWS-IF97 [20], [21].

Speed of sound

$$w(p,T,\psi_{\text{W}}) = \sqrt{-\frac{v^2}{M}\frac{c_p}{c_v}\left(\frac{\partial p}{\partial v}\right)_{T,\psi_{\text{W}}}}\,. \tag{3.110}$$

Isentropic exponent

$$\kappa(p,T,\psi_{\text{W}}) = \frac{w^2\,\tilde{\rho}}{p}\,. \tag{3.111}$$

Property libraries

The property libraries LibHyW83 and LibNEL02 [36] allow calculating properties of unsaturated and saturated humid air from the models by Hyland and Wexler [22], [37] as well as by Nelson and Sauer [38], [39], respectively.

3.2.3.3 Modified Redlich-Kwong Equation Proposed by Yan and Co-Workers

In the model developed by KTH, interaction parameters for different molecules a_{ij} $(i \neq j)$ used in the modified Redlich-Kwong equation of state were adjusted, the calculation method for the fugacity coefficients of water vapour at saturated pressure ($\phi^{\text{v}}_{\text{W}}$) was studied and Henry's constant of oxygen in water was correlated. More information can be found in the published papers by KTH [17], [40], and [41].

Modified Redlich-Kwong equation of state

$$p = \frac{RT}{v-b} - \frac{a}{\sqrt{T}\,v(v+b)} \tag{3.112}$$

where

$$a = \sum_i \sum_j \psi_i\,\psi_j\,a_{ij}$$

with $a_{ij} = a_{ji} = k_{ij}\left(a^0_{ii}\,a^0_{jj}\right)^{0.5}$ and $a_{ii} = a^0_{ii} + a^1_{ii}(T)$,

$$a_{\mathrm{ww}} = \begin{cases} 3448.07 - 16.0662\,T + 0.0205\,T^2, & (T < 323.15\,\mathrm{K}) \\ 5019.04 - 33.2805\,T + 0.0868942\,T^2 & \\ -1.01488\cdot 10^{-4}\,T^3 + 4.42162\cdot 10^{-8}\,T^4, & (323.15\,\mathrm{K} \le T \le 647\,\mathrm{K}) \\ 3.22518 + 0.347932\,T - 0.000369888\,T^2 & \\ +1.16667\cdot 10^{-7}\,T^3 & (T > 647\,\mathrm{K}) \end{cases} \tag{3.113}$$

$$b = \sum_i \psi_i\, b_i \;\text{ with }\; b_i = 0.0867\,\frac{R\,T_{\mathrm{c},i}}{p_{\mathrm{c},i}}\,.$$

Enthalpy

$$h = \sum_i \psi_i\, h_i^{\mathrm{o}}(T) + \frac{R\,T\,b}{v-b} - \frac{a}{(v+b)\sqrt{T}} - \frac{1}{b}\left[\frac{a}{\sqrt{T}} - T\,\frac{\mathrm{d}}{\mathrm{d}T}\left(\frac{a}{\sqrt{T}}\right)\right]\ln\left(\frac{v+b}{v}\right) \tag{3.114}$$

Entropy

$$s = \sum_i \psi_i\, s_i^{\mathrm{o}}(T, p_0) - R\ln\left(\frac{p}{p_0}\right) + R\ln\left(\frac{v-b}{v}\right) + \frac{1}{b}\,\frac{\mathrm{d}}{\mathrm{d}T}\left(\frac{a}{\sqrt{T}}\right)\ln\left(\frac{v+b}{v}\right) + R\ln\left(\frac{p\,v}{R\,T}\right) \tag{3.115}$$

where

$$\frac{\mathrm{d}}{\mathrm{d}T}\left(\frac{a}{\sqrt{T}}\right) = -\frac{a}{2\,T^{1.5}} + \frac{\psi_{\mathrm{w}}^2}{\sqrt{T}}\,\frac{\mathrm{d}a_{\mathrm{ww}}}{\mathrm{d}T},$$

$$h_i^{\mathrm{o}}(T) = C_{h1} + C_{h2}\,T + C_{h3}\,T^2,\ \text{and} \tag{3.116}$$

$$s_i^{\mathrm{o}}(T, p_0) = C_{s1} + C_{s2}\,T + C_{s3}\,T^2 + C_{s4}\,T^3 + C_{s5}\,T^4.$$

3.2.3.4 Multi-Component Model Proposed by Kunz *et al.*

The multi-component model of Kunz *et al.* [42] consists of a Helmholtz free energy equation, from which all the thermodynamic properties can be obtained using the Helmholtz free energy and its derivatives with respect to temperature and density. The equation is expressed as the sum of the ideal-gas contribution, the residual contribution, and the departure function and reads in its dimensionless form:

$$\frac{a(\rho,T,\Psi)}{R\,T} = \alpha(\delta,\tau,\Psi) = \alpha^{\mathrm{o}}(\rho,T,\Psi) + \sum_{i=1}^{N}\psi_i\,\alpha_{0,i}^{\mathrm{r}}(\delta,\tau) + \sum_{i=1}^{N-1}\sum_{j=i+1}^{N}\Delta\alpha_{ij}^{\mathrm{r}}(\delta,\tau,\Psi) \tag{3.117}$$

where

$\alpha^{\mathrm{o}}(\rho,T,\Psi)$ is the ideal-gas mixing contribution,

$\sum_{i=1}^{N}\psi_i\,\alpha_{0,i}^{\mathrm{r}}(\delta,\tau)$ represents the fundamental equations of i pure components,

$\sum_{i=1}^{N-1}\sum_{j=i+1}^{N}\Delta\alpha_{ij}^{\mathrm{r}}(\delta,\tau,\Psi)$ corresponds to the departure functions of the binary mixtures consisting of the pure components *i* and *j*.

The variables δ and τ are reduced density and reduced reciprocal temperature as described in [42]. This new fundamental equation can be used for calculating the thermodynamic properties of multi-component mixtures in particular of natural gas. The numerical details of the equation have not been published until the end of this work. Therefore, it could not be used for comparisons.

3.3 Saturated State of Humid Air

3.3.1 Saturation Pressures of Dry Air and Water

The saturation pressure of dry air can be calculated from the fundamental equation of Lemmon *et al.* [1], Eq. (3.1), by solving the Maxwell criterion. But, the critical temperature of dry air is 132.5306 K. That means the two-phase region of dry air will not be reached in heat cycles. Therefore, it is not necessary to calculate the saturation pressure of dry air in this work.

For calculating the saturation pressure of water for a given temperature, the international standard for scientific and general use IAPWS-95 [18], [19] can be used. The saturation pressure is derived from the fundamental equation, Eq. (3.8), by solving the Maxwell criterion. If the computational expenditure for solving the Maxwell criterion is too high, the international equation for the saturation pressure [43], [44] can be used. It has the dimensionless form

$$\beta_{\mathrm{s}} = \exp\left\{\frac{T_{\mathrm{c}}}{T}\left(n_1\,\vartheta + n_2\,\vartheta^{1.5} + n_3\,\vartheta^{3} + n_4\,\vartheta^{3.5} + n_5\,\vartheta^{4} + n_6\,\vartheta^{7.5}\right)\right\} \tag{3.118}$$

where $\beta_{\mathrm{s}} = \dfrac{p}{p_{\mathrm{c}}}$, $\vartheta = 1 - \dfrac{T}{T_{\mathrm{c}}}$, and $n_1 ... n_6$ are coefficients.

For the calculation of the saturation temperature from a given pressure, Eq. (3.118) has to be solved iteratively.

In addition, the industrial formulation IAPWS-IF97 [20], [21] can be used for practical calculations. The equation for describing the saturation line is an implicit quadratic equation which can be solved directly with regard to both, saturation pressure p_{s} and saturation temperature T_{s}. This equation reads in its dimensionless form

$$\beta_{\mathrm{s}}^2\,\vartheta_{\mathrm{s}}^2 + n_1\,\beta_{\mathrm{s}}^2\,\vartheta_{\mathrm{s}} + n_2\,\beta_{\mathrm{s}}^2 + n_3\,\beta_{\mathrm{s}}\,\vartheta_{\mathrm{s}}^2 + n_4\,\beta_{\mathrm{s}}\,\vartheta_{\mathrm{s}} + n_5\,\beta_{\mathrm{s}} + n_6\,\vartheta_{\mathrm{s}}^2 + n_7\,\vartheta_{\mathrm{s}} + n_8 = 0 \tag{3.119}$$

where $\beta_{\mathrm{s}} = \left(\dfrac{p_{\mathrm{s}}}{p_{\mathrm{r}}}\right)^{0.25}$ and $\vartheta_{\mathrm{s}} = \dfrac{T_{\mathrm{s}}}{T_{\mathrm{r}}} + \dfrac{n_9}{\dfrac{T_{\mathrm{s}}}{T_{\mathrm{r}}} - n_{10}}$,

with p_{r} and T_{r} as reducing constants and $n_1 ... n_{10}$ as coefficients.

Then the solution of Eq. (3.119) with regard to the saturation pressure is:

$$p_\mathrm{s} = p_\mathrm{r}\left[\frac{2C}{-B+\left(B^2-4AC\right)^{0.5}}\right]^4 \tag{3.120}$$

where

$A = \vartheta_\mathrm{s}^2 + n_1\,\vartheta_\mathrm{s} + n_2$,

$B = n_3\,\vartheta_\mathrm{s}^2 + n_4\,\vartheta_\mathrm{s} + n_5$, and

$C = n_6\,\vartheta_\mathrm{s}^2 + n_7\,\vartheta_\mathrm{s} + n_8$.

The solution of Eq. (3.119) for the saturation temperature reads:

$$T_\mathrm{s} = \frac{T_r}{2}\left\{n_{10} + D - \left[\left(n_{10}+D\right)^2 - 4\left(n_9 + n_{10}\,D\right)\right]^{0.5}\right\} \tag{3.121}$$

where

$$D = \frac{2G}{-F-(F^2-4EG)^{0.5}},$$

$E = \beta_\mathrm{s}^2 + n_3\,\beta_\mathrm{s} + n_6$,

$F = n_1\,\beta_\mathrm{s}^2 + n_4\,\beta_\mathrm{s} + n_7$, and

$G = n_2\,\beta_\mathrm{s}^2 + n_5\,\beta_\mathrm{s} + n_8$.

3.3.2 Poynting Effect for the Ideal-Mixing Model

The poynting effect describes the increase of the saturation partial pressure of water at a certain temperature in a gas atmosphere if the total pressure is increased. Hyland and Wexler [22], [37] as well as Nelson and Sauer [38], [39] used the name "enhancement factor" in lieu of "poynting effect". For calculating the poynting effect in the case of the ideal-mixing model, it is assumed that the liquid phase consists of pure water. That means, the phase equilibrium corresponds to that between saturated water vapour (steam) and saturated liquid water:

$$\mu''_\mathrm{W}(p_\mathrm{s,W}, T) = \mu'_\mathrm{W}(p_\mathrm{s,W}, T) \tag{3.122}$$

where

T is the given temperature and

$p_\mathrm{s,W}$ is the saturation pressure of water at temperature T.

For a change of the equilibrium, the following condition must be valid:

$$\mathrm{d}\mu''_\mathrm{W} = \mathrm{d}\mu'_\mathrm{W}. \tag{3.123}$$

Than follows for constant temperature

$$v''_{\mathrm{w}}\,\mathrm{d}p_{\mathrm{s,w}} = v'_{\mathrm{w}}\,\mathrm{d}p_{\mathrm{s,w}}\,. \tag{3.124}$$

The gas phase of water can be described as an ideal gas

$$v'' = \frac{R_{\mathrm{w}}\,T}{p_{\mathrm{s,w}}} \tag{3.125}$$

and the liquid phase as an incompressible liquid

$$v'_{\mathrm{w}} = v'_{\mathrm{w}}(T)\,. \tag{3.126}$$

The insertion of Eqs. (3.125) and (3.126) into Eq. (3.124) leads to the expression

$$\frac{\mathrm{d}p_{\mathrm{s,w}}}{p_{\mathrm{s,w}}} = \frac{v'_{\mathrm{w}}(T)}{R_{\mathrm{w}}\,T}\,\mathrm{d}p_{\mathrm{s,w}}\,. \tag{3.127}$$

The integration is assumed under assumption that the steam in saturated humid air has the partial pressure p_{s} and the liquid exists under mixture pressure p:

$$\int_{p_{\mathrm{s,w}}}^{p_{\mathrm{s}}} \frac{\mathrm{d}p_{\mathrm{s,w}}}{p_{\mathrm{s,w}}} = \int_{p_{\mathrm{s,w}}}^{p} \frac{v'_{\mathrm{w}}(T)}{R_{\mathrm{w}}\,T}\mathrm{d}p\,. \tag{3.128}$$

The integration leads to the equation

$$\ln\left(\frac{p_{\mathrm{s}}}{p_{\mathrm{s,w}}}\right) = \frac{v'_{\mathrm{w}}(T)}{R_{\mathrm{w}}\,T}(p - p_{\mathrm{s,w}})\,. \tag{3.129}$$

As result the saturation pressure of humid air is obtained:

$$p_{\mathrm{s}} = p_{\mathrm{s,w}}\exp\left\{\frac{v'_{\mathrm{w}}(T)}{R_{\mathrm{w}}\,T}(p - p_{\mathrm{s,w}})\right\} \tag{3.130}$$

where $p_{\mathrm{s,w}}$ is the saturation pressure of pure water calculated from IAPWS-95 [18], [19] or IAPWS-IF97 [20], [21].

The water in the vapour phase and in the liquid phase is treated as a real fluid, so that Eq. (3.123) leads to

$$\mu''(p_{\mathrm{s}},T) - \mu''(p_{\mathrm{s,w}},T) = \mu'(p,T) - \mu'(p_{\mathrm{s,w}},T) \tag{3.131}$$

where

$\mu''(p,T) = g_2(p,T)$ from IAPWS-IF97 [20], [21],

$\mu'(p,T) = g_1(p,T)$ from IAPWS-IF97 [20], [21],

and $p_{\mathrm{s,w}}$ is the saturation pressure of pure water.

Eq. (3.131) allows calculating p_{s} iteratively for a given temperature T and a given pressure p what is implemented in the developed property library LibHuGas [31].

The mole fraction of water $\psi_{s,w}$ in saturated humid air is then obtained by

$$\psi_{s,w} = \frac{p_s(p,T)}{p}, \tag{3.132}$$

and the poynting effect (enhancement factor) of the saturation pressure of water follows from

$$f = \frac{p_s(p,T)}{p_{s,w}(T)}. \tag{3.133}$$

3.3.3 Poynting Model Proposed by Rabinovich and Beketov

The model of Rabinovich and Beketov [35] calculates the poynting effect by using the enhancement factor *f*. At the saturated state, the enhancement factor is determined iteratively at particular values of *p* and *T* from a solubility equation and reads:

$$\ln(f) = \ln\left(\frac{Z(p,T,\psi_{s,w})}{Z_w(T,p_{s,w})}\right) + J(p,T) + 2\frac{B_{ww}}{v''_w} - \frac{2\left(B_{aw} + \left(B_{ww} - B_{aw}\right)\psi_{s,w}\right)}{v} - \frac{3C_{aaw}\left(1-\psi_{s,w}\right)^2}{2v^2} \tag{3.134}$$

where

f is a function of $\psi_{s,w}(p,T)$,

$v = v(p,T,\psi_{s,w})$ is the molar volume of humid air at particular values of *p*, *T*, and $\psi_{s,w}(p,T)$, and has to be derived iteratively from Eq. (3.71),

$v''_w = v_w(T,p_{s,w})$ is the molar volume of pure saturated water vapour,

$$J(p,T) = \frac{1}{RT}\int_{p_{s,w}}^{p} v_{w,con}(p,T)\,\mathrm{d}p \tag{3.135}$$

where

$v_{w,con}$ is the molar volume of condensed water calculated from the following expression

$$v_{w,con} = b_1 + b_2\,\theta + b_3\,\theta^2 + b_4\,\theta^3 + b_5\,\theta^4 + \left(b_6 + b_7\,\theta + b_8\,\theta^2\right)p,$$

with $\theta = \frac{T}{T_{t,w}}$, $b_1 ... b_8$ are coefficients, and $T_{t,w}$ is the triple point temperature of water.

B_{aw}, B_{ww}, and C_{aww} are temperature-dependent virial coefficients described in Section 3.2.3.1.

$Z(p,T,\psi_{s,w})$ describes the equation of state and is written in Section 3.2.3.1, too.

$$Z_{\mathrm{w}} = 1 + \frac{B_{\mathrm{ww}}}{v_{\mathrm{w}}} \tag{3.136}$$

where

Z_{w} is described by an equation of state of water vapour,

B_{ww} is a temperature-dependent virial coefficient of water, and

v_{w} is the molar volume of water vapour.

The value for $\psi_{\mathrm{s,w}}(p,T)$ in Eq. (3.134) has to be calculated in each step of the iteration according to

$$\psi_{\mathrm{s,w}} = \frac{f\, p_{\mathrm{s,w}}}{p}\,. \tag{3.137}$$

The initial value for f in (3.137) is 1.0. If the criterion $\left|\psi_{\mathrm{s,w_{new}}} - \psi_{\mathrm{s,w_{old}}}\right| \le \varepsilon$ with $\varepsilon = 10^{-6}$ is fulfilled, the iteration is completed.

If all the virial coefficients (B_{aa}, B_{aw}, B_{ww}, C_{aaa}, and C_{aaw}) for humid air are known, then the saturation composition $\psi_{\mathrm{s,w}}$ and the molar volume of humid air v at the phase equilibrium for each pair of values of p and T can be calculated by solving simultaneously Eqs. (3.71) and (3.134).

The iterative calculation is implemented in the property library LibRB95 [36].

After iterating the enhancement factor f, the mole fraction of water vapour $\psi_{\mathrm{s,w}}$ results from Eq. (3.137).

The saturation pressure p_{s} of humid air can be obtained from

$$p_{\mathrm{s}} = f\, p_{\mathrm{s,w}} = \psi_{\mathrm{s,w}}\, p\,. \tag{3.138}$$

3.3.4 Poynting Model Proposed by Hyland and Wexler in Combination with the Modification Proposed by Nelson and Sauer

The mole fraction of water in saturated humid air is:

$$\psi_{\mathrm{s,w}} = \frac{f\, p_{\mathrm{s,w}}}{p} \tag{3.139}$$

where $p_{\mathrm{s,w}}$ is the saturation pressure of pure water and p is the total pressure. The enhancement factor f considering the non-ideal behaviour of the mixture in the saturated state is given as a function of p and T. It can be derived iteratively from the isothermal compressibility of liquid water, from Henry's constant, and from the virial coefficients of air, of water, and of the mixture air-water using the relationship:

$$\ln(f) = \left[\frac{\left(1+\kappa_T\, p_{\mathrm{s,w}}\right)\left(p-p_{\mathrm{s,w}}\right)-\kappa_T\,\frac{\left(p^2-p_{\mathrm{s,w}}^2\right)}{2}}{RT}\right] v_{\mathrm{w,liq}} + \ln\left(1-\beta_{\mathrm{H}}\,\psi_{\mathrm{s,a}}\,p\right) +$$
$$\left[\frac{\psi_{\mathrm{s,a}}^2\,p}{RT}\right] B_{\mathrm{aa}} - \left[\frac{2\psi_{\mathrm{s,a}}^2\,p}{RT}\right] B_{\mathrm{aw}} - \left[\frac{p-p_{\mathrm{s,w}}-\psi_{\mathrm{s,a}}^2\,p}{RT}\right] B_{\mathrm{ww}} +$$
$$\left[\frac{\psi_{\mathrm{s,a}}^3\,p^2}{(RT)^2}\right] C_{\mathrm{aaa}} + \left[\frac{3\psi_{\mathrm{s,a}}^2\left(1-2\psi_{\mathrm{s,a}}\right)p^2}{2(RT)^2}\right] C_{\mathrm{aaw}} -$$
$$\left[\frac{3\psi_{\mathrm{s,a}}^2\left(1-\psi_{\mathrm{s,a}}\right)p^2}{(RT)^2}\right] C_{\mathrm{aww}} - \left[\frac{\left(1+2\psi_{\mathrm{s,a}}\right)\left(1-\psi_{\mathrm{s,a}}\right)^2\,p^2-p_{\mathrm{s,w}}^2}{2(RT)^2}\right] C_{\mathrm{www}} -$$
$$\left[\frac{\psi_{\mathrm{s,a}}^2\left(1-3\psi_{\mathrm{s,a}}\right)\left(1-\psi_{\mathrm{s,a}}\right)p^2}{(RT)^2}\right] B_{\mathrm{aa}}\,B_{\mathrm{ww}} - \left[\frac{2\psi_{\mathrm{s,a}}^3\left(2-3\psi_{\mathrm{s,a}}\right)p^2}{(RT)^2}\right] B_{\mathrm{aa}}\,B_{\mathrm{aw}} +$$
$$\left[\frac{6\psi_{\mathrm{s,a}}^2\left(1-\psi_{\mathrm{s,a}}\right)^2\,p^2}{(RT)^2}\right] B_{\mathrm{ww}}\,B_{\mathrm{aw}} - \left[\frac{3\psi_{\mathrm{s,a}}^4\,p^2}{2(RT)^2}\right] B_{\mathrm{aa}}^2 -$$
$$\left[\frac{2\psi_{\mathrm{s,a}}^2\left(1-\psi_{\mathrm{s,a}}\right)\left(1-3\psi_{\mathrm{s,a}}\right)p^2}{(RT)^2}\right] B_{\mathrm{aw}}^2 - \left[\frac{p_{\mathrm{s,w}}^2-\left(1+3\psi_{\mathrm{s,a}}\right)\left(1-\psi_{\mathrm{s,a}}\right)^3\,p^2}{2(RT)^2}\right] B_{\mathrm{ww}}^2 \tag{3.140}$$

where

κ_T is the isothermal compressibility of liquid water.

Hyland and Wexler [22], [37] defined κ_T to be:

$$\kappa_T = 10^{-11}\left[\frac{\sum_{k=1}^{5} J_k\,t^k}{1+J_6\,t}\right] \tag{3.141}$$

where $J_1 \ldots J_6$ are coefficients. Hyland and Wexler [22], [37] give different coefficients for temperature ranges of $0 < t \le 100°\mathrm{C}$ and of $100 < t \le 200°\mathrm{C}$.

Nelson and Sauer [38], [39] defined κ_T to be:

$$\kappa_T = 10^{-3}\left[\frac{J_1+J_2\,t}{1+J_3\,t+J_4\,t^2}\right]^2 \tag{3.142}$$

$J_1 \ldots J_4$ are a set of coefficients which are given for the following three pressure and temperature ranges:

$p \le 1\,\mathrm{MPa}$ and $t \le 179.9°\mathrm{C}$,

$p \le 2$ MPa and $t \le 212.4$°C, and

$p \le 5$ MPa and $t \le 263.9$°C.

$p_{s,w}$ is the saturation pressure calculated from IAPWS-IF97 [20], [21].

R is the molar gas constant with $R = 8.3144\ \mathrm{kJ\,kmol^{-1}\,K^{-1}}$.

$v_{w,liq}$ is the molar volume of saturated liquid water in $\mathrm{cm^3\,mol^{-1}}$.

β_H is the Henry's law constant and is calculated from the following equation:

$$\beta_H = \frac{1}{\beta_a\, 1.01325 \times 10^9} \tag{3.143}$$

where β_a is calculated from the following expression

$$\frac{1}{\beta_a} = \frac{\psi_{O_2}}{\beta_{O_2}} \frac{\psi_{N_2}}{\beta_{N_2}} \tag{3.144}$$

with

$\psi_{O_2} = 0.22$ and $\psi_{N_2} = 0.78$ are the mole fractions of oxygen and nitrogen in dry air,

$$\beta_{O_2} = \exp\left(\sum_{k=1}^{6} J_k\, X^{(k-1)} \right) \tag{3.145}$$

where J_1 … J_6 are coefficients,

$$\beta_{N_2} = \sum_{k=1}^{6} J_k\, X^{(k-1)} + \sum_{m=1}^{4} I_m\, X^{(-m)} \tag{3.146}$$

where J_1 … J_6 are coefficients, I_1 … I_4 are coefficients, and

$X = 1000\ \mathrm{K}\, T^{-1}$.

B and C are the temperature-dependent virial coefficients described in Section 3.2.3.2.

The value for $\psi_{s,a}(p,T)$ in Eq. (3.140) has to be calculated in each step of the iteration according to:

$$\psi_{s,a} = \frac{p - f\, p_{s,w}}{p}. \tag{3.147}$$

The initial value for f in relation (3.147) chosen for the iteration is 1.0. If the criterion $\left|\psi_{s,a_{new}} - \psi_{s,a_{old}}\right| \le \varepsilon$ with $\varepsilon = 10^{-6}$ is fulfilled, the iteration is completed.

The iterative calculation is implemented in the property libraries LibHyW83 [36], LibNEL02 [36], and LibHuAir [33].

After iterating the enhancement factor f, the mole fraction of water vapour $\psi_{s,w}$ results from

$$\psi_{\mathrm{s,w}} = \frac{f\, p_{\mathrm{s,w}}}{p}\,. \tag{3.148}$$

The saturation pressure p_{s} of humid air is obtained using

$$p_{\mathrm{s}} = f\, p_{\mathrm{s,w}} = \psi_{\mathrm{s,w}}\, p\,. \tag{3.149}$$

3.3.5 Poynting Model Proposed by Yan and Co-Workers

The saturated composition is calculated from phase equilibrium and Henry's law is used to describe the liquid phase ([17], [40], [41]):

$$\begin{aligned} p\,\psi_{\mathrm{w}}\,\phi_{\mathrm{w}} &= f_{0,\mathrm{w}}\,\psi_{\mathrm{w}} \\ p\,\psi_i\,\phi_i &= \beta_{\mathrm{H}_i}\,\psi_i \qquad (i = \text{nitrogen, oxygen}) \end{aligned} \tag{3.150}$$

where ψ_i is the mole fraction in the liquid phase, ϕ_i is the fugacity coefficient of component i in the vapour phase and is calculated from the used equation of state, and β_{H_i} is the Henry's law constant of component i. The expression reads

$$\begin{aligned} \ln\phi_i = {} & \ln\left(\frac{v}{v-b}\right) + \frac{b_i}{v-b} - \frac{2\sum_j \psi_j\, a_{ij}}{RT^{1.5}\, b}\ln\left(\frac{v+b}{v}\right) \\ & + \frac{a\, b_i}{RT^{1.5}\, b^2}\left[\ln\left(\frac{v+b}{v}\right) - \frac{b}{v+b}\right] - \ln\left(\frac{p\,v}{RT}\right) \end{aligned} \tag{3.151}$$

$$f_{0,\mathrm{w}} = \phi''_{\mathrm{w}}(T, p_{\mathrm{s,w}})\, p_{\mathrm{s,w}}(T) \exp\left\{\frac{1}{RT}\int_{p_{\mathrm{s,w}}}^{p} v_{\mathrm{w},i}(T,p)\,\mathrm{d}p\right\} \tag{3.152}$$

$$\beta_{\mathrm{H_{N_2}}} = 55.51 \exp\left\{\frac{\Delta g^{\mathrm{o}}_{\mathrm{N_2,gas}}(T,p)_m - \Delta g^{\mathrm{o}}_{\mathrm{N_2,liq}}(T,p)_m}{RT}\right\} \tag{3.153}$$

$$\begin{aligned} \ln\beta_{\mathrm{H_{O_2}}} = {} & Q_1 + Q_2\, p + Q_3\, p^2 + \left(Q_4 + Q_5\, p + Q_6\, p^2\right)T \\ & + \left(Q_7 + Q_8\, p + Q_9\, p^2\right)T^2 + \left(Q_{10} + Q_{11}\, p + Q_{12}\, p^2\right)\ln(T) \end{aligned} \tag{3.154}$$

where Δg^{o} is the Gibbs free energy of formation on a molarity basis calculated with an equation of state of Helgeson and co-workers [45].

3.3.6 Phase Equilibrium Using the Multi-Fluid Model Proposed by Kunz *et al.*

The mole fraction and other properties of saturated humid air are calculated by solving the fundamental equation of state for the mixture, Eq. (3.117), according to the phase equilibrium conditions [42].

4 Comparisons on Thermodynamic Properties of Dry and Humid Air

The following comparisons have been performed for the models listed in Table 4.1. The multi-component model of Kunz *et al.* [42] could not be considered because its numerical details were not available during the period of work in the AA-CAES project.

Table 4.1: Models for calculating thermodynamic properties of humid air used for comparisons.

Abbreviation	Model	Author(s)	Software	Section
IdGas	Ideal mixture of ideal gases	VDI-Guideline 4670 [16], [23]	LibIdGas [25] and LibFLUFT [26] from FHZI	3.2.1
HuAir	Ideal mixture of the real fluids dry air and water	Hellriegel [34]	LibHuAir [33] from FHZI	3.2.2.2
HuGas	Ideal mixture of the real fluids N_2, O_2, Ar, and water	Kleemann, Seibt [32]	LibHuGas [31] from FHZI	3.2.2.1
KTH	Modified Redlich-Kwong equation of state for the mixture	Yan and co-workers [17], [40], [41]	from KTH	3.2.3.3
RB	Virial equation for the mixture	Rabinovich, Beketov [35]	LibRB95 [36] from FHZI	3.2.3.1
NEL	Virial equation for the mixture	Nelson, Sauer [38], [39]	LibNel02 [36] from FHZI	3.2.3.2
HyW	Virial equation for the mixture	Hyland, Wexler [22], [37]	LibHyW83 [36] from FHZI, HumidAirTab [46]	3.2.3.2
SKU	Ideal mixture of the real fluids dry air and water	Span, Kretzschmar, Ulbig, Herrmann (this work)	LibSKU from this work	-

The SKU model included in Table 4.1 is a result of our investigation on the different models and therefore it was not described in Chap. 3. The numerical details and the mixing rules of the SKU model are shown in Chap. 5.

4.1 Comparisons for Dry Air

4.1.1 Comparison between Calculated Values and Experimental Density Data

For density of dry air, three new data sets measured within the AA-CAES project were checked for consistency with the fundamental equation of Lemmon *et al.* [1]. The data sets are summarized in Table 4.2. The new experimental data points have already been illustrated in Figure 2.5 as a pressure-temperature diagram.
The plots of Figure 4.1 show the deviations of the density values of dry air calculated for the different models from the experimental data of PTB 04 as a function of pressure and temperature.

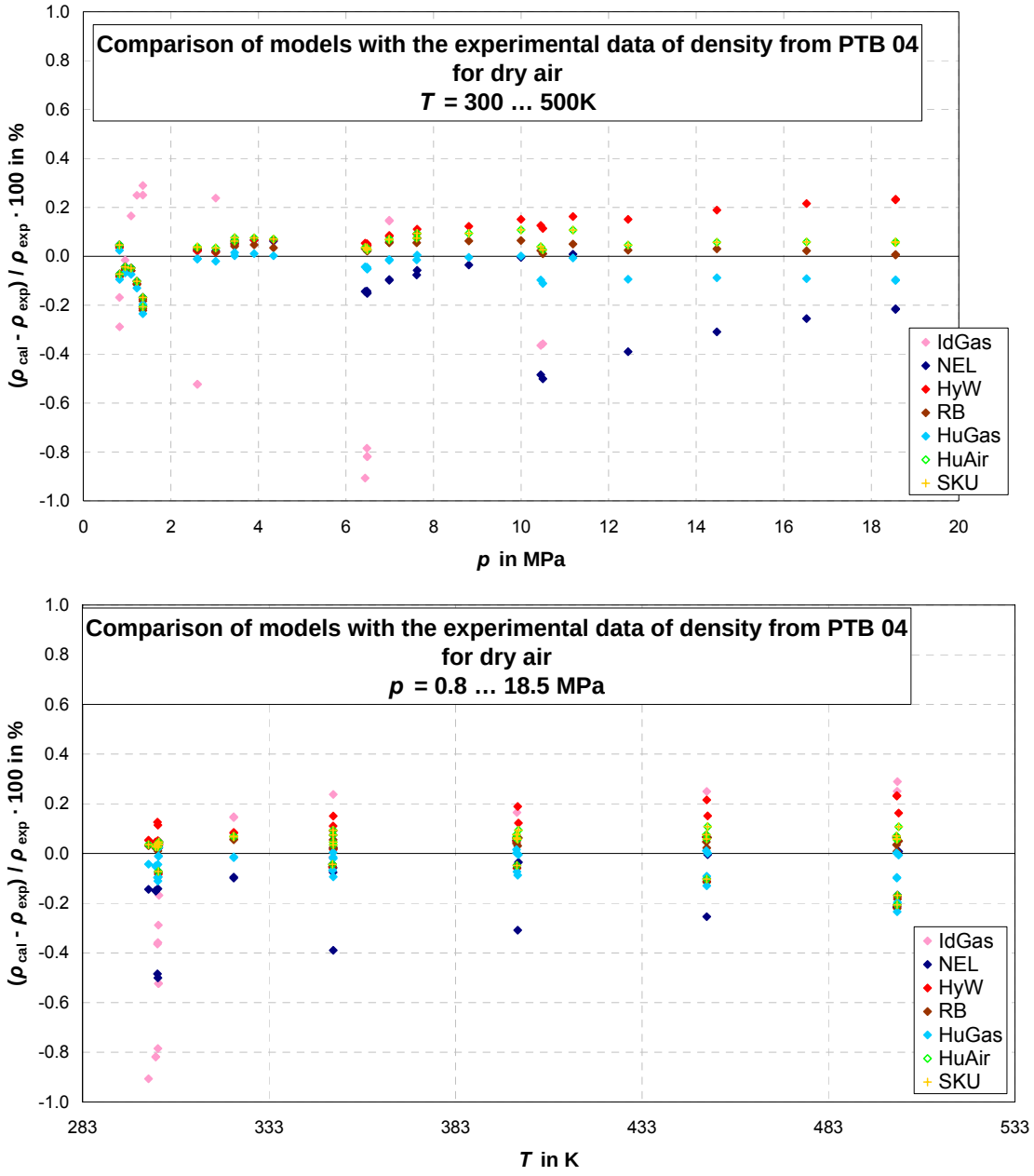

Figure 4.1: Percentage deviations of the density values of dry air calculated for models listed in Table 4.1 from the experimental data of PTB 04 [11] as a function of pressure and temperature.

Table 4.2: New experimental data for density and speed of sound of dry air generated within the AA-CAES project.

Abbreviation	Author(s)	T / K	p / MPa
PTB 04	Klingenberg, Ulbig 2007 (AA-CAES, 2004) [11]	300-500	0.8-18.6
ICSTM 04	Trusler 2004 (AA-CAES) [12]	295-546	0.9-15.8
RUB 05	Wöll 2005 (AA-CAES) [13]	298-500	0.1-17

The plots of Figure 4.2 illustrate the deviations of the density values of dry air calculated for different models from the experimental data of ICSTM 04 as a function of pressure and temperature.

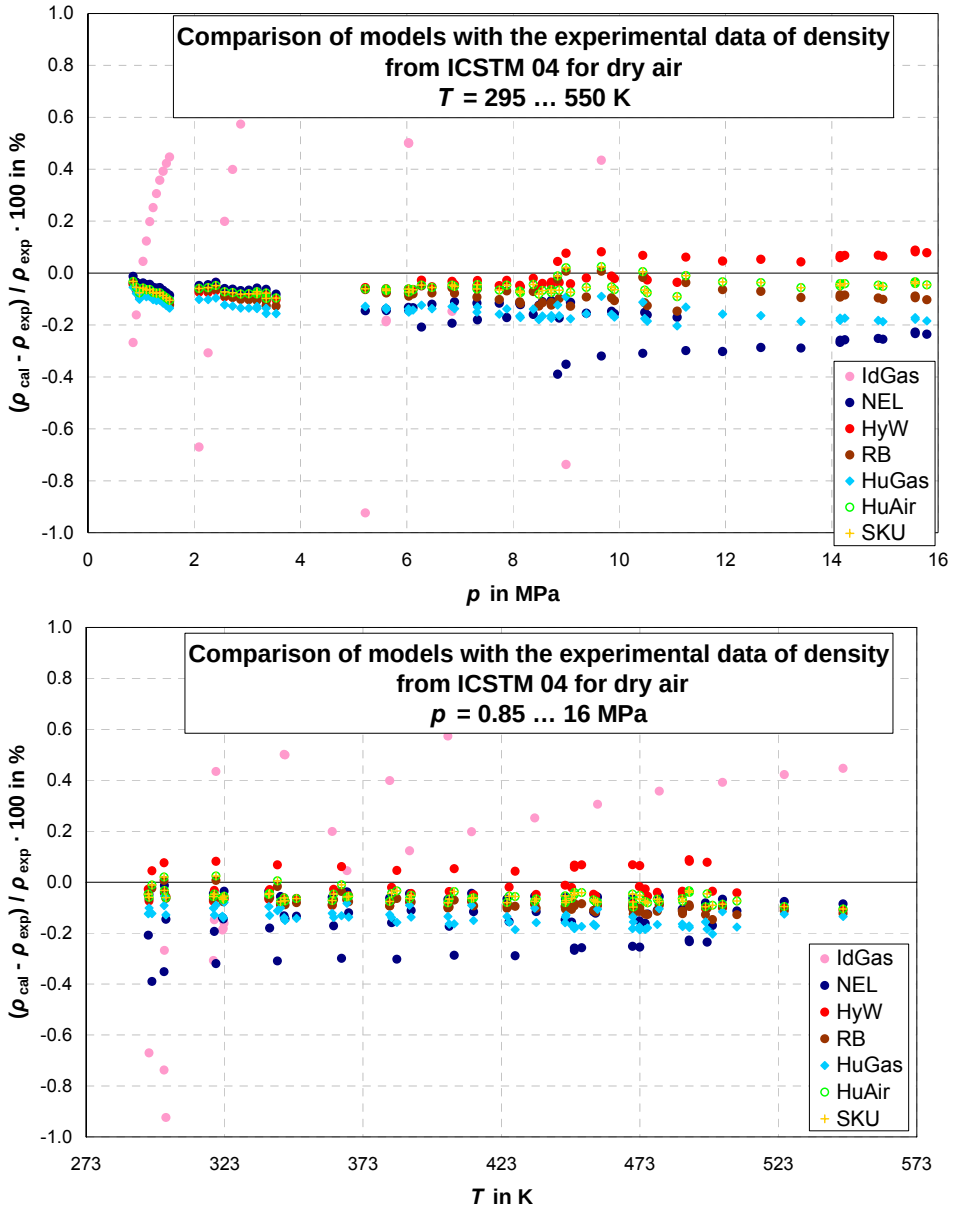

Figure 4.2: Percentage deviations of the density values of dry air calculated for the models listed in Table 4.1 from the experimental data of ICSTM 04 [12] as a function of pressure and temperature.

In Figure 4.3 the deviations of the density values of dry air calculated for the different models from the experimental data of RUB 05 are illustrated as a function of pressure and temperature.

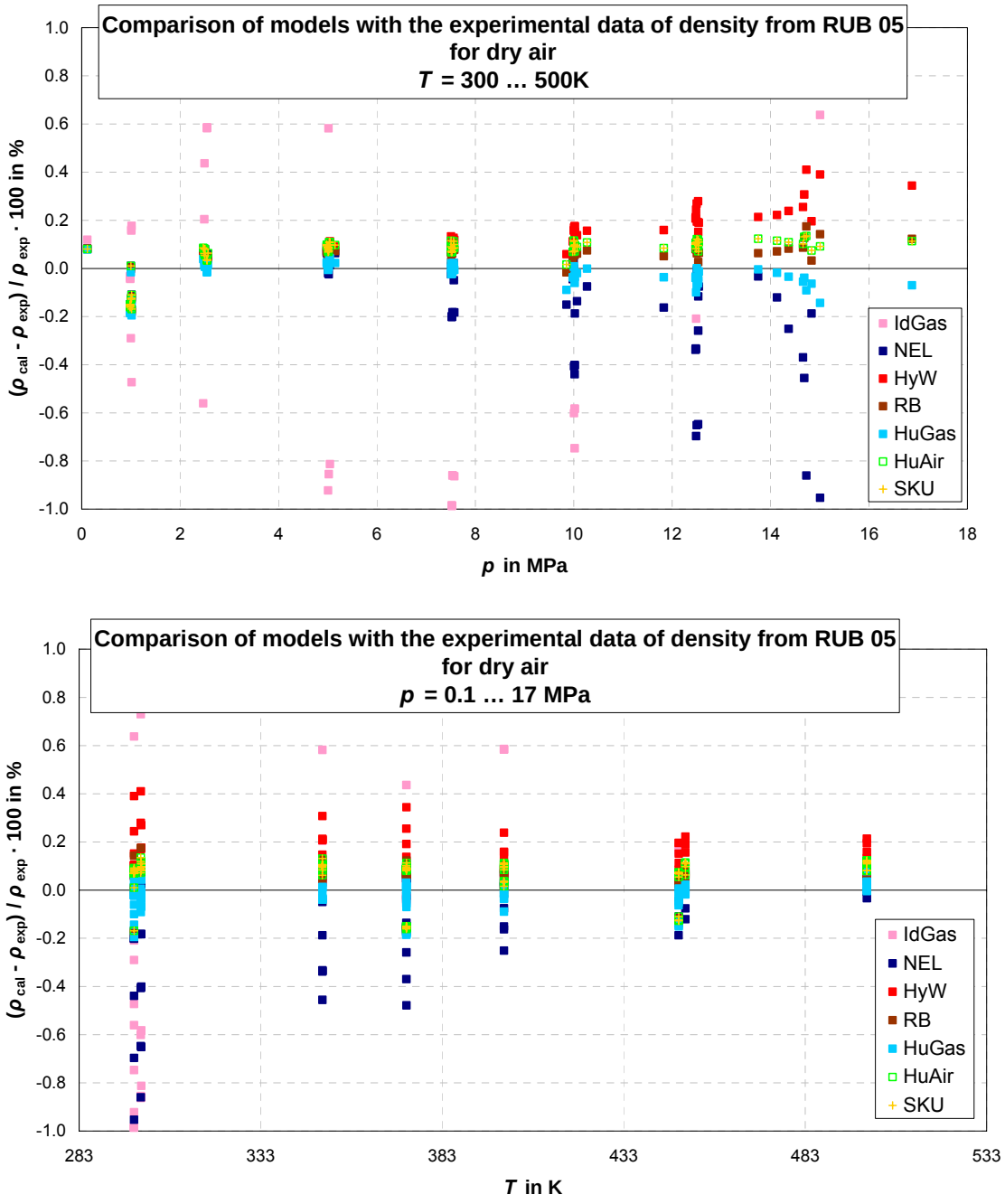

Figure 4.3: Percentage deviations of the density values of dry air calculated for the models listed in Table 4.1 from the experimental data of RUB 05 [13] as a function of pressure and temperature.

All models except the IdGas model show deviations from the experimental data for the density of dry air which are less than ± 1%. The NEL model calculates densities that are less than the experimental data and the uncertainty increases with increasing pressures. The values of density from HyW model are greater than the experimental data and the

other models in the entire pressure and temperature ranges. The HuAir, SKU, and RB models meet the experimental data within ± 0.2%. The SKU and HuAir models which base on the fundamental equation of Lemmon *et al.* [1] were found to be the most suitable models.

4.1.2 Comparison between Calculated Values and Experimental Speed of Sound Data

For dry air, experimental data for speed of sound were measured by Trusler at ICSTM in 2004 [12] (see Table 4.3).

Table 4.3: New experimental data for speed of sound of dry air generated within the AA-CAES project.

Abbreviation	Author	T / K	p / MPa
ICSTM 04	Trusler 2004 (AA-CAES) [12]	300-450	0.1-16.3

The new experimental data points for speed of sound of dry air have been plotted as a pressure-temperature diagram (see Figure 2.6).

The deviations of the calculated speed of sound values of dry air for the different models from the experimental data of ICSTM 04 are presented as a function of pressure for temperatures of 300 K, 350 K, 400 K, and 450 K in Figure 4.4.

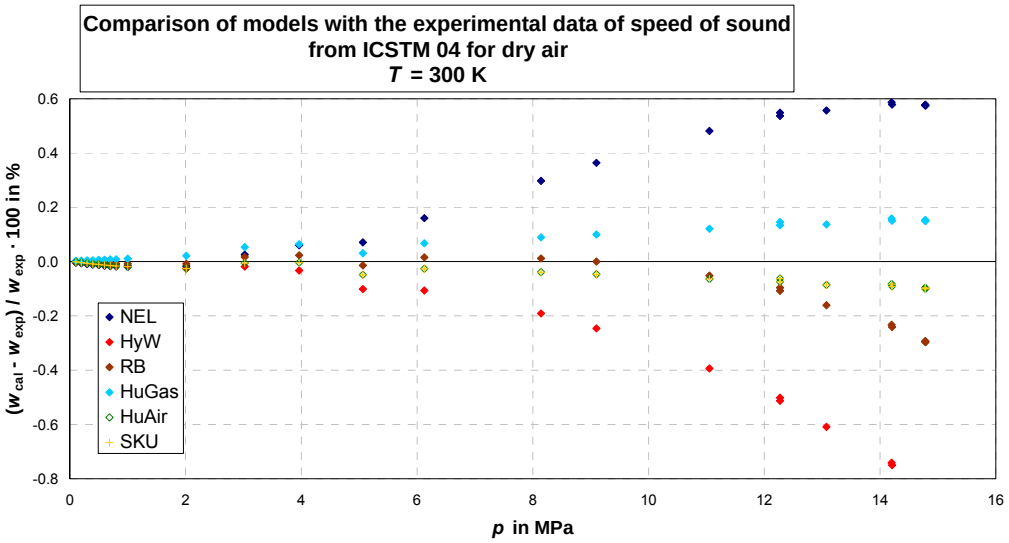

Figure 4.4: Percentage deviations of the speed of sound values of dry air calculated for the models listed in Table 4.1 from the experimental data of ICSTM 04 [12] as a function of pressure for temperatures of 300 K, 350 K, 400 K, and 450 K.

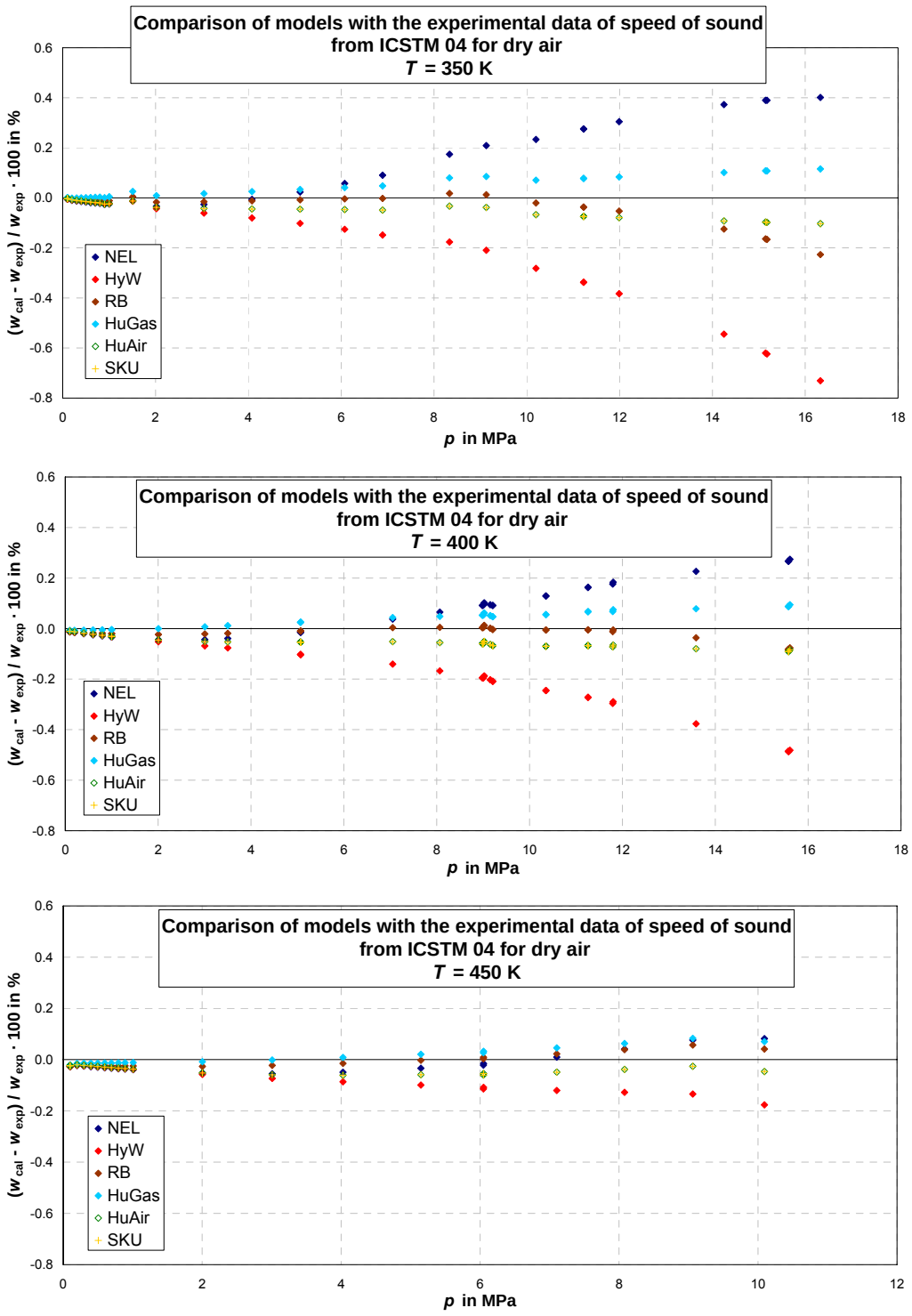

Figure 4.4: (continued)

Figure 4.4 reveals that all models represent the experimental data for speed of sound of dry air very well at low pressures. The deviations are within ± 0.1% for pressures less than 5 MPa. The deviations for all models increase with increasing pressure. The NEL model calculates values that are high, while the HyW model gives low values. The maximum deviation for the NEL model is + 0.6% at 300 K and 14 MPa. The HyW model leads to deviations up to – 0.9% at 300 K and 15 MPa. The RB, HuGas, HuAir, and SKU models describe the experimental data better than the NEL and HyW models. The speed

of sound values calculated from the best models SKU and HuAir do not deviate more than ± 0.1% from the experimental data.

4.2 Comparisons for the Gas Phase of Humid Air

4.2.1 Comparison between Calculated Values and Experimental Density Data

The experimental data sets available for the density of the gas phase of humid air are summarized in Table 4.4.

Table 4.4: Experimental data for the density of humid air.

Abbreviation	Author(s)	T / K	p / MPa
RUB 05	Wöll 2005 (AA-CAES) [13]	298-500	0.1-17
PTB 05	Klingenberg, Ulbig 2007 (AA-CAES, 2005) [11]	424-524	3.7-17
ICSTM 05	Trusler 2005 (AA-CAES) [14]	317-522	0.9-15.8
Japas 85	Japas, Franck 1985 [7]	620-673	27-264

All these data except Japas 85 were measured within the project AA-CAES. The data of Japas 85 were not taken into consideration due to the very high pressures, which are out of the range for the AA-CAES project. The experimental data points measured within the AA-CAES project for the density of humid air have already been presented in a pressure-temperature diagram in Figure 2.7.

The plots of Figure 4.5 show the deviations for the calculated density values of different models from the experimental data of RUB 05 for different mole fractions of water vapour over pressure and temperature.

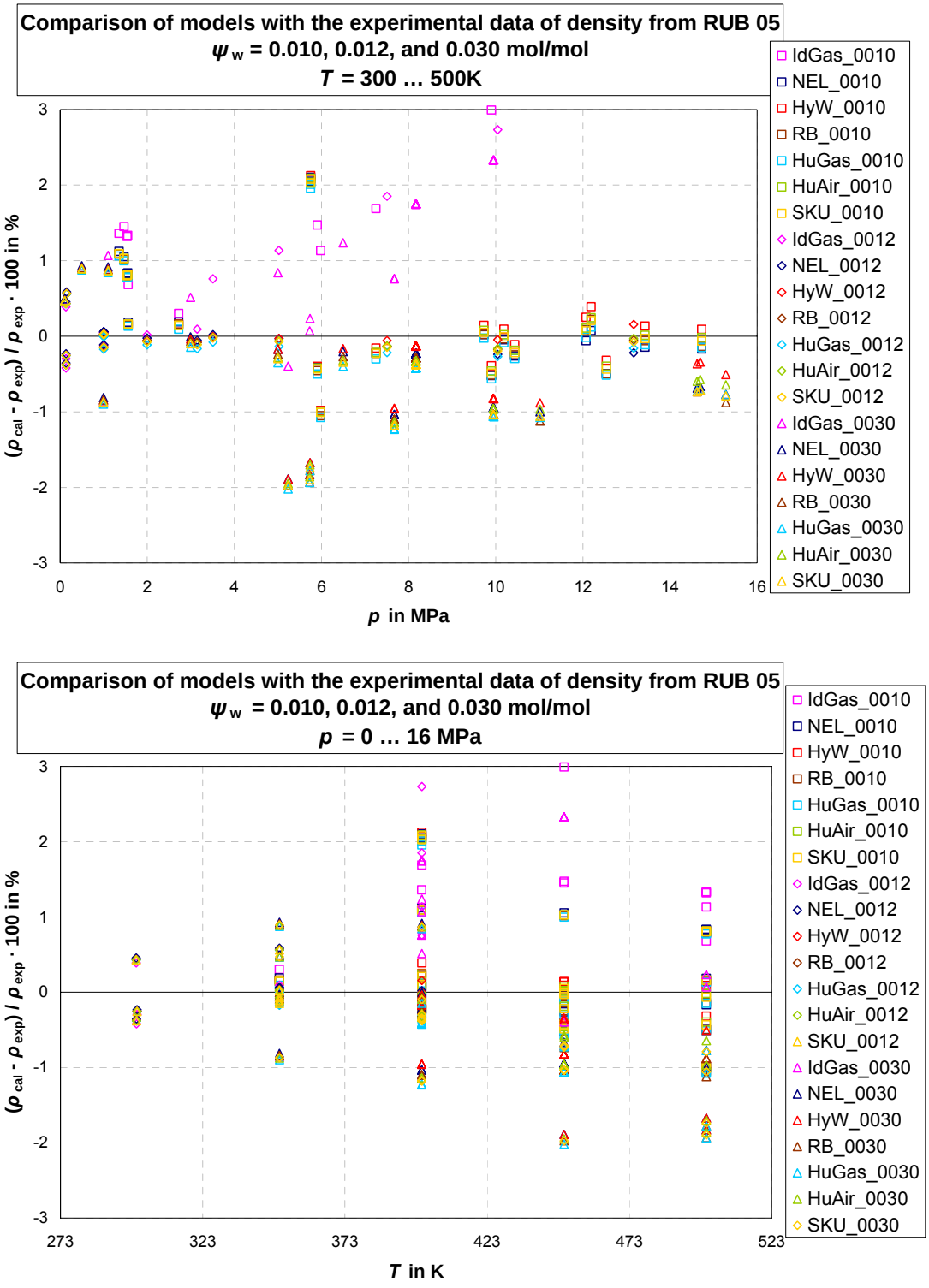

Figure 4.5: Percentage deviations of the density values of humid air calculated for the models listed in Table 4.1 from the experimental data of RUB 05 [13] as a function of pressure and temperature.

The deviations of all models apart from the IdGas model are less than ± 2%. Obviously, there is no significant difference between the models over the whole pressure and temperature ranges. The differences between the models are lower than their deviations from the experimental data.

In Figure 4.6 the deviations for the calculated density values of the different models from the experimental data of PTB 05 are illustrated for different mole fractions of water vapour over pressure and temperature.

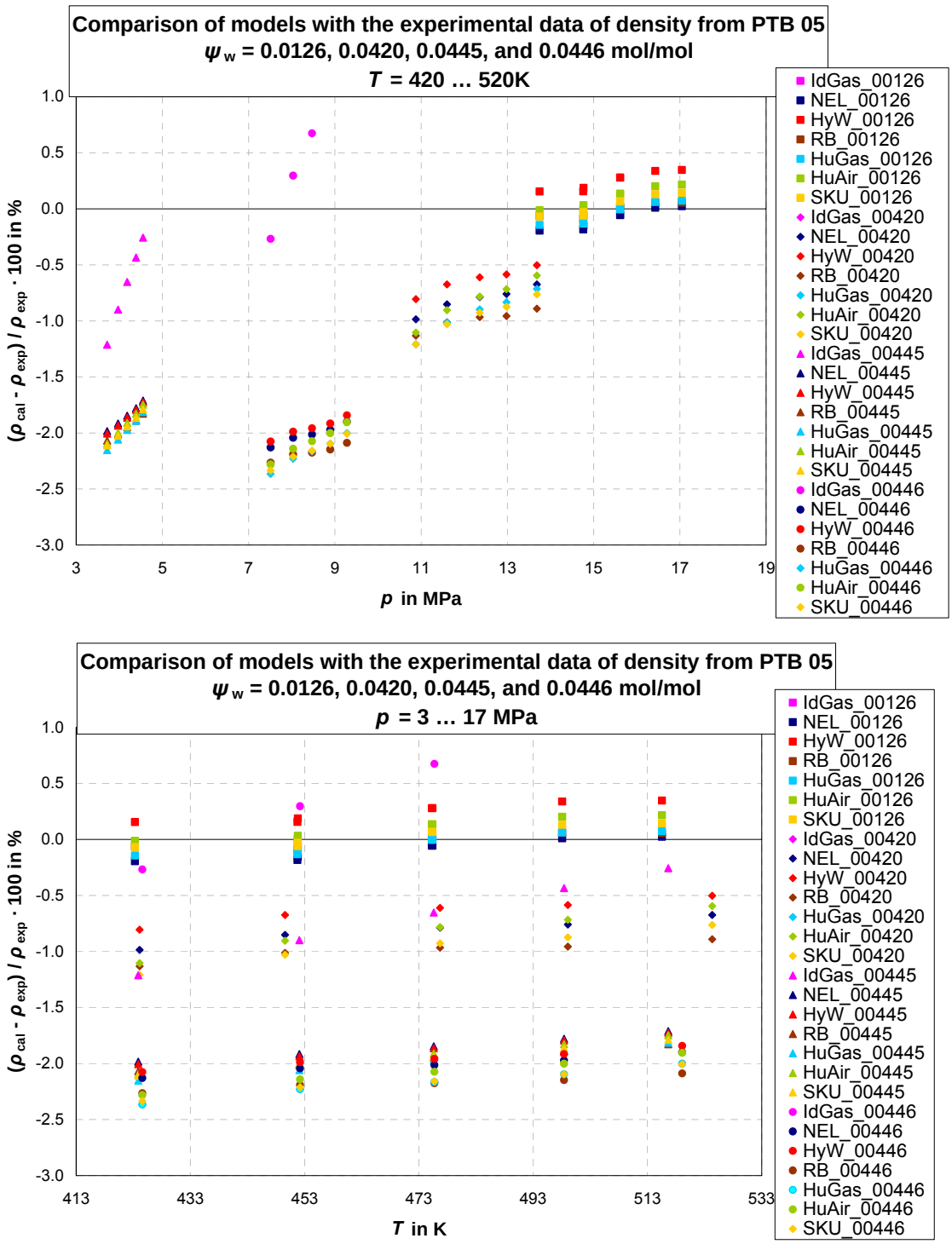

Figure 4.6: Percentage deviations of the density values of humid air calculated for the models listed in Table 4.1 from the experimental data of PTB 05 [11] as a function of pressure and temperature.

The calculated values for all models except for the IdGas model deviate up to ± 2.3% from the experimental data. The experimental data for the mole fraction of 1.26% of

water are described within ± 0.3%. The other three data sets for mole fractions of about 4% water are represented differently by the models. This seems to be due to the uncertainty of the experimental data, since the deviations of values calculated for different models from the experimental data are nearly identical. The values for the IdGas model show greater deviations from the experimental data.

Figure 4.7 presents the deviations of the calculated density values of the different models from the experimental data of ICSTM 05 for different mole fractions of water vapour over pressure and temperature.

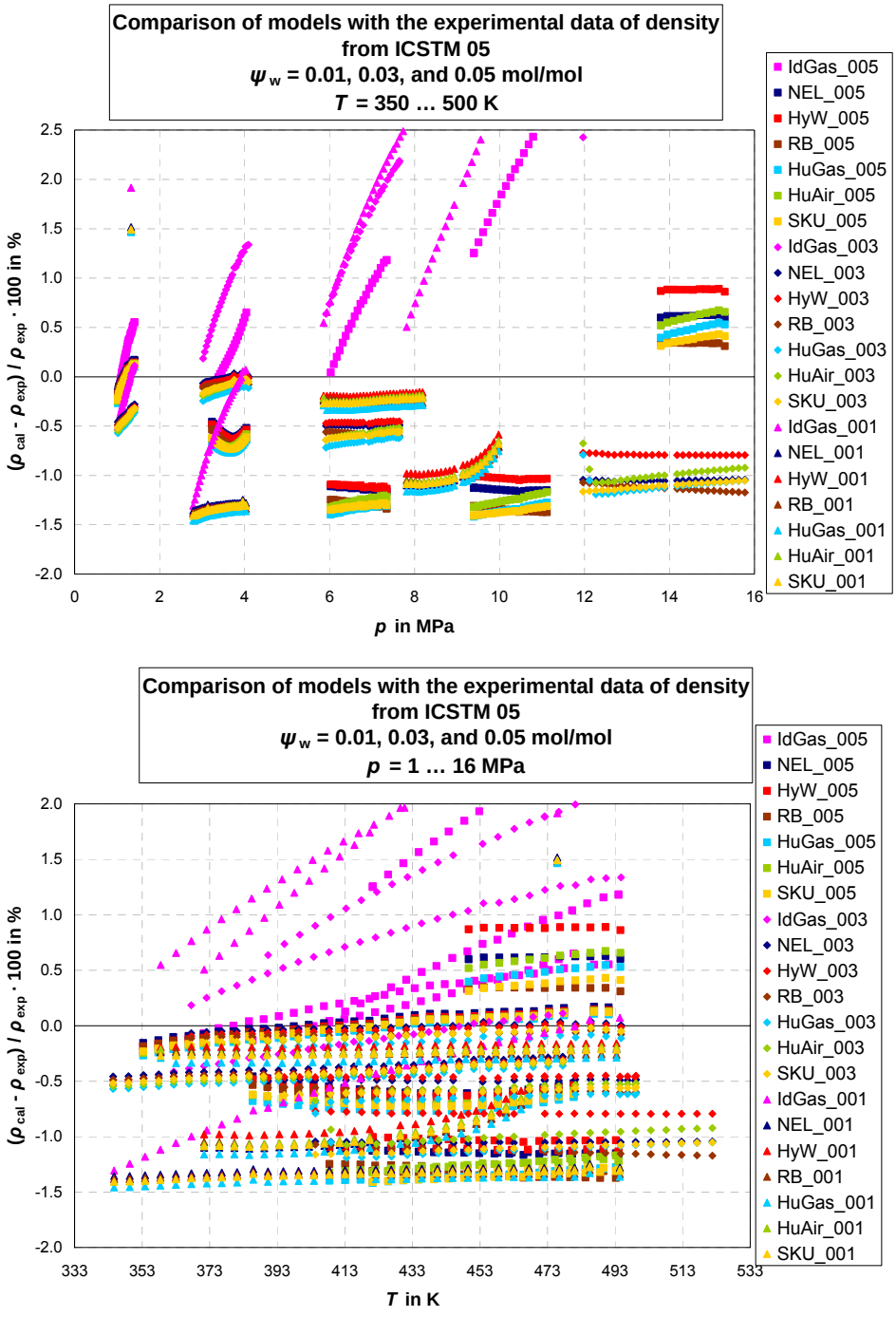

Figure 4.7: Percentage deviations of the density values of humid air calculated for the models listed in Table 4.1 from the experimental data of ICSTM 05 [14] as a function of pressure and temperature.

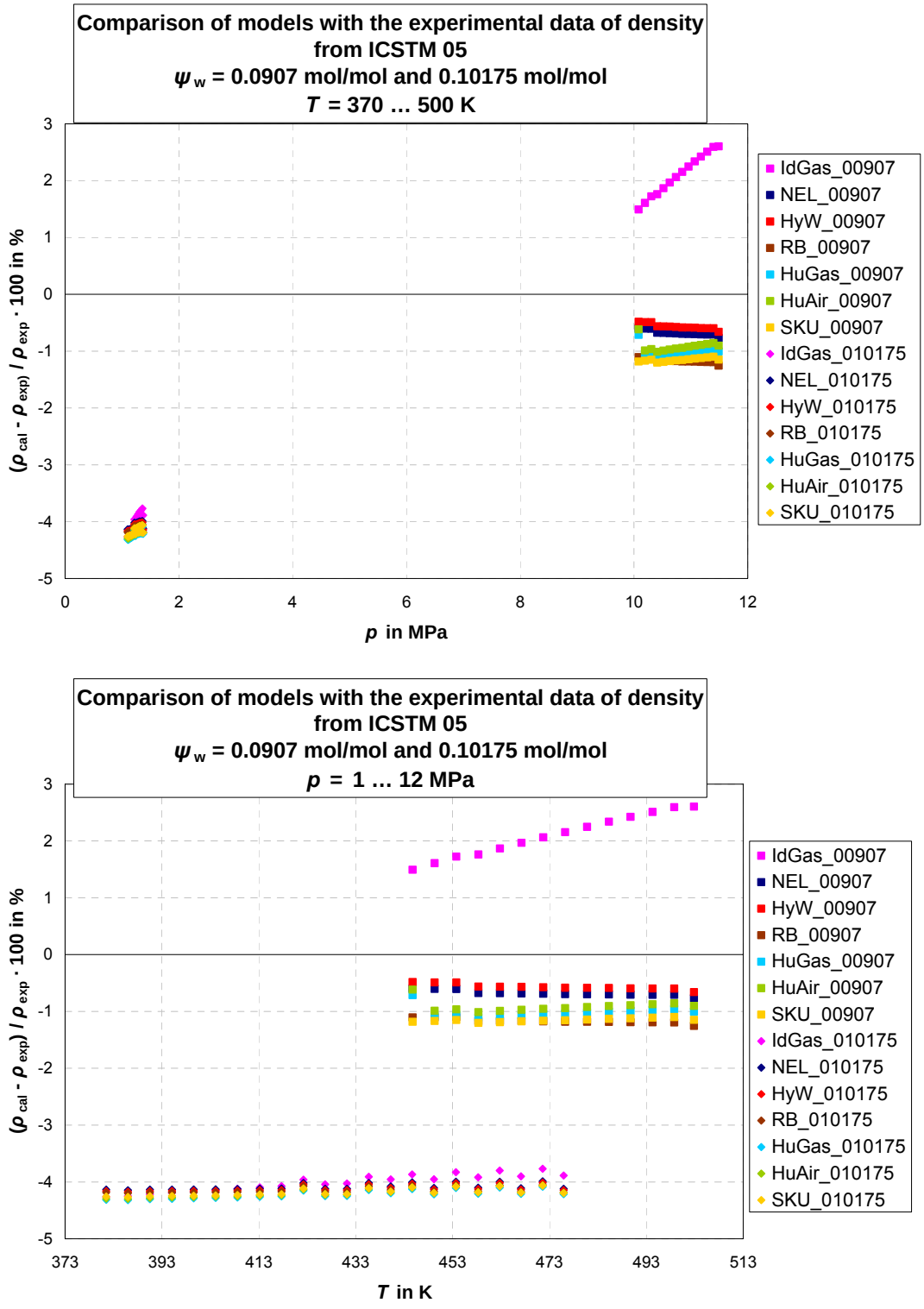

Figure 4.7: (continued 1)

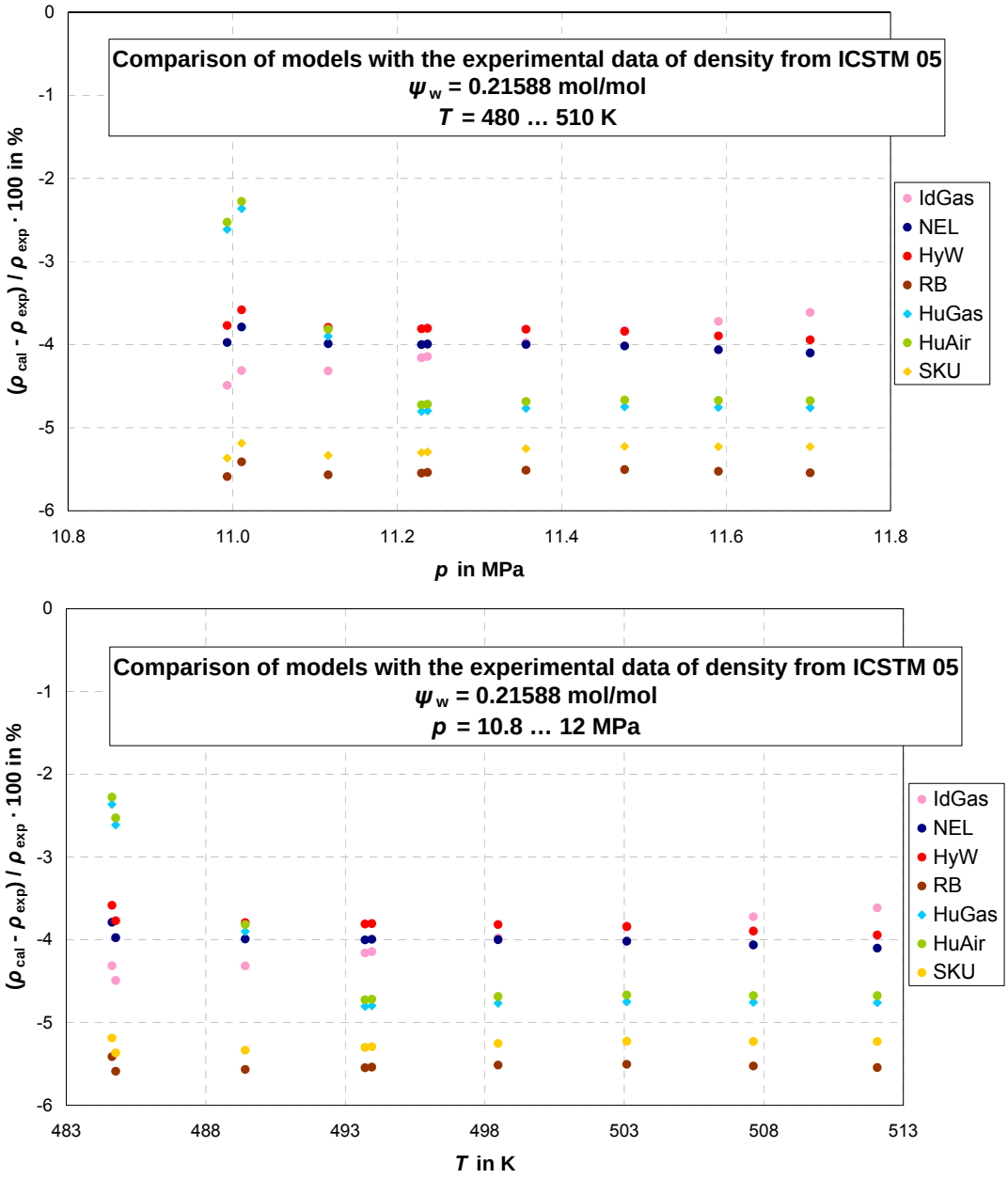

Figure 4.7: (continued 2)

For water mole fractions of approximately 1%, 3%, and 5%, the calculated values for all models show relative deviations less than ± 1.5% in density. For the water mole fraction of round about 10% the two data sets show different results for all models, whereas the different models calculate nearly the same values. If the water contents rise up to 20%, all models are characterised by deviations between – 4% and – 6%.

In summary, all models deviate from the experimental data. That means either the models do not describe the truth correctly or the experimental data are uncertain. There were heavy problems in measuring the properties of humid air because of corrosion in the measuring cells. However, for water contents between 1 and 5 mole%, which are of relevance for AA-CAES cycles, relative uncertainties of the calculated values for density up to – 2% have to be expected for the SKU model recommended for calculating AA-CAES cycles.

4.2.2 Comparison on Density Values Calculated from Different Models

The models listed in Table 4.1 were used for calculating the density of humid air at the pressures 0.1, 0.5, 1, 2, 4, 6, 10, and 15 MPa and at the temperatures 273.15, 300, 400, 600, 800, 1000, 1500, and 2000 K for each pressure, respectively. Figure 4.8 to Figure 4.15 show the relative deviations between density values calculated from the IdGas, NEL, HyW, RB, KTH, HuGas, and HuAir models to that calculated from the SKU model. The relative deviations are plotted over the mole fraction of water up to 50 mole% or up to the saturated state. The zero line in the following diagrams corresponds to the SKU model.

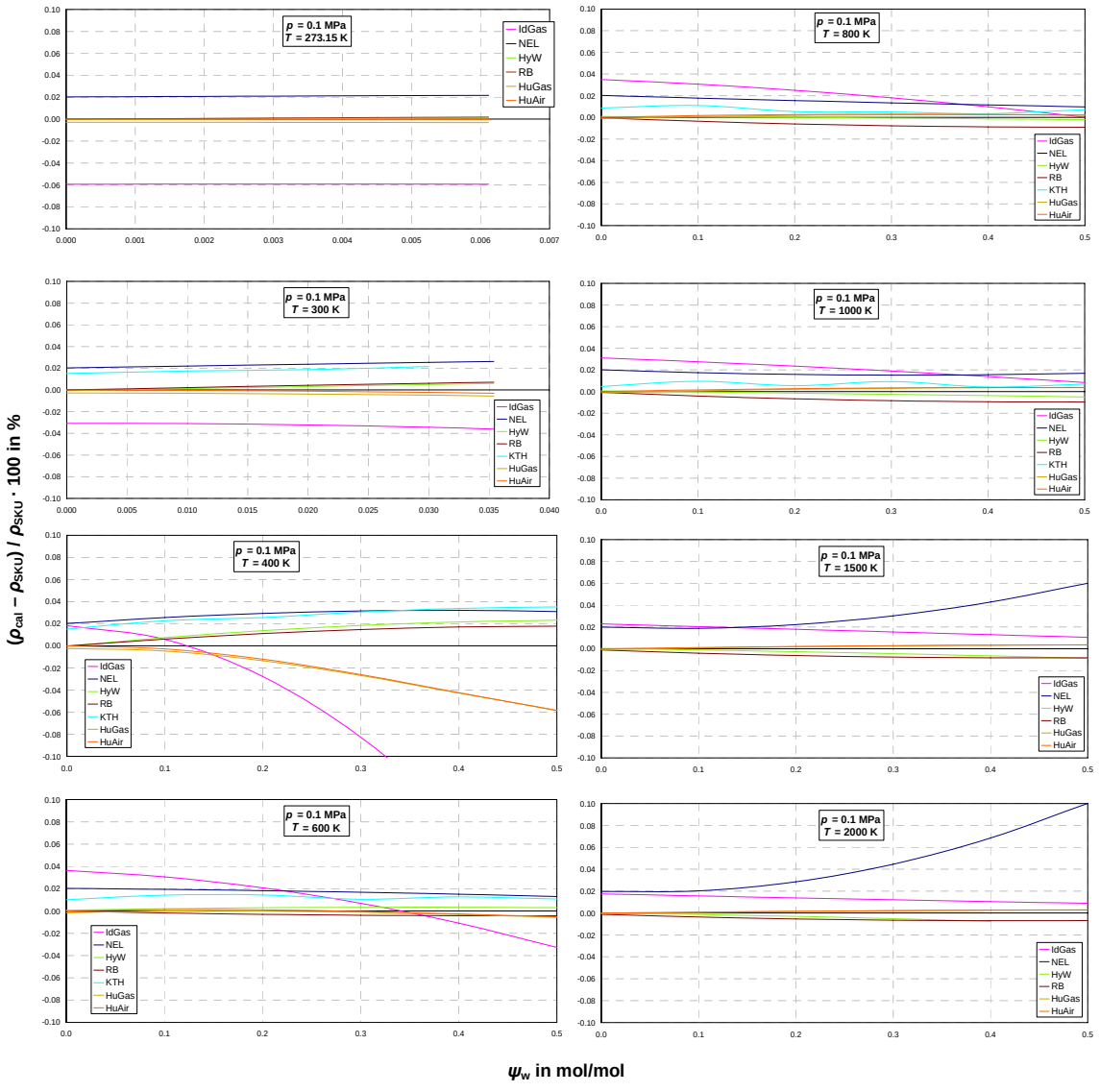

Figure 4.8: Relative deviations of the density values calculated for the different models from the density values calculated for the SKU ideal-mixing model, at pressure p = 0.1 MPa, plotted as a function of the mole fraction of water in air.

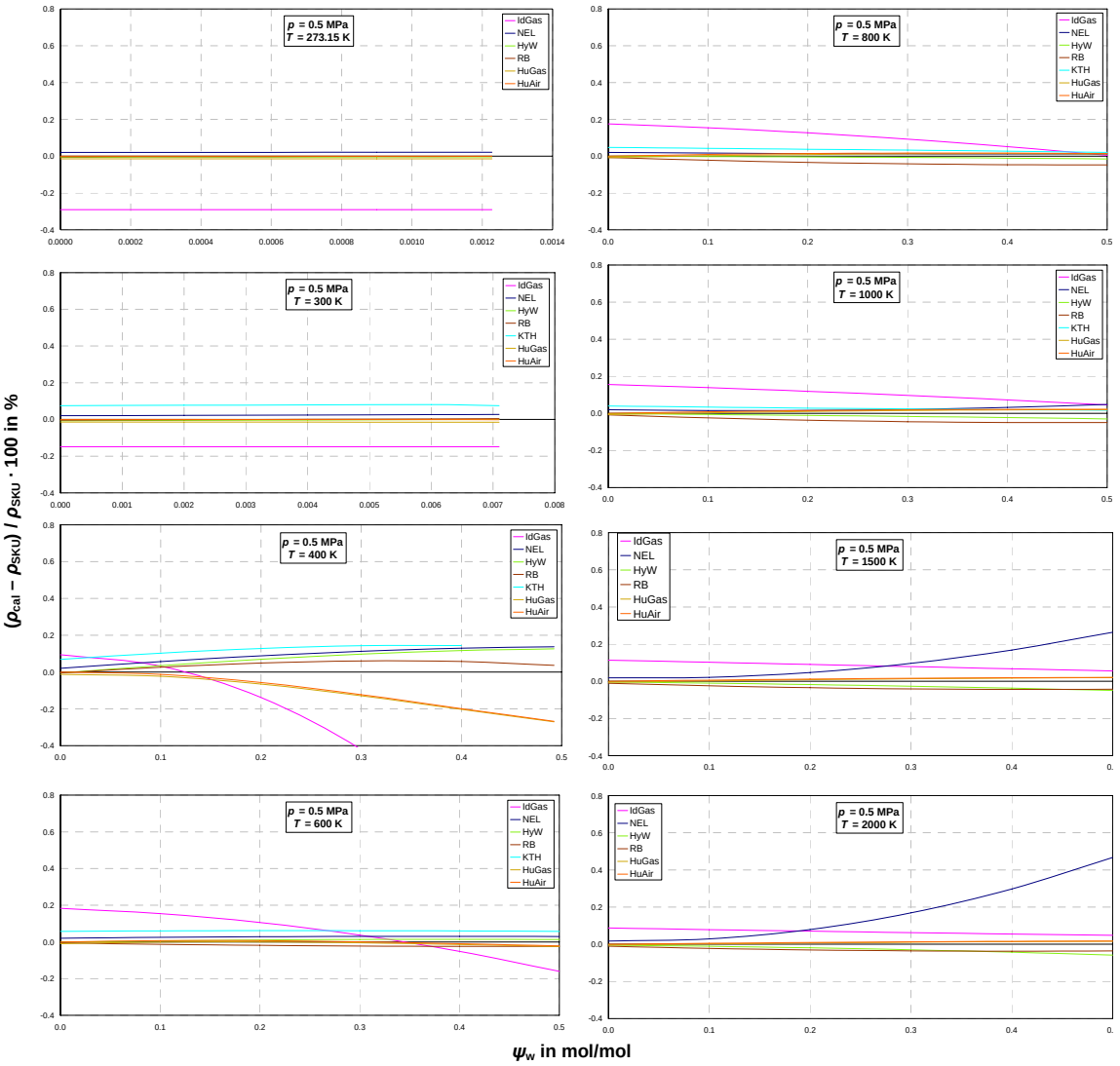

Figure 4.9: Relative deviations of the density values calculated for the different models from the density values calculated for the SKU ideal-mixing model, at pressure p = 0.5 MPa, plotted as a function of the mole fraction of water in air.

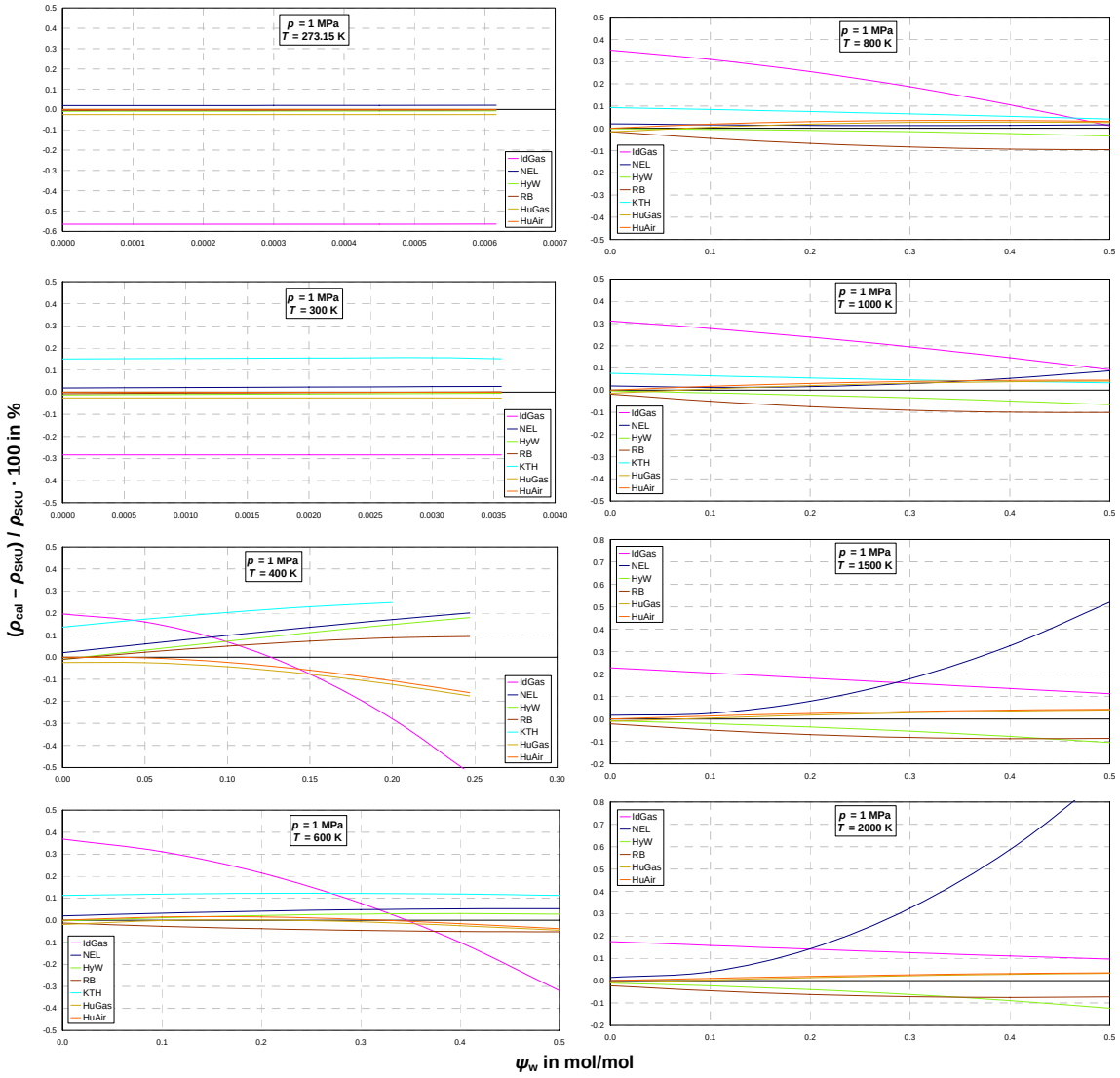

Figure 4.10: Relative deviations of the density values calculated for the different models from the density values calculated for the SKU ideal-mixing model, at pressure p = 1 MPa, plotted as a function of the mole fraction of water in air.

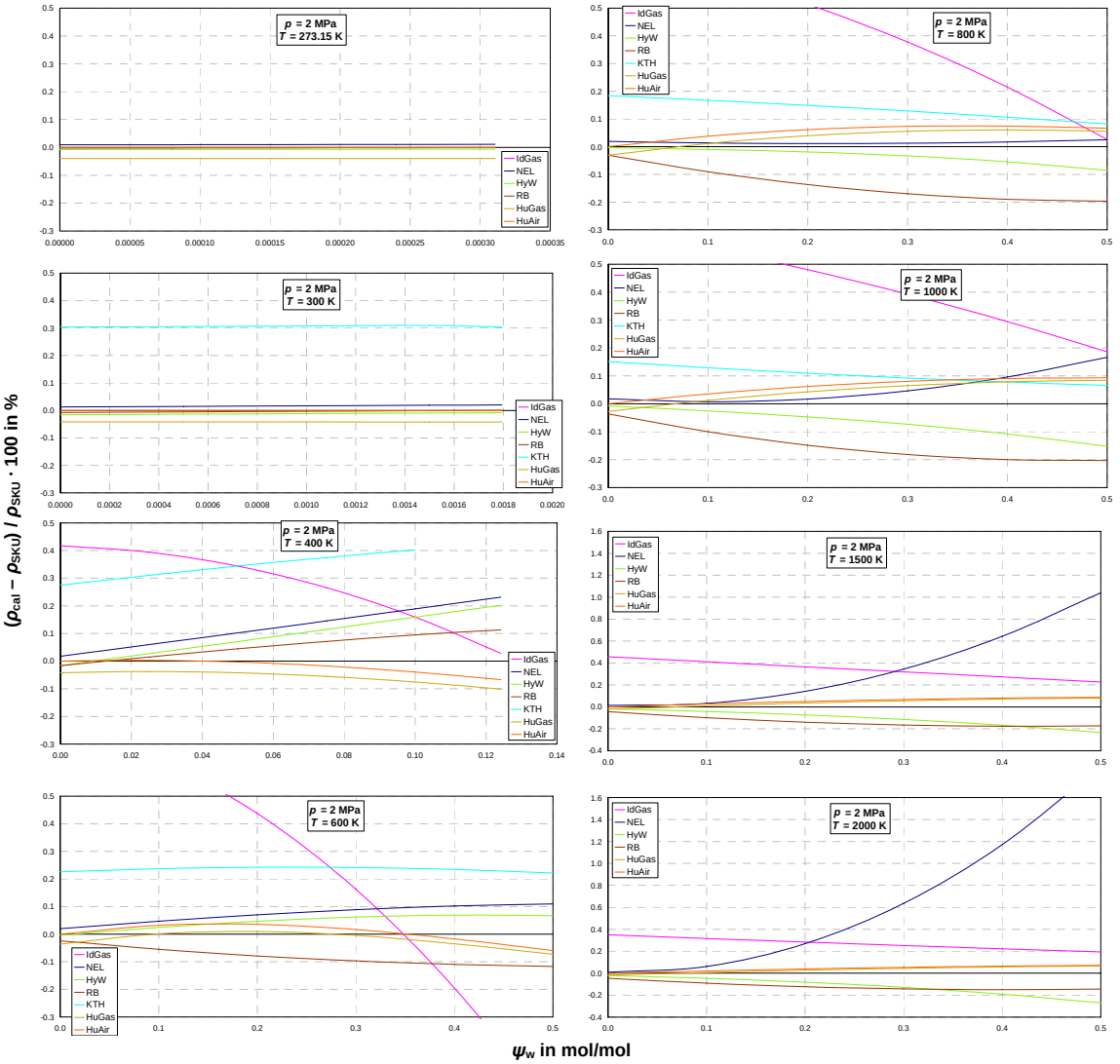

Figure 4.11: Relative deviations of the density values calculated for the different models from the density values calculated for the SKU ideal-mixing model, at pressure p = 2 MPa, plotted as a function of the mole fraction of water in air.

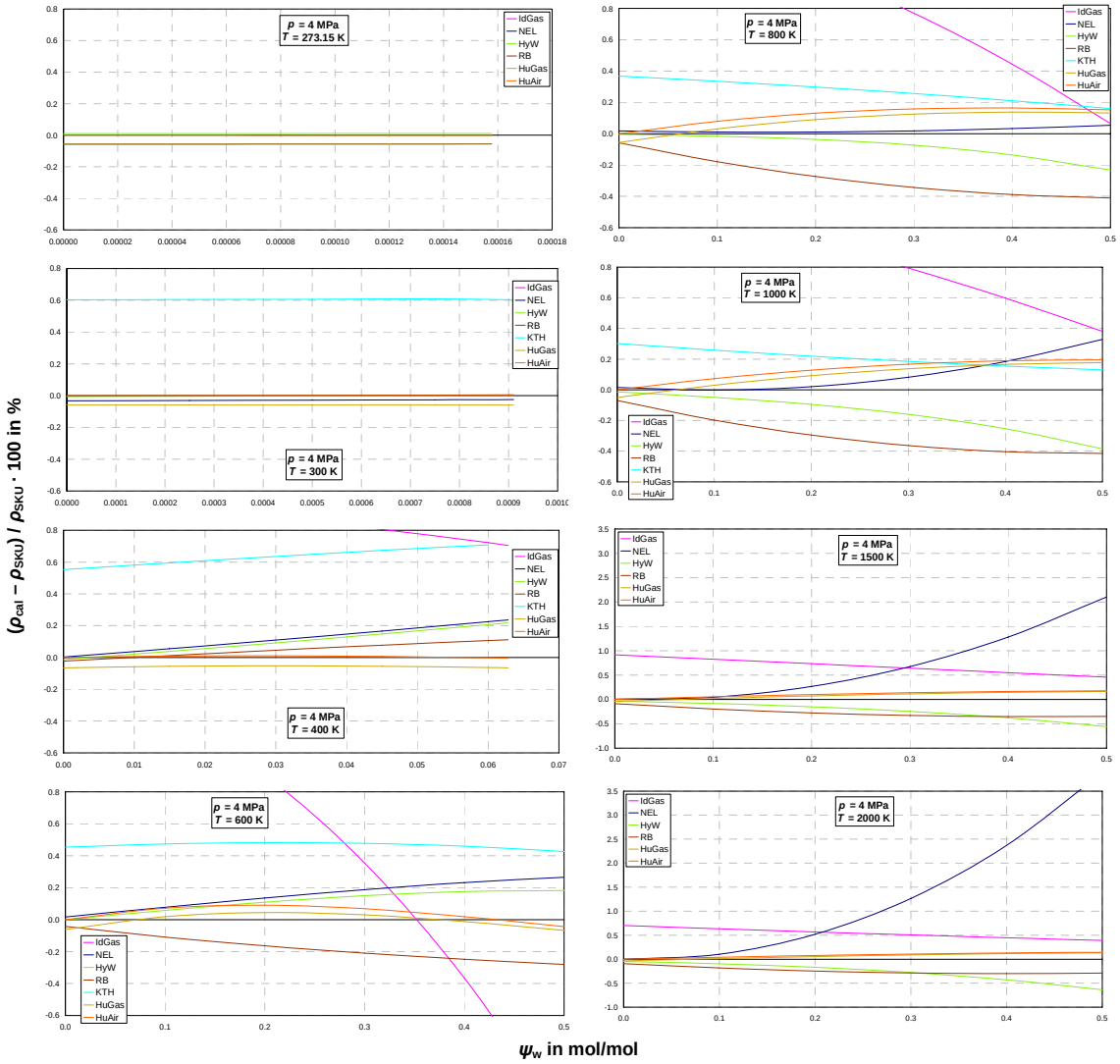

Figure 4.12: Relative deviations of the density values calculated for the different models from the density values calculated for the SKU ideal-mixing model, at pressure p = 4 MPa, plotted as a function of the mole fraction of water in air.

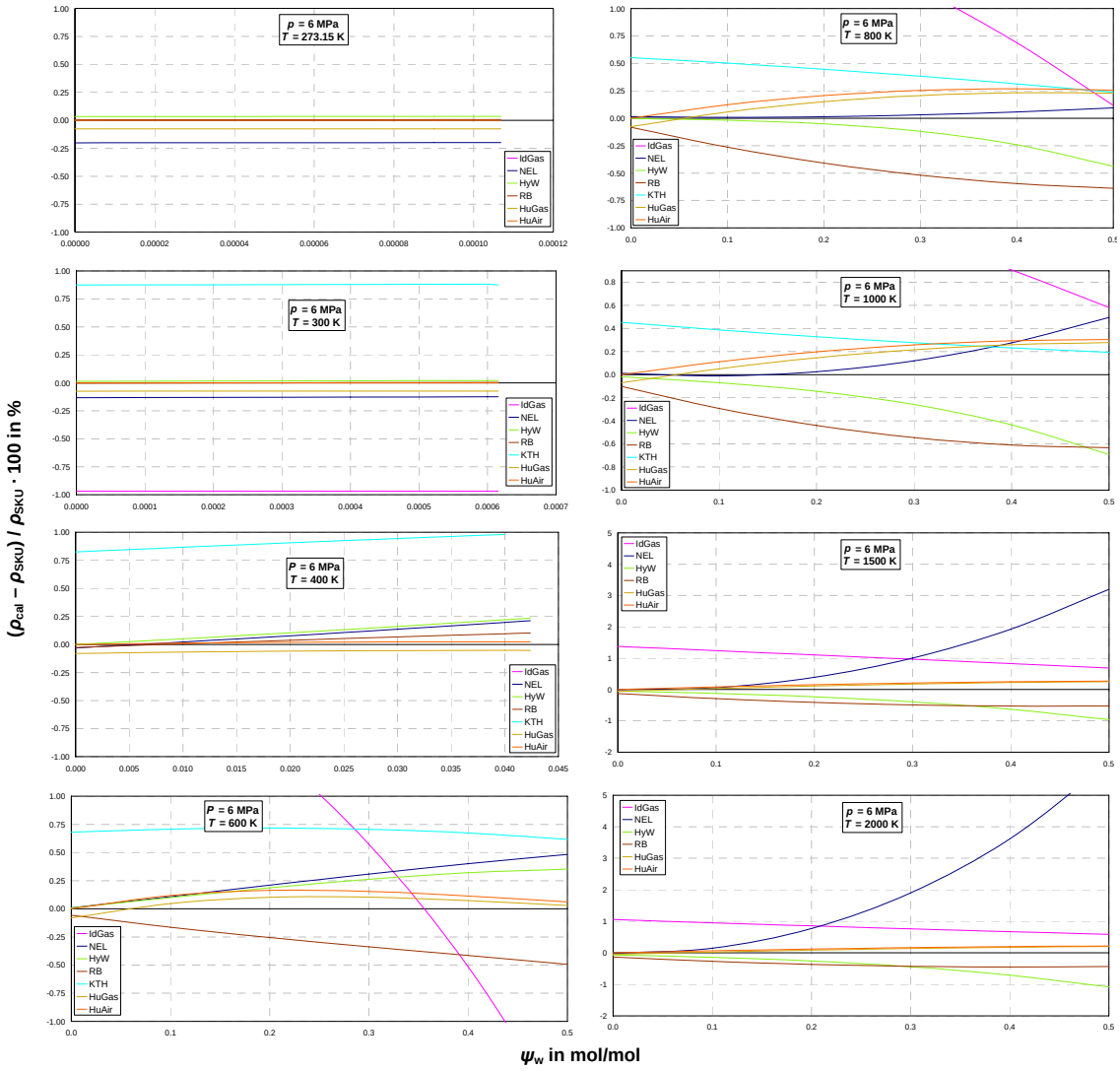

Figure 4.13: Relative deviations of the density values calculated for the different models from the density values calculated for the SKU ideal-mixing model, at pressure p = 6 MPa, plotted as a function of the mole fraction of water in air.

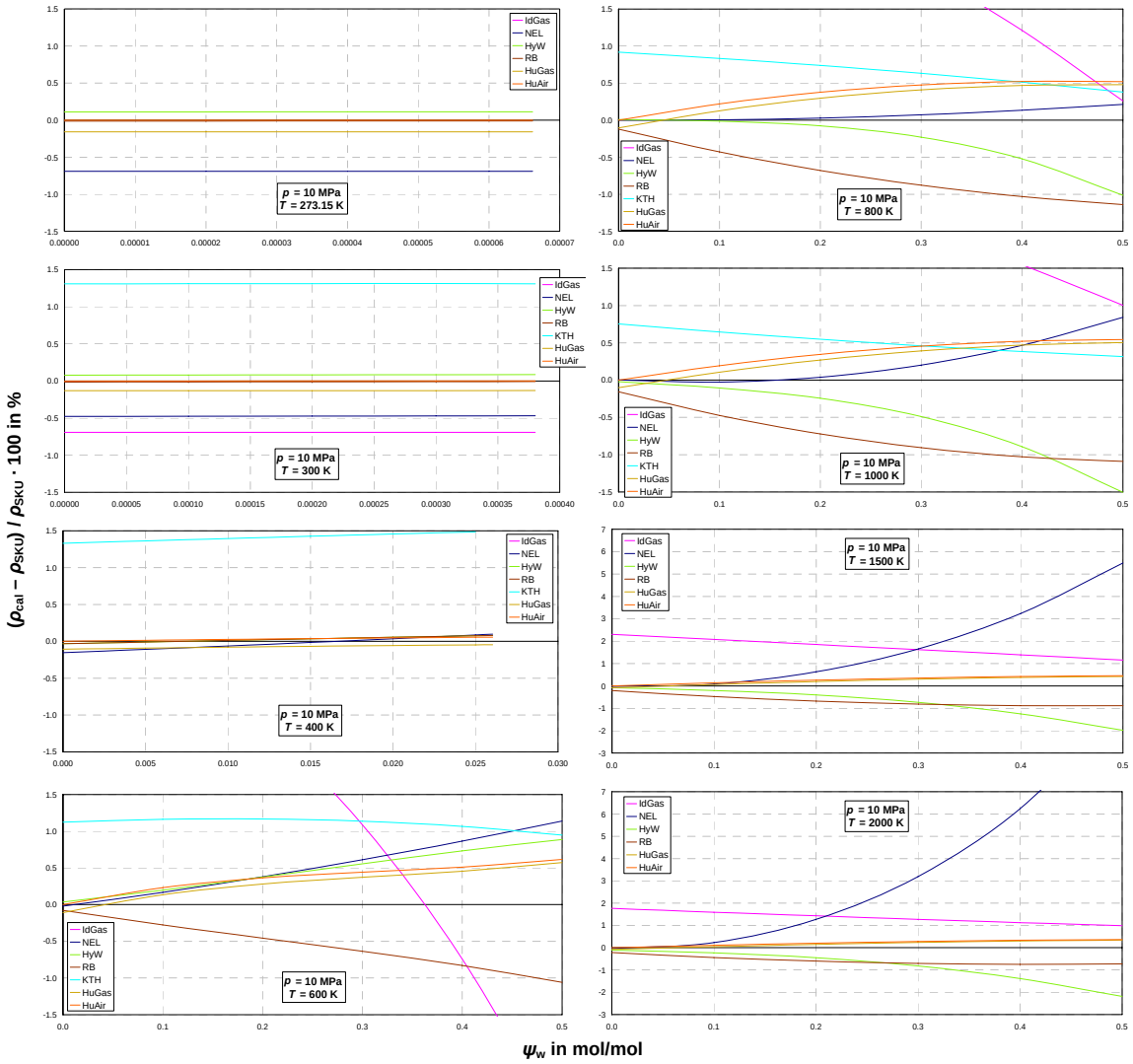

Figure 4.14: Relative deviations of the density values calculated for the different models from the density values calculated for the SKU ideal-mixing model, at pressure p = 10 MPa, plotted as a function of the mole fraction of water in air.

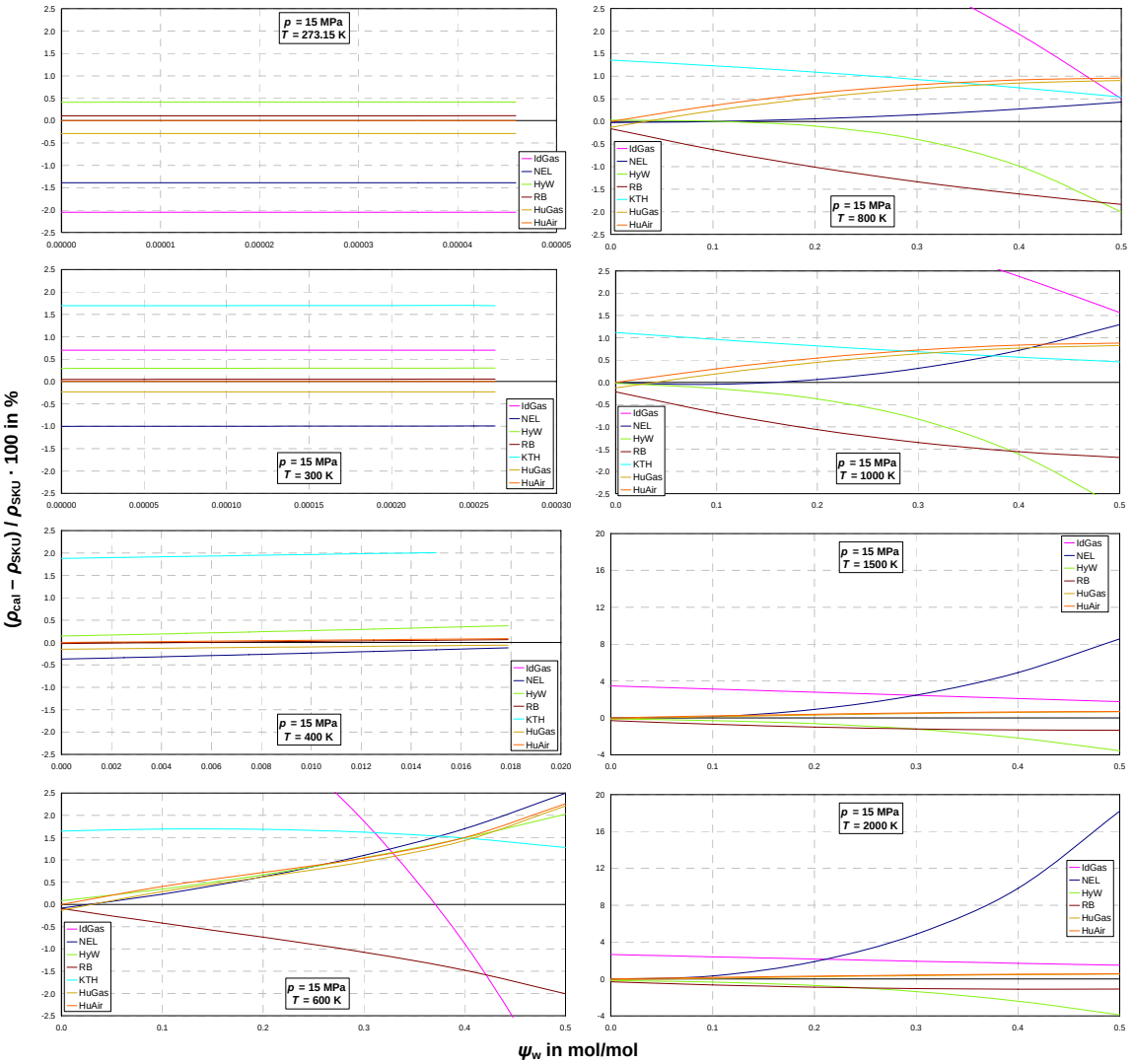

Figure 4.15: Relative deviations of the density values calculated for the different models from the density values calculated for the SKU ideal-mixing model, at pressure p = 15 MPa, plotted as a function of the mole fraction of water in air.

For dry air ($\psi_W = 0$), Figure 4.8 to Figure 4.15 show that SKU and HuAir are the most suitable models for the calculation of the density of dry air, which is the advantage of all models describing humid air as an ideal mixture of real dry air and water.

For humid air, the IdGas model shows the highest deviations in comparison with all the other models. As expected, the ideal mixing models HuGas and HuAir which are described in Sections 3.2.2.1 and 3.2.2.2 lead to nearly the same values as the SKU model. The differences increase with increasing pressure, but remain below ± 1.1%. An exception to the previous statement is shown in Figure 4.15 at 15 MPa and 600 K. Here, the deviations increase up to + 2.3% for $\psi_W = 0.5$. The RB model shows in the entire testing range another behaviour than the other models.

At pressures up to 4 MPa and temperatures between 400 and 600 K, the NEL, HyW, and KTH models show a slightly different behaviour compared with that of the HuAir and HuGas models, while the SKU model (zero line) calculates values between these two model groups.

At temperatures above 600 K, the NEL and HyW models show a completely different behaviour, when compared to each other. With increasing water content, the NEL model calculates too high values while the HyW model leads to values which are too low. At temperatures between 1500 K and 2000 K, the deviations of the NEL model compared to the SKU model amount up to + 18% and the deviations of the HyW model amount up to – 4%.

Concluding, the deviation curves show that the models NEL, HyW, RB, and KTH do behave differently to each other and to the SKU model. Therefore, it is difficult to draw conclusions from these figures. The HuAir and HuGas models correspond to the SKU model. Obviously, humid air can be treated as an ideal mixture of the real fluids dry air and steam (SKU model) with acceptable accuracy. The advantage of this model is that the crossover to dry air is better represented.

4.2.3 Comparison on Isobaric Heat Capacity Values Calculated from Different Models

The models listed in Table 4.1 were used for calculating the isobaric heat capacity of humid air at the pressures 0.1, 0.5, 1, 2, 4, 6, 10, and 15 MPa and at the temperatures 273.15, 300, 400, 600, 800, 1000, 1500, and 2000 K for each pressure, respectively. Figure 4.16 to Figure 4.23 show the relative deviations between isobaric heat capacity values calculated from the IdGas, NEL, HyW, RB, KTH, HuGas, and HuAir models to that calculated from the SKU model. The relative deviations are plotted over the mole fraction of water up to 50 mole% or up to the saturated state. The zero line in the following diagrams corresponds to the SKU model.

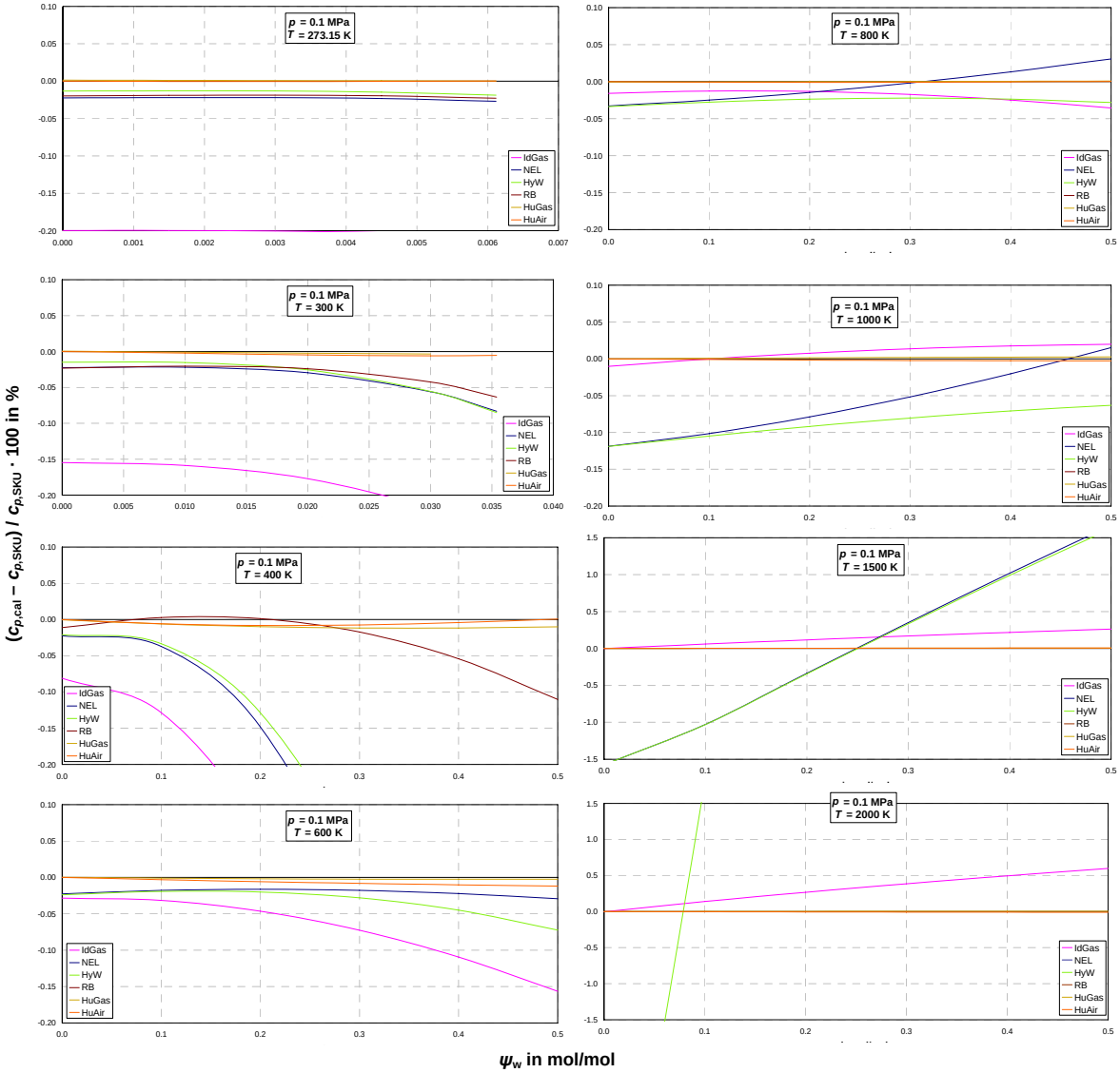

Figure 4.16: Relative deviations of the isobaric heat capacity values calculated for the different models from the values calculated for the SKU ideal-mixing model, at pressure p = 0.1 MPa, plotted as a function of the mole fraction of water in air.

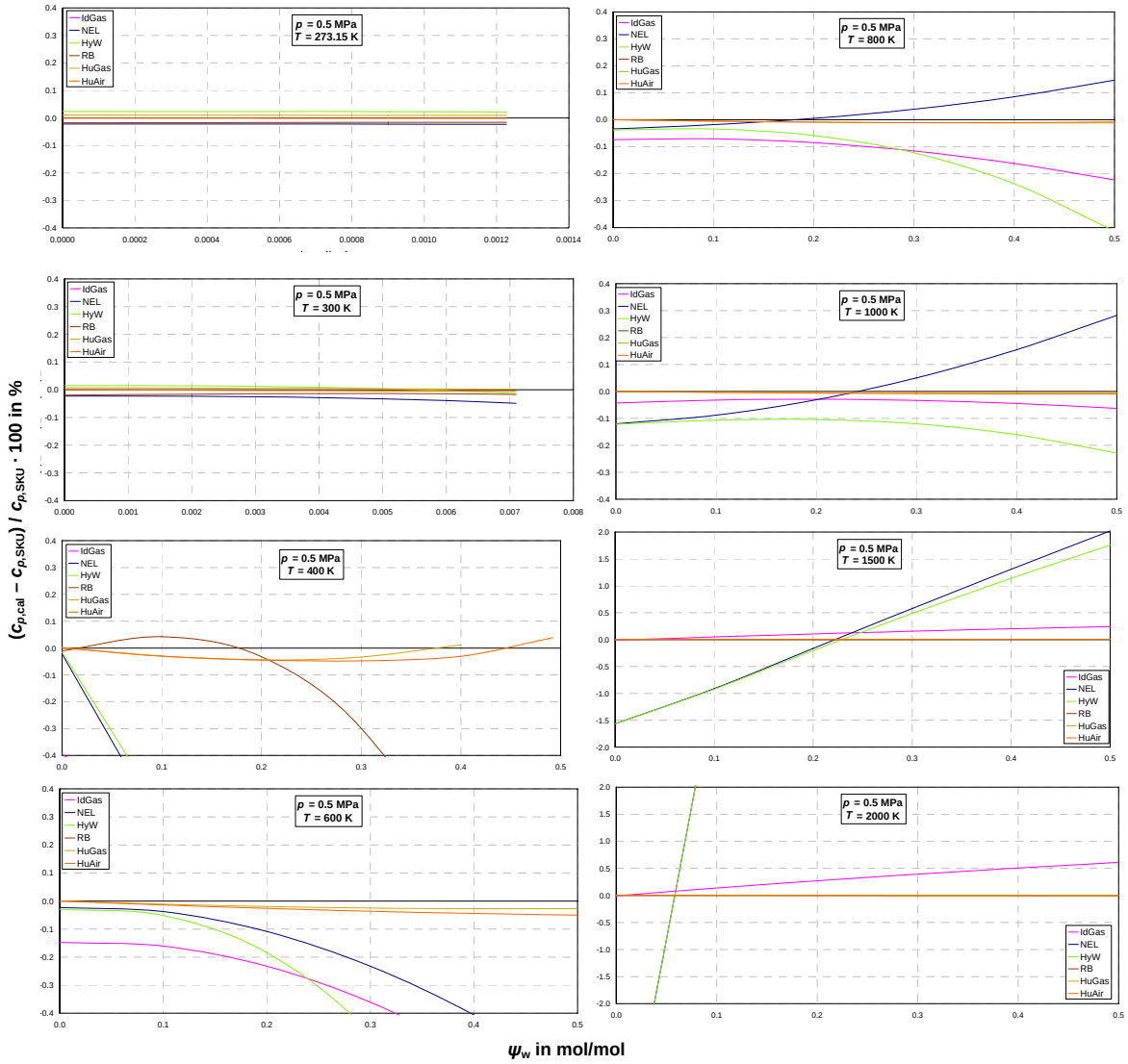

Figure 4.17: Relative deviations of the isobaric heat capacity values calculated for the different models from the values calculated for the SKU ideal-mixing model, at pressure p = 0.5 MPa, plotted as a function of the mole fraction of water in air.

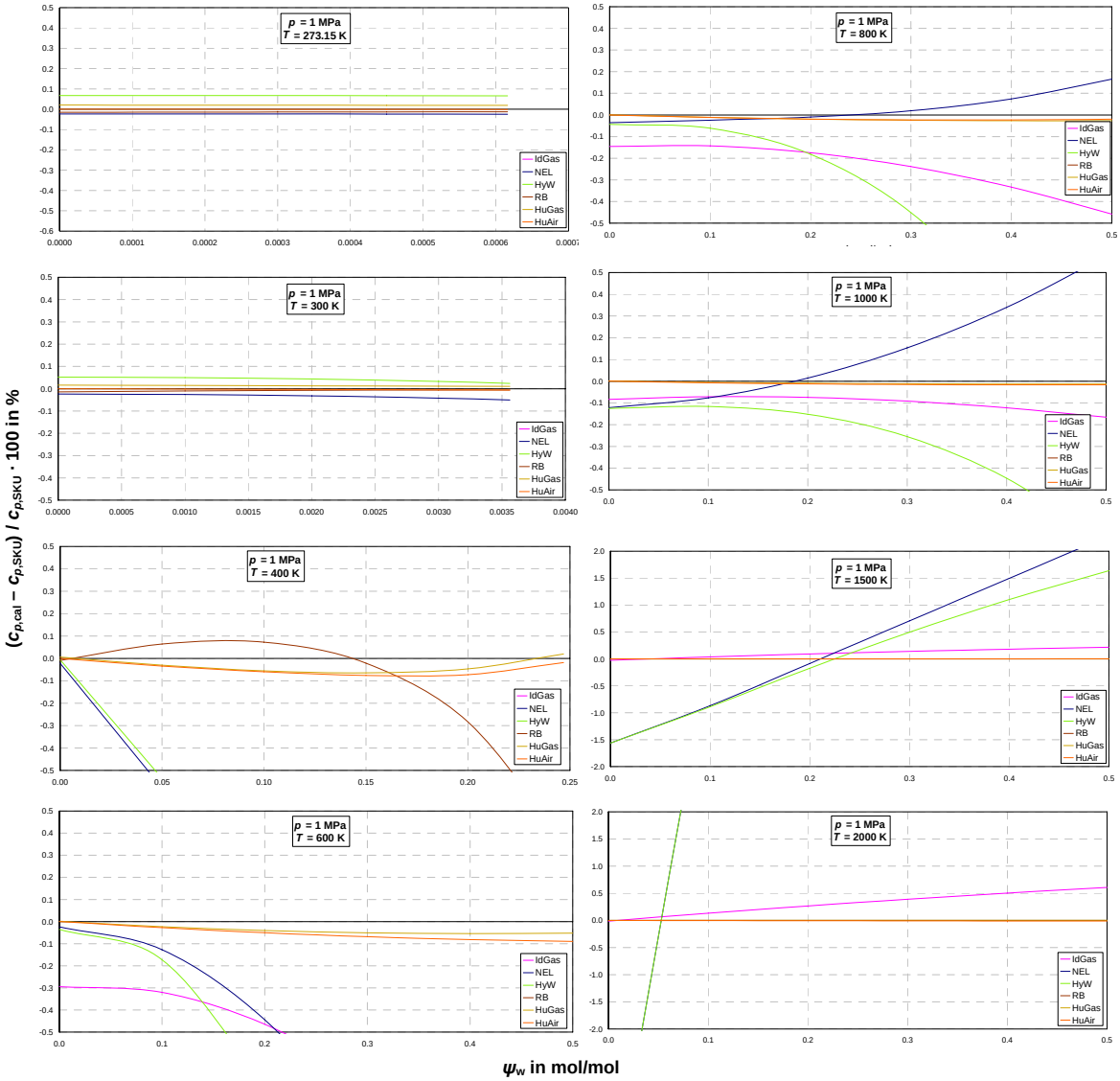

Figure 4.18: Relative deviations of the isobaric heat capacity values calculated for the different models from the values calculated for the SKU ideal-mixing model, at pressure p = 1 MPa, plotted as a function of the mole fraction of water in air.

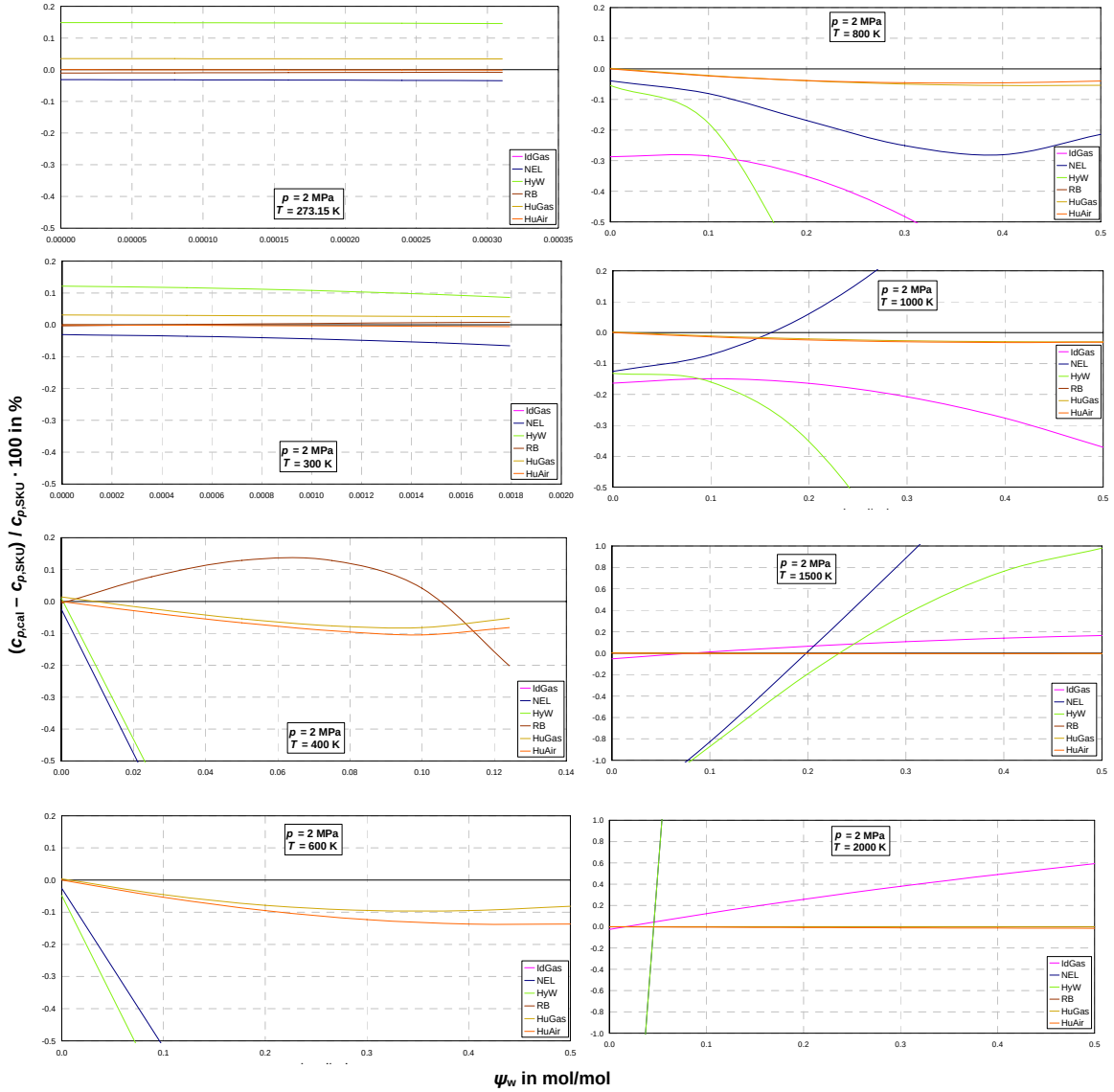

Figure 4.19: Relative deviations of the isobaric heat capacity values calculated for the different models from the values calculated for the SKU ideal-mixing model, at pressure p = 2 MPa, plotted as a function of the mole fraction of water in air.

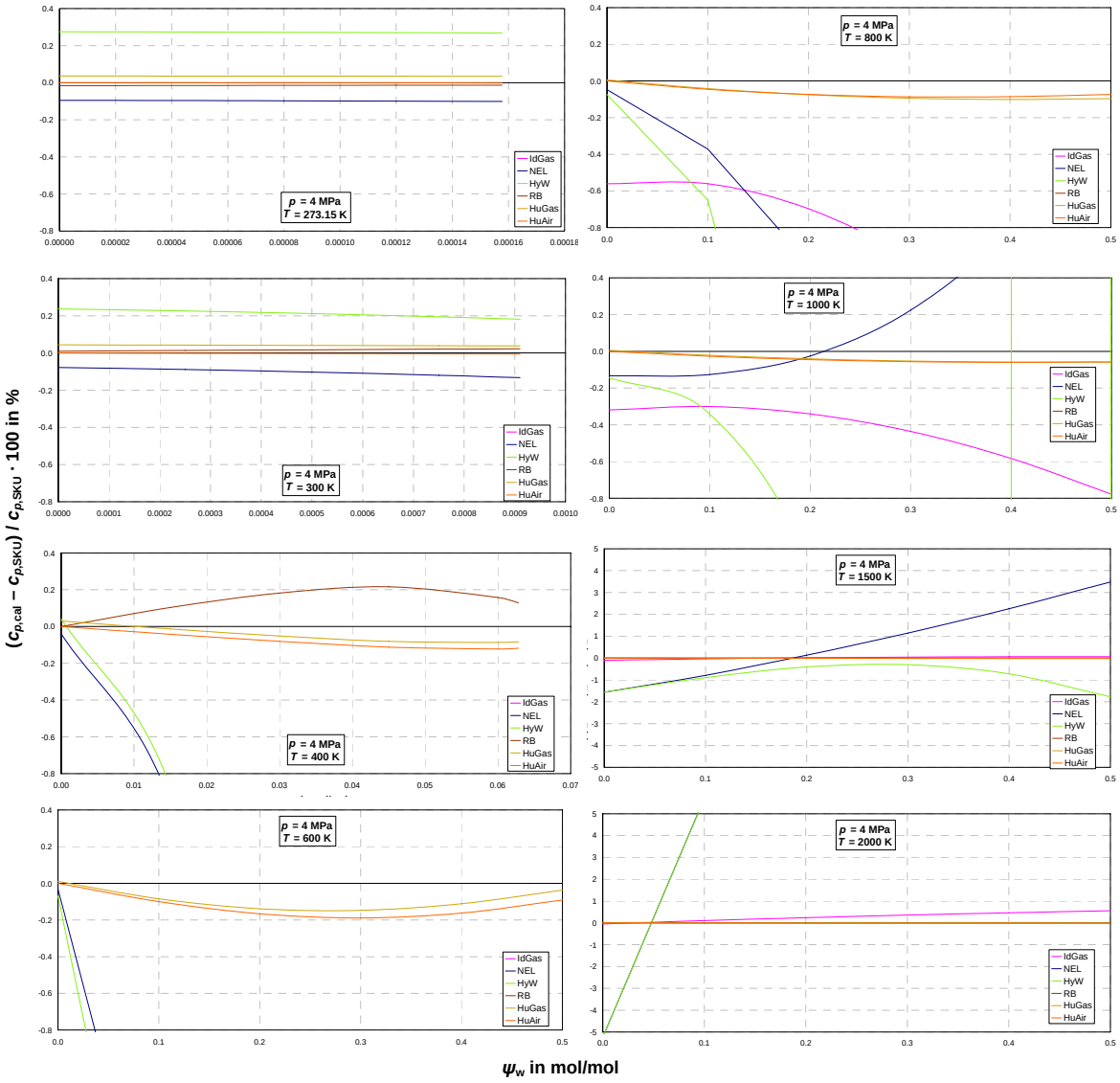

Figure 4.20: Relative deviations of the isobaric heat capacity values calculated for the different models from the values calculated for the SKU ideal-mixing model, at pressure p = 4 MPa, plotted as a function of the mole fraction of water in air.

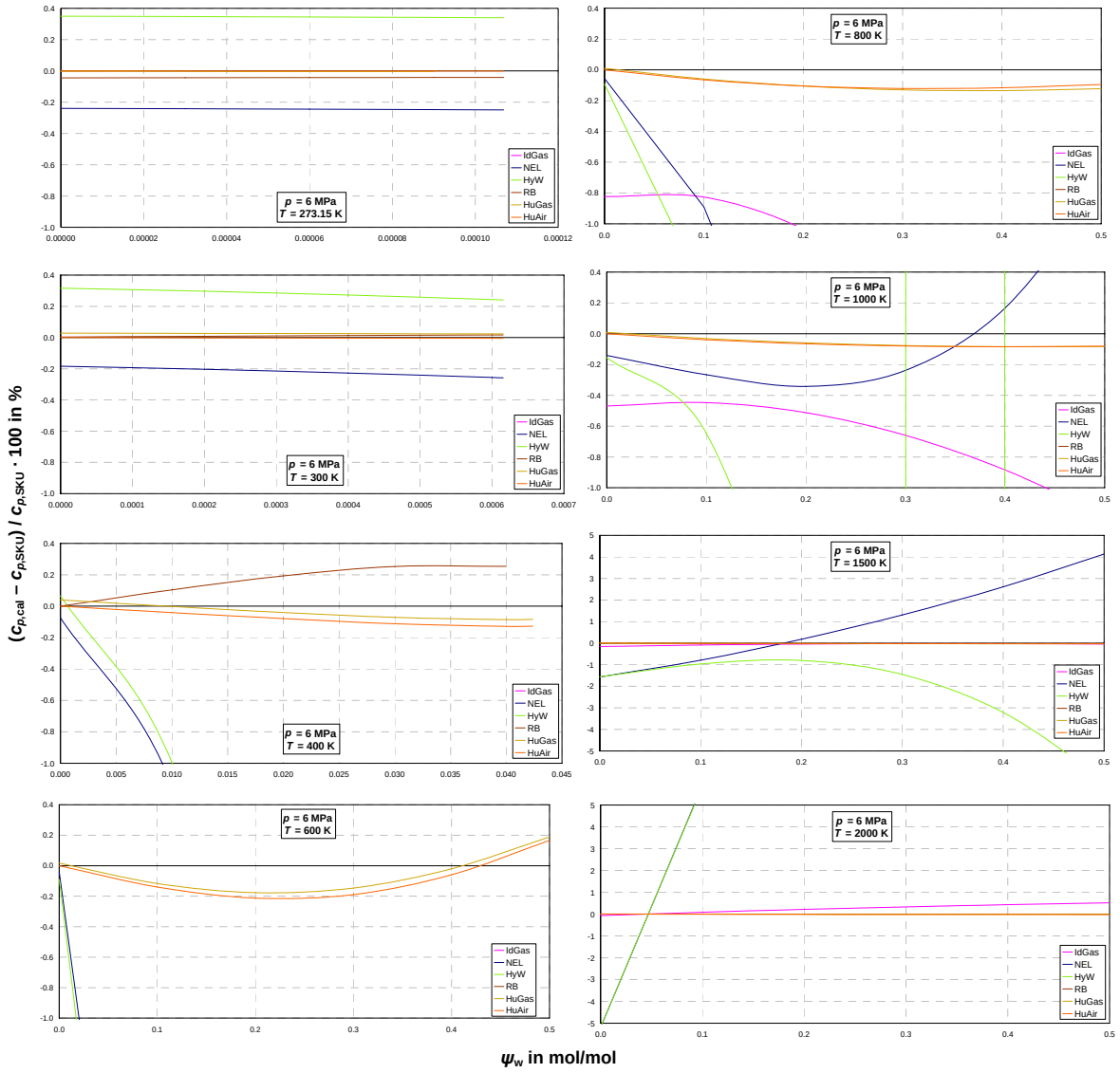

Figure 4.21: Relative deviations of the isobaric heat capacity values calculated for the different models from the values calculated for the SKU ideal-mixing model, at pressure p = 6 MPa, plotted as a function of the mole fraction of water in air.

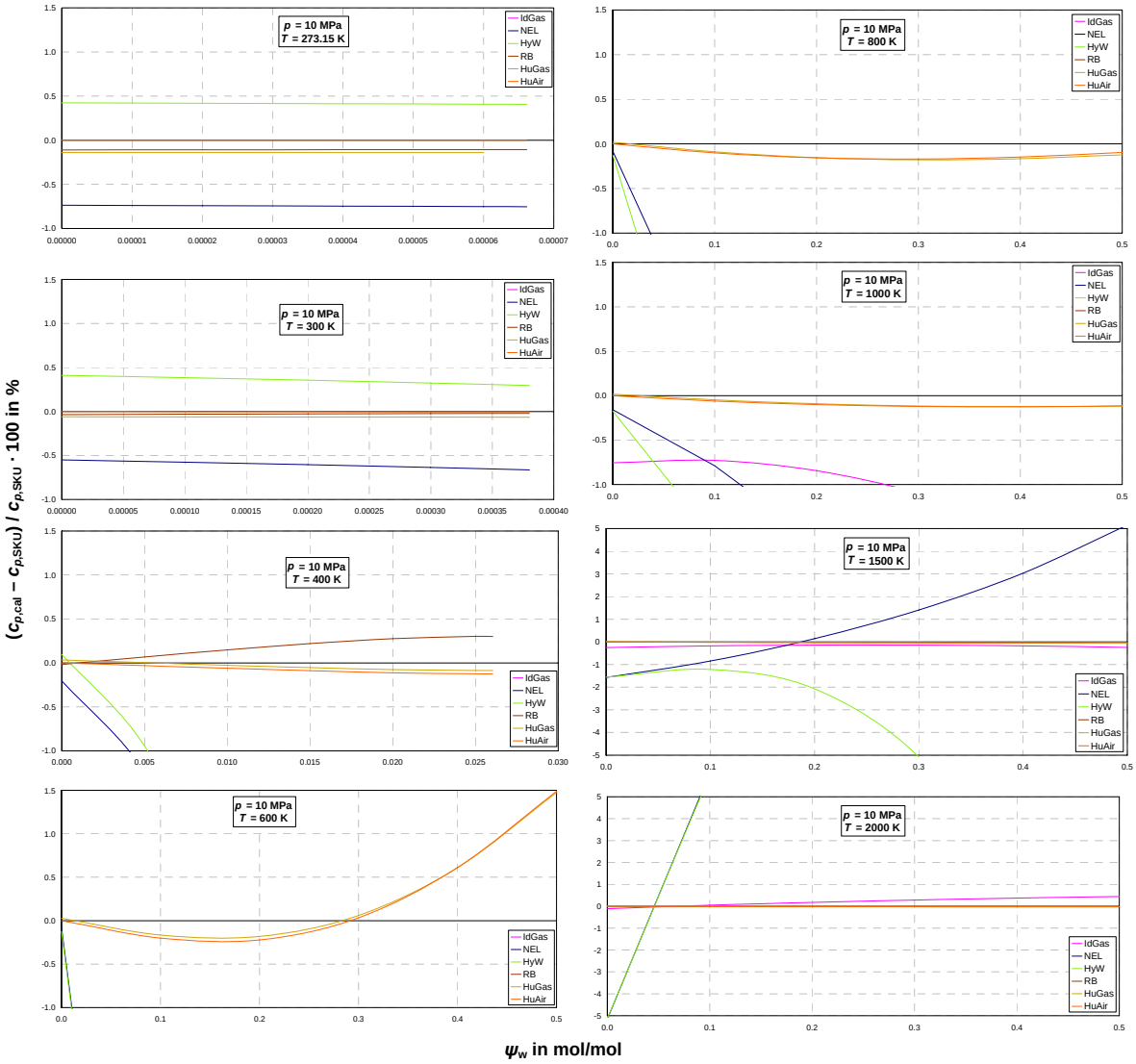

Figure 4.22: Relative deviations of the isobaric heat capacity values calculated for the different models from the values calculated for the SKU ideal-mixing model, at pressure p = 10 MPa, plotted as a function of the mole fraction of water in air.

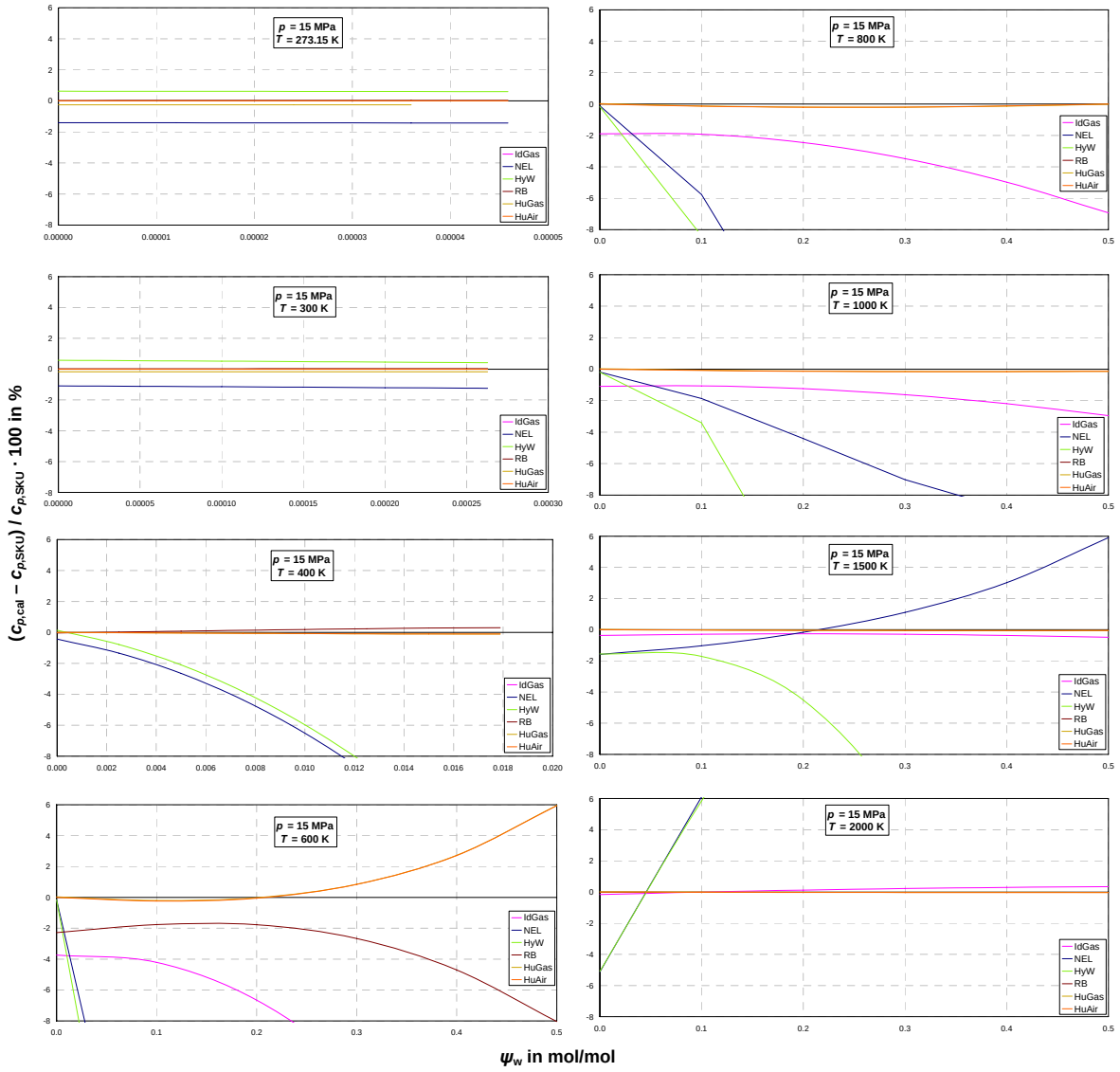

Figure 4.23: Relative deviations of the isobaric heat capacity values calculated for the different models from the values calculated for the SKU ideal-mixing model, at pressure p = 15 MPa, plotted as a function of the mole fraction of water in air.

For dry air ($\psi_w = 0$), Figure 4.16 to Figure 4.23 show that SKU and HuAir are the most suitable models for the calculation of the isobaric heat capacity of dry air, which is the advantage of all models describing humid air as an ideal mixture of real dry air and water.

For humid air, the IdGas model shows the highest deviations in comparison with all the other models. As expected, the ideal mixing models HuGas and HuAir which are described in Sections 3.2.2.1 and 3.2.2.2 lead to nearly the same values as the SKU model. The differences increase with increasing pressure, but remain below ± 0.2%. An exception to the previous statement is shown in Figure 4.22 and Figure 4.23 at 10 and 15 MPa and 600 K. Here, the deviations increase up to + 6% for $\psi_w = 0.5$.

At 273.15 and 300 K, the values for the RB model are similar to those of the HuAir model. At 400 K, the deviations are a little bit higher. Values for the RB model could not be calculated at temperatures greater than 400 K.

At temperatures above 300 K, the NEL and HyW models show a completely different behaviour, when compared to SKU, HuAir, and HuGas models. For temperatures greater than 1000 K and with increasing water content, the NEL model calculates too high values while the HyW model leads to values which are too low. The deviations of the NEL model compared to the SKU model amount up to + 48% and the deviations of the HyW model amount up to + 19%.

The NEL, RB, and HyW models do not show a uniform behaviour with regard to the deviation curves relative to the SKU model. Therefore, it is difficult to draw conclusions from these figures.

Concluding, humid air can be treated as an ideal mixture of the real fluids dry air and steam (SKU model) with acceptable accuracy. The advantage of this model is that the crossover to dry air is better represented.

4.2.4 Additional Comparison for the Gas Phase of Humid Nitrogen

An additional comparison between calculated density values and experimental data for the gas phase of nitrogen-water mixtures is given in this section. In order to show the ability of the ideal-mixing model HuGas, the experimental data of Fenghour and Wakeham (1993) [8] were compared with the values determined by the HuGas model.

The experimental data points for the density of nitrogen-water mixtures of Fenghour and Wakeham have already been presented as a part of the pressure-temperature diagram in Figure 2.4.

Figure 4.24 illustrates the deviations of the density values of nitrogen-water mixtures calculated for the HuGas model from the experimental data of Fenghour and Wakeham for mole fractions of water below 40% as a function of pressure and temperature.

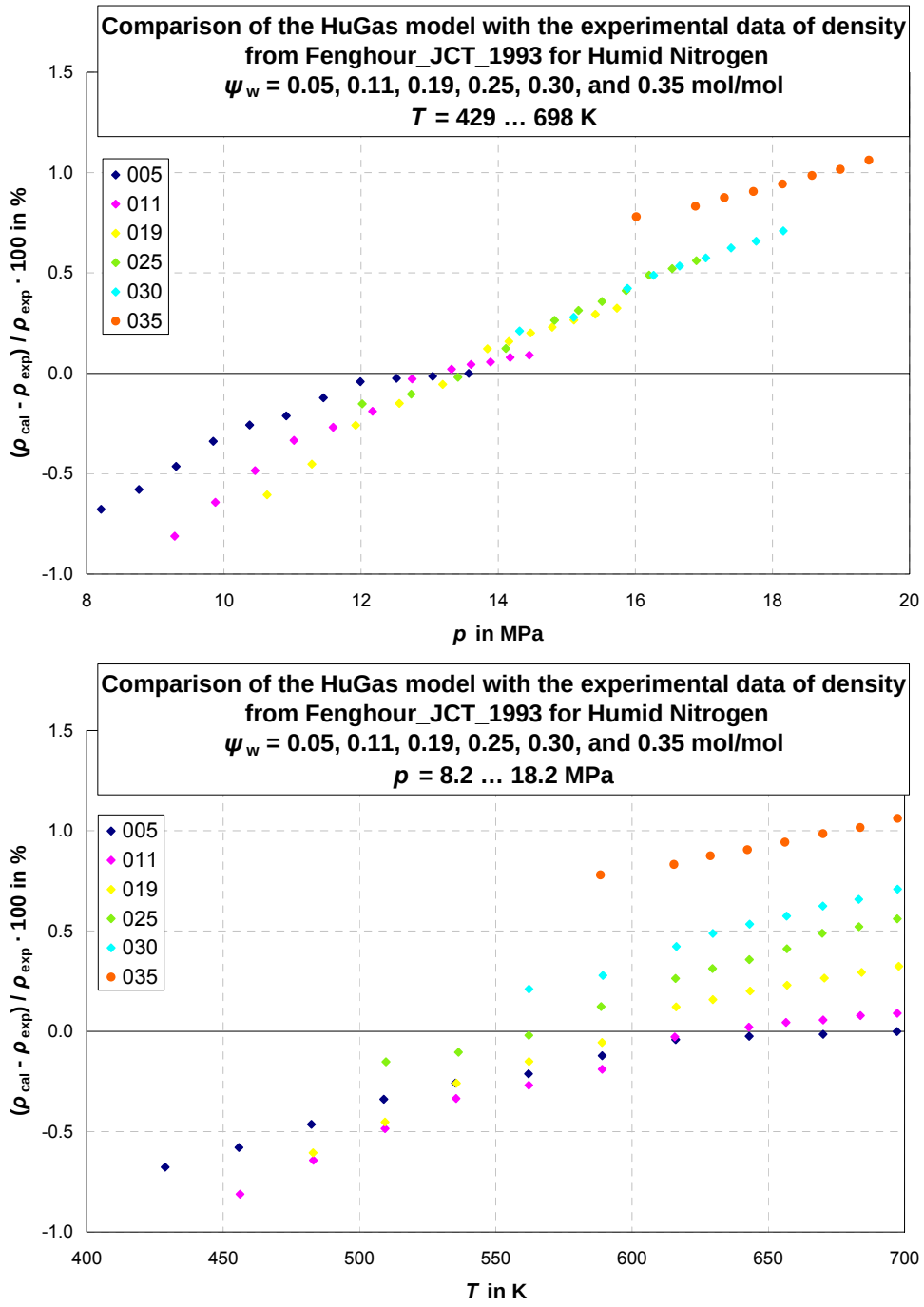

Figure 4.24: Relative deviations of the density values of nitrogen-water mixtures calculated for the HuGas model (listed in Table 4.1) from the experimental data of Fenghour and Wakeham (1993) [8] for mole fractions of water below 40% as a function of pressure and temperature.

Figure 4.24 makes obvious that the HuGas model is able to represent the experimental data for density within $\pm 1.1\%$. But the calculated values show systematic differences to the experimental data for density as a function of pressure and temperature. The calculated values are lower than the experimental ones at low pressures and temperatures. On the contrary, the calculated densities are higher than the experimental data at high pressures and temperatures.

4.3 Comparison on Composition of the Saturated State of Humid Air

4.3.1 Comparison between Calculated Values and Experimental Data for the Composition of Humid Air in the Saturated State

The available experimental data for the saturated state of humid air are summarized in Table 4.5. The dataset Kogl 07 [15] was measured within the project AA-CAES.

Table 4.5: Available experimental data for the saturated state of humid air.

Abbreviation	Property	Author(s)	T / K	p / MPa
Kogl 07	water-concentration enhancement factor	Koglbauer & Wendland 2007 (AA-CAES) [15]	293-413	0.1-25
Wylie 96	enhancement factor	Wylie & Fisher 1996 [6]	293-348	1.5-14
Hy 75	mole fraction of steam	Hyland *et al.* 1975 [3]	263-343	2-3.5
HW 73	mole fraction of steam	Hyland & Wexler 1973 [2]	303-323	1.0-10.3
Web 50	enhancement factor	Webster 1950 [5]	238-288	2.5-20
Poll 24	enhancement factor	Pollitzer & Strebel 1924 [4]	323	2.5-20
-	interaction coefficient	Goff & Bates 1941 [47]	278-298	0.1
-	solubility	Baldwin & Daniel 1952 [48], [49]	293	0.1
-	solubility	McKee 1953 [50]	273	3.5-20.7
-	solubility	Eichelberger 1955 [51]	298-338	6.7-24.1

Figure 4.25 presents an overview of the experimental data points for mole fraction of steam, steam-pressure enhancement factor, and water-concentration enhancement factor in a pressure-temperature diagram.

Figure 4.26 illustrates the deviations of the saturation-pressure values converted from the experimental data shown in Figure 4.25 for saturated humid air determined for different models.

Figure 4.26 and Figure 4.27 make obvious that the poynting correction of the ideal-mixing model HuGas, which is part of the property library LibHuGas and described in Section 3.3.2, does not represent the increase of the saturation pressure of steam in an appropriate manner. The deviations increase with increasing total pressure. The other models NEL, HyW, RB, and KTH represent the experimental data much better. The KTH model offers the best results with regard to the experimental data at pressures up to 14 MPa. At higher pressures, the RB model is characterised by the lowest deviations from the experimental data.

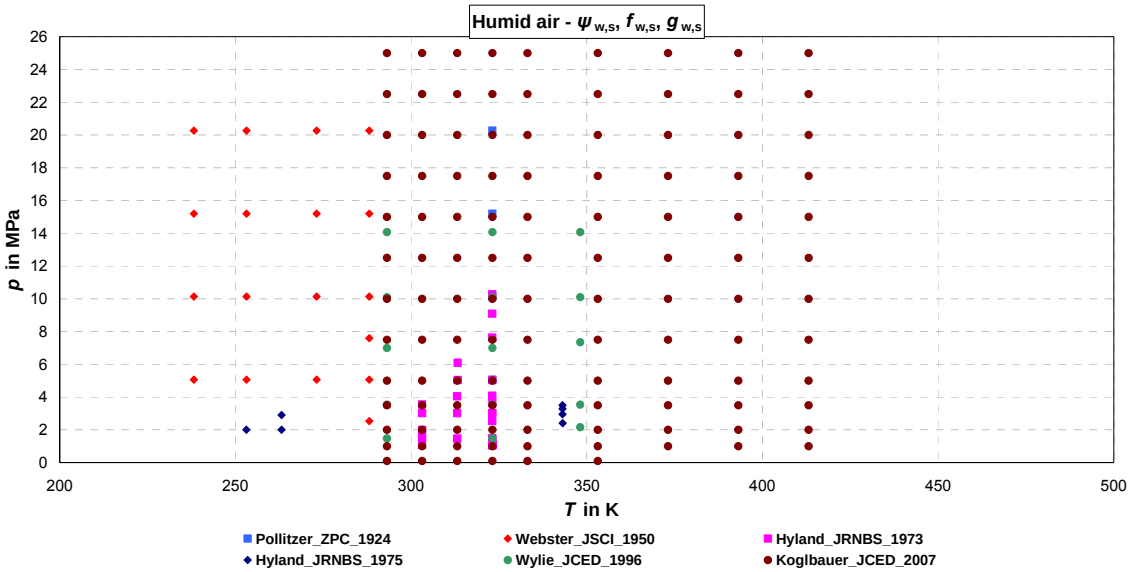

Figure 4.25: Pressure-temperature diagram with experimental data points for mole fraction of steam $\psi_{w,s}$, steam-pressure enhancement factor $f_{w,s}$, and water-concentration enhancement factor $g_{w,s}$ of humid air.

Figure 4.28 shows for the water-concentration enhancement factor experimentally determined by Wendland [15] once more that the poynting correction of the ideal-mixing model HuGas is too low. For the temperatures $T = 373$ K, $T = 393$ K, and $T = 413$ K, the values calculated from the NEL or HyW models are greater than the experimental data and the differences increase with increasing total pressure up to + 15% at 25 MPa. For $T = 333$ K and lower temperatures, the values calculated from the NEL or HyW models are less than the experimental data. The differences increase with increasing pressure up to – 10% at 22.5 MPa. For 353 K, the differences remain at – 3% also at high pressures. At pressures lower than 2 MPa the differences are less than 3%. The differences between the NEL and HyW models increase with increasing pressure up to 2%. This relatively small difference results from the fact that the NEL model is a further development of the HyW model. The RB model shows increasing deviations from the experimental data with increasing pressures up to – 20% at 25 MPa for temperatures between 303 K and 353 K. For the other isotherms, the differences increase with increasing pressure up from – 5% to – 10% at 25 MPa. The KTH model was not available for the comparison calculations with the Kogl 07 data.

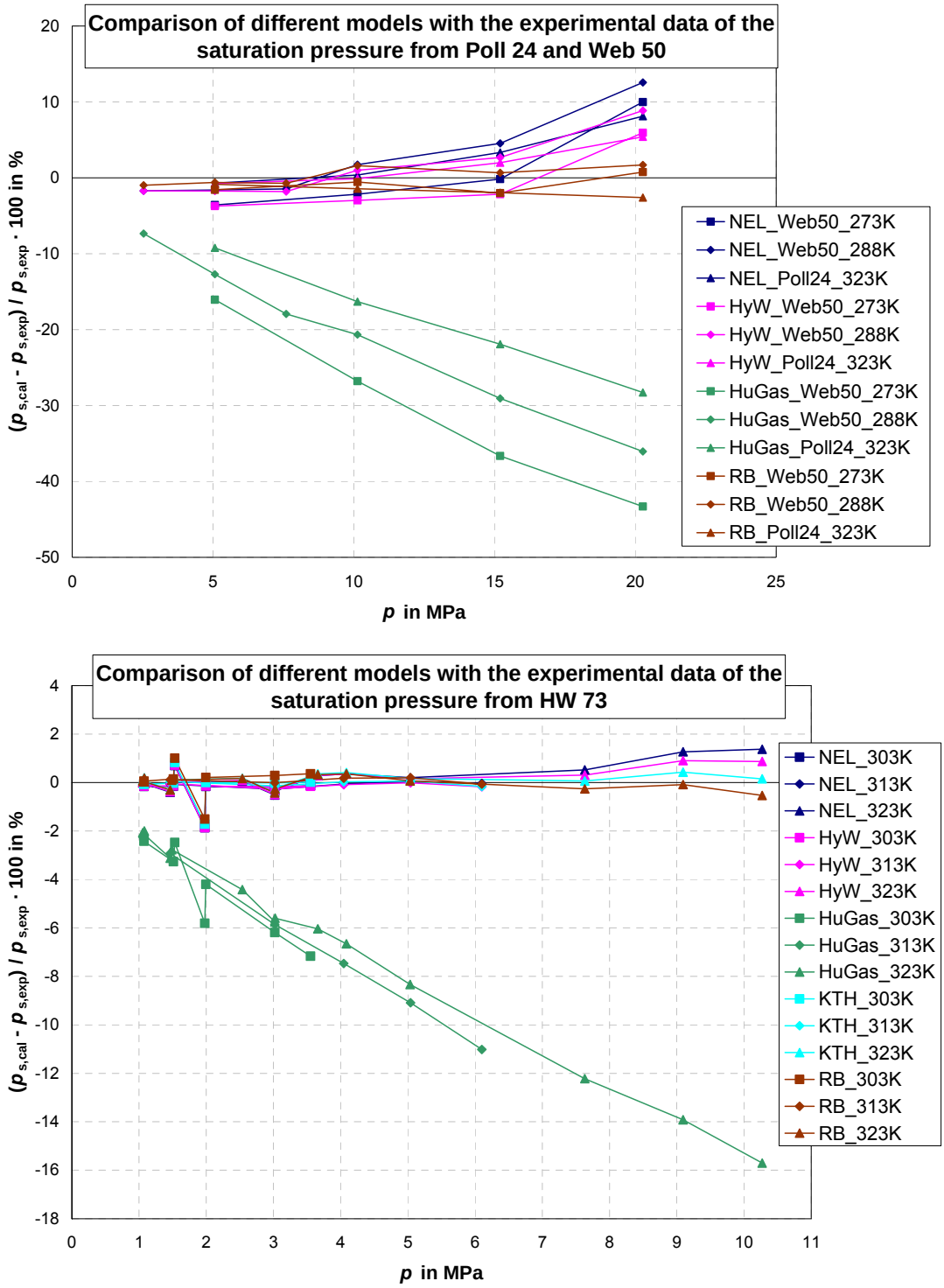

Figure 4.26: Relative deviations of saturation-pressure values for saturated humid air for the models listed in Table 4.1 from the experimental data of Table 4.5.

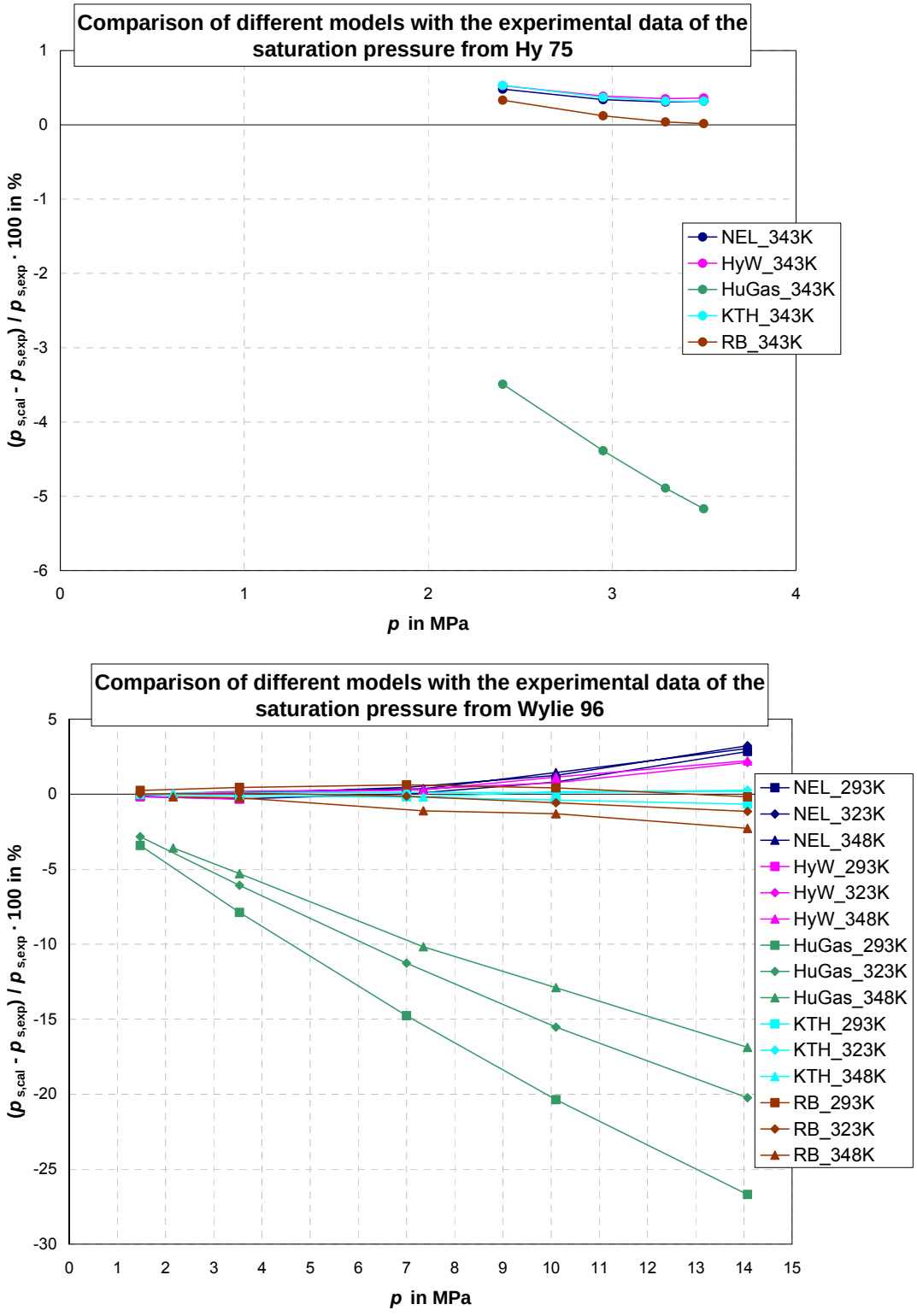

Figure 4.26: (continued)

Figure 4.27 summarises the results of the used models in comparison with all available experimental data except the Kogl 07 data.

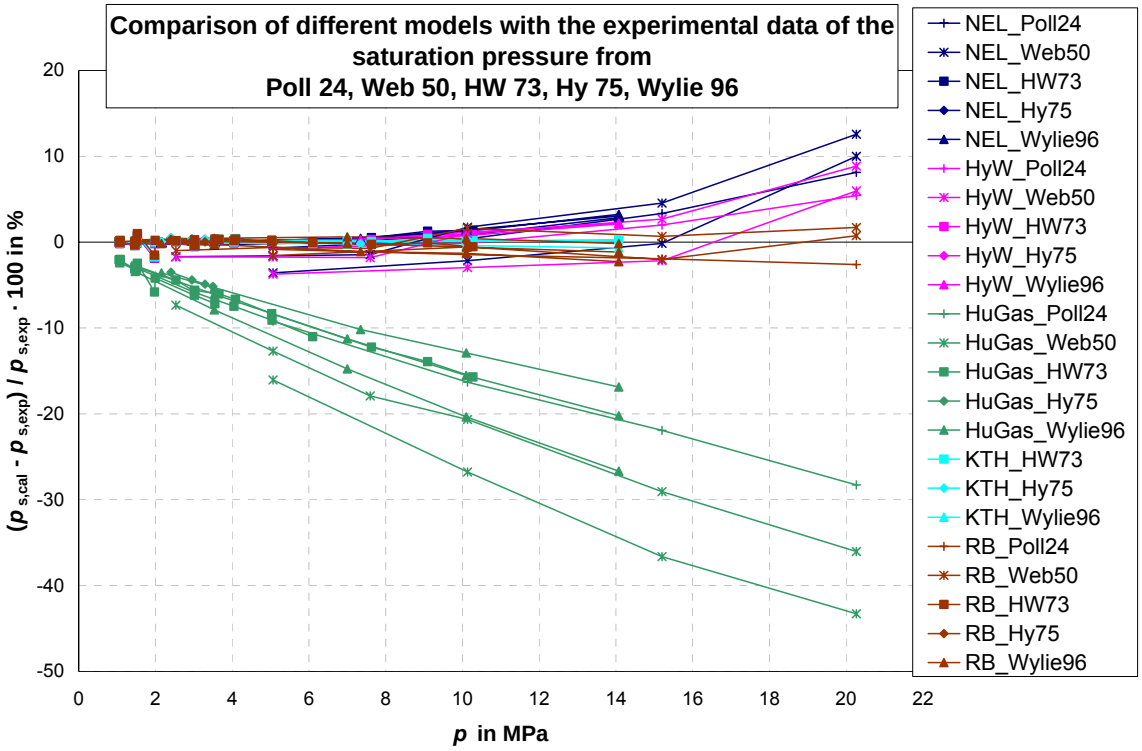

Figure 4.27: Summary of the relative deviations of saturation-pressure values for saturated humid air calculated for the models listed in Table 4.1 from the experimental data of Table 4.5.

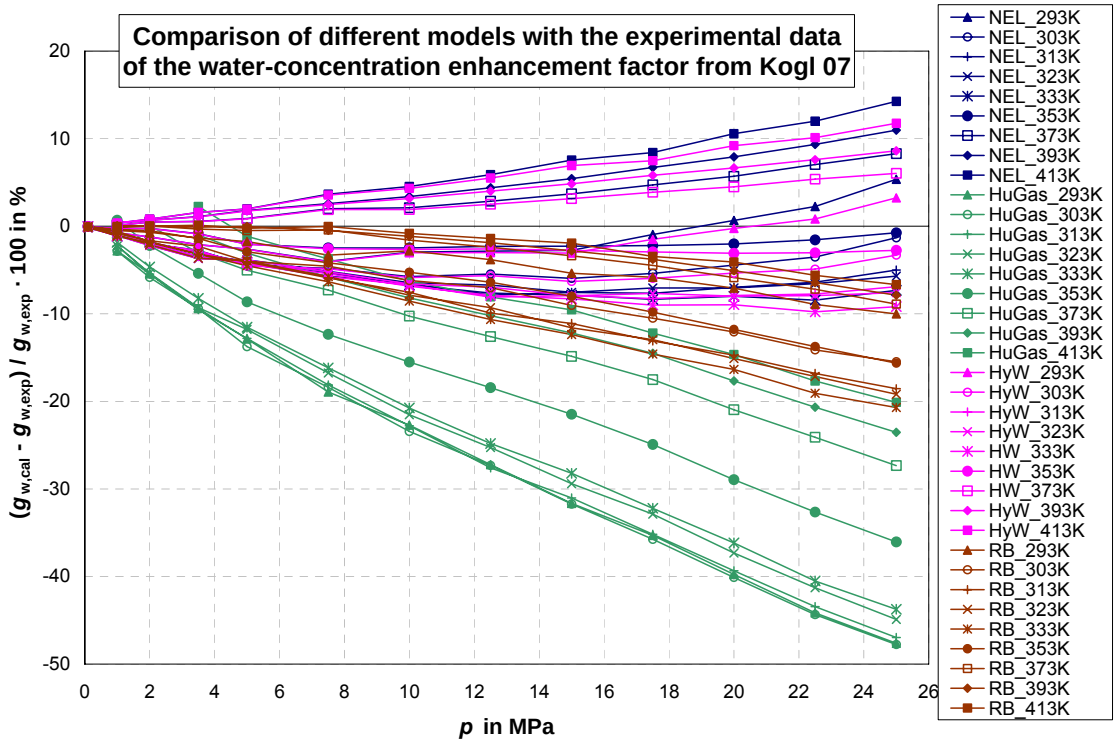

Figure 4.28: Relative deviations of the values of the water-concentration enhancement factor for saturated humid air calculated for the models listed in Table 4.1 from the experimental data of Koglbauer and Wendland [15].

4.3.2 Comparison on Calculated Partial Saturation-Pressure Values of Water Vapour for Different Models

A comparison of the partial saturation-pressure values of water vapour calculated from the models listed in Table 4.1 has been carried out. The results of these comparisons are presented in Figure 4.29 over temperature at certain values of constant total pressure. This corresponds to that of the mole fraction of water in the gas phase.

The multi-component model of Kunz *et al.* [42] could not be considered because its numerical details were not available during the period of work in the AA-CAES project.

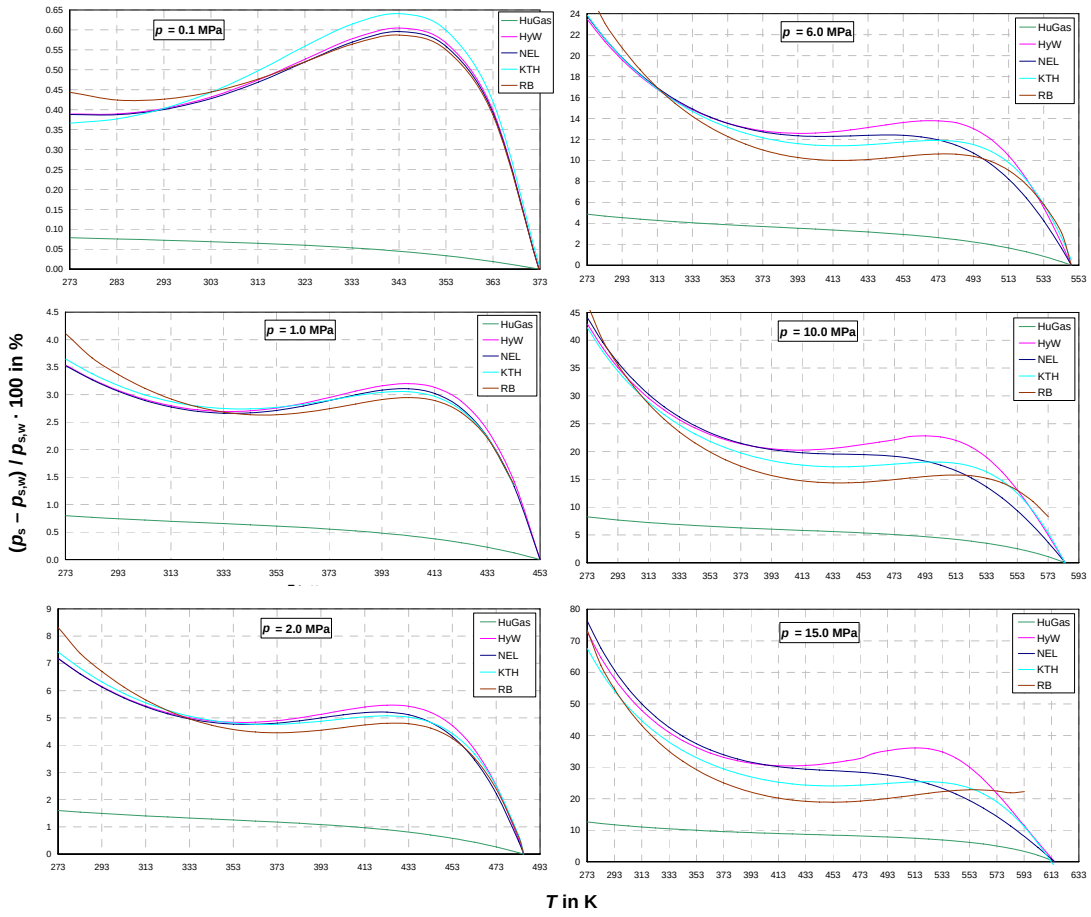

Figure 4.29: Relative enhancement of the partial saturation-pressure of steam in humid air for different models for certain pressures as a function of temperature.

Figure 4.29 makes evident that the poynting correction of the ideal-mixing model HuGas described in Section 3.3.2 does not represent the increase of the partial saturation-pressure of steam in an adequate manner. The HyW, NEL, RB, and KTH models show nearly the same behaviour, but differ a little bit at total pressures higher than 5 MPa. At the saturation temperature for the pressures 10 MPa and 15 MPa, the RB model is characterised by a problem in the calculation algorithm, because the values for the RB model do not reach zero at T_s.

Figure 4.30 summarises the results calculated for the enhancement of the saturation pressure of water in humid air for different models as a function of temperature for total

pressures from ambient to 15 MPa. While the maximum enhancement at 15 MPa and 273.15 K amounts to 13% for the HuGas model, the corresponding value amounts to 74% for the NEL model, to 72% for the HyW and RB models, and to 68% for the KTH model.

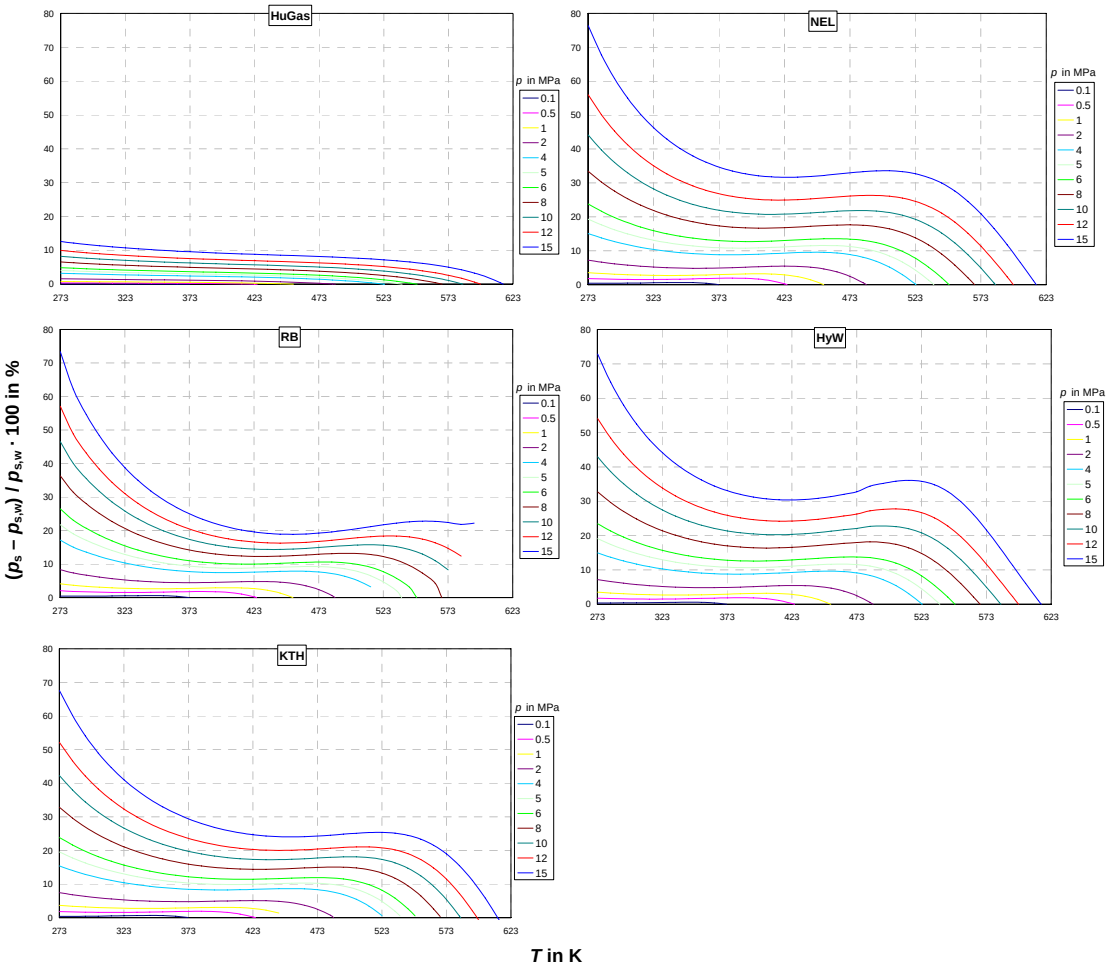

Figure 4.30: Relative change of enhancement of the saturation pressures for steam in humid air for different models at different constant total pressures as a function of temperature.

4.4 Conclusions from the Comparisons of the Investigated Models

Only experimental data generated within the AA-CAES project were suitable for comparisons concerning the density. In the case of the speed of sound, only one data set measured within the AA-CAES project at ICSTM was used for a comparison.

The following three statements based on the results for the deviations of the calculated values from the experimental data shall be given.

- No significant differences occur between all models apart from the IdGas model for density in comparison to experimental data. This behaviour was found for all three data sets measured independently with different techniques. That means either the models do not describe the truth correctly or the experimental data are uncertain. There were heavy problems in measuring the properties of humid air because of corrosion in the measuring cells. In general, relative deviations of the calculated density values from the experimental data up to – 2% have to be

expected for water contents between 1 and 5 mole% which are of relevance for AA-CAES cycles.

- In the case of the speed of sound, the RB, HuGas, HuAir, and SKU models show a better agreement with the experimental data than the HyW and NEL models.
- The IdGas, KTH, NEL, and HyW models and to a certain degree the HuGas model do not meet the experimental data for density and speed of sound for dry air in comparison with the SKU and HuAir models.

Table 4.6 summarizes the ability of the various models, considered in the project including the new model SKU, to represent experimental data for different thermodynamic properties of dry and humid air. The symbols have the following meanings:

— shows that the model does not describe the experimental data in an acceptable manner,
○ shows that the model represents the experimental data in an acceptable manner,
+ shows that the model predicts the experimental data very well,
an empty cell shows that this model was not considered in this comparison.

Finally, the following statements are to be added:

- The SKU and HuAir models have the advantage that dry air is calculated very accurately because of the used fundamental equation of state by Lemmon *et al.* However, the poynting correction of the HuGas model calculates values that are too low for the partial saturation-pressure of steam and therefore for the steam content of saturated humid air.
- The KTH, RB, NEL, and HyW models calculate the poynting correction with more realistic results.
- The RB model cannot be used at temperatures above 400 K.
- The NEL and KTH models show significant deviations for the density at high temperatures and pressures.

Table 4.6: Qualitative judgement of the considered models including the new SKU model to represent experimental data for different thermodynamic properties of dry and humid air.

	IdGas	HuGas	HuAir	KTH	RB	HyW	NEL	SKU
Density, exp. data (4.1.1 and 4.2.1)[1]	—	○	○	○	○	○	○	○
Speed of sound, exp. data (4.1.2)[1]		+	+		+	○	○	+
Saturated state, exp. data (4.3.1)[2]		—	+[3]	+	+	+	+	+[3]

Table 4.7 gives an overview of the comparison of calculated values from the considered models over wide pressure and temperature ranges. The symbols have the following meanings:

- — shows that the model deviates from the values calculated using the SKU model in the considered ranges of pressure (0.1 MPa to 15 MPa) and temperature (273.15 K to 2000 K),
- ○ shows that the model leads to minor problems in comparison to values calculated with the SKU model in the considered ranges of pressure (0.1 MPa to 15 MPa) and temperature (273.15 K to 2000 K),
- + shows that the model leads to reasonable results in comparison to values calculated with the SKU model in the considered ranges of pressure (0.1 MPa to 15 MPa) and temperature (273.15 K to 2000 K),
  an empty cell shows that this model was not considered in this comparison.

It is evident that the SKU model is favourable to calculate the thermodynamic properties of dry and humid air. The NEL model is to be preferred to calculate the saturation composition of humid air. As a consequence, the NEL model was included as part of the SKU model for calculating thermodynamic properties of humid air.
The multi-component model of Kunz *et al.* [42] should be considered in further investigations.

[1] Comparisons to experimental data for dry and humid air considered for the judgement are given in these sections of Chapter 4.
[2] Comparisons to experimental data for humid air only considered for the judgement are given in this section of Chapter 4.
[3] The composition of the saturated state of humid air is calculated using the NEL model.

Table 4.7: Qualitative judgement of the considered models including the new SKU model to predict thermodynamic properties for dry and humid air in the ranges of pressure (0.1 MPa to 15 MPa) and temperature (273.15 K to 2000 K).

	IdGas	**HuGas**	**HuAir**	**KTH**	**RB**	**HyW**	**NEL**	**SKU**
Density, cal. values (4.2.2)[4]	−	+	+	−	+	○	○	+
Isobaric heat capacity, cal. values (4.2.3)[4]	−	+	+		○	○	○	+
Saturated state, cal. values (4.3.2)[4]		−	+[5]	+	○	+	+	+[5]

[4] Comparisons between different models for dry and humid air considered for the judgement are given in this section of Chapter 4.

[5] The composition of the saturated state of humid air is calculated using the NEL model.

5 Recommended Model for Thermodynamic Properties

The recommended SKU model (SKU is the shortcut of Span[6], Kretzschmar[7], Ulbig[8], and Herrmann[9]) treats humid air as an ideal mixture of the real fluids dry air and water. The thermodynamic properties of dry air are calculated from the NIST standard of Lemmon *et al.* [1], those of steam and liquid water from the IAPWS-95 standard [18], [19], and those of ice crystals from the IAPWS Release 2006 [52], [53]. Additional contributions to the thermodynamic properties due to the dissociation of the components at high temperatures result from a model described in the VDI-Guideline 4670 [16], [23].
The calculation of the saturated state composition is performed with the NEL model [38], [39], which was investigated with correlated second virial coefficients for water-water interactions and air-water interactions by Harvey *et al.* [55], [56].
The model SKU can be used in the following ranges of temperature and pressure:

T = 243.15 K … 2000 K and p = 611.2 Pa … 100 MPa,

with the limitation that the partial pressure of steam is restricted to 16 MPa.

5.1 Dry Air

The thermodynamic properties of dry air are calculated using the NIST standard of Lemmon *et al.* [1]. It consists of a fundamental equation for the molar Helmholtz energy a_a as a function of molar density ρ_a and temperature T. The dimensionless form reads

$$\frac{a_\mathrm{a}(\rho_\mathrm{a},T)}{R^{Lem}T} = \alpha_\mathrm{a}(\delta_\mathrm{a},\tau_\mathrm{a}) = \alpha_\mathrm{a}^\mathrm{o}(\delta_\mathrm{a},\tau_\mathrm{a}) + \alpha_\mathrm{a}^\mathrm{r}(\delta_\mathrm{a},\tau_\mathrm{a}) \tag{5.1}$$

where

$\alpha_\mathrm{a}^\mathrm{o}(\delta_\mathrm{a},\tau_\mathrm{a})$ is the ideal-gas contribution,

$\alpha_\mathrm{a}^\mathrm{r}(\delta_\mathrm{a},\tau_\mathrm{a})$ is the residual contribution,

with

$$\delta_\mathrm{a} = \frac{\rho_\mathrm{a}}{\rho_\mathrm{j,a}} \tag{5.2}$$

is the reduced density, where ρ_a is the molar density of dry air,

$$\tau_\mathrm{a} = \frac{T_\mathrm{j,a}}{T_\mathrm{a}} \tag{5.3}$$

is the reciprocal reduced temperature, and $\rho_\mathrm{j,a}$, $T_\mathrm{j,a}$, R^{Lem} taken from Table 5.1.

[6] Prof. Dr.-Ing. Roland Span, Lehrstuhl für Thermodynamik, Ruhr-Universität Bochum, Germany.
[7] Prof. Dr.-Ing. Hans-Joachim Kretzschmar, Department of Technical Thermodynamics, University of Applied Sciences Zittau/Goerlitz, Germany.
[8] Dr.-Ing. Peter Ulbig, Department of Analytical Measuring Techniques and Pressure, Physikalisch-Technische Bundesanstalt Braunschweig, Germany.
[9] Dipl.-Ing. (FH) Sebastian Herrmann, Chair of Technical Thermodynamics / Department of Physical Chemistry, University of Rostock, Germany.

This fundamental equation allows calculating all thermodynamic properties from the equation itself and from its first, second, and mixed derivatives with respect to reduced density and reciprocal reduced temperature:

$$\alpha^{\mathrm{o}}_{\delta,\mathrm{a}} = \left(\frac{\partial \alpha^{\mathrm{o}}}{\partial \delta}\right)_{\tau_\mathrm{a},\mathrm{a}},\ \alpha^{\mathrm{o}}_{\delta\delta,\mathrm{a}} = \left(\frac{\partial^2 \alpha^{\mathrm{o}}}{\partial \delta^2}\right)_{\tau_\mathrm{a},\mathrm{a}},\ \alpha^{\mathrm{o}}_{\tau,\mathrm{a}} = \left(\frac{\partial \alpha^{\mathrm{o}}}{\partial \tau}\right)_{\delta_\mathrm{a},\mathrm{a}},$$

$$\alpha^{\mathrm{o}}_{\tau\tau,\mathrm{a}} = \left(\frac{\partial^2 \alpha^{\mathrm{o}}}{\partial \tau^2}\right)_{\delta_\mathrm{a},\mathrm{a}},\ \alpha^{\mathrm{o}}_{\delta\tau,\mathrm{a}} = \left(\frac{\partial^2 \alpha^{\mathrm{o}}}{\partial \delta\, \partial \tau}\right)_{\mathrm{a}}, \tag{5.4}$$

$$\alpha^{\mathrm{r}}_{\delta,\mathrm{a}} = \left(\frac{\partial \alpha^{\mathrm{r}}}{\partial \delta}\right)_{\tau_\mathrm{a},\mathrm{a}},\ \alpha^{\mathrm{r}}_{\delta\delta,\mathrm{a}} = \left(\frac{\partial^2 \alpha^{\mathrm{r}}}{\partial \delta^2}\right)_{\tau_\mathrm{a},\mathrm{a}},\ \alpha^{\mathrm{r}}_{\tau,\mathrm{a}} = \left(\frac{\partial \alpha^{\mathrm{r}}}{\partial \tau}\right)_{\delta_\mathrm{a},\mathrm{a}},$$

$$\alpha^{\mathrm{r}}_{\tau\tau,\mathrm{a}} = \left(\frac{\partial^2 \alpha^{\mathrm{r}}}{\partial \tau^2}\right)_{\delta_\mathrm{a},\mathrm{a}},\ \alpha^{\mathrm{r}}_{\delta\tau,\mathrm{a}} = \left(\frac{\partial^2 \alpha^{\mathrm{r}}}{\partial \delta\, \partial \tau}\right)_{\mathrm{a}}. \tag{5.5}$$

The most important thermodynamic properties are:

Molar and specific volume and density

Using the fundamental equation the molar density ρ_a (or molar volume $v_\mathrm{a} = 1/\rho_\mathrm{a}$) can be calculated iteratively for from the following expression:

$$p_\mathrm{a}(\rho_\mathrm{a}, T) = R^{Lem}\, T \rho_\mathrm{a} \left[1 + \delta_\mathrm{a}\, \alpha^{\mathrm{r}}_{\delta,\mathrm{a}}\right]. \tag{5.6}$$

After iterating ρ_a, the mass density $\tilde{\rho}_\mathrm{a}$ (or specific volume $\tilde{v}_\mathrm{a} = 1/\tilde{\rho}_\mathrm{a}$) is calculated from the equation

$$\tilde{\rho}_\mathrm{a} = \rho_\mathrm{a}\, M_\mathrm{a}\,. \tag{5.7}$$

Isobaric heat capacity

$$c_{p,\mathrm{a}}(\rho_\mathrm{a}, T) = R^{Lem} \left[-\tau_\mathrm{a}^2 \left(\alpha^{\mathrm{o}}_{\tau\tau,\mathrm{a}} + \alpha^{\mathrm{r}}_{\tau\tau,\mathrm{a}}\right) + \frac{\left(1 + \delta_\mathrm{a}\, \alpha^{\mathrm{r}}_{\delta,\mathrm{a}} - \delta_\mathrm{a}\, \tau_\mathrm{a}\, \alpha^{\mathrm{r}}_{\delta\tau,\mathrm{a}}\right)^2}{1 + 2\,\delta_\mathrm{a}\, \alpha^{\mathrm{r}}_{\delta,\mathrm{a}} + \delta_\mathrm{a}^2\, \alpha^{\mathrm{r}}_{\delta\delta,\mathrm{a}}} \right],\ \tilde{c}_{p,\mathrm{a}} = \frac{c_{p,\mathrm{a}}}{M_\mathrm{a}}. \tag{5.8}$$

Isochoric heat capacity

$$c_{v,\mathrm{a}}(\rho_\mathrm{a}, T) = -R^{Lem} \tau_\mathrm{a}^2 \left(\alpha^{\mathrm{o}}_{\tau\tau,\mathrm{a}} + \alpha^{\mathrm{r}}_{\tau\tau,\mathrm{a}}\right),\ \tilde{c}_{v,\mathrm{a}} = \frac{c_{v,\mathrm{a}}}{M_\mathrm{a}}. \tag{5.9}$$

Enthalpy

$$h_\mathrm{a}(\rho_\mathrm{a}, T) = R^{Lem}\, T \left[\tau_\mathrm{a} \left(\alpha^{\mathrm{o}}_{\tau,\mathrm{a}} + \alpha^{\mathrm{r}}_{\tau,\mathrm{a}}\right) + \delta_\mathrm{a}\, \alpha^{\mathrm{r}}_{\delta,\mathrm{a}} + 1\right],\ \tilde{h}_\mathrm{a} = \frac{h_\mathrm{a}}{M_\mathrm{a}}. \tag{5.10}$$

Internal energy

$$u_\mathrm{a}(\rho_\mathrm{a},T) = R^{Lem}\,T\,\tau_\mathrm{a}\left(\alpha^\mathrm{o}_{\tau,\mathrm{a}} + \alpha^\mathrm{r}_{\tau,\mathrm{a}}\right),\quad \tilde{u}_\mathrm{a} = \frac{u_\mathrm{a}}{M_\mathrm{a}}\,. \tag{5.11}$$

Entropy

$$s_\mathrm{a}(\rho_\mathrm{a},T) = R^{Lem}\left[\tau_\mathrm{a}\left(\alpha^\mathrm{o}_{\tau,\mathrm{a}} + \alpha^\mathrm{r}_{\tau,\mathrm{a}}\right) - \alpha^\mathrm{o}_\mathrm{a} - \alpha^\mathrm{r}_\mathrm{a}\right],\quad \tilde{s}_\mathrm{a} = \frac{s_\mathrm{a}}{M_\mathrm{a}}\,. \tag{5.12}$$

Speed of sound

$$w_\mathrm{a}(\rho_\mathrm{a},T) = \sqrt{\frac{1}{M_\mathrm{a}}\frac{c_{p,\mathrm{a}}}{c_{v,\mathrm{a}}}\left(\frac{\partial p}{\partial \rho}\right)_{T,\mathrm{a}}}\,, \tag{5.13}$$

where

$$\left(\frac{\partial p}{\partial \rho}\right)_{T,\mathrm{a}}(\rho_\mathrm{a},T) = R^{Lem}\,T\left(1 + 2\,\delta_\mathrm{a}\,\alpha^\mathrm{r}_{\delta,\mathrm{a}} + \delta_\mathrm{a}^2\,\alpha^\mathrm{r}_{\delta\delta,\mathrm{a}}\right). \tag{5.14}$$

Isentropic exponent

$$\kappa_\mathrm{a}(\rho_\mathrm{a},T) = \frac{w_\mathrm{a}^2\,\rho_\mathrm{a}}{p\,M_\mathrm{a}}\,. \tag{5.15}$$

Table 5.1: Constants used in the equations by Lemmon *et al.* [1].

Constant	**Air** [1]
M_a / kg kmol^{-1}	28.958 6
$\tilde{R}_\mathrm{a}$ / kJ kg^{-1} K^{-1}	(0.287 117)[10]
R^{Lem} / kJ kmol^{-1} K^{-1}	8.314 510
$T_{\mathrm{j,a}}$ / K	132.631 2
$\rho_{\mathrm{j,a}}$ / kmol m^{-3}	10.447 7

5.2 Steam, Liquid Water, and Ice

Steam and liquid water

For calculating the thermodynamic properties of steam and water, the international standard for scientific and general use IAPWS-95 [18], [19] is applied. This standard consists of a fundamental equation for the specific Helmholtz energy $\tilde{a}_\mathrm{w}$ as a function of density $\tilde{\rho}_\mathrm{w}$ and temperature T. The dimensionless form reads:

[10] Calculated from the equation $\tilde{R}_\mathrm{a} = R^{Lem} / M_\mathrm{a}$.

$$\frac{\tilde{a}_\mathrm{w}(\tilde{\rho}_\mathrm{w},T)}{\tilde{R}_\mathrm{w}\,T}=\alpha_\mathrm{w}(\delta_\mathrm{w},\tau_\mathrm{w})=\alpha_\mathrm{w}^\mathrm{o}(\delta_\mathrm{w},\tau_\mathrm{w})+\alpha_\mathrm{w}^\mathrm{r}(\delta_\mathrm{w},\tau_\mathrm{w}) \tag{5.16}$$

where

$\alpha_\mathrm{w}^\mathrm{o}(\delta_\mathrm{w},\tau_\mathrm{w})$ is the ideal-gas contribution,

$\alpha_\mathrm{w}^\mathrm{r}(\delta_\mathrm{w},\tau_\mathrm{w})$ is the residual contribution,

with

$\delta_\mathrm{w}=\dfrac{\tilde{\rho}_\mathrm{w}}{\tilde{\rho}_\mathrm{c,w}}$ is the reduced density, (5.17)

$\tau_\mathrm{w}=\dfrac{T_\mathrm{c,w}}{T_\mathrm{w}}$ is the reciprocal reduced temperature, (5.18)

and $\tilde{\rho}_\mathrm{c,w}$, $T_\mathrm{c,w}$, $\tilde{R}_\mathrm{w}$ from Table 5.2.

All thermodynamic properties are calculated from density and temperature using Eq. (5.16).

$$\alpha_{\delta,\mathrm{w}}^\mathrm{o}=\left(\frac{\partial\alpha^\mathrm{o}}{\partial\delta}\right)_{\tau_\mathrm{w},\mathrm{w}},\ \alpha_{\delta\delta,\mathrm{w}}^\mathrm{o}=\left(\frac{\partial^2\alpha^\mathrm{o}}{\partial\delta^2}\right)_{\tau_\mathrm{w},\mathrm{w}},\ \alpha_{\tau,\mathrm{w}}^\mathrm{o}=\left(\frac{\partial\alpha^\mathrm{o}}{\partial\tau}\right)_{\delta_\mathrm{w},\mathrm{w}},$$
$$\alpha_{\tau\tau,\mathrm{w}}^\mathrm{o}=\left(\frac{\partial^2\alpha^\mathrm{o}}{\partial\tau^2}\right)_{\delta_\mathrm{w},\mathrm{w}},\ \alpha_{\delta\tau,\mathrm{w}}^\mathrm{o}=\left(\frac{\partial^2\alpha^\mathrm{o}}{\partial\delta\,\partial\tau}\right)_\mathrm{w}, \tag{5.19}$$

$$\alpha_{\delta,\mathrm{w}}^\mathrm{r}=\left(\frac{\partial\alpha^\mathrm{r}}{\partial\delta}\right)_{\tau_\mathrm{w},\mathrm{w}},\ \alpha_{\delta\delta,\mathrm{w}}^\mathrm{r}=\left(\frac{\partial^2\alpha^\mathrm{r}}{\partial\delta^2}\right)_{\tau_\mathrm{w},\mathrm{w}},\ \alpha_{\tau,\mathrm{w}}^\mathrm{r}=\left(\frac{\partial\alpha^\mathrm{r}}{\partial\tau}\right)_{\delta_\mathrm{w},\mathrm{w}},$$
$$\alpha_{\tau\tau,\mathrm{w}}^\mathrm{r}=\left(\frac{\partial^2\alpha^\mathrm{r}}{\partial\tau^2}\right)_{\delta_\mathrm{w},\mathrm{w}},\ \alpha_{\delta\tau,\mathrm{w}}^\mathrm{r}=\left(\frac{\partial^2\alpha^\mathrm{r}}{\partial\delta\,\partial\tau}\right)_\mathrm{w}. \tag{5.20}$$

The most important properties are:

Density and specific and molar volume

Using the fundamental equation the mass density $\tilde{\rho}_\mathrm{w}$ (or specific volume $\tilde{v}_\mathrm{w}=1/\tilde{\rho}_\mathrm{w}$) can be calculated iteratively for from the following expression:

$$p(\tilde{\rho}_\mathrm{w},T)=\tilde{R}_\mathrm{w}\,T\tilde{\rho}_\mathrm{w}\left[1+\delta_\mathrm{w}\,\alpha_{\delta,\mathrm{w}}^\mathrm{r}\right]. \tag{5.21}$$

After iterating $\tilde{\rho}_\mathrm{w}$, the molar density ρ_w (or molar volume $v_\mathrm{w}=1/\rho_\mathrm{w}$) is calculated from the equation

$$\tilde{\rho}_\mathrm{w}=\rho_\mathrm{w}\,M_\mathrm{w}. \tag{5.22}$$

Isobaric heat capacity

$$\tilde{c}_{p,\mathrm{w}}(\tilde{\rho}_\mathrm{w},T)=\tilde{R}_\mathrm{w}\left[-\tau_\mathrm{w}^2\left(\alpha_{\tau\tau,\mathrm{w}}^\mathrm{o}+\alpha_{\tau\tau,\mathrm{w}}^\mathrm{r}\right)+\frac{\left(1+\delta_\mathrm{w}\,\alpha_{\delta,\mathrm{w}}^\mathrm{r}-\delta_\mathrm{w}\,\tau_\mathrm{w}\,\alpha_{\delta\tau,\mathrm{w}}^\mathrm{r}\right)^2}{1+2\,\delta_\mathrm{w}\,\alpha_{\delta,\mathrm{w}}^\mathrm{r}+\delta_\mathrm{w}^2\,\alpha_{\delta\delta,\mathrm{w}}^\mathrm{r}}\right],$$

$$c_{p,\mathrm{w}}=\tilde{c}_{p,\mathrm{w}}M_\mathrm{w}\,. \tag{5.23}$$

Isochoric heat capacity

$$\tilde{c}_{v,\mathrm{w}}(\tilde{\rho}_\mathrm{w},T)=-\tilde{R}_\mathrm{w}\tau_\mathrm{w}^2\left(\alpha_{\tau\tau,\mathrm{w}}^\mathrm{o}+\alpha_{\tau\tau,\mathrm{w}}^\mathrm{r}\right),\quad c_{v,\mathrm{w}}=\tilde{c}_{v,\mathrm{w}}M_\mathrm{w}\,. \tag{5.24}$$

Enthalpy

$$\tilde{h}_\mathrm{w}(\tilde{\rho}_\mathrm{w},T)=\tilde{R}_\mathrm{w}\,T\left[\tau_\mathrm{w}\left(\alpha_{\tau,\mathrm{w}}^\mathrm{o}+\alpha_{\tau,\mathrm{w}}^\mathrm{r}\right)+\delta_\mathrm{w}\,\alpha_{\delta,\mathrm{w}}^\mathrm{r}+1\right],\quad h_\mathrm{w}=\tilde{h}_\mathrm{w}M_\mathrm{w}\,. \tag{5.25}$$

Internal energy

$$\tilde{u}_\mathrm{w}(\tilde{\rho}_\mathrm{w},T)=\tilde{R}_\mathrm{w}\,T\tau_\mathrm{w}\left(\alpha_{\tau,\mathrm{w}}^\mathrm{o}+\alpha_{\tau,\mathrm{w}}^\mathrm{r}\right),\quad u_\mathrm{w}=\tilde{u}_\mathrm{w}M_\mathrm{w}\,. \tag{5.26}$$

Entropy

$$\tilde{s}_\mathrm{w}(\tilde{\rho}_\mathrm{w},T)=\tilde{R}_\mathrm{w}\left[\tau_\mathrm{w}\left(\alpha_{\tau,\mathrm{w}}^\mathrm{o}+\alpha_{\tau,\mathrm{w}}^\mathrm{r}\right)-\alpha_\mathrm{w}^\mathrm{o}-\alpha_\mathrm{w}^\mathrm{r}\right],\quad s_\mathrm{w}=\tilde{s}_\mathrm{w}M_\mathrm{w}\,. \tag{5.27}$$

Speed of sound

$$w_\mathrm{w}(\tilde{\rho}_\mathrm{w},T)=\sqrt{\frac{\tilde{c}_{p,\mathrm{w}}}{\tilde{c}_{v,\mathrm{w}}}\left(\frac{\partial p}{\partial\tilde{\rho}}\right)_{T,\mathrm{w}}} \tag{5.28}$$

where

$$\left(\frac{\partial p}{\partial\tilde{\rho}}\right)_{T,\mathrm{w}}(\tilde{\rho}_\mathrm{w},T)=\tilde{R}_\mathrm{w}\,T\left(1+2\,\delta_\mathrm{w}\,\alpha_{\delta,\mathrm{w}}^\mathrm{r}+\delta_\mathrm{w}^2\,\alpha_{\delta\delta,\mathrm{w}}^\mathrm{r}\right). \tag{5.29}$$

Isentropic exponent

$$\kappa_\mathrm{w}(\tilde{\rho}_\mathrm{w},T)=\frac{w_\mathrm{w}^2\,\tilde{\rho}_\mathrm{w}}{p}\,. \tag{5.30}$$

Ice

The thermodynamic properties of the ice crystals (i) in ice fog are calculated on the basis of the IAPWS Release on an equation of state for the Gibbs energy of H_2O Ice Ih [52], [53] using an equation for the Gibbs energy g_i as function of pressure p and temperature T:

$$g_{\mathrm{i}}(p,T) = g_{0,\mathrm{i}} - s_{0,\mathrm{i}}\, T_{\mathrm{t,i}}\, \tau_{\mathrm{i}} + T_{\mathrm{t,i}} \operatorname{Re}\left\{ \sum_{k=1}^{2} r_{k,\mathrm{i}} \left[\left(t_{k,\mathrm{i}} - \tau_{\mathrm{i}}\right) \ln\left(t_{k,\mathrm{i}} - \tau_{\mathrm{i}}\right) + \left(t_{k,\mathrm{i}} + \tau_{\mathrm{i}}\right) \ln\left(t_{k,\mathrm{i}} + \tau_{\mathrm{i}}\right) - 2\, t_{k,\mathrm{i}} \ln\left(t_{k,\mathrm{i}}\right) - \frac{\tau_{\mathrm{i}}^2}{t_{k,\mathrm{i}}} \right] \right\} \tag{5.31}$$

where

$$g_{0,\mathrm{i}}(p) = \sum_{k=0}^{4} g_{0k,\mathrm{i}} \left(\pi_{\mathrm{i}} - \pi_{0,\mathrm{i}}\right)^k \quad \text{and} \tag{5.32}$$

$$r_{2,\mathrm{i}}(p) = \sum_{k=0}^{2} r_{2k,\mathrm{i}} \left(\pi_{\mathrm{i}} - \pi_{0,\mathrm{i}}\right)^k \tag{5.33}$$

are pressure dependent expressions with

$g_{00,\mathrm{i}} \ldots g_{04,\mathrm{i}}$ are real coefficients,

$r_{20,\mathrm{i}} \ldots r_{22,\mathrm{i}}$ are complex coefficients,

$s_{0,\mathrm{i}}$ is a complex coefficient,

$n_{1,\mathrm{i}}$, $t_{1,\mathrm{i}}$, and $t_{2,\mathrm{i}}$ are complex coefficients.

All these coefficients are obtained from [52], [53], and

$$\pi_{\mathrm{i}} = \frac{p_{\mathrm{i}}}{p_{\mathrm{t,i}}}, \quad \pi_{0,\mathrm{i}} = \frac{p_{0,\mathrm{i}}}{p_{\mathrm{t,i}}}, \quad \tau_{\mathrm{i}} = \frac{T_{\mathrm{i}}}{T_{\mathrm{t,i}}}, \tag{5.34}$$

with $p_{\mathrm{t,i}}$, $p_{0,\mathrm{i}}$, and $T_{\mathrm{t,i}}$ from Table 5.2.

Important thermodynamic properties are given as:

Specific and molar volume

$$v_{\mathrm{i}}(p,T) = \left(\frac{\partial g_{\mathrm{i}}}{\partial p} \right)_T, \quad v_{\mathrm{i}} = \tilde{v}_{\mathrm{i}} M_{\mathrm{w}}. \tag{5.35}$$

Isobaric heat capacity

$$c_{p,\mathrm{i}}(p,T) = T \left(\frac{\partial s_{\mathrm{i}}}{\partial T} \right)_p, \quad c_{p,\mathrm{i}} = \tilde{c}_{p,\mathrm{i}} M_{\mathrm{w}}. \tag{5.36}$$

Enthalpy

$$\tilde{h}_{\mathrm{i}}(p,T) = g_{\mathrm{i}} + T\, \tilde{s}_{\mathrm{i}}, \quad h_{\mathrm{i}} = \tilde{h}_{\mathrm{i}} M_{\mathrm{w}}. \tag{5.37}$$

Internal energy

$$\tilde{u}_{\mathrm{i}}(p,T) = g_{\mathrm{i}} + T\, \tilde{s}_{\mathrm{i}} - p \tilde{v}_{\mathrm{i}}, \quad u_{\mathrm{i}} = \tilde{u}_{\mathrm{i}} M_{\mathrm{w}}. \tag{5.38}$$

Entropy

$$s_{\mathrm{i}}(p,T) = -\left(\frac{\partial g_{\mathrm{i}}}{\partial T}\right)_p , \quad s_{\mathrm{i}} = \tilde{s}_{\mathrm{i}} M_{\mathrm{w}} . \tag{5.39}$$

Table 5.2: Constants taken from IAPWS-95 [18], [19] for water and steam and from Feistel and Wagner [52], [53] for ice.

Constant	**Water and Steam** [18], [19]	Constant	**Ice** [52], [53]
M_{w} / kg kmol^{-1}	18.015 268	$R^{(11)}$ / kJ kmol^{-1} K^{-1}	8.314 472
$\tilde{R}_{\mathrm{w}}$ / kJ kg^{-1} K^{-1}	0.461 518 05	$T_{\mathrm{t,i}}$ / K	273.16
R^{95} / kJ kmol^{-1} K^{-1}	(8.314 371)[12]	$p_{0,\mathrm{i}}$ / MPa	0.101 325
$T_{\mathrm{c,w}}$ / K	647.096	$p_{\mathrm{t,i}}$ / MPa	0.000 611 657
$\tilde{\rho}_{\mathrm{c,w}}$ / kg m^{-3}	322.0		

5.3 Ideal Mixture of Dry Air and Steam, Liquid Water, or Ice

The SKU model allows calculating the thermodynamic properties of unsaturated and saturated humid air and of liquid fog and of ice fog. The treatment of these systems corresponds to an ideal mixing of real fluids, which means they are considered to be ideal mixtures of dry air and steam (and liquid water in case of liquid fog or ice in case of ice fog). The calculation procedure for unsaturated humid air is summarised in Section 5.3.1. The calculation for liquid fog and ice fog is described in the Sections 5.3.3 and 5.3.4. The virial equation of Nelson and Sauer is used for calculating the composition of the saturated state of humid air. This algorithm is presented in Section 5.4.

5.3.1 Composition of Humid Air

The humidity ratio (absolute humidity) x_{w} is defined as the quotient of the mass of water m_{w} in humid air divided by the mass of dry air m_{a} in humid air:

$$x_{\mathrm{w}} = \frac{m_{\mathrm{w}}}{m_{\mathrm{a}}} = \frac{m_{\mathrm{w}}}{\left(m - m_{\mathrm{w}}\right)}, \tag{5.40}$$

where m is the mass of the mixture humid air.

With the mole fraction ψ_{w} of water in humid air one obtains

$$x_{\mathrm{w}} = \varepsilon \frac{\psi_{\mathrm{w}}}{\left(1 - \psi_{\mathrm{w}}\right)}, \tag{5.41}$$

where ε is the quotient of the molar masses of dry air and water, Eq. (5.42).

[11] These value of the molar gas constant *R* is identically with the current value recommend by Mohr and Taylor [54]. Therefore, no particular label, e.g., "Lem" for air (**Lem**mon *et al.*), "95" for water and steam (IAPWS-**95**), is used.

[12] Calculated value.

The quotient of the molar masses of water and dry air is defined as

$$\varepsilon = \frac{M_\mathrm{w}}{M_\mathrm{a}} = \frac{\tilde{R}_\mathrm{a}}{\tilde{R}_\mathrm{w}}. \tag{5.42}$$

By solving Eq. (5.41) in terms of ψ_w one obtains

$$\psi_\mathrm{w} = \frac{x_\mathrm{w}}{\left(\varepsilon + x_\mathrm{w}\right)} \text{ and } \psi_\mathrm{a} = 1 - \psi_\mathrm{w}. \tag{5.43}$$

The molar mass of humid air M is calculated from the equation

$$M = \psi_\mathrm{a} M_\mathrm{a} + \psi_\mathrm{w} M_\mathrm{w}, \tag{5.44}$$

where M_a and M_w are the molar masses of dry air and water, given in Table 5.1 and Table 5.2.

Then, the specific gas constant of humid air results from

$$\tilde{R} = R / M. \tag{5.45}$$

For certain users, the mass fraction of water ξ_w in humid air is of interest. It can be obtained from the expression

$$\xi_\mathrm{w} = \frac{x_\mathrm{w}}{\left(1 + x_\mathrm{w}\right)} = \frac{M_\mathrm{w}}{M}\psi_\mathrm{w}, \; \xi_\mathrm{a} = 1 - \xi_\mathrm{w}. \tag{5.46}$$

Table 5.3: Constants and values used for the calculation of psychrometric properties of humid air.

Quantity	Symbol	Value	Reference
Universal molar gas constant	R	8.314 472 kJ/(kmol K)	[54]
Molar mass of dry air	M_a	28.958 6 kg/kmol	[1]
Molar mass of water	M_w	18.015 268 kg/kmol	[18], [19]
Specific gas constant of dry air	$\tilde{R}_\mathrm{a}$	≅ 0.287 116 kJ/(kg K)	
Specific gas constant of water	$\tilde{R}_\mathrm{w}$	≅ 0.461 524 kJ/(kg K)	
Quotient: $M_\mathrm{w} / M_\mathrm{a} = \tilde{R}_\mathrm{a} / \tilde{R}_\mathrm{w}$	ε	≅ 0.621 945	

5.3.2 Unsaturated and Saturated Humid Air

To implement the ideal mixing of real fluids for unsaturated humid air, the fundamental equation of state proposed by Lemmon *et al.* [1] is applied for dry air, whereas the scientific formulation IAPWS-95 [18], [19] is utilized for steam.

In addition for unsaturated or saturated humid air, the water content can be specified by the quantity relative humidity. The relative humidity φ is defined as the quotient of the mole fraction of water vapour ψ_w in humid air divided by the mole fraction of water vapour in the saturation state $\psi_\mathrm{s,w}$ at given total pressure p and temperature T:

$$\varphi = \frac{\psi_\mathrm{w}}{\psi_\mathrm{s,w}} \tag{5.47}$$

with the definition range $0 \le \varphi \le 1$; the value $\varphi = 0$ for dry air and $\varphi = 1$ for saturated humid air.

With the partial pressure of water vapour

$$p_{\mathrm{w}} = \psi_{\mathrm{w}}\, p \tag{5.48}$$

and the saturation pressure of humid air

$$p_{\mathrm{s}} = \psi_{\mathrm{s,w}}\, p \tag{5.49}$$

according Eq. (5.118), where p is the total pressure of humid air, one obtains

$$\varphi = \frac{p_{\mathrm{w}}}{p_{\mathrm{s}}}. \tag{5.50}$$

This equation is valid for $p_{\mathrm{w}} \le p_{\mathrm{s}}$.

As relation between humidity ratio and relative humidity the following equation is obtained

$$W = \varepsilon \frac{\varphi\, p_{\mathrm{s}}}{\left(p - \varphi\, p_{\mathrm{s}}\right)} \tag{5.51}$$

with ε as quotient of the molar masses of water and dry air, Eq. (5.42), and $p_{\mathrm{s}} = f\, p_{\mathrm{s,w}}$, where $f(p,T)$ is the vapour-pressure enhancement factor calculated from Eq. (5.103) for given total pressure p and temperature T. The saturation pressure of pure water $p_{\mathrm{s,w}}$ is calculated for given temperature T from Eq. (3.120).

Saturation State

The saturation state of humid air is characterized by

$p_{\mathrm{w}} = p_{\mathrm{s}}(p,T)$ according Eq. (5.118),

$\psi_{\mathrm{w}} = \psi_{\mathrm{s,w}}$ according Eq. (5.102),

$\varphi = 1$,

and therefore by

$$W_{\mathrm{s}} = \varepsilon \frac{\psi_{\mathrm{s,w}}}{\left(1 - \psi_{\mathrm{s,w}}\right)}, \tag{5.52}$$

where $\psi_{\mathrm{s,w}}$ is the mole fraction of water vapour in saturated humid air and ε is given in Eq. (5.42).

The equations for unsaturated humid air from the SKU model are given as follows:

Molar density and molar volume

The molar density ρ has to be calculated iteratively from the following expression for the mixture pressure p, temperature T, and composition Ψ:

$$p(\rho,T,\Psi) = \psi_{\mathrm{a}}\, p_{\mathrm{a}}(\rho,T) + p_{\mathrm{w}}(\rho_{\mathrm{w}},T) \tag{5.53}$$

where

ψ_a is the molar fraction of dry air in humid air,

p_a is the partial pressure of dry air at temperature T and molar mixture density ρ and reads:

$$p_a = \rho T R^{Lem}\left[1+\delta_a \alpha^r_{\delta,a}(\delta_a,\tau_a)\right] \tag{5.54}$$

with $\alpha^r_{\delta,a}$ from Eq. (5.5), $\delta_a = \rho/\rho_{j,a}$, $\tau_a = T_{j,a}/T$, where $\rho_{j,a}$, $T_{j,a}$, and R^{Lem} from Table 5.1,

p_w is the partial pressure of steam at temperature T and molar partial density of steam ρ_w and reads:

$$p_w = \rho_w T R^{95}\left[1+\delta_w \alpha^r_{\delta,w}(\delta_w,\tau_w)\right] \tag{5.55}$$

with $\alpha^r_{\delta,w}$ from Eq. (5.20), $\delta_w = \tilde{\rho}_w/\tilde{\rho}_{c,w}$, $\tau_w = T_{c,w}/T_w$, where

$\tilde{\rho}_w = \rho_w M_w$,

$\rho_w = \psi_w \rho$ with $\psi_w = 1-\psi_a$, and

$\tilde{\rho}_{c,w}$, $T_{c,w}$, R^{95}, and M_w from Table 5.2.

After iterating ρ, the molar volume v, the mass density $\tilde{\rho}$, and the specific volume $\tilde{v}$ are calculated from the equations

$$v = \frac{1}{\rho},\ \tilde{\rho} = \rho M \text{, and } \tilde{v} = \frac{v}{M} \tag{5.56}$$

with the molar mass M of the mixture resulting from Eq. (5.44).

For the application to humid combustion gases with *I* components as recommended in the ASME Report STP-TS-012 [57], the following equation for iteratively calculating the molar density ρ of the mixture can be used:

$$p(\rho,T,\Psi) = \sum_{i=1,i\neq w}^{I}\left[\psi_i\, p_i(\rho,T)\right] + p_w(\rho_w,T) \tag{5.57}$$

where Ψ is the vector of the mole fractions,

ψ_i is the mole fraction of the component *i*,

p_i is the partial pressure of the component *i* calculated for ρ and T from the fundamental equation of the component *i*,

p_w is the partial pressure of steam calculated for ρ_w and T from the fundamental equation of steam, and

$\rho_w = \psi_w \rho$ is the partial density of steam, where ψ_w is the mole fraction of steam.

Isobaric heat capacity

$$c_p(\rho,T,\Psi)=\psi_{\mathrm{a}}\,c_{p,\mathrm{a}}(\rho,T)+\psi_{\mathrm{w}}\,c_{p,\mathrm{w}}(\rho_{\mathrm{w}},T)+\Delta c_{p,\mathrm{dis}}(p,T,\Psi)\,,\quad \tilde{c}_p=\frac{c_p}{M} \tag{5.58}$$

where: Dry air

$$c_{p,\mathrm{a}}(\rho,T)=R^{Lem}\left[-\tau_{\mathrm{a}}^2\left(\alpha^{\mathrm{o}}_{\tau\tau,\mathrm{a}}+\alpha^{\mathrm{r}}_{\tau\tau,\mathrm{a}}\right)+\frac{\left(1+\delta_{\mathrm{a}}\,\alpha^{\mathrm{r}}_{\delta,\mathrm{a}}-\delta_{\mathrm{a}}\,\tau_{\mathrm{a}}\,\alpha^{\mathrm{r}}_{\delta\tau,\mathrm{a}}\right)^2}{1+2\,\delta_{\mathrm{a}}\,\alpha^{\mathrm{r}}_{\delta,\mathrm{a}}+\delta_{\mathrm{a}}^2\,\alpha^{\mathrm{r}}_{\delta\delta,\mathrm{a}}}\right] \tag{5.59}$$

Steam

$$c_{p,\mathrm{w}}(\rho_{\mathrm{w}},T)=R^{95}\left[-\tau_{\mathrm{w}}^2\left(\alpha^{\mathrm{o}}_{\tau\tau,\mathrm{w}}+\alpha^{\mathrm{r}}_{\tau\tau,\mathrm{w}}\right)+\frac{\left(1+\delta_{\mathrm{w}}\,\alpha^{\mathrm{r}}_{\delta,\mathrm{w}}-\delta_{\mathrm{w}}\,\tau_{\mathrm{w}}\,\alpha^{\mathrm{r}}_{\delta\tau,\mathrm{w}}\right)^2}{1+2\,\delta_{\mathrm{w}}\,\alpha^{\mathrm{r}}_{\delta,\mathrm{w}}+\delta_{\mathrm{w}}^2\,\alpha^{\mathrm{r}}_{\delta\delta,\mathrm{w}}}\right] \tag{5.60}$$

Dissociation at temperatures $T\geq 1200$ K

$\Delta c_{p,\mathrm{dis}}(p,T,\Psi)$ results from Eq. (5.89),

and M results from Eq. (5.44).

For the application of humid combustion gases with *I* components as recommended in the ASME Report STP-TS-012 [57], the following equation can be used:

$$c_p(\rho,T,\Psi)=\sum_{i=1,i\neq\mathrm{w}}^{I}\left[\psi_i\,c_{p,i}(\rho,T)\right]+\psi_{\mathrm{w}}\,c_{p,\mathrm{w}}(\rho_{\mathrm{w}},T)\,. \tag{5.61}$$

The dissociation part is not considered in the ASME report.

Isochoric heat capacity

$$c_v(\rho,T,\Psi)=\psi_{\mathrm{a}}\,c_{v,\mathrm{a}}(\rho,T)+\psi_{\mathrm{w}}\,c_{v,\mathrm{w}}(\rho_{\mathrm{w}},T)+\Delta c_{p,\mathrm{dis}}(p,T,\Psi)\,,\quad \tilde{c}_v=\frac{c_v}{M} \tag{5.62}$$

where: Dry air

$$c_{v,\mathrm{a}}(\rho,T)=-R^{Lem}\,\tau_{\mathrm{a}}^2\left(\alpha^{\mathrm{o}}_{\tau\tau,\mathrm{a}}+\alpha^{\mathrm{r}}_{\tau\tau,\mathrm{a}}\right) \tag{5.63}$$

Steam

$$c_{v,\mathrm{w}}(\rho_{\mathrm{w}},T)=-R^{95}\,\tau_{\mathrm{w}}^2\left(\alpha^{\mathrm{o}}_{\tau\tau,\mathrm{w}}+\alpha^{\mathrm{r}}_{\tau\tau,\mathrm{w}}\right) \tag{5.64}$$

Dissociation at temperatures $T\geq 1200$ K

$\Delta c_{p,\mathrm{dis}}(p,T,\Psi)$ results from Eq. (5.89),

and M results from Eq. (5.44).

For the application of humid combustion gases with *I* components as recommended in the ASME Report STP-TS-012 [57], the following equation can be used:

$$c_v(\rho,T,\Psi) = \sum_{i=1,i\neq \mathrm{w}}^{I} \left[\psi_i\, c_{v,i}(\rho,T)\right] + \psi_\mathrm{w}\, c_{v,\mathrm{w}}(\rho_\mathrm{w},T)\,. \tag{5.65}$$

The dissociation part is not considered in the ASME report.

Enthalpy

$$h(\rho,T,\Psi) = \psi_\mathrm{a}\, h_\mathrm{a}(\rho,T) + \psi_\mathrm{w}\, h_\mathrm{w}(\rho_\mathrm{w},T) + \Delta h_\mathrm{dis}(p,T,\Psi)\,,\quad \tilde{h} = \frac{h}{M} \tag{5.66}$$

where: Dry air

$$h_\mathrm{a}(\rho,T) = R^{Lem}\, T\left[1 + \tau_\mathrm{a}\left(\alpha^\mathrm{o}_{\tau,\mathrm{a}} + \alpha^\mathrm{r}_{\tau,\mathrm{a}}\right) + \delta_\mathrm{a}\, \alpha^\mathrm{r}_{\delta,\mathrm{a}}\right] \tag{5.67}$$

Steam

$$h_\mathrm{w}(\rho_\mathrm{w},T) = R^{95}\, T\left[1 + \tau_\mathrm{w}\left(\alpha^\mathrm{o}_{\tau,\mathrm{w}} + \alpha^\mathrm{r}_{\tau,\mathrm{w}}\right) + \delta_\mathrm{w}\, \alpha^\mathrm{r}_{\delta,\mathrm{w}}\right] \tag{5.68}$$

Dissociation at temperatures $T \geq 1200$ K

$\Delta h_\mathrm{dis}(p,T,\Psi)$ results from Eq. (5.90),

and M results from Eq. (5.44).

For the application of humid combustion gases with *I* components as recommended in the ASME Report STP-TS-012 [57], the following equation can be used:

$$h(\rho,T,\Psi) = \sum_{i=1,i\neq \mathrm{w}}^{I} \left[\psi_i\, h_i(\rho,T)\right] + \psi_\mathrm{w}\, h_\mathrm{w}(\rho_\mathrm{w},T)\,. \tag{5.69}$$

The dissociation part is not considered in the ASME report.

Internal energy

$$u(\rho,T,\Psi) = \psi_\mathrm{a}\, u_\mathrm{a}(\rho,T) + \psi_\mathrm{w}\, u_\mathrm{w}(\rho_\mathrm{w},T) + \Delta h_\mathrm{dis}(p,T,\Psi)\,,\quad \tilde{u} = \frac{u}{M} \tag{5.70}$$

where: Dry air

$$u_\mathrm{a}(\rho,T) = R^{Lem}\, T\tau_\mathrm{a}\left(\alpha^\mathrm{o}_{\tau,\mathrm{a}} + \alpha^\mathrm{r}_{\tau,\mathrm{a}}\right) \tag{5.71}$$

Steam

$$u_\mathrm{w}(\rho_\mathrm{w},T) = R^{95}\, T\tau_\mathrm{w}\left(\alpha^\mathrm{o}_{\tau,\mathrm{w}} + \alpha^\mathrm{r}_{\tau,\mathrm{w}}\right) \tag{5.72}$$

Dissociation at temperatures $T \geq 1200$ K

$\Delta h_\mathrm{dis}(p,T,\Psi)$ results from Eq. (5.90),

and M results from Eq. (5.44).

For the application of humid combustion gases with *I* components as recommended in the ASME Report STP-TS-012 [57], the following equation can be used:

$$u(\rho,T,\Psi) = \sum_{i=1,i\neq \mathrm{w}}^{I} \left[\psi_i\, u_i(\rho,T)\right] + \psi_\mathrm{w}\, u_\mathrm{w}(\rho_\mathrm{w},T)\,. \tag{5.73}$$

The dissociation part is not considered in the ASME report.

Entropy

$$s(\rho,T,\Psi) = \psi_\mathrm{a}\, s_\mathrm{a}(\rho,T) + \psi_\mathrm{w}\, s_\mathrm{w}(\rho_\mathrm{w},T) + \Delta s_\mathrm{irr} + \Delta s_\mathrm{dis}(p,T,\Psi)\,,\quad \tilde{s} = \frac{s}{M} \tag{5.74}$$

where: Dry air

$$s_\mathrm{a}\left(\rho,T\right) = R^{Lem}\left[\tau_\mathrm{a}\left(\alpha^\mathrm{o}_{\tau,\mathrm{a}} + \alpha^\mathrm{r}_{\tau,\mathrm{a}}\right) - \alpha^\mathrm{o}_\mathrm{a} - \alpha^\mathrm{r}_\mathrm{a}\right] + \Delta s_\mathrm{irr,a} \tag{5.75}$$

and $\Delta s_\mathrm{irr,a}$ is the irreversible contribution of the dry air entropy,

$$\Delta s_\mathrm{irr,a} = -R^\mathrm{Lem} \sum_{i,i\neq \mathrm{w}} \left[\frac{\psi_i}{\psi_\mathrm{a}} \ln\left(\frac{\psi_i}{\psi_\mathrm{a}}\right)\right],$$

$$\Delta s_\mathrm{irr,a} = -R^\mathrm{Lem}\left[-0,56354\right] = 4,68559\,\mathrm{kJ\,kmol^{-1}\,K^{-1}},$$

where the components of dry air are $i = \mathrm{N_2}$, $\mathrm{O_2}$, and Ar.

Steam

$$s_\mathrm{w}(\rho_\mathrm{w},T) = R^{95}\left[\tau_\mathrm{w}\left(\alpha^\mathrm{o}_{\tau,\mathrm{w}} + \alpha^\mathrm{r}_{\tau,\mathrm{w}}\right) - \alpha^\mathrm{o}_\mathrm{w} - \alpha^\mathrm{r}_\mathrm{w}\right] \tag{5.76}$$

Irreversible mixing entropy of humid air

$$\Delta s_\mathrm{irr} = -R\left[\psi_\mathrm{a} \ln\left(\psi_\mathrm{a}\right) + \psi_\mathrm{w} \ln\left(\psi_\mathrm{w}\right)\right],$$

where R results from Eq. (5.45).

Dissociation at temperatures $T \geq 1200$ K

$\Delta s_\mathrm{dis}(p,T,\Psi)$ results from Eq. (5.91),

and M results from Eq. (5.44).

For the application of humid combustion gases with *I* components as recommended in the ASME Report STP-TS-012 [57], the following equation can be used:

$$s(\rho,T,\Psi) = \sum_{i=1,i\neq \mathrm{w}}^{I} \left[\psi_i\, s_i(\rho,T)\right] + \psi_\mathrm{w}\, s_\mathrm{w}(\rho_\mathrm{w},T) + \Delta s_\mathrm{irr}\,, \tag{5.77}$$

where the irreversible mixing entropy of the humid combustion gases

$$\Delta s_\mathrm{irr} = -R\sum_{i=1}^{I} \psi_i \ln(\psi_i)\ .$$

The dissociation part is not considered in the ASME report.

Speed of sound

$$w(\rho,T,\Psi) = w^\mathrm{o}(T,\Psi)\left[\psi_\mathrm{a}\, \frac{w_\mathrm{a}(\rho,T)}{w^\mathrm{o}_\mathrm{a}(T)} + \psi_\mathrm{w}\, \frac{w_\mathrm{w}(\rho_\mathrm{w},T)}{w^\mathrm{o}_\mathrm{w}(T)}\right] \tag{5.78}$$

where: $$w^{\mathrm{o}}(T,\Psi)=\sqrt{\frac{c_p^{\mathrm{o}}(T,\Psi)}{c_p^{\mathrm{o}}(T,\Psi)-R}\frac{R}{M}T}\,, \tag{5.79}$$

$$c_p^{\mathrm{o}}(T,\Psi)=\psi_{\mathrm{a}}c_{p,\mathrm{a}}^{\mathrm{o}}(T)+\psi_{\mathrm{w}}c_{p,\mathrm{w}}^{\mathrm{o}}(T)\,, \tag{5.80}$$

$$c_{p,\mathrm{a}}^{\mathrm{o}}(T)=-R^{Lem}\tau_{\mathrm{a}}^2\alpha_{\tau\tau,\mathrm{a}}^{\mathrm{o}}\,, \tag{5.81}$$

$$c_{p,\mathrm{w}}^{\mathrm{o}}(T)=-R^{95}\tau_{\mathrm{w}}^2\alpha_{\tau\tau,\mathrm{w}}^{\mathrm{o}}\,, \tag{5.82}$$

M results from Eq. (5.44), R results from Eq. (5.45),
R^{Lem} results from Table 5.1, and R^{95} results from Table 5.2.

Dry air

$$w_{\mathrm{a}}(\rho,T)=\sqrt{\frac{1}{M_{\mathrm{a}}}\frac{c_{p,\mathrm{a}}}{c_{v,\mathrm{a}}}\left(\frac{\partial p}{\partial\rho}\right)_{T,\mathrm{a}}}\,, \tag{5.83}$$

$$w_{\mathrm{a}}^{\mathrm{o}}(T)=\sqrt{\frac{c_{p,\mathrm{a}}^{\mathrm{o}}(T)}{c_{p,\mathrm{a}}^{\mathrm{o}}(T)-R^{Lem}}\frac{R^{Lem}}{M_{\mathrm{a}}}T}\,, \tag{5.84}$$

M_{a} and R^{Lem} results from Table 5.1.

Steam

$$w_{\mathrm{w}}(\tilde{\rho}_{\mathrm{w}},T)=\sqrt{\frac{\tilde{c}_{p,\mathrm{w}}}{\tilde{c}_{v,\mathrm{w}}}\left(\frac{\partial p}{\partial\tilde{\rho}}\right)_{T,\mathrm{w}}}\,, \tag{5.85}$$

$$w_{\mathrm{w}}^{\mathrm{o}}(T)=\sqrt{\frac{c_{p,\mathrm{w}}^{\mathrm{o}}(T)}{c_{p,\mathrm{w}}^{\mathrm{o}}(T)-R^{95}}\frac{R^{95}}{M_{\mathrm{w}}}T}\,, \tag{5.86}$$

M_{w} and R^{95} results from Table 5.2.

For the application of humid combustion gases with I components as recommended in the ASME Report STP-TS-012 [57], the following equation can be used:

$$w(\rho,T,\Psi)=w^{\mathrm{o}}(T,\Psi)\left\{\sum_{i=1,i\neq\mathrm{w}}^{I}\left[\psi_i\frac{w_i(\rho,T)}{w_i^{\mathrm{o}}(T)}\right]+\psi_{\mathrm{w}}\frac{w_{\mathrm{w}}(\rho_{\mathrm{w}},T)}{w_{\mathrm{w}}^{\mathrm{o}}(T)}\right\}, \tag{5.87}$$

where

$$w^{\mathrm{o}}(T,\Psi)=\sqrt{\frac{c_p^{\mathrm{o}}(T,\Psi)}{c_p^{\mathrm{o}}(T,\Psi)-R}\frac{R}{M}T}\,.$$

Isentropic exponent

$$\kappa=\frac{w^2\rho}{p}M\,. \tag{5.88}$$

where

w, ρ, p are speed of sound, the molar density of the mixture, and the pressure of the mixture, and M results from Eq. (5.44).

The terms $\Delta c_{p,\mathrm{dis}}$, Δh_{dis}, and Δs_{dis} are needed for isobaric and isochoric heat capacities, c_p and c_v, for enthalpy h, for internal energy u, and for entropy s. They consider the influence of the dissociation at temperatures greater than 1200 K and mole fractions of oxygen greater than or equal to 1%. The algorithms of the VDI-Guideline 4670 [16], [23] contain a simplified model for the dissociation at high temperatures given as:

$$\Delta c_{p,\mathrm{dis}} = \Delta c_{p,\mathrm{dis}}(p,T,\Psi), \tag{5.89}$$

$$\Delta h_{\mathrm{dis}} = \Delta h_{\mathrm{dis}}(p,T,\Psi), \tag{5.90}$$

$$\Delta s_{\mathrm{dis}} = \Delta s_{\mathrm{dis}}(p,T,\Psi), \tag{5.91}$$

where Ψ is the vector of the mole fractions of the components.

5.3.3 Liquid Fog

Liquid fog is treated as an ideal mixture of saturated humid air and of water droplets in the calculation of its thermodynamic properties. But it makes no sense to calculate the isobaric heat capacity c_p and therefore the thermal diffusivity a and the Prandtl number Pr in the case of liquid fog.

The values of the constants for dry air used in this section are taken from Table 5.1, and the values of the constants for steam and water used in the following equations are taken from Table 5.2.
Important thermodynamic properties are given for liquid fog ($x_{\mathrm{w}} > x_{\mathrm{s,w}}$ and $273.16 \le T < 647.096\,\mathrm{K}$) as follows:

Molar and specific volume and density

$$v = \frac{\left(\dfrac{1+x_{\mathrm{w,s}}}{\dfrac{1}{\tilde{v}_{\mathrm{a}}} + \dfrac{1}{\tilde{v}_{\mathrm{w,v}}}} \right) + \left(x_{\mathrm{w}} - x_{\mathrm{w,s}}\right)\tilde{v}_{\mathrm{w,liq}}}{1+x_{\mathrm{w}}} M\,. \tag{5.92}$$

$$\tilde{\rho} = \frac{M}{v}\,. \tag{5.93}$$

Enthalpy, Entropy, and Internal energy

$$z(p,T,\Psi) = \frac{M}{\left(1+x_{\mathrm{w}}\right)}\left[\tilde{z}_{\mathrm{a}} + x_{\mathrm{w,s}}\,\tilde{z}_{\mathrm{w,v}} + \left(x_{\mathrm{w}} - x_{\mathrm{w,s}}\right)\tilde{z}_{\mathrm{w,liq}}\right] \tag{5.94}$$

where $\tilde{z} = \tilde{h}$ (for specific enthalpy), $\tilde{z} = \tilde{s}$ (for specific entropy), or $\tilde{z} = \tilde{u}$ (for specific internal energy):

$\tilde{z}_\mathrm{a} = \tilde{z}(p_\mathrm{a}, T)$ specific value of the corresponding property for air obtained from Lemmon *et al.* [1]

and $p_\mathrm{a} = p - p_\mathrm{s,w}$ is the partial pressure of air in the mixture in MPa,

$\tilde{z}_\mathrm{w,v} = \tilde{z}(p_\mathrm{s,w}, T)$ specific value of the corresponding property for water vapour obtained from IAPWS-95 [18], [19]

and $p_\mathrm{s,w} = f(p,T)$ is the partial pressure of water vapour of the saturated state obtained from Nelson and Sauer [38], [39] in MPa,

$\tilde{z}_\mathrm{w,liq} = \tilde{z}(p,T)$ specific value of the corresponding property for liquid water obtained from IAPWS-95,

$x_\mathrm{w} = \dfrac{\xi_\mathrm{w}}{1-\xi_\mathrm{w}}$ humidity ratio in $\mathrm{kg_w\,kg_a^{-1}}$

ξ_w mass fraction of water in $\mathrm{kg_w\,kg^{-1}}$,

$x_\mathrm{w,s} = \dfrac{R_\mathrm{a}}{R_\mathrm{w}} \dfrac{p_\mathrm{s,w}}{p - p_\mathrm{s,w}}$ humidity ratio of the saturated state at given pressure p and temperature T in $\mathrm{kg_w\,kg_a^{-1}}$, R_a from Table 5.1, R_w from Table 5.2, and

$M = \psi_\mathrm{a} M_\mathrm{a} + \psi_\mathrm{w} M_\mathrm{w}$ molar mass of the mixture in $\mathrm{kg\,kmol^{-1}}$, M_a from Table 5.1, M_w from Table 5.2,

with

$\psi_\mathrm{a} = 1 - \psi_\mathrm{w}$ mole fraction of air

$\psi_\mathrm{w} = \dfrac{x_\mathrm{w}}{\left(\dfrac{M_\mathrm{w}}{M_\mathrm{a}} + x_\mathrm{w}\right)}$ mole fraction of water.

Speed of sound

$$w(p,T,\Psi) = \gamma_\mathrm{s,w}\, w_\mathrm{s,w} + \gamma_\mathrm{w,liq}\, w_\mathrm{w,liq} \tag{5.95}$$

where

$w_\mathrm{s,w} = \sqrt{10^6\, p\, \tilde{v}_\mathrm{s,w}\, \kappa_\mathrm{s,w}}$ speed of sound of the saturated state of water vapour in $\mathrm{m\,s^{-1}}$

with

$\tilde{v}_{\mathrm{s,w}} = \dfrac{1}{\dfrac{1}{\tilde{v}_{\mathrm{a}}} + \dfrac{1}{\tilde{v}_{\mathrm{w,v}}}}$ specific volume of the saturated state of water vapour in $\mathrm{m^3\,kg^{-1}}$

where

$\tilde{v}_{\mathrm{a}} = \tilde{v}(p_{\mathrm{a}}, T)$ value of the specific volume of dry air obtained from Lemmon *et al.* [1] in $\mathrm{m^3\,kg^{-1}}$

$p_{\mathrm{a}} = p - p_{\mathrm{s,w}}$ is the partial pressure of air in the mixture in MPa,

$\tilde{v}_{\mathrm{w,v}} = \tilde{v}(p_{\mathrm{s,w}}, T)$ value of the specific volume of water vapour obtained from IAPWS-95 [18], [19] in $\mathrm{m^3\,kg^{-1}}$

$p_{\mathrm{s,w}} = f(p, T)$ is the partial pressure of water vapour of the saturated state obtained from Nelson and Sauer [38], [39] in MPa,

$\kappa_{\mathrm{s,w}} = f\left[\tilde{v}, c_p, c_v, p, \left(\dfrac{\partial p}{\partial \tilde{v}}\right)_T\right]$ isentropic exponent of the saturated state of water vapour, the calculation is described in the following item

$w_{\mathrm{w,liq}} = w(p, T)$ speed of sound of pure water obtained from IAPWS-95, in $\mathrm{m\,s^{-1}}$

$\gamma_{\mathrm{w,liq}} = \dfrac{\tilde{v}_{\mathrm{w,liq}}\left(x_{\mathrm{w}} - x_{\mathrm{w,s}}\right)}{\left[\dfrac{1 + x_{\mathrm{w,s}}}{\dfrac{1}{\tilde{v}_{\mathrm{a}}} + \dfrac{1}{\tilde{v}_{\mathrm{w,v}}}} + \tilde{v}_{\mathrm{w,liq}}\left(x_{\mathrm{w}} - x_{\mathrm{w,s}}\right)\right]}$ is the volume fraction of liquid water

with

$\tilde{v}_{\mathrm{w,liq}} = \tilde{v}(p, T)$ value of the specific volume of liquid water obtained from IAPWS-95,

$\gamma_{\mathrm{s,w}} = 1 - \gamma_{\mathrm{w,liq}}$ volume fraction of steam at the saturated state.

Isentropic exponent

$$\kappa = \gamma_{\mathrm{s,w}}\,\kappa_{\mathrm{s,w}} + \gamma_{\mathrm{w,liq}}\,\kappa_{\mathrm{w,liq}} \tag{5.96}$$

where

$\kappa_{\mathrm{s,w}} = -\dfrac{\tilde{v}_{\mathrm{s,w}}\,\tilde{c}_p}{p\,\tilde{c}_v}\left(\dfrac{\partial p}{\partial \tilde{v}}\right)_T$ value of the isentropic exponent of the saturated state of water vapour

with

$$\tilde{v}_{\mathrm{s,w}} = \frac{1}{\frac{1}{\tilde{v}_{\mathrm{a}}} + \frac{1}{\tilde{v}_{\mathrm{w,v}}}}$$ specific volume of the saturated state of water vapour,

$$\tilde{c}_p = \frac{\tilde{c}_{p,\mathrm{a}} + x_{\mathrm{w,s}}\,\tilde{c}_{p,\mathrm{w,v}}}{1 + x_{\mathrm{w,s}}}$$ specific isobaric heat capacity of the saturated state,

where

$\tilde{c}_{p,\mathrm{a}} = \tilde{c}_p(p_{\mathrm{a}}, T)$ value of the specific isobaric heat capacity of air obtained from Lemmon *et al.*

$\tilde{c}_{p,\mathrm{w,v}} = \tilde{c}_p(p_{\mathrm{s,w}}, T)$ value of the specific isobaric heat capacity of water vapour obtained from IAPWS-95,

$$\tilde{c}_v = \frac{\tilde{c}_{v,\mathrm{a}} + x_{\mathrm{w,s}}\,\tilde{c}_{v,\mathrm{w,v}}}{1 + x_{\mathrm{w,s}}}$$ specific isochoric heat capacity of the saturated state,

where

$\tilde{c}_{v,\mathrm{a}} = \tilde{c}_v(p_{\mathrm{a}}, T)$ value of the specific isochoric heat capacity of air obtained from Lemmon *et al.*

$\tilde{c}_{v,\mathrm{w,v}} = \tilde{c}_v(p_{\mathrm{s,w}}, T)$ value of the specific isochoric heat capacity of water vapour obtained from IAPWS-95,

$$\left(\frac{\partial p}{\partial \tilde{v}}\right)_T = \frac{1}{\xi_{\mathrm{a}}\left(\frac{\partial \tilde{v}}{\partial p}\right)_{T,\mathrm{a}}} + \frac{1}{\xi_{\mathrm{s,w}}\left(\frac{\partial \tilde{v}}{\partial p}\right)_{T,\mathrm{w}}}$$

where

Dry air

$$\left(\frac{\partial \tilde{v}}{\partial p}\right)_{T,\mathrm{a}}(\tilde{v}_{\mathrm{a}}, T) = -\frac{\tilde{v}_{\mathrm{a}}^2}{R_{\mathrm{a}}\,T\left(1 + 2\,\delta_{\mathrm{a}}\,\alpha^r_{\delta,\mathrm{a}} + \delta_{\mathrm{a}}^2\,\alpha^r_{\delta\delta,\mathrm{a}}\right)},$$

Water and steam

$$\left(\frac{\partial \tilde{v}}{\partial p}\right)_{T,\mathrm{w}}(\tilde{v}_{\mathrm{w}}, T) = -\frac{\tilde{v}_{\mathrm{w}}^2}{R_{\mathrm{w}}\,T\left(1 + 2\,\delta_{\mathrm{w}}\,\alpha^r_{\delta,\mathrm{w}} + \delta_{\mathrm{w}}^2\,\alpha^r_{\delta\delta,\mathrm{w}}\right)},$$

$\xi_{\mathrm{a}} = 1 - \xi_{\mathrm{s,w}}$ mass fraction of dry air in the mixture at the saturated state,

$$\xi_{\mathrm{s,w}} = \frac{x_{\mathrm{w,s}}}{1 + x_{\mathrm{w,s}}}$$ mass fraction of water vapour of the saturated state.

$\kappa_{\mathrm{w,liq}} = \kappa(p, T)$ isentropic exponent of liquid water obtained from IAPWS-95.

5.3.4 Ice Fog

Ice fog is treated as an ideal mixture of saturated humid air and of ice crystals using the algorithms for the calculation of the thermodynamic properties of unsaturated humid air. As an assumption, the ice crystals are considered to be equally distributed in the total volume or volume flow. But the properties molar isobaric heat capacity c_p, molar isochoric heat capacity c_v, thermal diffusivity *a*, and Prandtl number cannot be calculated in the case of ice fog. The reason is that the definition of $c_p = (\partial h / \partial T)_p$ would lead to infinite values of c_p, if the enthalpy of evaporation is considered.

The values of the constants for dry air used in this section are taken from Table 5.1, and the values of the constants for steam, water, and ice used in the following equations are taken from Table 5.2.

Important thermodynamic properties are given for ice fog ($\xi_\mathrm{w} > \xi_\mathrm{s,w}$ and $243.15 \le T < 273.16\ \mathrm{K}$ [13]) as:

Molar enthalpy, molar entropy, and molar internal energy

$$z = \frac{M}{(1+x_\mathrm{w})}\left[\tilde{z}_\mathrm{a} + \tilde{z}_\mathrm{w,v}\, x_\mathrm{w,s} + \tilde{z}_\mathrm{w,i}\left(x_\mathrm{w} - x_\mathrm{w,s}\right)\right] \tag{5.97}$$

where $\tilde{z} = \tilde{h}$ (for molar enthalpy), $\tilde{z} = \tilde{s}$ (for molar entropy), or $\tilde{z} = \tilde{u}$ (for molar internal energy)

$\tilde{z}_\mathrm{a} = \tilde{z}(p_\mathrm{s,a}, T)$ specific value of the corresponding property for air obtained from Lemmon *et al.* [1]

and $p_\mathrm{s,a} = p - p_\mathrm{s,w}$ is the partial pressure of air in the mixture in MPa,

$\tilde{z}_\mathrm{w,v} = \tilde{z}(p_\mathrm{s,w}, T)$ specific value of the corresponding property for water vapour obtained from IAPWS-95 [18], [19]

and $p_\mathrm{s,w} = f(p,T)$ is the partial pressure of water vapour of the saturated state obtained from Nelson and Sauer [38], [39] in MPa,

for enthalpy *h* and entropy *s*:

$\tilde{z}_\mathrm{w,i} = \tilde{z}(p,T)$ specific value of the corresponding property for ice obtained from Feistel and Wagner [52], [53],

for internal energy *u*:

$\tilde{u}_\mathrm{w,i} = \tilde{h}_\mathrm{w,i}(p,T) - p\,\tilde{v}_\mathrm{w,i}(p,T)$,

$\tilde{h}_\mathrm{w,i}$ and $\tilde{v}_\mathrm{w,i}$ obtained from IAPWS [52].

[13] For simplifying the use of the library, the ice fog was assigned to temperatures below the triple-point temperature 273.16 K of water.

Speed of sound

$$w = w_{\mathrm{s,w}} \tag{5.98}$$

with

$w_{\mathrm{s,w}} = \sqrt{p\,\tilde{v}_{\mathrm{s,w}}\,\kappa_{\mathrm{s,w}}}$ speed of sound of the saturated state of water vapour (from Section 5.3.3).

Isentropic exponent

$$\kappa = \kappa_{\mathrm{s,w}} \tag{5.99}$$

with

$\kappa_{\mathrm{s,w}} = -\dfrac{\tilde{v}_{\mathrm{s,w}}\,c_p}{p\,c_v}\left(\dfrac{\partial p}{\partial \tilde{v}}\right)_T$ isentropic exponent of the saturated state of water vapour (from Section 5.3.3).

Molar volume

$$v = \frac{\left(\dfrac{1+x_{\mathrm{w,s}}}{\dfrac{1}{\tilde{v}_{\mathrm{a}}}+\dfrac{1}{\tilde{v}_{\mathrm{w,v}}}}\right)+\left(x_{\mathrm{w}}-x_{\mathrm{w,s}}\right)\tilde{v}_{\mathrm{w,i}}}{1+x_{\mathrm{w}}} M \tag{5.100}$$

where

$\tilde{v}_{\mathrm{a}} = \tilde{v}(p_{\mathrm{s,a}}, T)$ specific volume of air obtained from Lemmon *et al.* [1] in $\mathrm{m^3\,kg^{-1}}$

$\tilde{v}_{\mathrm{w,v}} = \tilde{v}(p_{\mathrm{s,w}}, T)$ specific volume of water vapour obtained from IAPWS-95 [18], [19] in $\mathrm{m^3\,kg^{-1}}$

$\tilde{v}_{\mathrm{w,i}} = \tilde{v}(T)$ specific volume of ice crystals obtained from [52], [53] in $\mathrm{m^3\,kg^{-1}}$.

Mass density

$$\tilde{\rho} = \frac{M}{v} \tag{5.101}$$

where v is the molar volume in $\mathrm{m^3\,kmol^{-1}}$.

Some basic variables used in the equations for liquid fog as well as in that for ice fog are given for the sake of completeness as follows:

$x_{\mathrm{w}} = \dfrac{\xi_{\mathrm{w}}}{1-\xi_{\mathrm{w}}}$ humidity ratio in $\mathrm{kg_w\,kg_a^{-1}}$

ξ_w mass fraction of water in $\mathrm{kg_w\,kg^{-1}}$

$x_{\mathrm{w,s}}(p,T) = \dfrac{\tilde{R}_\mathrm{a}}{\tilde{R}_\mathrm{w}} \dfrac{p_\mathrm{s,w}}{p - p_\mathrm{s,w}}$ humidity ratio of the saturated state at given pressure p and temperature T in $\mathrm{kg_w\,kg_a^{-1}}$, $\tilde{R}_\mathrm{a}$ from Table 5.1, $\tilde{R}_\mathrm{w}$ from Table 5.2, and

$M = \psi_\mathrm{a} M_\mathrm{a} + \psi_\mathrm{w} M_\mathrm{w}$ molar mass of the mixture in $\mathrm{kg\,kmol^{-1}}$, M_a from Table 5.1, M_w from Table 5.2,

where

$\psi_\mathrm{a} = 1 - \psi_\mathrm{w}$ mole fraction of air, and

$\psi_\mathrm{w} = \dfrac{x_\mathrm{w}}{\left(\dfrac{M_\mathrm{w}}{M_\mathrm{a}} + x_\mathrm{w}\right)}$ mole fraction of water,

$\gamma_{\mathrm{s,w}} = 1 - \gamma_\mathrm{w}$ volume fraction of liquid water of the saturated state,

$\gamma_\mathrm{w} = \dfrac{\tilde{v}_{\mathrm{w,liq}}\left(x_\mathrm{w} - x_{\mathrm{w,s}}\right)}{\left[\dfrac{1 + x_{\mathrm{w,s}}}{\dfrac{1}{\tilde{v}_\mathrm{a}} + \dfrac{1}{\tilde{v}_{\mathrm{w,v}}}} + \tilde{v}_{\mathrm{w,liq}}\left(x_\mathrm{w} - x_{\mathrm{w,s}}\right)\right]}$ is the volume fraction of liquid water,

where $\tilde{v}_{\mathrm{w,liq}} = \tilde{v}(p,T)$ is the value for the specific volume of liquid water obtained from IAPWS-95.

5.4 Composition of Saturated Humid Air

The mole fraction of water in saturated humid air is:

$$\psi_{\mathrm{s,w}} = \frac{f\, p_{\mathrm{s,w}}}{p} \tag{5.102}$$

where $p_{\mathrm{s,w}}$ is the saturation pressure of pure water and p is the total pressure. The enhancement factor f considering the non-ideal behaviour of the mixture in the saturated state is given as a function of p and T and can be derived iteratively from the isothermal compressibility of liquid water, from Henry's constant, and from the virial coefficients of air, of water, and of the mixture air-water using the relationship:

$$\ln(f) = \left[\frac{\left(1+\kappa_T\, p_{\mathrm{s,w}}\right)\left(p - p_{\mathrm{s,w}}\right) - \kappa_T \dfrac{\left(p^2 - p_{\mathrm{s,w}}^2\right)}{2}}{RT} \right] v_{\mathrm{w,liq}} + \ln\left(1 - \beta_{\mathrm{H}}\, \psi_{\mathrm{s,a}}\, p\right) +$$
$$\left[\frac{\psi_{\mathrm{s,a}}^2\, p}{RT}\right] B_{\mathrm{aa}} - \left[\frac{2\psi_{\mathrm{s,a}}^2\, p}{RT}\right] B_{\mathrm{aw}} - \left[\frac{p - p_{\mathrm{s,w}} - \psi_{\mathrm{s,a}}^2\, p}{RT}\right] B_{\mathrm{ww}} +$$
$$\left[\frac{\psi_{\mathrm{s,a}}^3\, p^2}{(RT)^2}\right] C_{\mathrm{aaa}} + \left[\frac{3\psi_{\mathrm{s,a}}^2\left(1-2\psi_{\mathrm{s,a}}\right)p^2}{2(RT)^2}\right] C_{\mathrm{aaw}} -$$
$$\left[\frac{3\psi_{\mathrm{s,a}}^2\left(1-\psi_{\mathrm{s,a}}\right)p^2}{(RT)^2}\right] C_{\mathrm{aww}} - \left[\frac{\left(1+2\psi_{\mathrm{s,a}}\right)\left(1-\psi_{\mathrm{s,a}}\right)^2 p^2 - p_{\mathrm{s,w}}^2}{2(RT)^2}\right] C_{\mathrm{www}} -$$
$$\left[\frac{\psi_{\mathrm{s,a}}^2\left(1-3\psi_{\mathrm{s,a}}\right)\left(1-\psi_{\mathrm{s,a}}\right)p^2}{(RT)^2}\right] B_{\mathrm{aa}}\, B_{\mathrm{ww}} - \left[\frac{2\psi_{\mathrm{s,a}}^3\left(2-3\psi_{\mathrm{s,a}}\right)p^2}{(RT)^2}\right] B_{\mathrm{aa}}\, B_{\mathrm{aw}} +$$
$$\left[\frac{6\psi_{\mathrm{s,a}}^2\left(1-\psi_{\mathrm{s,a}}\right)^2 p^2}{(RT)^2}\right] B_{\mathrm{ww}}\, B_{\mathrm{aw}} - \left[\frac{3\psi_{\mathrm{s,a}}^4\, p^2}{2(RT)^2}\right] B_{\mathrm{aa}}^2 -$$
$$\left[\frac{2\psi_{\mathrm{s,a}}^2\left(1-\psi_{\mathrm{s,a}}\right)\left(1-3\psi_{\mathrm{s,a}}\right)p^2}{(RT)^2}\right] B_{\mathrm{aw}}^2 - \left[\frac{p_{\mathrm{s,w}}^2 - \left(1+3\psi_{\mathrm{s,a}}\right)\left(1-\psi_{\mathrm{s,a}}\right)^3 p^2}{2(RT)^2}\right] B_{\mathrm{ww}}^2 \tag{5.103}$$

where p is the total pressure, T is the temperature of the mixture humid air, $\psi_{\mathrm{s,w}}$ is the mole fraction of water in saturated humid air with $\psi_{\mathrm{s,w}} = 1 - \psi_{\mathrm{s,a}}$, and $R = 8.3144\ \mathrm{kJ\,kmol^{-1}\,K^{-1}}$ is the value of the universal molar gas constant from [39]. Furthermore, $p_{\mathrm{s,w}} = p_{\mathrm{s}}^{97}(T)$ is the saturation pressure for temperatures $T \geq 273.15\ \mathrm{K}$ obtained from IAPWS-IF97 [20], [21] according to Eq. (3.120).

κ_T is the isothermal compressibility of liquid water obtained from IAPWS-95 [18], [19] for temperatures $T \geq 273.15\ \mathrm{K}$:

$$\kappa_T = -\frac{1}{v_{\mathrm{w,liq}}}\left(\frac{\partial v}{\partial p}\right)_{T,\mathrm{w}} \tag{5.104}$$

with

$v_{\mathrm{w,liq}} = v(p,T)$ is the molar volume of liquid water, and

$$\left(\frac{\partial v}{\partial p}\right)_{T,\mathrm{w}}(v_{\mathrm{w}},T) = -\frac{v_{\mathrm{w}}^2}{R_{\mathrm{w}}\, T\left(1 + 2\,\delta_{\mathrm{w}}\, \alpha_{\delta,\mathrm{w}}^{\mathrm{r}} + \delta_{\mathrm{w}}^2\, \alpha_{\delta\delta,\mathrm{w}}^{\mathrm{r}}\right)},$$

where this partial derivative for water is taken from IAPWS-95 [18], [19] in Sec. 5.2.

For temperatures $T \geq 273.15\,\mathrm{K}$ $\overline{v}_\mathrm{w} = \overline{v}_\mathrm{liq}(p_\mathrm{w,s}, T)$ is the molar volume of saturated liquid water of IAPWS-IF97.

β_H is the Henry's law constant and is calculated from the following equation valid for $T \geq 273.15\,\mathrm{K}$ and $T \leq T_\mathrm{s}(p)$, whereas $T_\mathrm{s}(p)$ is the saturation temperature for a given pressure:

$$\beta_\mathrm{H} = \frac{10^{-9}}{1.01325\beta_\mathrm{a}} \tag{5.105}$$

where

$$\frac{1}{\beta_\mathrm{a}} = \frac{\psi_{\mathrm{O}_2}}{\beta_{\mathrm{O}_2}} + \frac{\psi_{\mathrm{N}_2}}{\beta_{\mathrm{N}_2}} \tag{5.106}$$

with

$\psi_{\mathrm{O}_2} = 0.22$ is the mole fraction of oxygen in dry air,

$\psi_{\mathrm{N}_2} = 0.78$ is the mole fraction of nitrogen in dry air,

$$\beta_{\mathrm{O}_2} = \exp\left\{\sum_{k=1}^{6} J_k\, X^{(k-1)}\right\} \tag{5.107}$$

where $J_1 \ldots J_6$ are coefficients obtained by Nelson and Sauer [38], [39]:

$$\begin{aligned}
J_1 &= -0.197\,867\,73 \times 10^{2} \\
J_2 &= 0.233\,930\,48 \times 10^{2} \\
J_3 &= -0.989\,849\,83 \times 10^{1} \\
J_4 &= 0.223\,631\,72 \times 10^{1} \\
J_5 &= -0.296\,184\,34 \times 10^{0} \\
J_6 &= 0.170\,849\,32 \times 10^{-1}
\end{aligned}$$

$$\beta_{\mathrm{N}_2} = \sum_{k=1}^{6} J_k\, X^{(k-1)} + \sum_{m=1}^{4} I_m\, X^{(-m)} \tag{5.108}$$

where $J_1 \ldots J_6$ and $I_1 \ldots I_4$ are coefficients obtained by Nelson and Sauer:

$$\begin{aligned}
J_1 &= -0.288\,743\,088 \times 10^{6} \\
J_2 &= 0.111\,167\,594 \times 10^{6} \\
J_3 &= -0.279\,882\,964 \times 10^{5} \\
J_4 &= 0.444\,444\,530 \times 10^{4} \\
J_5 &= -0.404\,940\,980 \times 10^{3} \\
J_6 &= 0.161\,931\,127 \times 10^{2}
\end{aligned}$$

$$
\begin{aligned}
I_1 &= 0.491\,323\,518 \times 10^6 \\
I_2 &= -0.529\,382\,752 \times 10^6 \\
I_3 &= 0.328\,398\,259 \times 10^6 \\
I_4 &= -0.895\,056\,879 \times 10^5
\end{aligned}
$$

with $X = 1000\,\mathrm{K}\,T^{-1}$.

β_H is zero for $T \geq 273.15\,\mathrm{K}$ and $T > T_\mathrm{s}(p)$.

Nelson and Sauer [38], [39] determined the temperature dependent virial coefficients to be:

$$B_\mathrm{aa}(T)/(\mathrm{cm}^3\,\mathrm{mol}^{-1}) = \sum_{k=1}^{7} b_k \left(\frac{T}{\mathrm{K}}\right)^{(1-k)} \tag{5.109}$$

where b_1 … b_7 are:

$$
\begin{aligned}
b_1 &= 0.318\,317\,63 \times 10^2 \\
b_2 &= -0.719\,511\,95 \times 10^3 \\
b_3 &= -0.653\,813\,70 \times 10^7 \\
b_4 &= 0.159\,298\,28 \times 10^{10} \\
b_5 &= -0.255\,888\,42 \times 10^{12} \\
b_6 &= 0.223\,003\,82 \times 10^{14} \\
b_7 &= -0.827\,934\,65 \times 10^{15}
\end{aligned}
$$

$$C_\mathrm{aaa}(T)/(\mathrm{cm}^6\,\mathrm{mol}^{-2}) = \sum_{k=1}^{7} c_k \left(\frac{T}{\mathrm{K}}\right)^{(1-k)} \tag{5.110}$$

where c_1 … c_7 are:

$$
\begin{aligned}
c_1 &= 0.129\,753\,78 \times 10^4 \\
c_2 &= 0.460\,213\,28 \times 10^5 \\
c_3 &= 0.408\,131\,54 \times 10^8 \\
c_4 &= -0.320\,239\,10 \times 10^{10} \\
c_5 &= 0.229\,647\,85 \times 10^{12} \\
c_6 &= -0.536\,834\,67 \times 10^{13} \\
c_7 &= -0.211\,839\,15 \times 10^{15}
\end{aligned}
$$

$$C_\mathrm{aaw}(T)/(\mathrm{cm}^6\,\mathrm{mol}^{-2}) = \sum_{k=1}^{5} c_k \left(\frac{T}{\mathrm{K}}\right)^{(1-k)} \tag{5.111}$$

where c_1 … c_5 are:

$$
\begin{aligned}
c_1 &= 0.482\,737 \times 10^{3} \\
c_2 &= 0.105\,678 \times 10^{6} \\
c_3 &= -0.656\,394 \times 10^{8} \\
c_4 &= 0.294\,442 \times 10^{11} \\
c_5 &= -0.319\,317 \times 10^{13}
\end{aligned}
$$

$$
C_{\mathrm{aww}}(T)/(\mathrm{cm}^6\,\mathrm{mol}^{-2}) = -10^{-6} \exp\left\{ \sum_{k=1}^{4} c_k \left(\frac{T}{\mathrm{K}} \right)^{(1-k)} \right\} \tag{5.112}
$$

where $c_1 \ldots c_4$ are:

$$
\begin{aligned}
c_1 &= -0.107\,288\,7 \times 10^{2} \\
c_2 &= 0.347\,804 \times 10^{4} \\
c_3 &= -0.383\,383 \times 10^{6} \\
c_4 &= 0.334\,060 \times 10^{8}
\end{aligned}
$$

$$
C_{\mathrm{www}}(T)/(\mathrm{cm}^6\,\mathrm{mol}^{-2}) = -10^{-6} \exp\left\{ \sum_{k=1}^{7} c_k \left(\frac{T}{\mathrm{K}} \right)^{(k-1)} \right\} \tag{5.113}
$$

where $c_1 \ldots c_7$ are:

$$
\begin{aligned}
c_1 &= -0.656\,627\,660\,6 \times 10^{1} \\
c_2 &= 0.389\,467\,951\,6 \times 10^{0} \\
c_3 &= -0.342\,810\,205\,37 \times 10^{-2} \\
c_4 &= 0.133\,392\,491\,8 \times 10^{-4} \\
c_5 &= -0.272\,640\,407\,8 \times 10^{-7} \\
c_6 &= 0.283\,936\,913\,6 \times 10^{-10} \\
c_7 &= -0.118\,911\,433\,0 \times 10^{-13}
\end{aligned}
$$

The second virial coefficients for water-water (B_{ww}) and air-water (B_{aw}) molecule interactions given by Nelson and Sauer was replaced with the recommended calculation proposed by Harvey *et al.* Harvey and Huang [55] determined the temperature dependent second virial coefficient of air and water B_{aw} to be:

$$
B_{\mathrm{aw}}(T)/(\mathrm{cm}^3\,\mathrm{mol}^{-1}) = \sum_{i=1}^{3} b_i (T^*)^{d_i} \tag{5.114}
$$

where $b_1 \ldots b_3$ and $d_1 \ldots d_3$ are

b_1	=	$0.665\,567 \times 10^2$	d_1	=	–0.237
b_2	=	$-0.238\,834 \times 10^3$	d_2	=	–1.048
b_3	=	$-0.176\,755 \times 10^3$	d_3	=	–3.183

and $T^* = T/(100\,\mathrm{K})$.

Harvey and Lemmon [56] determined the temperature dependent second virial coefficient of water and water B_{ww} to be:

$$B_{\mathrm{ww}}(T)/(\mathrm{cm}^3\,\mathrm{mol}^{-1}) = 10^3 \sum_{i=1}^{3} b_i (T^*)^{d_i} \tag{5.115}$$

where $b_1 \ldots b_3$ and $d_1 \ldots d_3$ are:

b_1	=	$0.344\,04 \times 10^0$	d_1	=	–0.5
b_2	=	$-0.758\,26 \times 10^0$	d_2	=	–0.8
b_3	=	$-0.242\,19 \times 10^2$	d_3	=	–3.35
b_4	=	$-0.397\,82 \times 10^4$	d_4	=	–8.3

and $T^* = T/(100\,\mathrm{K})$.

The value for $\psi_{\mathrm{s,a}}(p,T)$ in Eq. (5.103) has to be calculated in each step of the iteration according to:

$$\psi_{\mathrm{s,a}} = \frac{p - f\,p_{\mathrm{s,w}}}{p}\,. \tag{5.116}$$

The initial value for f in relation (5.116) chosen for the iteration is 1.0. If the criterion $\left|\psi_{\mathrm{s,a_{new}}} - \psi_{\mathrm{s,a_{old}}}\right| \le \varepsilon$ with $\varepsilon = 10^{-8}$ is fulfilled, the iteration is completed.

After iterating the enhancement factor f, the mole fraction of water vapour $\psi_{\mathrm{s,w}}$ results from

$$\psi_{\mathrm{s,w}} = \frac{f\,p_{\mathrm{s,w}}}{p}\,. \tag{5.117}$$

The saturation pressure p_{s} of humid air is obtained using

$$p_{\mathrm{s}} = f\,p_{\mathrm{s,w}} = \psi_{\mathrm{s,w}}\,p\,. \tag{5.118}$$

6 Conclusions

Different models for calculating thermodynamic properties of humid air have been compared. The implemented algorithms of the models have been described in Section 3 of this work. The models were verified by comparing the calculated results for a certain model with the available experimental data as well as with the results for the other models in Section 4. Section 5 comprises the description of the new SKU model developed and recommended for the calculation of the thermodynamic properties for humid air. For calculating the thermodynamic properties of humid air, the recommended model is composed of the following two models:

- Ideal mixture of the real fluids dry air and water
- Virial equation for the mixture by Nelson and Sauer used for calculating the saturated composition of humid air (poynting correction).

In addition, a procedure to calculate the thermodynamic properties of humid air in case of liquid fog and ice fog is recommended.

The ideal-mixing model for the calculation of the thermodynamic properties of humid air uses the most accurate equations of state for the real fluids dry air and water, and for ice in the case of ice fog.

Further investigations with regard to the thermodynamic properties of humid air should incorporate the multi-fluid model of Kunz *et al.* which was not yet available during this project. Further experimental data for the thermodynamic properties of humid air are needed for further improvements of the corresponding calculation algorithms.

7 References

[1] Lemmon, E. W.; Jacobsen, R. T.; Penoncello, S. G.; Friend, D. G.: Thermodynamic Properties of Air and Mixtures of Nitrogen, Argon, and Oxygen from 60 to 2000 K at Pressures to 2000 MPa. *J. Phys. Chem. Ref. Data* **29**, 331-385 (2000).

[2] Hyland, R. W.; Wexler, A.: The Enhancement of Water Vapor in Carbon Dioxide–Free Air at 30, 40, and 50 °C. *J. Res. NBS* **77A**, 115-131 (1973).

[3] Hyland, R. W.: A Correlation for the Second Interaction Virial Coefficients and Enhancement Factors for Humid Air. *J. Res. NBS* **79A**, 551-560 (1975).

[4] Pollitzer, F.; Strebel, E.: Over the Influence of Indifferent Gases on the Saturation Steam Concentration of Liquids. *Z. phys. Chem.* **110**, 768-785 (1924) (in German).

[5] Webster, T. J.: The Effect on Water Vapor Pressure of Super-Imposed Air Pressure. *J. S. C. I.* **69**, 343-346 (1950).

[6] Wylie, R. G.; Fisher, R. S.: Molecular Interaction of Water Vapor and Air. *J. Chem. Eng. Data* **41,** 133-142 **(**1996).

[7] Japas, M. L.; Franck, E. U.: High Pressure Phase Equilibria and *PVT*-Data of the Water-Oxygen System Including Water-Air to 673 K and 250 MPa. *Ber. Bunsenges. Phys. Chem.* **89**, 1268-1275 (1985).

[8] Fenghour, A.; Wakeham, W. A.; Ferguson, D.; Scott, A. C.; Watson, J. T. R.: Densities of (Water+Nitrogen) in the Temperature Range 533 K to 703 K and at Pressures up to 31 MPa. *J. Chem. Thermodyn.* **25**, 1151-1159 (1993).

[9] Saddington, A. W.; Krase, N. W.: Vapor-Liquid Equilibria in the System Nitrogen-Water. *J. Amer. Chem. Soc.* **56**, 353-361 (1934).

[10] Abdulagatov, I. M.; Bazaev, A. R.; Ramazanova, A. E.: *P-V-T-x* Measurements of Aqueous Mixtures at Supercritical Conditions. *Int. J. Thermophys.* **14**, 231-250 (1993).

[11] Klingenberg, G.; Ulbig, P.: Isochoric *ppT* Measurements on Dry and Humid Air. *J. Chem. Eng. Data* **52**, 1413-1419 (2007).

[12] Trusler, J. P. M.: Experimental Data for the Density and Speed of Sound of Dry Air. Imperial College of London, Department of Chemical Engineering and Chemical Technology, internal communication within the AA-CAES project (2004).

[13] Wöll, O.: Measurements on Dynamic Viscosity and Density of Dry and Humid Air and Further Development of a Combined Viscosity Density Measuring System. Dissertation, Ruhr-Universität Bochum, Faculty of Mechanical Engineering, Bochum (2005) (in German).

[14] Trusler, J. P. M.: Experimental Data for the Density of Humid Air. Imperial College of London, Department of Chemical Engineering and Chemical Technology, internal communication within the AA-CAES project (2005).

[15] Koglbauer, G.; Wendland, M.: Water Vapor Concentration Enhancement in Compressed Humid Air Measured by Fourier Transform Infrared Spectroscopy. *J. Chem. Eng. Data* **52**, 1672-1677 (2007).

[16] VDI-Guideline 4670: *Thermodynamic Properties of Humid Air and Combustion Gases.* Beuth, Berlin (2003).

[17] Ji, X.; Yan, J.: Thermodynamic Properties for Humid Gases from 298 to 573 K and up to 200 bar. *Appl. Therm. Eng.* **26**, 251-258 (2006).

[18] Wagner, W.; Pruß, A.: The IAPWS Formulation 1995 for the Thermodynamic Properties of Ordinary Water Substance for General and Scientific Use. *J. Phys. Chem. Ref. Data* **31**, 387-535 (2002).

[19] IAPWS. Release on the IAPWS Formulation 1995 for the Thermodynamic Properties of Ordinary Water Substance for General and Scientific Use. 1995; available from the IAPWS Executive Secretary, Dr. R. B. Dooley, Structural Integrity Associates, Inc., Oakville, Ontario L6J 7L7, Canada, www.iapws.org.

[20] IAPWS. Release on the IAPWS Industrial Formulation 1997 for the Thermodynamic Properties of Water and Steam IAPWS-IF97. 1997; available from the IAPWS Executive Secretary, Dr. R. B. Dooley, Structural Integrity Associates, Inc., Oakville, Ontario L6J 7L7, Canada, www.iapws.org.

[21] Wagner, W.; Cooper, J. R.; Dittmann, A.; Kijima, J.; Kretzschmar, H.-J.; Kruse, A.; Mares, R.; Oguchi, K.; Sato, H.; Stöcker, I.; Sifner, O.; Takaishi, Y.; Tanishita, I.; Trübenbach, J.; Willkommen, Th.: The IAPWS Industrial Formulation 1997 for the Thermodynamic Properties of Water and Steam. *J. Eng. Gas Turb. Power* **122**, 150-184 (2000).

[22] Hyland, R. W.; Wexler, A.: Formulations for the Thermodynamic Properties of the Saturated Phases of H_2O from 173.15 K to 473.15 K. *ASHRAE Trans*. **89**, 500-519 (1983).

[23] Bücker, D.; Span, R.; Wagner, W.: Thermodynamic Property Models for Humid Air and Combustion Gases. *J. Eng. Gas Turb. Power* **125**, 374-384 (2003).

[24] McBride, B. J.; Gordon, S.; Renor, M. A.: Coefficients for Calculating Thermodynamic and Transport Properties of Individual Species. *NASA Technical Memorandum* **4513** (1993).

[25] Kretzschmar, H.-J.; Stöcker, I.; Jähne, I.; Knobloch, K.; Karich, J.: Property Library LibIdGas for Combustion Gases Calculated as Ideal Gas Mixture from VDI-Guideline 4670 and Add-In FluidEXL for MS Excel. Zittau/Goerlitz University of Applied Sciences, Department of Technical Thermodynamics, Zittau (2003), available from http://thermodynamics-zittau.de.

[26] Kretzschmar, H.-J.; Stöcker, I.; Jähne, I.; Knobloch, K.; Hellriegel, T.: Property Library LibIdAir for Humid Air Calculated as Ideal Mixture of Ideal Gases and Water from VDI-Guideline 4670 and Add-In FluidEXL for MS Excel. Zittau/Goerlitz University of Applied Sciences, Department of Technical Thermodynamics, Zittau (2003), available from http://thermodynamics-zittau.de.

[27] Span, R.; Lemmon, E. W.; Jacobsen, R. T.; Wagner, W.; Yokozeki, A.: A Reference Equation of State for the Thermodynamic Properties of Nitrogen for Temperatures from 63.151 to 1000 K and Pressures to 2200 MPa. *J. Phys. Chem. Ref. Data* **29**, 1361-1433 (2000).

[28] de Reuck, K. M.; Wagner, W.: *Oxygen, International Thermodynamic Tables of the Fluid State-9.* Blackwell Scientific Publications LTD, Oxford (1987).

[29] Schmidt, R.; Wagner, W.: A New Form of the Equation of State for Pure Substances and its Application to Oxygen. *Fluid Phase Equil*. **19**, 175-200 (1985).

[30] Tegeler, Ch.; Span, R.; Wagner, W.: A New Equation of State for Argon Covering the Fluid Region for Temperatures from the Melting Line to 700 K at Pressure up to 1000 MPa. *J. Phys. Chem. Ref. Data* **28**, 779-850 (1999).

[31] Kretzschmar, H.-J.; Stöcker, I.; Jähne, I.; Knobloch, K.; Kleemann, L.; Seibt, D.: Property Library LibHuGas for Humid Combustion Gases Calculated as Ideal Mixtures of Real Fluids and Add-In FluidEXL for MS Excel. Zittau/Goerlitz University of Applied Sciences, Department of Technical Thermodynamics, Zittau (2002-2005), available from http://thermodynamics-zittau.de.

[32] Kleemann, L.; Seibt, D.: Calculation of the Thermophysical Properties of Humid Combustion Gases and Humid Air in Power-Cycle Modelling. Diploma Thesis, Zittau/Goerlitz University of Applied Sciences, Faculty of Mechanical Engineering, Zittau (2002) (in German).

[33] Kretzschmar, H.-J.; Stöcker, I.; Jähne, I.; Knobloch, K.; Hellriegel, T.; Kleemann, L.; Seibt, D.: Property Library LibHuAir for Humid Air Calculated as Ideal Mixture of Real Fluids and Add-In FluidEXL for MS Excel. Zittau/Goerlitz University of Applied Sciences, Department of Technical Thermodynamics, Zittau (2001-2005), available from http://thermodynamics-zittau.de.

[34] Hellriegel, T.: Calculation of the Thermodynamic Property Functions of Humid Air in Power-Cycle Modelling. Diploma Thesis, Zittau/Goerlitz University of Applied Sciences, Faculty of Mechanical Engineering, Zittau (2001) (in German).

[35] Rabinovich, V. A.; Beketov, V. G.: *Humid Gases, Thermodynamic Properties.* Begell House, New York (1995).

[36] Herrmann, S.: Determination of Thermodynamic and Transport Properties for Humid Air for Power Cycle Calculations. Diploma thesis, Zittau/Goerlitz University of Applied Sciences, Department of Technical Thermodynamics, Zittau (2006).

[37] Hyland, R. W.; Wexler, A.: Formulations for the Thermodynamic Properties of Dry Air from 173.15 K to 473.15 K, and of Saturated Moist Air From 173.15 K to 372.15 K, at Pressures to 5 MPa. *ASHRAE Trans.* **89**, 520-535 (1983).

[38] Nelson, H. F.; Sauer, H. J.: Formulation of High-Temperature Properties for Humid Air. *HVAC&R Research* **8**, 311-334 (2002).

[39] Gatley, D. P.: *Understanding Psychrometrics,* 2nd ed., ASHRAE, Atlanta (2005).

[40] Ji, X.; Lu, X.; Yan, J.: Survey of Experimental Data and Assessment of Calculation Methods of Properties for the Air–Water Mixture. *Appl. Therm. Eng.* **23**, 2213-2228 (2003).

[41] Ji, X.; Yan, J.: Saturated Thermodynamic Properties for the Air-Water System at Elevated Temperatures and Pressures. *Chem. Eng. Sci.* **58**, 5069-5077 (2003).

[42] Kunz, O.; Klimeck, R.; Wagner, W.; Jaeschke, M.: The GERG-2004 Wide-Range Equation of State for Natural Gases and Other Mixtures. *Fortschr.-Ber. VDI*, *Reihe 6: Energietechnik*, *Nr. 557*, VDI-Verlag, Düsseldorf (2007).

[43] IAPWS. Revised Supplementary Release on Saturation Properties of Ordinary Water Substance. 1992; available from the IAPWS Executive Secretary, Dr. R. B. Dooley, Structural Integrity Associates, Inc., Oakville, Ontario L6J 7L7, Canada, www.iapws.org.

[44] Wagner, W.; Pruss, A.: International Equations for the Saturation Properties of Ordinary Water Substance. Revised According to the International Temperature Scale of 1990. *J. Phys. Chem. Ref. Data* **22**, 783-787 (1993).

[45] Johnson, J. W.; Oelkers, E. H.; Helgeson, H. C.: SUPCRT92: A Software Package for Calculating the Standard Molal Thermodynamic Properties of Minerals, Gases, Aqueous Species, and Reactions from 1 to 5000 bar and 0 to 1000°C, *Comp. & Geosci.* **18**, 899-947 **(**1992).

[46] HumidAirTab V1.0, Thermodynamic Properties of Humid Air (Psychrometrics). ChemicaLogic Corp., Burlington MA, USA (1999).

[47] Goff, J. A.; Bates, A. C.: The Interaction Constant for Humid Air. *ASHVE Trans.* **47**, 373-390 (1941).

[48] Baldwin, R. R.; Daniel, S. G.: Determination of the Solubility of Gases in Liquids with Particular Reference to Viscous Liquids. *J. Appl. Chem.* **2**, 161-165 (1952).

[49] Baldwin, R. R.; Daniel, S. G.: The Solubility of Gases in Lubricating Oils and Fuels. *J. Inst. Petrol.* **39**, 105-124 (1953).

[50] McKee, O. L. Jr.: Ph.D. thesis, Purdue University, Department of Mechanical Engineering (1953). In Battino, R.: *Oxygen and Ozone*, *IUPAC Solubility Data Series 7*. Pergamon Press, Oxford, Chap. 2.1, p. 461 (1981).

[51] Eichelberger, W. C.: Solubility of Air in Brine at High Pressures. *Ind. Eng. Chem.* **47**, 2223-2228 (1955).

[52] IAPWS. Release on an Equation of State for H_2O Ice Ih. 2006; available from the IAPWS Executive Secretary, Dr. R. B. Dooley, Structural Integrity Associates, Inc., Oakville, Ontario L6J 7L7, Canada, www.iapws.org.

[53] Feistel, R.; Wagner, W.: A New Equation of State for H_2O Ice Ih. *J. Phys. Chem. Ref. Data* **35**, 1021-1047 (2006).

[54] Mohr, P. J.; Taylor, P. N.: CODATA Recommended Values of the Fundamental Physical Constants: 2002. *Rev. Mod. Phys.* **77**, 1-107 (2005).

[55] Harvey, A. H.; Huang, P. H.: First-Principles Calculation of the Air-Water Second Virial Coefficient. *Int. J. Thermophys.* **28**, 556-565 (2007).

[56] Harvey, A. H.; Lemmon, E. W.: Correlation for the Second Virial Coefficient of Water. *J. Phys. Chem. Ref. Data* **33**, 369-376 (2004).

[57] ASME. STP-TS-012 Thermophysical Properties of Working Gases used in Gas Turbine Applications. Prepared by ASME Air Properties Committee, ASME Standards Technology, LLC, New York (2008).

Part B

Transport Properties

1 Nomenclature

Symbols

Variable	Description
a_i	Coefficients
$a_{0i} \ldots a_{3i}$	Coefficients
A	Constant
A_i	Coefficients
A_{ij}^*	Temperature dependent ratio of collision integrals for *i-j* interactions
b_i	Coefficients
$b_{0i} \ldots b_{3i}$	Coefficients
B	Constant
B_i	Coefficients
B_{ij}^*	Temperature dependent relationship of collision integrals for *i-j* interactions
c_p	Specific isobaric heat capacity
c_V	Specific isochoric heat capacity
C	Constant
C_i	Coefficients
$c_{p\mathrm{m}}$	Molar isobaric heat capacity
$c_{V\mathrm{m}}$	Molar isochoric heat capacity
d_i	Exponents, coefficients
D	Constant
D_{ij}	Binary diffusion coefficient
E	Constant
F	Constant
F_c	Factor for molecular structure and polar effects
G	Constant
G_i	Parameters characterizing the density dependence of transport properties
h_i	Coefficients
h_{ij}	Coefficients
H	Constant
H_c	Pseudo-critical viscosity
H_i	Parameters characterizing the density dependence of transport properties
H_{ij}	Elements of determinant for calculating the viscosity of dense fluid mixtures

i	Exponent
k_B	Boltzmann`s constant
K_c	Pseudo-critical thermal conductivity
K_c	Concentration equilibrium constant
K_p	Pressure equilibrium constant
l_i	Exponents, coefficients
l_{ij}	Coefficients
L_{ij}	Elements of determinant for calculating the thermal conductivity of dense fluid mixtures
m	Mass
M	Molar mass
n	Number of terms in η^R and λ^R
N	Number of components of the mixture
N_i	Coefficients
N_A	Avogadro's constant
p	Pressure
q_D	Effective cutoff wave number
Q	Function
R	Universal molar gas constant
R_0	Universal amplitude
S	Constant, function
S_η	Effective cross section for the viscosity
t_i	Exponents
T	Temperature
v	Specific volume
V	Volume
W	Absolute humidity, constant
$\overline{x}$	Molar composition in general
x	Mole fraction
Y	Packing fraction
Y_i	Elements of determinant for calculating the transport properties of dense fluid mixtures
Z	Collision number
α	Parameter considering the contribution of internal degrees of freedom to thermal conductivity
α_{ij}	Parameter accounting for the mean free-path shortening for *i-j* interactions, interaction parameter in 3PCS model

β	Parameter considering the contribution of internal degrees of freedom to thermal conductivity
β_{ij}	Interaction parameter in 3PCS model
β_η	Parameter
β_λ	Parameter
γ	Critical exponent, volume fraction
γ_i	Parameters
γ_{ij}	Parameter accounting for the mean free-path shortening for *i-j* interactions, interaction parameter in 3PCS model
Γ	Amplitude of the asymptotic power law for $\tilde{\chi}$
δ	Reduced density
ΔH_d	Enthalpy of dimerisation reaction
ε	Scaling factor for energy, potential energy parameter
η	Dynamic viscosity
η_{ij}^0	Interaction viscosity in the limit of zero density
κ	Correction factor for hydrogen-bonding effects, bulk viscosity, scaling factor for thermal conductivity
λ	Thermal conductivity
λ_{ij}^0	Interaction thermal conductivity in the limit of zero density
μ	Dipole moment
ν	Kinematic viscosity, critical exponent
ξ	Correlation length, mass fraction
ξ_0	Amplitude of the asymptotic power law for ξ
ρ	Mass density
ρ_m^*	Switch-over molar density
σ	Scaling factor for length, potential length parameter
τ	Reciprocal reduced temperature
Φ_{ij}	Interaction parameter
$\overline{\chi}$	Contact value of pseudo-radial distribution function
$\overline{\chi}_{ij}$	Contact value of pseudo-radial distribution function in dense fluid mixture
$\tilde{\chi}$	Dimensionless generalized susceptibility
ψ	Scaling factor for viscosity; **Note:** In Part A ψ is used as mole fraction.
Ψ	Term considering the contribution of internal degrees of freedom to thermal conductivity
ω	Acentric factor
$\tilde{\Omega}$	Term of the enhancement of thermal conductivity in the critical region

$\tilde{\Omega}_0$	Correction term of the enhancement of thermal conductivity in the critical region
$\Omega^{(2,2)}$	Collision integral for viscosity and thermal conductivity

Superscripts

0	Limit of zero-density
1	Contribution to transport property related but not identical to residual part
2	Contribution to transport property accounting for the critical enhancement
adj	Adjusted
C	Contribution due to critical enhancement
o	Ideal-gas contribution
R	Residual contribution
*	Reduced variable

Subscripts

a	Component dry air
c	Critical
cal	Calculated
d	Dimer
exp	Experimental
i	Subindex for components of the mixture, for coefficients, and for exponents
ij	Subindex for interacting components of the mixture
ice	Ice
k	Kinetic contribution
liq	Liquid
m	Molar, monomer
md	Monomer-dimer interaction
mix	Mixture
p	Potential contribution
r	Reduced variable
ref	Reference
rf1, rf2	Reference fluids 1 and 2
R	Contribution to thermal conductivity due to reaction
s	Saturated state
vap	Vapour
w	Component water

Abbreviations

Abbreviation	Description
AA-CAES	Advanced Adiabatic Compressed Air Energy Storage, Project in the Fifth Framework Programme by the European Commission, Contract-No. ENK6-CT-2002-00611, www.cordis.lu.
FHZI	Zittau/Goerlitz University of Applied Science, Department of Technical Thermodynamics, Prof. Dr. H.-J. Kretzschmar, Zittau, Germany.
HuAir	Ideal mixture of the real fluids dry air and water (water from IAPWS-IF97) from FHZI; Software: LibHuAir from FHZI.
int	Internal contribution to the thermal conductivity.
Lib	Shortcut for 'Library'; corresponds to a property library, e.g., LibHuAir which includes functions for the calculation of humid air.
LHA	LibHuAir.
mon	Translational monatomic contribution to the thermal conductivity.
3PCS	Three-Parameter Corresponding States Model of Scalabrin *et al.*
RUB	Ruhr-Universität Bochum.
VW	Model of Vesovic and Wakeham.

2 Overview on Data from the Literature and Newly Measured Data

2.1 Data from the Literature

2.1.1 Dry Air

The collection of experimental data concerning the transport properties of dry air consists of 33 literature sources selected for the database. 19 of them contain results for the viscosity and 14 for the thermal conductivity. Only reliable data were selected, prepared, and incorporated into the database of the project AA-CAES, some older measurements were left out. For each data set a description file was added giving information about the method applied for the measurements, the preparation of the air used, the experimental uncertainty reported by the authors, and some additional remarks. Furthermore, some correlations and calculation methods handling dry air as a pure component (taken from the atmosphere) or as a mixture of nitrogen, oxygen, and argon were included. A comprehensive analysis of available experimental transport property data was given by Lemmon and Jacobsen [1].

2.1.2 Humid Air

Only a few experimental data for the transport properties of humid air are available. Two data sets for the viscosity [2], [3] and one set for the thermal conductivity [4] could be considered for the further evaluation of transport property models. All measurements on humid air reported in the open literature were restricted to atmospheric pressure and low temperatures (see Figure 2.1), but covered the complete range of composition. In most cases values for the densities of the mixtures were not given and had to be calculated from the equation of state.

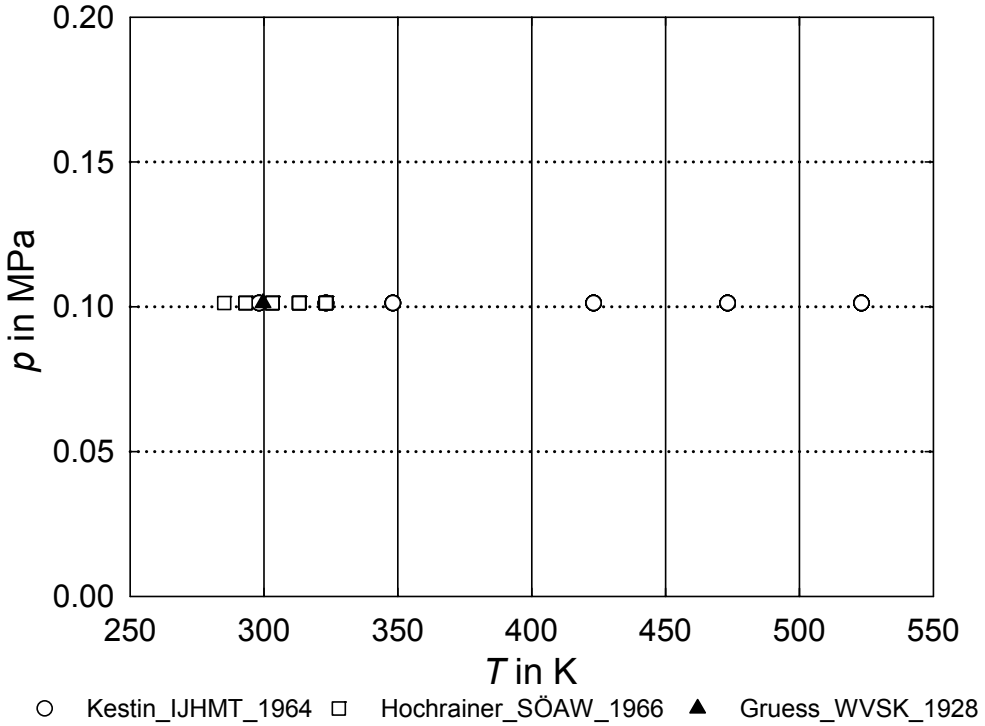

Figure 2.1: Pressure-temperature diagram with data points for the viscosity of humid air given by Kestin and Whitelaw (1964) [2] and by Hochrainer and Munczak (1966) [3] as well as for the thermal conductivity of humid air given by Grüß and Schmick (1928) [4].

2.1.3 Aqueous Mixtures

In addition, results of measurements for the viscosity of $N_2 + H_2O$ and $CH_4 + H_2O$ mixtures were reported by Assael *et al.* [5]. These measurements were carried out in the temperature range between 313 and 455 K near atmospheric pressure by means of a vibrating-wire viscometer.

2.2 Newly Measured Data

2.2.1 Dry Air

Measurements of the viscosity of dry air were carried out within this project at Ruhr-Universität Bochum [6], using a rotating-cylinder viscometer combined with a single-sinker densimeter, in the range between ambient temperature and 500 K up to a maximum pressure of 17 MPa. In addition, new experimental data on the thermal conductivity of dry air were provided by the co-workers from the Universidade de Lisboa [7]. Their measurements were performed with the transient hot-wire technique along three isotherms between 316 K and 436 K and at pressures up to 10 MPa. A comparison of the newly measured data with available transport property correlations is given in a later section.

2.2.2 Humid Air

In addition, the working group at Ruhr-Universität Bochum performed some measurements of the viscosity of humid air at small mole fractions of water in the temperature range between 298 and 500 K and pressures up to 15 MPa. These data points are plotted in Figure 2.2. New experimental data on the thermal conductivity of humid air should be determined by the working group of the Universidade de Lisboa, but have not become available until now.

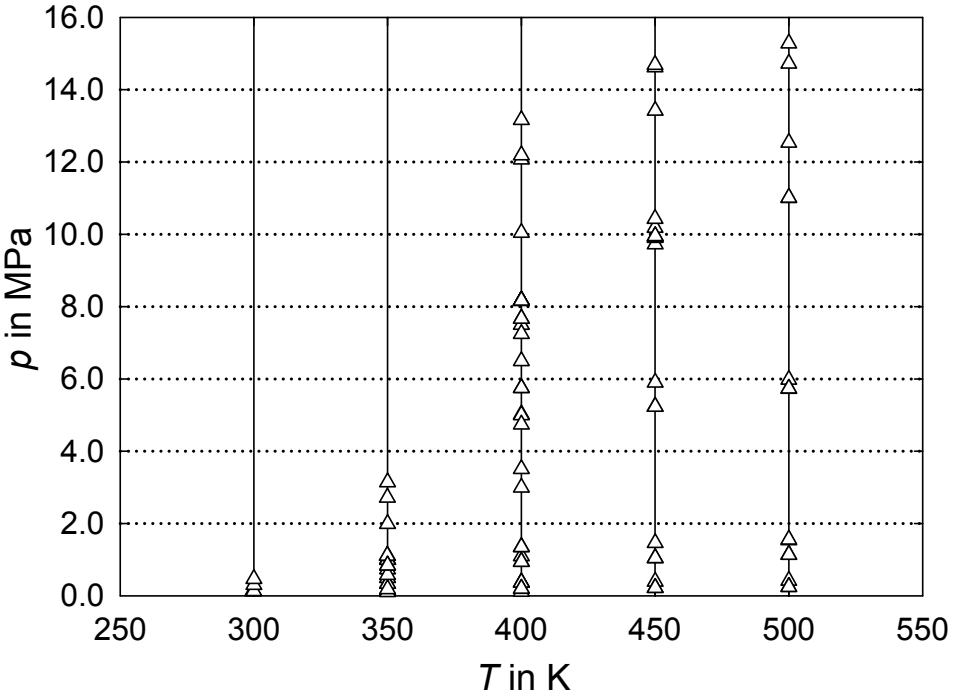

Figure 2.2: Pressure-temperature diagram with data points for the viscosity of humid air measured within the project by Wöll (RUB, 2005) [6].

3 Description of Models for Transport Properties

3.1 Transport Properties of Dry Air and Pure Water

The validity ranges and the uncertainties of correlations for the transport properties of dry air, argon, and water needed in the calculations of this section are summarized in Table 3.1.

Table 3.1: Validity ranges and uncertainties of correlations for the transport properties of dry air, argon, and water.

	Dry air [1]	**Argon [1]**	**Water [8], [9]**
Viscosity			
Temperature range	70-775 K	84-575 K (extrapolation possible)	273-1173 K
Max. pressure	100 MPa	100 MPa	300-1000 MPa
Uncertainty	Dilute gas: ± 1% High pressures: ± 2-5% Larger uncertainties near to critical point	Dilute gas: ± 0.5% High pressures: ± 1-2% Larger uncertainties near to critical point	Dilute gas: ± 1-2% Medium pressures: ± 2-3% High pressures and near to critical point: ± 5-8%
Thermal conductivity			
Temperature range	70-1100 K	89-980 K (extrapolation possible)	273-1073 K
Max. pressure	100 MPa	100 MPa	40-100 MPa
Uncertainty	Dilute gas: ± 2% High pressures: ± 3-5% Larger uncertainties near to critical point: > 10%	Dilute gas: ± 2% High pressures: ± 2-3% Larger uncertainties near to critical point: ± 5%	Dilute gas: ± 2% Medium pressures: ± 3% High pressures and near to critical point: ± 8%

3.1.1 Dry Air

Ambient air is a mixture of several components with varying mole fractions. Since the composition of the mixture influences the thermophysical properties, all experimenters of the project AA-CAES used samples of dry air with the same composition (mole fractions of nitrogen: 0.7820, oxygen: 0.2090, argon: 0.0090). Older measurements reported in the literature were normally performed on dried ambient air with small differences in the composition. Nevertheless, all these data were used as basis to develop correlations for the viscosity and the thermal conductivity of dry air. This makes possible calculation of the transport properties of dry air as a pseudo-pure component.

In addition, the transport properties of dry air can be determined by considering it to be a mixture of several pure components.

3.1.1.1 Dry Air as Mixture of Nitrogen, Oxygen, and Argon

The treatment of dry air as an ideal or a real mixture of the pure components nitrogen, oxygen, and argon requires a suitable mixing model. Such a model should be based on reliable correlations for the transport properties of the pure components. The formulations given by Lemmon and Jacobsen [1] and used in the AA-CAES project were developed using a large number of experimental data available in the literature and can be used to calculate the viscosity and thermal conductivity of nitrogen, oxygen, and argon over large ranges of temperature and pressure.

The viscosity of the pure fluids is expressed according to Lemmon and Jacobsen [1] with the following equation:

$$\eta = \eta^0(T) + \eta^{\mathrm{R}}(\tau, \delta)\,. \tag{3.1}$$

The viscosity of the dilute gas η^0 depends on the temperature T, whereas the residual part of viscosity η^{R} is a function of the reciprocal reduced temperature $\tau = T_{\mathrm{c}} / T$ and the reduced density $\delta = \rho / \rho_{\mathrm{c}}$. The critical parameters T_{c} and ρ_{c} are given in Table 3.4 at the end of this section. Since the enhancement of the viscosity in the vicinity of the critical point is comparably small and negligible for most practical applications, no critical contribution was included in the equation by Lemmon and Jacobsen. The dilute-gas viscosity (in μPa s) follows from:

$$\eta^0(T) = \frac{0.0266958\sqrt{MT}}{\sigma^2 \Omega^{(2,2)*}(T^*)}\,, \tag{3.2}$$

where M is the molar mass, σ is a scaling factor for length, and $\Omega^{(2,2)*}$ is the reduced collision integral for viscosity and thermal conductivity given as

$$\Omega^{(2,2)*}(T^*) = \exp\left\{\sum_{i=0}^{4} b_i \left[\ln\left(T^*\right)\right]^i\right\} \tag{3.3}$$

with

$$T^* = k_{\mathrm{B}} T / \varepsilon\,. \tag{3.4}$$

Here $\varepsilon / k_{\mathrm{B}}$ denotes a scaling factor for energy, k_{B} is Boltzmann`s constant. The coefficients of the collision integral equation are summarized to be:

$b_0 = 0.431$, $b_1 = -0.4623$, $b_2 = 0.08406$, $b_3 = 0.005341$, $b_4 = -0.00331$.

The residual fluid contribution to the viscosity follows from

$$\eta^{\mathrm{R}}(\tau, \delta) = \sum_{i=1}^{n} N_i \tau^{t_i} \delta^{d_i} \exp\left(-\gamma_i \delta^{l_i}\right). \tag{3.5}$$

All coefficients and exponents needed in Eq. (3.5) are summarized in Table 3.2. The parameter γ_i equals zero, if l_i is zero, and is unity, if l_i is not zero.

Table 3.2: Coefficients and exponents of the residual fluid viscosity relationship [Eq. (3.5)] taken from Lemmon and Jacobsen [1].

i	N_i	t_i	d_i	l_i	i	N_i	t_i	d_i	l_i
		Nitrogen					**Oxygen**		
1	10.72	0.1	2	0	1	17.67	0.05	1	0
2	0.03989	0.25	10	1	2	0.4042	0.0	5	0
3	0.001208	3.2	12	1	3	0.0001077	2.10	12	0
4	–7.402	0.9	2	2	4	0.3510	0.0	8	1
5	4.620	0.3	1	3	5	–13.67	0.5	1	2
		Argon					**Air**		
1	12.19	0.42	1	0	1	10.72	0.2	1	0
2	13.99	0.0	2	0	2	1.122	0.05	4	0
3	0.005027	0.95	10	0	3	0.002019	2.4	9	0
4	–18.93	0.5	5	2	4	–8.876	0.6	1	1
5	–6.698	0.9	1	4	5	-0.02916	3.6	8	1
6	–3.827	0.8	2	4					

Similar to the formulations given above for the viscosity, the thermal conductivity of the pure fluids is expressed as function of temperature as well as of reciprocal reduced temperature and of reduced density:

$$\lambda = \lambda^0(T) + \lambda^{\mathrm{R}}(\tau,\delta) + \lambda^{\mathrm{C}}(\tau,\delta), \tag{3.6}$$

where λ^0 is the thermal conductivity of the dilute gas, λ^{R} is the residual fluid contribution to the thermal conductivity, and λ^{C} is the contribution of the critical enhancement in the vicinity of the critical point which cannot be neglected in the case of the thermal conductivity. The reciprocal reduced temperature τ and the reduced density δ have already been introduced in connection with the viscosity equations.

The dilute-gas term of the thermal conductivity (in $\mathrm{mW\,m^{-1}\,K^{-1}}$) reads:

$$\lambda^0 = N_1 \left[\frac{\eta^0(T)}{1\ \mu\mathrm{Pa\ s}} \right] + N_2 \tau^{t_2} + N_3 \tau^{t_3}, \tag{3.7}$$

whereas the residual contribution to the thermal conductivity is given as:

$$\lambda^{\mathrm{R}} = \sum_{i=4}^{n} N_i \tau^{t_i} \delta^{d_i} \exp\left(-\gamma_i \delta^{l_i}\right). \tag{3.8}$$

The coefficients and exponents needed in the last two equations are summarized in Table 3.3. As already mentioned above, the value of the parameter γ_i depends on the values of the exponent l_i and equals either zero or unity.

Table 3.3: Coefficients and exponents of the dilute gas and of the residual fluid thermal conductivity equations [Eq. (3.7) and Eq. (3.8)] taken from Lemmon and Jacobsen [1].

i	N_i	t_i	d_i	l_i	i	N_i	t_i	d_i	l_i
	Nitrogen					**Oxygen**			
1	1.511				1	1.036			
2	2.117	–1.0			2	6.283	–0.9		
3	–3.332	–0.7			3	–4.262	–0.6		
4	8.862	0.0	1	0	4	15.31	0.0	1	0
5	31.11	0.03	2	0	5	8.898	0.0	3	0
6	–73.13	0.2	3	1	6	–0.7336	0.3	4	0
7	20.03	0.8	4	2	7	6.728	4.3	5	2
8	–0.7096	0.6	8	2	8	–4.374	0.5	7	2
9	0.2672	1.9	10	2	9	–0.4747	1.8	10	2
	Argon					**Air**			
1	0.8158				1	1.308			
2	–0.4320	–0.77			2	1.405	–1.1		
3	0.0	–1.0			3	–1.036	–0.3		
4	13.73	0.0	1	0	4	8.743	0.1	1	0
5	10.07	0.0	2	0	5	14.76	0.0	2	0
6	0.7375	0.0	4	0	6	–16.62	0.5	3	2
7	–33.96	0.8	5	2	7	3.793	2.7	7	2
8	20.47	1.2	6	2	8	–6.142	0.3	7	2
9	–2.274	0.8	9	2	9	–0.3778	1.3	11	2
10	–3.973	0.5	1	4					

The contribution to the thermal conductivity of the fluid due to the enhancement in the critical region is calculated by means of a model developed by Olchowy and Sengers [10]. Thus the critical enhancement of the thermal conductivity results as:

$$\lambda^{\mathrm{C}} = \rho c_p \frac{k_{\mathrm{B}} R_0 T}{6\pi\xi\eta(T,\rho)}\left(\tilde{\Omega} - \tilde{\Omega}_0\right), \tag{3.9}$$

where

$$\tilde{\Omega} = \frac{2}{\pi}\left[\left(\frac{c_p - c_V}{c_p}\right)\tan^{-1}\left(\xi / q_{\mathrm{D}}\right) + \frac{c_V}{c_p}\left(\xi / q_{\mathrm{D}}\right)\right] \tag{3.10}$$

and

$$\tilde{\Omega}_0 = \frac{2}{\pi}\left\{1 - \exp\left[\frac{-1}{\left(\xi / q_{\mathrm{D}}\right)^{-1} + \frac{1}{3}\left(\xi / q_{\mathrm{D}}\right)^2\left(\rho_{\mathrm{c}} / \rho\right)^2}\right]\right\}. \tag{3.11}$$

The correlation length ξ follows from

$$\xi = \xi_0 \left[\frac{\tilde{\chi}(T,\rho) - \tilde{\chi}(T_{\mathrm{ref}},\rho)\frac{T_{\mathrm{ref}}}{T}}{\Gamma} \right]^{\nu/\gamma} , \tag{3.12}$$

with

$$\tilde{\chi}(T,\rho) = \frac{p_{\mathrm{c}}\rho}{\rho_{\mathrm{c}}^2}\left(\frac{\partial\rho}{\partial p}\right)_T . \tag{3.13}$$

In these equations, R_0, ν, and γ are theoretically based constants with values of $R_0 = 1.01$, $\nu = 0.63$, and $\gamma = 1.2415$, whereas the fluid-specific terms q_{D}, ξ_0, and Γ were derived from a fit to experimental data in the critical region. The specific isobaric and isochoric heat capacities, c_p and c_V, as well as the first derivative of mass density with respect to pressure are available from the equation of state given by Lemmon *et al.* [11]. The reference temperature T_{ref} (see Table 3.4) was chosen to be twice the critical temperature T_{c}. At temperatures higher than T_{ref} the bracket term in Eq. (3.12) becomes negative and the critical enhancement should be set zero.

Table 3.4: Parameters of the viscosity and thermal conductivity equations.

Parameter	Nitrogen	Argon	Oxygen	Air
T_{c} / K	126.192	150.687	154.581	132.6312
ρ_{mc} / mol dm^{-3}	11.1839	13.40743	13.63	10.4477
p_{c} / MPa	3.3958	4.863	5.043	3.78502
M / g mol^{-1}	28.01348	39.948	31.9988	28.9586
$\varepsilon/k_{\mathrm{B}}$ / K	98.94	143.2	118.5	103.3
σ / nm	0.3656	0.335	0.3428	0.360
ξ_0 / nm	0.17	0.13	0.24	0.11
Γ	0.055	0.055	0.055	0.055
q_{D} / nm	0.40	0.32	0.51	0.31
T_{ref} / K	252.384	301.374	309.162	265.262

If a suitable mixing model is available, the transport properties of dry air can be derived in large ranges of temperature and pressure using the equations for the viscosity and thermal conductivity of the pure fluids nitrogen, oxygen, and argon.

3.1.1.2 Dry Air as Pseudo-Pure Component

The formulations for the viscosity and thermal conductivity reported by Lemmon and Jacobsen [1] can also be applied to calculate the transport properties of dry air treated as pseudo-pure component. The parameters and coefficients needed for these calculations have already been given in the tables of the foregoing section.

3.1.2 Water and Steam

The International Association for the Properties of Water and Steam (IAPWS) provided formulations for the calculation of the viscosity [8] as well as of the thermal conductivity [9] of ordinary water substance over large ranges of temperature and pressure.
The viscosity of water and steam is given in reduced form according to the following equation developed for general and scientific use:

$$\eta_\mathrm{r} = \eta_\mathrm{r}^0(T_\mathrm{r})\,\eta_\mathrm{r}^1(T_\mathrm{r},\rho_\mathrm{r})\,\eta_\mathrm{r}^2(T_\mathrm{r},\rho_\mathrm{r}) \tag{3.14}$$

Because all quantities are used in their reduced forms, the reference values to perform the reduction are given first together with the corresponding equations. In this connection it is to be noted that the values of the reference constants are close to, but not identical to the critical constants given in the equation of state [12], [13].

Table 3.5: Reference constants and relationships to reduce viscosities and thermal conductivities for water and steam.

Reference constants	Reduced quantities	
$T^* = 647.226$ K	$T_\mathrm{r} = T/T^*$	(3.15)
$\rho^* = 317.763$ kg m^{-3}	$\rho_\mathrm{r} = \rho/\rho^*$	(3.16)
$p^* = 22.115$ MPa	$p_\mathrm{r} = p/p^*$	(3.17)
$\eta^* = 55.071\ \mu$Pa s	$\eta_\mathrm{r} = \eta/\eta^*$	(3.18)
$\lambda^* = 0.4945$ W m^{-1} K^{-1}	$\lambda_\mathrm{r} = \lambda/\lambda^*$	(3.19)

The first term of Eq. (3.14) represents the reduced viscosity coefficient in the dilute-gas limit and follows from:

$$\eta_\mathrm{r}^0(T_\mathrm{r}) = \frac{\sqrt{T_\mathrm{r}}}{\sum_{i=0}^{3} \frac{h_i}{T_\mathrm{r}^i}}. \tag{3.20}$$

The coefficients h_i in this equation were determined to be:

$h_0 = 1.000000$ $\quad$ $h_1 = 0.978197$
$h_2 = 0.579829$ $\quad$ $h_3 = -0.202354$.

The second multiplicative factor is related but not identical with the residual contribution of viscosity and reads as

$$\eta_\mathrm{r}^1(T_\mathrm{r},\rho_\mathrm{r}) = \exp\left[\rho_\mathrm{r}\sum_{i=0}^{5}\sum_{j=0}^{6} h_{ij}\left(\frac{1}{T_\mathrm{r}}-1\right)^i\left(\rho_\mathrm{r}-1\right)^j\right] \tag{3.21}$$

with the coefficients h_{ij} summarized in the table given below. All h_{ij} values with combinations of the indices i and j not given in this table are equal zero.

Table 3.6: Coefficients h_{ij} for $\eta_{\mathrm{r}}^{1}(T_{\mathrm{r}},\rho_{\mathrm{r}})$.

i	j	h_{ij}	i	j	h_{ij}
0	0	$h_{00}=$ 0.5132047	2	2	$h_{22}=$ –1.263184
1	0	$h_{10}=$ 0.3205656	0	3	$h_{03}=$ 0.1778064
4	0	$h_{40}=$ –0.7782567	1	3	$h_{13}=$ 0.4605040
5	0	$h_{50}=$ 0.1885447	2	3	$h_{23}=$ 0.2340379
0	1	$h_{01}=$ 0.2151778	3	3	$h_{33}=$ –0.4924179
1	1	$h_{11}=$ 0.7317883	0	4	$h_{04}=$ –0.04176610
2	1	$h_{21}=$ 1.241044	3	4	$h_{34}=$ 0.1600435
3	1	$h_{31}=$ 1.476783	1	5	$h_{15}=$ –0.01578386
0	2	$h_{02}=$ –0.2818107	3	6	$h_{36}=$ –0.003629481
1	2	$h_{12}=$ –1.070786			

The last term of Eq. (3.14) accounts for the enhancement of the viscosity in the vicinity of the critical point and has only to be considered in a limited range of temperature and density and is described by the following equations:

$$\eta_{\mathrm{r}}^{2}(T_{\mathrm{r}},\rho_{\mathrm{r}}) = 0.922\ \tilde{\chi}^{0.0263} \qquad \text{if} \quad \tilde{\chi} \geq 21.93 \tag{3.22}$$

$$\eta_{\mathrm{r}}^{2}(T_{\mathrm{r}},\rho_{\mathrm{r}}) = 1 \qquad \text{if} \quad \tilde{\chi} < 21.93\ . \tag{3.23}$$

For industrial use the function η_{r}^{2} can be taken to be unity in the complete range of temperature and pressure or density, respectively.
The values for $\tilde{\chi}$ result from the equation of state according to the definition:

$$\tilde{\chi} = \rho_{\mathrm{r}} \left(\frac{\partial \rho_{\mathrm{r}}}{\partial p_{\mathrm{r}}} \right)_{T_{\mathrm{r}}}\ . \tag{3.24}$$

$\eta_{\mathrm{r}}^{2}(T_{\mathrm{r}},\rho_{\mathrm{r}})$ can be chosen in ranges located outside the critical region to be equal unity to allow simplified calculations, what means to avoid the determination of $\tilde{\chi}$ for points beyond that region. This follows from the experience that the thermodynamically stable areas with $\eta_{\mathrm{r}}^{2} > 1$ are situated within the following boundaries:

$$0.996 \leq T_{\mathrm{r}} \leq 1.01 \tag{3.25}$$

$$0.71 \leq \rho_{\mathrm{r}} \leq 1.36\ . \tag{3.26}$$

It is to be noted that these two equations are not part of the formal definition of the IAPWS formulation.

The equation for the thermal conductivity of ordinary water substance developed for scientific use differs from that shown for the viscosity and is given in reduced form as follows:

$$\lambda_r = \lambda_r^0(T_r)\,\lambda_r^1(T_r,\rho_r) + \lambda_r^2(T_r,\rho_r) \tag{3.27}$$

The reason for that is the much larger influence of the critical enhancement in the case of the thermal conductivity taken into consideration by a separate summand λ_r^2.
The first term in Eq. (3.27) represents the thermal conductivity in the dilute-gas limit and is written in reduced form as

$$\lambda_r^0(T_r) = \frac{\sqrt{T_r}}{\sum_{i=0}^{3} \frac{l_i}{T_r^i}} \tag{3.28}$$

with the following coefficients l_i:

$l_0 = 1.000000$ $\quad$ $l_1 = 6.978267$
$l_2 = 2.599096$ $\quad$ $l_3 = -0.998254.$

The second factor is given similarly to the corresponding term in the viscosity equation:

$$\lambda_r^1(T_r,\rho_r) = \exp\left[\rho_r \sum_{i=0}^{4}\sum_{j=0}^{5} l_{ij}\left(\frac{1}{T_r}-1\right)^i (\rho_r - 1)^j\right]. \tag{3.29}$$

The coefficients required in Eq. (3.29) are listed in the following table, whereas all values of l_{ij} not given are equal zero.

Table 3.7: Coefficients l_{ij} for $\lambda_r^1(T_r,\rho_r)$.

i	j	l_{ij}	i	j	l_{ij}
0	0	$l_{00} = 1.3293046$	2	2	$l_{22} = 4.9874687$
1	0	$l_{10} = 1.7018363$	3	2	$l_{32} = 4.3786606$
2	0	$l_{20} = 5.2246158$	0	3	$l_{03} = 0.018660751$
3	0	$l_{30} = 8.7127675$	1	3	$l_{13} = -0.76736002$
4	0	$l_{40} = -1.8525999$	2	3	$l_{23} = -0.27297694$
0	1	$l_{01} = -0.40452437$	3	3	$l_{33} = -0.91783782$
1	1	$l_{11} = -2.2156845$	0	4	$l_{04} = -0.12961068$
2	1	$l_{21} = -10.124111$	1	4	$l_{14} = 0.37283344$
3	1	$l_{31} = -9.5000611$	2	4	$l_{24} = -0.43083393$
4	1	$l_{41} = 0.93404690$	0	5	$l_{05} = 0.044809953$
0	2	$l_{02} = 0.24409490$	1	5	$l_{15} = -0.11203160$
1	2	$l_{12} = 1.6511057$	2	5	$l_{25} = 0.13333849$

As already mentioned above, the additive term $\lambda_r^2(T_r,\rho_r)$ of Eq. (3.27) represents the contribution resulting for the enhancement of thermal conductivity in the vicinity of the critical point and is defined as:

$$\lambda_{\mathrm{r}}^{2}(T_{\mathrm{r}},\rho_{\mathrm{r}}) = \frac{0.0013848}{\eta_{\mathrm{r}}^{0}(T_{\mathrm{r}})\,\eta_{\mathrm{r}}^{1}(T_{\mathrm{r}},\rho_{\mathrm{r}})}\left(\frac{T_{\mathrm{r}}}{\rho_{\mathrm{r}}}\right)^{2}\left(\frac{\partial p_{\mathrm{r}}}{\partial T_{\mathrm{r}}}\right)_{\rho_{\mathrm{r}}}^{2}\tilde{\chi}^{0.4678}\,\rho_{\mathrm{r}}^{1/2} \cdot \exp\left[-18.66\left(T_{\mathrm{r}}-1\right)^{2}-\left(\rho_{\mathrm{r}}-1\right)^{4}\right] \quad . \tag{3.30}$$

Here the contributions $\eta_{\mathrm{r}}^{0}(T_{\mathrm{r}})$ and $\eta_{\mathrm{r}}^{1}(T_{\mathrm{r}},\rho_{\mathrm{r}})$ follow from the viscosity equations described above including the definition of the quantity $\tilde{\chi}$.

In addition to the formulation for the thermal conductivity of ordinary water substance for general and scientific use, the IAPWS also provides equations for industrial use given here for completeness. The main difference between both equations is related to the treatment of the enhancement in the vicinity of the critical point which is assumed to be a finite value in the following equation instead of infinity justified by theory.
The reduced thermal conductivity results in the whole range of temperature and density according to the following equation:

$$\lambda_{\mathrm{r}} = \lambda_{\mathrm{r}}^{0}(T_{\mathrm{r}}) + \lambda_{\mathrm{r}}^{1}(\rho_{\mathrm{r}}) + \lambda_{\mathrm{r}}^{2}(T_{\mathrm{r}},\rho_{\mathrm{r}})\,. \tag{3.31}$$

The first term represents again the dilute-gas thermal conductivity and is given as function of temperature

$$\lambda_{\mathrm{r}}^{0}(T_{\mathrm{r}}) = \sqrt{T_{\mathrm{r}}}\sum_{i=0}^{3} a_i T_{\mathrm{r}}^{\,i}\,, \tag{3.32}$$

whereas the second term λ_{r}^{1} in the industrial equation is written as a function of density only:

$$\lambda_{\mathrm{r}}^{1}(\rho_{\mathrm{r}}) = b_0 + b_1\rho_{\mathrm{r}} + b_2\exp\left[B_1\left(\rho_{\mathrm{r}}+B_2\right)^{2}\right]. \tag{3.33}$$

Finally, the third term is given as:

$$\lambda_{\mathrm{r}}^{2}(T_{\mathrm{r}},\rho_{\mathrm{r}}) = \left(\frac{d_1}{T_{\mathrm{r}}^{10}}+d_2\right)\rho_{\mathrm{r}}^{9/5}\exp\left[C_1\left(1-\rho_{\mathrm{r}}^{14/5}\right)\right] + \mathrm{d}_3\,S\,\rho_{\mathrm{r}}^{Q}\exp\left[\left(\frac{Q}{1+Q}\right)\left(1-\rho_{\mathrm{r}}^{1+Q}\right)\right] + d_4\exp\left(C_2 T_{\mathrm{r}}^{3/2}+\frac{C_3}{\rho_{\mathrm{r}}^{5}}\right). \tag{3.34}$$

Here S and Q are functions of ΔT_{r} given as:

$$Q = 2 + \frac{C_5}{\Delta T_{\mathrm{r}}^{3/5}} \tag{3.35}$$

$$S = \begin{cases} \dfrac{1}{\Delta T_{\mathrm{r}}} & \text{for} \quad T_{\mathrm{r}} \geq 1 \\ \dfrac{C_6}{\Delta T_{\mathrm{r}}^{3/5}} & \text{for} \quad T_{\mathrm{r}} < 1 \end{cases}, \tag{3.36}$$

with

$$\Delta T_r = \left| T_r - 1 \right| + C_4 \,. \tag{3.37}$$

All coefficients required to calculate the contributions of the thermal conductivity as well the reference constants needed to perform the reduction of the different quantities are summarized in Table 3.8.

Table 3.8: Reference constants and coefficients for the industrial thermal conductivity formulation for water and steam.

Reference constants			
$T^* = 647.26$ K	$\rho^* = 317.7$ kg m^{-3}	$\lambda^* = 1$ W m^{-1} K^{-1}	
Coefficients for λ_r^0			
$a_0 = 0.0102811$	$a_1 = 0.0299621$	$a_2 = 0.0156146$	$a_3 = -0.00422464$
Coefficients for λ_r^1			
$b_0 = -0.397070$	$b_1 = 0.400302$	$b_2 = 1.060000$	
$B_1 = -0.171587$	$B_2 = 2.392190$		
Coefficients for λ_r^2			
$d_1 = 0.0701309$	$d_2 = 0.0118520$	$d_3 = 0.00169937$	$d_4 = -1.0200$
$C_1 = 0.642857$	$C_2 = -4.11717$	$C_3 = -6.17937$	$C_4 = 0.00308976$
$C_5 = 0.0822994$	$C_6 = 10.0932$		

3.2 Transport Properties of Humid Air

General models for the prediction of transport properties of gaseous mixtures at high pressures are hardly applicable to mixtures containing polar substances like water. As a consequence, only the model of Chung *et al.* [14], [15] was selected for the investigation. It is obvious that a suitable model for the prediction of the transport properties of gaseous mixtures should be able to reproduce the properties of the pure components at least. Furthermore, it is reasonable to consider dry air in the humid-air mixture as a pseudo-pure component. Therefore, models which can use correlations of the transport properties of dry air [1] and water [8], [9] were particularly taken into consideration. A prediction procedure treating humid air as an ideal mixture of real fluids has been proposed by co-workers of work package 4 [16]. Furthermore, a more theoretically founded model recommended by Vesovic and Wakeham [17], [18] was considered in the evaluation. In addition, a three-parameter corresponding states model [19], [20] requiring only some values under saturation conditions as well as transport equations of two reference fluids has been tested.

3.2.1 Multiparameter Correlation of Chung *et al.*

Chung *et al.* [14], [15] presented a prediction method for the viscosity and thermal conductivity of polar, nonpolar, and associating fluids in wide ranges of temperature and pressure. It requires temperature and molar density as well as the critical constants, acentric factor, dipole moment, and an empirically determined association factor as input parameters. In addition, the composition is needed for the prediction of the transport properties of mixtures. The mixing rules given for all parameters are based on the conformal solution model. Then the same empirically correlated density-dependent functions are applied to pure fluids and fluid mixtures.

Viscosity

The viscosity of the dilute gas is given according to the kinetic gas theory as:

$$\eta^0 = 2.669 \cdot 10^{-6} \frac{(MT)^{1/2}}{\sigma^2 \Omega^{(2,2)*}(T^*)} . \tag{3.38}$$

Here, η^0 is the viscosity in Pa s, M is the molar mass in g mol^{-1}, T is the temperature in K, and σ is the potential length parameter in 10^{-10} m. The reduced collision integral $\Omega^{(2,2)*}$ can be written as a function of the reduced temperature T^*

$$\Omega^{(2,2)*}(T^*) = \left(\frac{A}{T^{*B}}\right) + \frac{C}{\exp\left(DT^*\right)} + \frac{E}{\exp\left(FT^*\right)} + GT^{*B} \sin\left(ST^{*W} - H\right) \tag{3.39}$$

$$T^* = k_\mathrm{B} T / \varepsilon , \tag{3.40}$$

where k_B is Boltzmann`s constant and $\varepsilon / k_\mathrm{B}$ is the potential energy parameter in K. A to H as well as S and W are constants. The potential parameters are related to the critical temperature T_c and the critical molar volume V_mc (in cm^3 mol^{-1}). A factor F_c is adopted to account for molecular structure and polar effects.

$$\sigma = 0.809 \; V_\mathrm{mc}^{1/3} \tag{3.41}$$

$$\varepsilon / k_\mathrm{B} = T_\mathrm{c} / 1.2593 \tag{3.42}$$

$$F_\mathrm{c} = 1 - 0.2756\omega + 0.059035\mu_\mathrm{r}^4 + \kappa \tag{3.43}$$

Here, ω is the acentric factor, μ_r is a reduced dipole moment, and κ is a correction factor for hydrogen-bonding effects in associating fluids which is empirically derived from experimental viscosity data. Finally, the viscosity of the dilute gas results as:

$$\eta^0 = 4.0785 \cdot 10^{-6} \frac{(MT)^{1/2}}{V_\mathrm{mc}^{2/3} \Omega^{(2,2)*}(T^*)} F_\mathrm{c} . \tag{3.44}$$

The viscosity of dense fluids as a function of temperature T and molar density ρ_m follows from:

$$\eta = \eta_\mathrm{k} + \eta_\mathrm{p} \tag{3.45}$$

$$\eta_\mathrm{k} = \eta^0 \left(1/G_2 + A_6 Y\right) \tag{3.46}$$

$$\eta_\mathrm{p} = \left[3.6344 \cdot 10^{-6} \frac{\left(MT_\mathrm{c}\right)^{1/2}}{V_\mathrm{mc}^{2/3}}\right] A_7 Y^2 G_2 \exp\left(A_8 + \frac{A_9}{T^*} + \frac{A_{10}}{T^{*2}}\right) \tag{3.47}$$

$$Y = \rho_\mathrm{m} V_\mathrm{mc} / 6 \tag{3.48}$$

$$G_1 = \left(1.0 - 0.5Y\right)/\left(1-Y\right)^3 \tag{3.49}$$

$$G_2 = \left\{A_1\left[1 - \exp\left(-A_4 Y\right)\right]/Y + A_2 G_1 \exp\left(A_5 Y\right) + A_3 G_1\right\}/\left(A_1 A_4 + A_2 + A_3\right). \tag{3.50}$$

The coefficients A_i are linear functions of the acentric factor, of the reduced dipole moment, and of the association factor:

$$A_i = a_{0i} + a_{1i}\omega + a_{2i}\mu_\mathrm{r}^4 + a_{3i}\kappa \qquad (i = 1,10). \tag{3.51}$$

Thermal Conductivity

The thermal conductivity of a dilute gas is related to the viscosity:

$$\lambda^0 = 311.8 \left(\frac{\eta^0}{M}\right)\Psi \tag{3.52}$$

$$\Psi = 1 + \alpha\left(\frac{0.215 + 0.28288\alpha - 1.061\beta + 0.26665Z}{0.6366 + \beta Z + 1.061\alpha\beta}\right) \tag{3.53}$$

$$\alpha = \frac{c_{V\mathrm{m}}^\mathrm{o}}{R} - \frac{3}{2} \tag{3.54}$$

$$\beta = 0.786231 - 0.710907\omega + 1.31683\omega^2 \tag{3.55}$$

$$Z = 2.0 + 10.5T_\mathrm{r}^2 \tag{3.56}$$

$$T_\mathrm{r} = T/T_\mathrm{c}. \tag{3.57}$$

Here, λ^0 is given in $\mathrm{W\,m^{-1}\,K^{-1}}$, whereas $c_{V\mathrm{m}}^\mathrm{o}$ is the molar ideal-gas heat capacity at constant volume obtainable from correlations in the literature or using the equation of state.

The thermal conductivity of a dense fluid or fluid mixture results from:

$$\lambda = \lambda_\mathrm{k} + \lambda_\mathrm{p} \tag{3.58}$$

$$\lambda_\mathrm{k} = \lambda^0 \left(1/H_2 + B_6 Y\right) \tag{3.59}$$

$$\lambda_{\mathrm{p}} = \left[0.12715 \, \frac{\left(T_{\mathrm{c}} / M\right)^{1/2}}{V_{\mathrm{mc}}^{2/3}} \right] B_7 Y^2 H_2 T_{\mathrm{r}}^{1/2} \,. \tag{3.60}$$

Y and G_1 are obtained as described for the viscosity, H_2 is calculated similar to G_2 using the coefficients B_i given as:

$$B_i = b_{0i} + b_{1i}\omega + b_{2i}\mu_{\mathrm{r}}^4 + b_{3i}\kappa \qquad (i = 1,7) \,. \tag{3.61}$$

Remarks concerning the implementation of this model on humid air:

The model was tested for several pure components. In particular, the transport properties of dry air (as pseudo-pure component) and water vapour were calculated at temperatures between 300 and 1150 K and at pressures up to 25 MPa and were compared with available correlations from the literature. The results for the viscosity of dry air were in reasonable agreement with the correlation of Lemmon and Jacobsen [1] (± 2.5%), whereas larger differences up to 15% occurred for its thermal conductivity. Although this model was developed on the basis of experimental data of different substances including water, the calculated viscosity values differed from the IAPWS formulation [8] by – 6.5% to + 13%, whereas deviations up to 50% were found for the thermal conductivity related to the IAPWS formulation [9]. Since a suitable model should be able to reproduce the properties of the pure components, this procedure is by no means applicable for the prediction of the transport properties of humid air. Hence this model was not considered in the further evaluation.

3.2.2 Program Package LibHuAir

The program package LibHuAir developed by Kretzschmar *et al.* from the Zittau/Goerlitz University of Applied Sciences [16] includes equations for the calculation of the thermodynamic and transport properties of humid air.

The viscosity of humid air is calculated as an ideal mixture of dry air and of water vapour both characterised by real behaviour. Input parameters are the temperature T, the total pressure p, and the composition of the mixture (mass fraction of water). The properties of the pure or pseudo-pure components are determined as functions of temperature and of partial density ρ_i and summed up according to their volume fractions γ_i. Thus, the viscosity of unsaturated and saturated humid air results as:

$$\eta_{\mathrm{mix}} = \gamma_{\mathrm{a}} \, \eta_{\mathrm{a}}(T, \rho_{\mathrm{a}}) + \gamma_{\mathrm{w}} \, \eta_{\mathrm{w}}(T, \rho_{\mathrm{w}}) \,. \tag{3.62}$$

The volume fraction of each component is given as:

$$\gamma_i = \frac{V_i}{V_{\mathrm{mix}}} = \frac{m_i \; v_i}{m_{\mathrm{mix}} \; v_{\mathrm{mix}}} = \xi_i \, \frac{v_i}{v_{\mathrm{mix}}} \tag{3.63}$$

with

$$v_{\mathrm{mix}} = \frac{1}{\dfrac{1}{v_{\mathrm{a}}(T, p_{\mathrm{a}})} + \dfrac{1}{v_{\mathrm{w}}(T, p_{\mathrm{w}})}} = \frac{1}{\rho_{\mathrm{mix}}} = \frac{1}{\rho_{\mathrm{a}}(T, p_{\mathrm{a}}) + \rho_{\mathrm{w}}(T, p_{\mathrm{w}})} . \tag{3.64}$$

Here, V_i and V_{mix} are the volumes in m^3, v_i and v_{mix} are the specific volumes in $\mathrm{m}^3\ \mathrm{kg}^{-1}$, m_i and m_{mix} are the masses in kg, and ξ_i is the mass fraction. In addition, p_i is the partial pressure. The specific density of the mixture ρ_{mix} can also be derived and used in calculations with other models.

The thermal conductivity of humid air is calculated according to the same procedure. Properties of the mixture are not necessary for this procedure. Only the transport property equations of the pure components are needed.

Remarks concerning the implementation of this model on humid air:

At temperatures below the critical temperature and near to the saturation line of water, the evaluation of the transport properties of humid air needs a careful inspection of the partial density ρ_{w} which is calculated for the partial pressure p_{w} using the equation of state. The reason for that is that ρ_{w} could become greater than the density of the saturated pure vapour because the mixture density calculation in the LibHuAir package, leads to increased values of the saturated vapour pressure $p_{\mathrm{s}}\left(T, p, \bar{x}\right)$ by taking into account the so-called poynting correction. This situation has to be avoided, since the transport property values η_{w} and λ_{w} are calculated for the partial density ρ_{w} and the correlations of the transport properties of pure water are not valid in the two-phase region.

In contrast to the other models, the LibHuAir package contains the algorithms for the calculation of the thermodynamic and the transport properties of humid air, but also provides the equations of state and the viscosity and thermal conductivity correlations for the pure components. With respect to a comparison of different prediction models, the same formulations for the pure or pseudo-pure components should be used. In the case of dry air, the equation of state given by Lemmon *et al.* [11] and the transport property correlations of Lemmon and Jacobsen [1] are used in all models. It is important to note that the IAPWS makes available different formulations of the thermophysical properties of water for industrial and scientific uses. The original version of LibHuAir applies formulations for industrial use both for the thermodynamic properties [21] as well as for the transport properties [8], [9], whereas the formulations for scientific use [8], [9], [12], [13] are utilised in the other prediction models leading to small differences in the calculated transport property values, particularly close to the critical point.

3.2.3 Model of Vesovic and Wakeham

The method proposed by Vesovic and Wakeham [17], [18] to predict the transport properties of a dense fluid mixture is based on a rigid-sphere model. The real behaviour of the fluids is taken into account by the contact value of the pseudo-radial distribution

function derived from the transport property correlations of the pure components. Furthermore, the temperature, the molar density of the mixture, and the composition are needed as input quantities. Experimental data of the mixture are not necessary for the calculation, but can be used for an improvement of the method. In addition, it is to be noted that Vesovic and Wakeham treated the transport properties in the way that the contributions resulting from the enhancement near to the critical point are excluded.

Viscosity

The viscosity of a dense fluid mixture containing N components is given as

$$\eta_{\mathrm{mix}}(T,\rho_{\mathrm{m}},\overline{x}) = -\begin{vmatrix} H_{11} & \cdots & H_{1N} & Y_1 \\ \vdots & & \vdots & \vdots \\ H_{N1} & \cdots & H_{NN} & Y_N \\ Y_1 & \cdots & Y_N & 0 \end{vmatrix} \Bigg/ \begin{vmatrix} H_{11} & \cdots & H_{1N} \\ \vdots & & \vdots \\ H_{N1} & \cdots & H_{NN} \end{vmatrix} + \kappa_{\mathrm{mix}} \tag{3.65}$$

$$Y_i = x_i \left(1 + \sum_{j=1}^{N} \frac{m_j}{m_i + m_j} x_j \alpha_{ij} \overline{\chi}_{ij} \rho_{\mathrm{m}} \right) \tag{3.66}$$

$$H_{ii} = \frac{x_i^2 \overline{\chi}_{ii}}{\eta_i^0} + \sum_{\substack{j=1 \\ j \neq i}}^{N} \frac{x_i x_j \overline{\chi}_{ij}}{2 A_{ij}^* \eta_{ij}^0} \frac{m_i m_j}{\left(m_i + m_j\right)^2} \left(\frac{20}{3} + \frac{4 m_j}{m_i} A_{ij}^* \right) \tag{3.67}$$

$$H_{ij} = -\frac{x_i x_j \overline{\chi}_{ij}}{2 A_{ij}^* \eta_{ij}^0} \frac{m_i m_j}{\left(m_i + m_j\right)^2} \left(\frac{20}{3} - 4 A_{ij}^* \right) \quad (i \neq j) \tag{3.68}$$

$$\kappa_{\mathrm{mix}} = \frac{16}{5\pi} \frac{15}{16} \rho_{\mathrm{m}}^2 \sum_{i=1}^{N} \sum_{j=1}^{N} x_i x_j \overline{\chi}_{ij} \alpha_{ij}^2 \eta_{ij}^0 \tag{3.69}$$

Here x_i and x_j are the mole fractions of the fluids i and j, whereas m_i and m_j are their molecular masses, κ_{mix} is the bulk viscosity, and ρ_{m} is the molar density. The viscosity coefficient of the pure components in the limit of zero density is expressed as η_i^0, while the parameter α_{ii} and α_{ij}, related to the second pressure virial coefficient, account for the mean free-path shortening of a collision between like or unlike molecules. The interaction viscosity in the limit of zero density η_{ij}^0 can be determined from experimental data of the mixture or with the help of an extended corresponding states principle. A_{ij}^* characterises a temperature-dependent ratio of collision integrals and is approximately 1.1.

The contact value of the pseudo-radial distribution function $\overline{\chi}_i$ follows from the viscosity of the pure component η_i after subtracting the critical enhancement η_i^{C}:

$$\bar{\chi}_i(T,\rho_\mathrm{m}) = \frac{\beta_\eta\left(\eta_i - \rho_\mathrm{m}\alpha_{ii}\eta_i^0\right)}{2\rho_\mathrm{m}^2\alpha_{ii}^2\eta_i^0} \pm \beta_\eta\left[\left(\frac{\eta_i - \rho_\mathrm{m}\alpha_{ii}\eta_i^0}{2\rho_\mathrm{m}^2\alpha_{ii}^2\eta_i^0}\right)^2 - \frac{1}{\beta_\eta\rho_\mathrm{m}^2\alpha_{ii}^2}\right]^{1/2}. \tag{3.70}$$

In order to ensure a physically reasonable behaviour and a smooth transition between the two roots, a so-called switch-over molar density ρ_m^* and a value of α_{ii} are needed as functions of temperature. For that purpose, the derivative of the viscosity with respect to density is compared iteratively with the ratio of viscosity to molar density:

$$\left[\frac{\partial\eta_i(T,\rho_\mathrm{m})}{\partial\rho_\mathrm{m}}\right]_T = \frac{\eta_i(T,\rho_\mathrm{m})}{\rho_\mathrm{m}^*}. \tag{3.71}$$

Then the parameter α_{ii} can be derived using the value ρ_m^* which fulfils the foregoing equation:

$$\frac{\eta_i(T,\rho_\mathrm{m}^*)}{\rho_\mathrm{m}^*\alpha_{ii}\eta_i^0} = 1 + \frac{2}{\sqrt{\beta_\eta}} \tag{3.72}$$

with

$$\frac{1}{\beta_\eta} = \frac{1}{4} + \left(\frac{16}{5\pi}\right)\frac{15}{16}.$$

The values of the pseudo-radial distribution functions have to be unity in the limit of zero density so that the negative root is used first and the positive one is applied at densities higher than the switch-over density.
The quantities characterising the interaction between unlike molecules of species i and j are obtained from the following mixing rules:

$$\alpha_{ij} = \frac{1}{8}\left(\alpha_{ii}^{1/3} + \alpha_{jj}^{1/3}\right)^3 \tag{3.73}$$

$$\bar{\chi}_{ij} = 1 + \frac{2}{5}\sum_{k=1}^{N} x_k\left(\bar{\chi}_k - 1\right) + \frac{\frac{6}{5}\left(\bar{\chi}_i - 1\right)^{1/3}\left(\bar{\chi}_j - 1\right)^{1/3}\sum_{k=1}^{N} x_k\left(\bar{\chi}_k - 1\right)^{2/3}}{\left(\bar{\chi}_i - 1\right)^{1/3} + \left(\bar{\chi}_j - 1\right)^{1/3}}. \tag{3.74}$$

Thermal Conductivity

In contrast to the viscosity the thermal conductivity of a dense fluid mixture consists of a translational (mon - monatomic) and an internal (int) contribution:

$$\lambda_\mathrm{mix}(T,\rho_\mathrm{m}) = \lambda_\mathrm{mix}(\mathrm{mon})(T,\rho_\mathrm{m}) + \lambda_\mathrm{mix}(\mathrm{int})(T,\rho_\mathrm{m}). \tag{3.75}$$

The translational contribution is given similar to the formulae for the viscosity:

$$\lambda_{\mathrm{mix}}(\mathrm{mon})(T,\rho_{\mathrm{m}}) = -\begin{vmatrix} L_{11} & \cdots & L_{1N} & Y_1 \\ \vdots & & \vdots & \vdots \\ L_{N1} & \cdots & L_{NN} & Y_N \\ Y_1 & \cdots & Y_N & 0 \end{vmatrix} \Bigg/ \begin{vmatrix} L_{11} & \vdots & L_{1N} \\ \vdots & & \vdots \\ L_{N1} & \cdots & L_{NN} \end{vmatrix} + \kappa_{\mathrm{mix}} \tag{3.76}$$

$$Y_i = x_i \left[1 + \sum_{j=1}^{N} \frac{2m_i m_j}{\left(m_i + m_j\right)^2} x_j \gamma_{ij} \overline{\chi}_{ij} \rho_{\mathrm{m}} \right] \tag{3.77}$$

$$\begin{aligned} L_{ii} = {} & \frac{x_i^2 \overline{\chi}_{ii}}{\lambda_i^0(\mathrm{mon})} \\ & + \sum_{\substack{j=1 \\ j\neq i}}^{N} \left[\frac{x_i x_j \overline{\chi}_{ij}}{2A_{ij}^* \lambda_{ij}^0(\mathrm{mon}) \left(m_i + m_j\right)^2} \left(\frac{15}{2} m_i^2 + \frac{25}{4} m_j^2 - 3m_j^2 B_{ij}^* + 4 m_i m_j A_{ij}^* \right) \right] \end{aligned} \tag{3.78}$$

$$L_{ij} = -\frac{x_i x_j \overline{\chi}_{ij}}{2A_{ij}^* \lambda_{ij}^0(\mathrm{mon})} \frac{m_i m_j}{\left(m_i + m_j\right)^2} \left(\frac{55}{4} - 3B_{ij}^* - 4A_{ij}^* \right) \quad (i \neq j) \tag{3.79}$$

$$\kappa_{\mathrm{mix}} = \frac{16}{5\pi} \frac{10}{9} \rho_{\mathrm{m}}^2 \sum_{i=1}^{N} \sum_{j=1}^{N} \frac{m_i m_j}{\left(m_i + m_j\right)^2} x_i x_j \overline{\chi}_{ij} \gamma_{ij}^2 \lambda_{ij}^0(\mathrm{mon}) . \tag{3.80}$$

Here $\lambda_i^0(\mathrm{mon})$ and $\lambda_{ij}^0(\mathrm{mon})$ are the translational contributions of the thermal conductivity in the limit of zero density which can be derived from the corresponding values of the viscosity in the same limit:

$$\lambda_i^0(\mathrm{mon}) = \frac{5}{2} \left[\frac{c_{V\mathrm{m}}^{\mathrm{o}}(\mathrm{mon})}{M_i} \right] \eta_i^0 . \tag{3.81}$$

$c_{V\mathrm{m}}^{\mathrm{o}}(\mathrm{mon})$ is the molar ideal-gas heat capacity of a monatomic gas at constant volume. B_{ij}^* represents a temperature-dependent relationship between different collision integrals and amounts to approximately 1.1 to 1.2 for the extended corresponding states principle. The parameters γ_{ii} and γ_{ij} characterise the shortening of the mean free-path of a collision between like or unlike molecules.

Furthermore, the contribution resulting for the consideration of internal degrees of freedom is given as:

$$\lambda_{\mathrm{mix}}(\mathrm{int})(T,\rho_{\mathrm{m}}) = \sum_{i=1}^{N} \left[\frac{\lambda_i^0 - \lambda_i^0(\mathrm{mon})}{\overline{\chi}_{ii}} \right] \left[1 + \sum_{\substack{j=1 \\ j\neq i}}^{N} \frac{x_j \lambda_i^0(\mathrm{mon}) \overline{\chi}_{ij} A_{ii}^*}{x_i \lambda_{ij}^0(\mathrm{mon}) \overline{\chi}_{ii} A_{ij}^*} \right]^{-1} . \tag{3.82}$$

The contact value of the pseudo-radial distribution function $\overline{\chi}_i$ follows from the thermal conductivity of the pure component λ_i after subtracting the critical enhancement λ_i^{C}:

$$\overline{\chi}_i(T,\rho_{\mathrm{m}}) = \frac{\beta_\lambda\left[\lambda_i - \rho_{\mathrm{m}}\gamma_{ii}\lambda_i^0(\mathrm{mon})\right]}{2\rho_{\mathrm{m}}^2\gamma_{ii}^2\lambda_i^0(\mathrm{mon})} \pm \beta_\lambda\left\{\left[\frac{\lambda_i - \rho_{\mathrm{m}}\gamma_{ii}\lambda_i^0(\mathrm{mon})}{2\rho_{\mathrm{m}}^2\gamma_{ii}^2\lambda_i^0(\mathrm{mon})}\right]^2 - \frac{\lambda_i^0}{\beta_\lambda\rho_{\mathrm{m}}^2\gamma_{ii}^2\lambda_i^0(\mathrm{mon})}\right\}^{1/2} \tag{3.83}$$

The switch-over molar density ρ_{m}^* and the parameter γ_{ii} are derived from:

$$\left[\frac{\partial\lambda_i(T,\rho_{\mathrm{m}})}{\partial\rho_{\mathrm{m}}}\right]_T = \frac{\lambda_i(T,\rho_{\mathrm{m}})}{\rho_{\mathrm{m}}^*} \tag{3.84}$$

$$\frac{\lambda_i(T,\rho_{\mathrm{m}}^*)}{\rho_{\mathrm{m}}^*\gamma_{ii}\lambda_i^0(\mathrm{mon})} = 1 + \frac{2}{\sqrt{\beta_\lambda}}\left[\frac{\lambda_i^0}{\lambda_i^0(\mathrm{mon})}\right]^{1/2} \tag{3.85}$$

with $\frac{1}{\beta_\lambda} = \frac{1}{4} + \left(\frac{16}{5\pi}\right)\frac{5}{18}$.

The analogous mixing rules as formulated for the prediction of the viscosity are applied to determine the mixture quantities $\overline{\chi}_{ij}$ and γ_{ij}.

Remarks concerning the implementation of the model on humid air:

The prediction of the transport properties of mixtures by means of this model requires that the transport properties of the pure components have to be known at the same temperature and density as the mixture. This is necessary, since the transport properties of the pure components are needed for the complete temperature range up to high densities in order to determine the switch-over molar density ρ_{m}^*, the mean free-path shortening parameters α_{ii} and γ_{ii}, and particularly the contact value of the pseudo-radial distribution function $\overline{\chi}_i$. But the implementation of the procedure for mixtures containing water as one of the components leads to several problems. Water can be a liquid under the conditions of interest and has to be treated as a hypothetical fluid that has the same properties as the real component in the single-phase region, but does not undergo a phase separation. Hence the calculation procedure at temperatures below the critical temperature is the following one. First, the viscosity or thermal conductivity is calculated at the given temperature and at the density of the saturated vapour. Then the density dependence of the considered transport property of an isotherm at a supercritical reference temperature T_{ref} is shifted into the two-phase region. Finally, the transport property value at the density of the mixture results in that way that the contribution of the change in density is added to the value at the saturated density of the subcritical isotherm. The reason for doing so is that the residual contributions of the viscosity η^{R} and of the

thermal conductivity λ^{R} of a fluid in the supercritical or gaseous states are nearly independent of the temperature. In our investigation the reference temperature was chosen to be T_{ref} = 650 K marginally higher than the critical temperature.

Surprisingly, the density dependence of the contact values of the pseudo-radial distribution function, resulting for isotherms from the transport properties of the pure components, showed an unexpected behaviour for water. In the case of the viscosity the $\overline{\chi}_{w}$ values are larger than unity for all isotherms and pass through a maximum that decreases with increasing temperature. In Figure 3.1 and all following ones the dashed vertical line characterises the critical density.

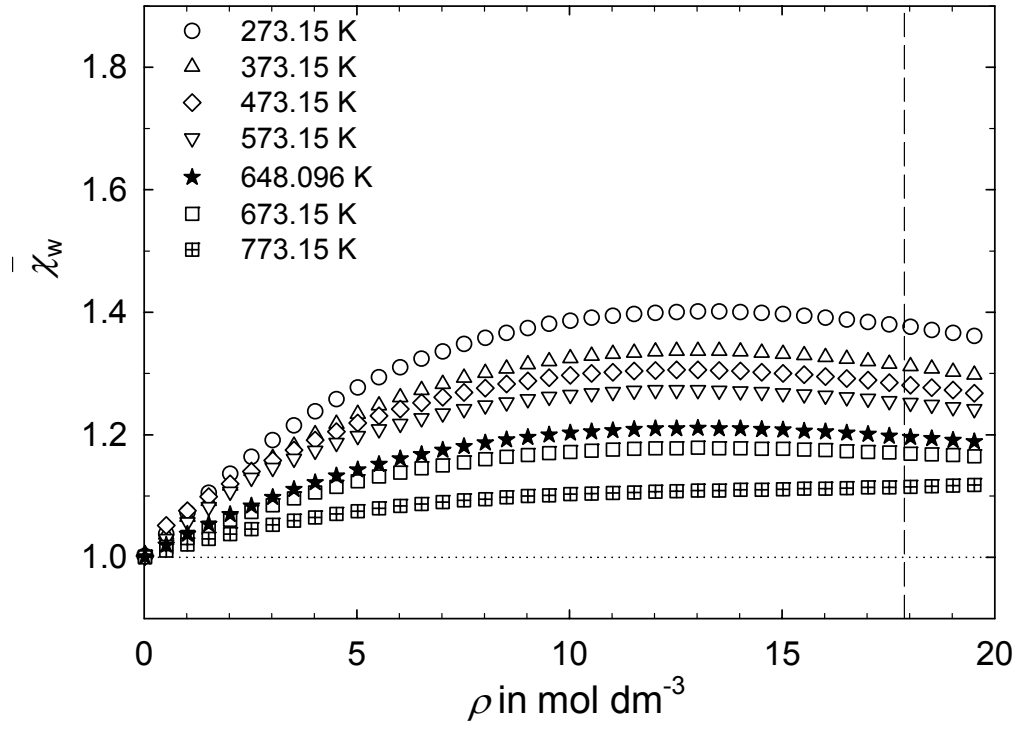

Figure 3.1: Contact value of the pseudo-radial distribution function for the viscosity of water as a function of temperature.

In contrast to the viscosity, the contact values for the thermal conductivity decrease below unity with increasing density. This behaviour was found for the subcritical isotherms, for which water is treated as hypothetical fluid, as well as for the supercritical isotherms. The deviations from unity decrease with increasing temperature. In connection with Figure 3.2 it is to be noticed that for subcritical isotherms a jump in the $\overline{\chi}_{w}$ values occurs at the saturated density due to the transition to the hypothetical fluid, distinctly detected for the 473.15 K isotherm.

Note that such problems do not occur for the contact values of the pseudo-radial distribution functions of dry air for which the $\overline{\chi}_{a}$ values are unity in the limit of zero density and rise smoothly with increasing density as expected and shown in Figure 3.3. The small deviations found for the isotherm near the critical temperature in the case of the viscosity could be caused by the uncertainty of the correlation in this region.

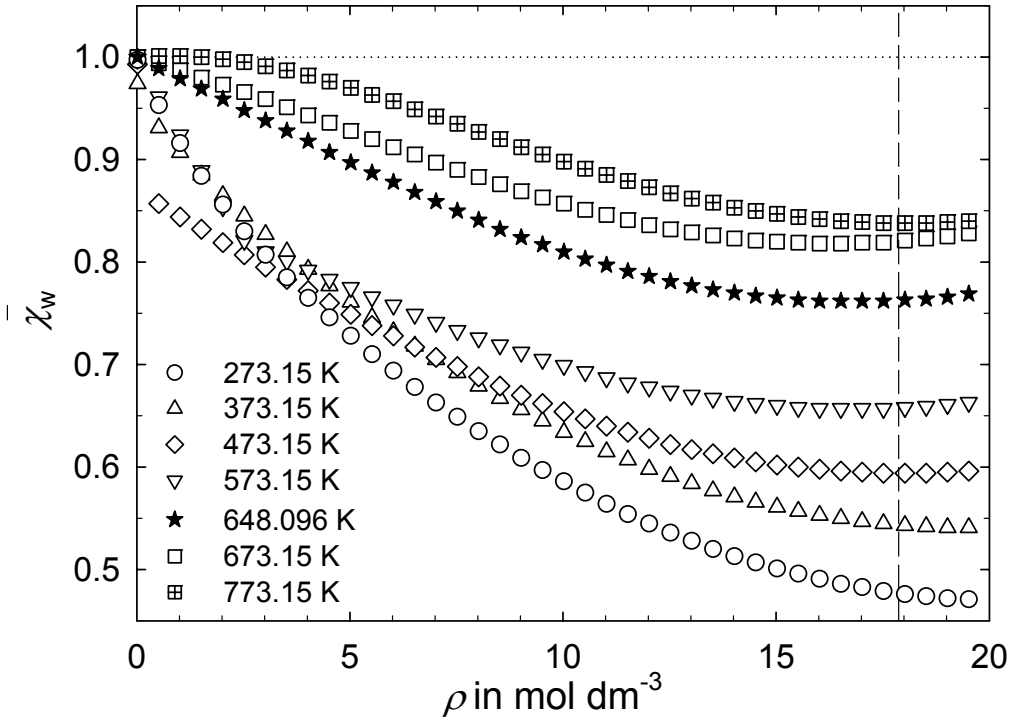

Figure 3.2: Contact value of the pseudo-radial distribution function for the thermal conductivity of water as a function of temperature.

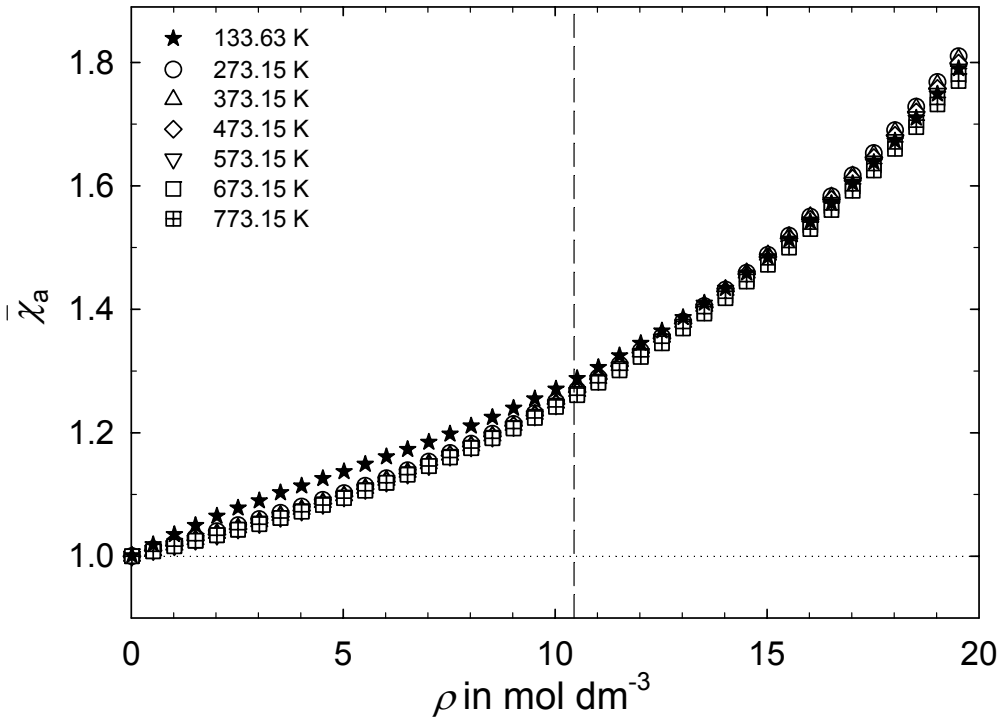

Figure 3.3: Contact value of the pseudo-radial distribution function for the viscosity of air as a function of temperature.

On the other hand, the $\bar{\chi}_a$ values of the near critical isotherm resulting for the thermal conductivity (see Figure 3.4) show larger deviations certainly due to the inadequate treatment of the critical enhancement. But the uncertainties of $\bar{\chi}_a$ in this range are

without any importance, since the temperatures considered for the calculations of the project are much higher.

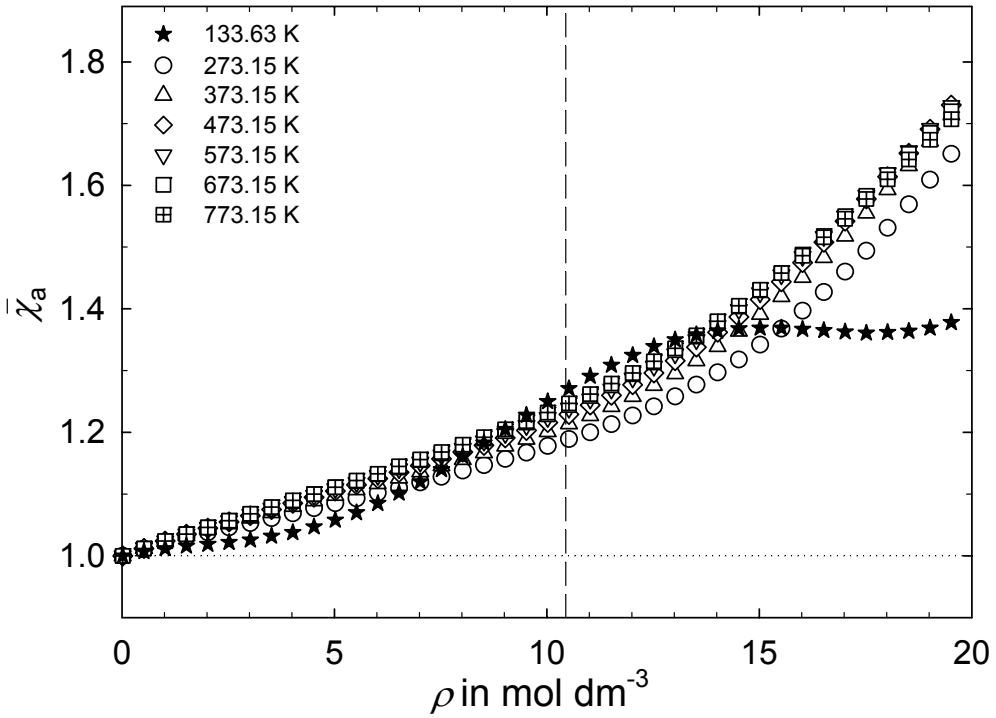

Figure 3.4: Contact value of the pseudo-radial distribution function for the thermal conductivity of air as a function of temperature.

The rather unexpected behaviour of the contact value of the pseudo-radial distribution function of water derived from its thermal conductivity has been further investigated. As it is known from the literature, the thermal conductivity of reacting gaseous mixtures in chemical equilibrium may be higher than that of non-reacting mixtures. General equations to calculate the increase in thermal conductivity due to chemical reaction were proposed by Butler and Brokaw [22], [23]. In the case of associating fluids such as methanol, the additional contribution to the thermal conductivity results from the formation of higher associates. If only the dimerisation of water $2\,\mathrm{H_2O} \rightleftarrows (\mathrm{H_2O})_2$ is considered, the thermal conductivity due to the chemical reaction λ_R can be formulated as a function of the temperature T and the pressure p:

$$\lambda_\mathrm{R} = \frac{pD_\mathrm{md}}{RT}\frac{\Delta H_\mathrm{d}^2}{RT^2}\frac{x_\mathrm{m}x_\mathrm{d}}{\left(x_\mathrm{m}+2x_\mathrm{d}\right)^2}. \tag{3.86}$$

Here, x_m and x_d are the mole fractions of the monomers and dimers, D_md is the binary diffusion coefficient, ΔH_d is the enthalpy of the dimerisation reaction, and R is the universal gas constant. Values of the pressure equilibrium constant K_p and of the enthalpy of dimerisation derived from experimental thermal conductivity data at moderately low pressures in the temperature range between 358 and 386 K were reported by Curtiss *et al.* [24]. Strictly speaking, all these quantities are required in the complete

temperature and pressure ranges considered in the project as prerequisite for the calculation of the thermal conductivity contribution λ_R. The binary diffusion coefficient between the monomers and dimers D_{md} can be derived by means of the kinetic gas theory using an extended corresponding states principle. The pressure equilibrium constant K_p and the enthalpy of the dimerisation ΔH_d can statistically-mechanically be calculated starting with the ab initio potential hypersurface for the interaction between two water molecules [25], [26]. The mole fractions of the monomers and dimers x_m and x_d follow from the concentration equilibrium constant K_c which is related to K_p. Values of the contribution due to dimerisation λ_R, of the critical enhancement λ^C and of the total thermal conductivity λ as well as of the mole fraction of dimers are given in Table 3.9 for several isotherms along the saturated vapour curve.

Table 3.9: Contributions to the thermal conductivity along the saturated vapour curve.

T	ρ_m	x_d	λ_R	λ^C	λ
K	mol dm^{-3}		10^{-3} W m^{-1} K^{-1}	10^{-3} W m^{-1} K^{-1}	10^{-3} W m^{-1} K^{-1}
273.15	0.00027	0.00050	0.092	0.000	17.071
323.15	0.00462	0.00372	0.562	0.000	20.365
373.15	0.03320	0.01325	1.582	0.000	25.096
423.15	0.14143	0.03296	3.064	0.000	31.595
473.15	0.43636	0.06541	4.608	0.072	40.113
523.15	1.10829	0.11188	5.776	0.613	51.262
573.15	2.56290	0.17515	6.333	4.661	69.652
623.15	6.30366	0.27065	6.238	41.671	135.869
643.15	11.20814	0.34725	5.949	189.556	324.243

The table shows that the content of dimers can amount to nearly 35% in the vicinity of the critical point. Similarly, the absolute value of the contribution λ_R increases when approaching the critical point, but the maximum of its proportion related to the total value of the thermal conductivity (about 12%) is already attained 200 K lower. Furthermore, the table makes evident that the critical enhancement becomes the main contribution of thermal conductivity near to the critical point. Consequently, in addition to the critical enhancement the contribution λ_R has been subtracted from the total value of thermal conductivity to re-evaluate the contact value of the pseudo-radial distribution function. The results are illustrated in Figure 3.5 to be compared with Figure 3.2. The new $\overline{\chi}_w$ values are increased in the whole density range and pass through a maximum at moderate densities. Unfortunately, these changes are not large enough to lead to a behaviour expected for a nonpolar fluid.

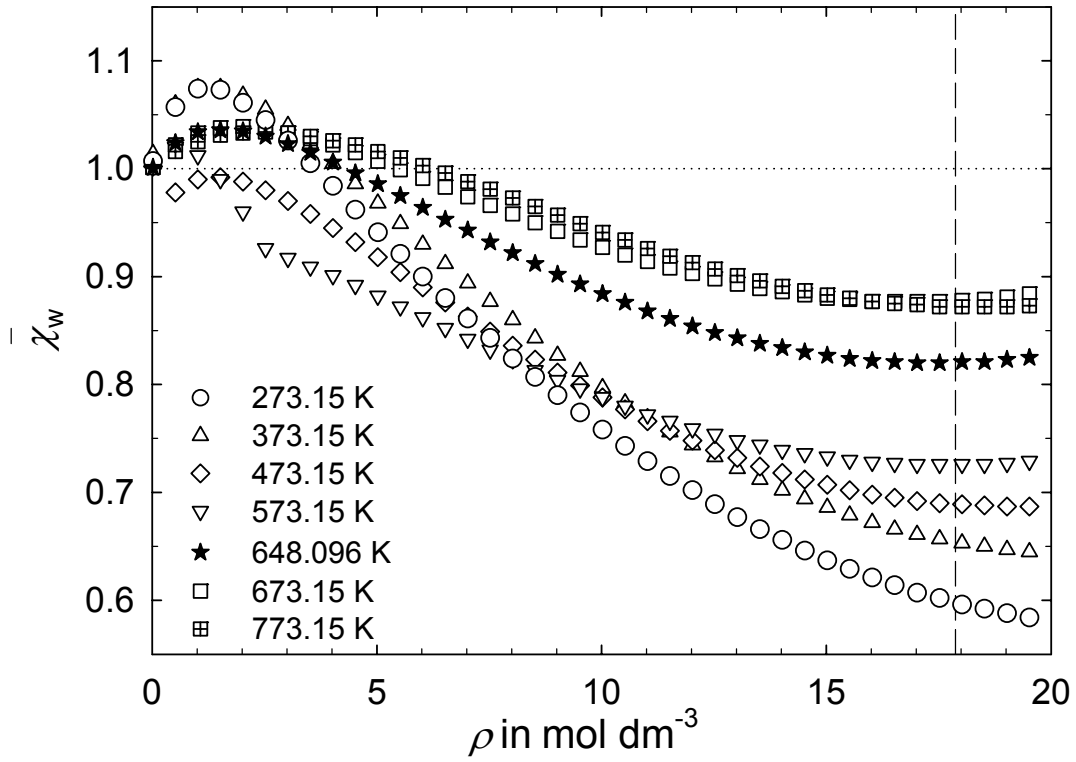

Figure 3.5: Contact value of the pseudo-radial distribution function for the thermal conductivity of water after subtraction of the contribution considering the dimerisation reaction.

It must be pointed out that for the final calculation of the thermal conductivity the contributions due to the dimerisation reaction and to the critical enhancement, omitted in the determination of the contact values of the pseudo-radial distribution function, have to be added according to the partial molar density of water $\rho_{\mathrm{m,w}}$ as given in the following relationship:

$$\lambda_{\mathrm{mix,total}}(T,\rho_{\mathrm{m}}) = \lambda_{\mathrm{mix,mod}}(T,\rho_{\mathrm{m}}) + \lambda^{\mathrm{C}}(T,\rho_{\mathrm{m,w}}) + \lambda_{\mathrm{R}}(T,\rho_{\mathrm{m,w}}) \tag{3.87}$$

Here it is to be noted that the contribution $\lambda_{\mathrm{mix,mod}}$ corresponds to the usual one of the Vesovic-Wakeham procedure apart from the fact that the $\bar{\chi}_{\mathrm{w}}$ values have been derived after subtraction of the contribution considering the dimerisation reaction. In the usual case the thermal conductivity of the mixture is calculated according to

$$\lambda_{\mathrm{mix,total}}(T,\rho_{\mathrm{m}}) = \lambda_{\mathrm{mix}}(T,\rho_{\mathrm{m}}) + \lambda^{\mathrm{C}}(T,\rho_{\mathrm{m,w}})\,. \tag{3.88}$$

Furthermore, it could happen that, as a consequence of $\bar{\chi}_{\mathrm{w}} < 1$ in the case of the thermal conductivity, unreasonable values result for the interaction quantities $\bar{\chi}_{ij}$, $\bar{\chi}_{ii}$, and $\bar{\chi}_{jj}$ for high mole fractions of water, if the common mixing rule is applied. This would also lead to inadequate results for the thermal conductivity of the mixture and can be avoided by using the following simpler alternative mixing rules for the interaction quantities:

$$\bar{\chi}_{ii} = \bar{\chi}_i \tag{3.89}$$

$$\bar{\chi}_{jj} = \bar{\chi}_j \tag{3.90}$$

$$\bar{\chi}_{ij} = \left(\bar{\chi}_i \bar{\chi}_j \right)^{1/2} . \tag{3.91}$$

In addition, the interaction viscosity in the limit of zero density needed in the Vesovic-Wakeham procedure is determined based on an extended corresponding states principle [27]. A so-called universal correlation with a reduced effective cross section for the viscosity S_η^* is applied using universal coefficients a_k derived from the Hartree-Fock Dispersion (HFD) potentials of the rare gases [28]. First, individual scaling factors σ_{ii} and ε_{ii} were calculated from experimental data of the pure components. Then the scaling factors for the interaction between the unlike molecules σ_{ij} and ε_{ij} were derived with the help of common mixing rules:

$$\sigma_{ij} = \frac{1}{2}\left(\sigma_{ii} + \sigma_{jj} \right) \tag{3.92}$$

$$\varepsilon_{ij} = \left(\varepsilon_{ii} \varepsilon_{jj} \right)^{1/2} . \tag{3.93}$$

Finally, the interaction viscosity follows from:

$$\eta_{ij}^0(T) = \frac{0.021357 \left(\frac{2 M_i M_j}{M_i + M_j} T \right)^{1/2}}{\sigma_{ij}^2 S_\eta^*(T_{ij}^*)} \tag{3.94}$$

with

$$S_\eta^*(T_{ij}^*) = \exp\left\{ \sum_{k=0}^{4} a_k \left[\ln\left(T_{ij}^* \right) \right]^k \right\} \tag{3.95}$$

and

$$T_{ij}^* = \frac{k_\mathrm{B}\, T}{\varepsilon_{ij}} . \tag{3.96}$$

3.2.4 Three-Parameter Corresponding States Model of Scalabrin *et al.*

Scalabrin *et al.* [19], [20] developed a three-parameter corresponding states model for the prediction of the viscosity and thermal conductivity of dense fluids and fluid mixtures. Input quantities are temperature, total pressure and, in the case of mixtures, the composition. Transport property correlations have to be available over wide ranges of temperature and pressure for two chosen reference fluids. In addition, the parameters needed are critical temperature and pressure as well as a transport property scaling factor derived from at least one experimental data point of the saturated liquid. The parameters of the mixture are determined as functions of the composition using mixing rules based on a one-fluid model approach.

Viscosity

The viscosity of a pure fluid is formulated in a reduced form as:

$$\eta_{\mathrm{r},i}(T_{\mathrm{r},i}, p_{\mathrm{r},i}, \psi_i) = \frac{\eta_i(T, p, \psi_i)}{H_{\mathrm{c},i}} = \eta_{\mathrm{r,rf1}} + \frac{\psi_i - \psi_{\mathrm{rf1}}}{\psi_{\mathrm{rf2}} - \psi_{\mathrm{rf1}}}\left(\eta_{\mathrm{r,rf2}} - \eta_{\mathrm{r,rf1}}\right) \tag{3.97}$$

with

$$H_{\mathrm{c},i} = \frac{M_i^{1/2} p_{\mathrm{c},i}^{2/3}}{R^{1/6} N_{\mathrm{A}}^{1/3} T_{\mathrm{c},i}^{1/6}} \qquad T_{\mathrm{r},i} = \frac{T}{T_{\mathrm{c},i}} \qquad p_{\mathrm{r},i} = \frac{p}{p_{\mathrm{c},i}} \tag{3.98}$$

where M is the molar mass in $\mathrm{kg\,mol^{-1}}$, $T_{\mathrm{c},i}$ and $p_{\mathrm{c},i}$ are the critical temperature and pressure of the fluid under consideration in K and MPa, N_{A} is Avogadro's constant, and R is the universal gas constant. The viscosity coefficient reduced with a pseudo-critical viscosity value $H_{\mathrm{c},i}$ is characterised by the subscript r. The subscripts rf1 and rf2 indicate the properties of two reference fluids. The viscosity scaling factor ψ_i can be derived for all considered fluids as an arithmetic mean of three values at T_{r} equal to 0.7, 0.8, and 0.9:

$$\psi_i = \frac{1}{3}\sum_{j=1}^{3}\left[\left(\log\eta_{\mathrm{r},i} - \log\eta_{\mathrm{r,CH_4}}\right)_{T_{\mathrm{r}}(j)}\right]^{\text{saturated liquid}} \tag{3.99}$$

Here the logarithm of the saturated liquid viscosity of the fluid is related to the saturated liquid viscosity of the reference fluid methane at the same reduced temperature, both in reduced form. Scalabrin *et al.* tabulated such ψ_i values for several fluids, but the calculation can also be done without knowledge of values for methane. It should also be possible to use viscosity data of the saturated vapour for an adequate description of gas mixtures.

The prediction of the mixture viscosity can be performed in the following way. The critical temperature and pressure of the mixture are calculated for a given composition:

$$T_{\mathrm{c,mix}} / p_{\mathrm{c,mix}} = \sum_i \sum_j x_i x_j T_{\mathrm{c},ij} / p_{\mathrm{c},ij} \tag{3.100}$$

$$T_{\mathrm{c,mix}}^2 \Big/ p_{\mathrm{c,mix}} = \sum_i \sum_j x_i x_j T_{\mathrm{c},ij}^2 \Big/ p_{\mathrm{c},ij} \tag{3.101}$$

$$T_{\mathrm{c},ij} = \alpha_{ij}\left(T_{\mathrm{c},i}\ T_{\mathrm{c},j}\right)^{1/2} \tag{3.102}$$

$$p_{\mathrm{c},ij} = 8T_{\mathrm{c},ij} \Bigg/ \left\{\ \beta_{ij}\left[\left(T_{\mathrm{c},i}/p_{\mathrm{c},i}\right)^{1/3} + \left(T_{\mathrm{c},j}/p_{\mathrm{c},j}\right)^{1/3}\right]^3\right\}. \tag{3.103}$$

The interaction parameters α_{ij} and β_{ij} can be derived from experimental data or can be chosen to be unity. Then the reduced quantities $T_{\mathrm{r,mix}} = T / T_{\mathrm{c,mix}}$ and $p_{\mathrm{r,mix}} = p / p_{\mathrm{c,mix}}$ are determined. The densities corresponding to the chosen temperature T and pressure p

are obtained for each reference fluid from the equation of state and are used to get the viscosity as a function of temperature and molar density (here i = 1,2):

$$T_{\mathrm{rf}i} = T_{\mathrm{r,mix}} T_{\mathrm{c,rf}i} \tag{3.104}$$

$$p_{\mathrm{rf}i} = p_{\mathrm{r,mix}} p_{\mathrm{c,rf}i} \tag{3.105}$$

$$\eta_{\mathrm{r,rf}i} = \frac{\eta_{\mathrm{rf}i}(T_{\mathrm{rf}i}, \rho_{\mathrm{m,rf}i})}{H_{\mathrm{c,rf}i}} \qquad \text{with} \qquad \rho_{\mathrm{m,rf}i} = \rho_{\mathrm{m}}(T_{\mathrm{rf}i}, p_{\mathrm{rf}i}) \,. \tag{3.106}$$

The reduction is performed with individual values of the pseudo-critical viscosity $H_{\mathrm{c,rf}i}$. Finally, the viscosity of the mixture results using an analogous value $H_{\mathrm{c,mix}}$:

$$\eta_{\mathrm{mix}}(T, p, \bar{x}) = H_{\mathrm{c,mix}} \left[\eta_{\mathrm{r,rf1}} + \frac{\psi_{\mathrm{mix}} - \psi_{\mathrm{rf1}}}{\psi_{\mathrm{rf2}} - \psi_{\mathrm{rf1}}} \left(\eta_{\mathrm{r,rf2}} - \eta_{\mathrm{r,rf1}} \right) \right] \tag{3.107}$$

$$\psi_{\mathrm{mix}} = \sum_{i=1}^{N} x_i \psi_i \,. \tag{3.108}$$

Here $\bar{x}$ corresponds again to the molar composition of the mixture.

Thermal Conductivity

In contrast to the viscosity the thermal conductivity of a mixture is separated in a dilute-gas term λ^0_{mix} and a residual contribution $\lambda^{\mathrm{R}}_{\mathrm{mix}}$:

$$\lambda_{\mathrm{mix}}(T, p, \bar{x}) = \lambda^0_{\mathrm{mix}}(T, \bar{x}) + \lambda^{\mathrm{R}}_{\mathrm{mix}}(T, p, \bar{x}) \tag{3.109}$$

The thermal conductivity of the dilute-gas mixture can be determined with the Wassiljewa equation modified by Mason and Saxena [29]:

$$\lambda^0_{\mathrm{mix}}(T, \bar{x}) = \sum_{i=1}^{N} \frac{x_i \lambda_i^0(T)}{\sum_{i=1}^{N} x_i \Phi_{ij}} \tag{3.110}$$

with

$$\Phi_{ij} = \frac{\varepsilon_{ij} \left[1 + \left(\lambda_i^0 / \lambda_j^0 \right)^{1/2} \left(M_i / M_j \right)^{1/4} \right]^2}{\left[8 \left(1 + M_i / M_j \right) \right]^{1/2}} \,. \tag{3.111}$$

Here λ_i^0 corresponds to the dilute-gas thermal conductivity of the ith component of the mixture. M_i is the molar mass, and ε_{ij} is a numerical constant near to unity and can be used as a correlation parameter if experimental data of the mixture are available.

The residual contribution to the thermal conductivity λ_i^{R} of a pure fluid is defined as:

$$\lambda_i^{\mathrm{R}}(T, \rho_{\mathrm{m}}) = \lambda_i(T, \rho_{\mathrm{m}}) - \lambda_i^0(T) \,, \tag{3.112}$$

and the corresponding scaling parameter κ_i results from

$$\kappa_i = \frac{1}{3}\sum_{j=1}^{3}\left[\left(\lambda_{\mathrm{r},i}^{\mathrm{R}} - \lambda_{\mathrm{r,CH_4}}^{\mathrm{R}}\right)_{T_\mathrm{r}(j)}\right]^{\text{saturated liquid}} . \tag{3.113}$$

Then the residual contribution to the thermal conductivity of the mixture is obtained similar to the viscosity:

$$\lambda_{\mathrm{mix}}^{\mathrm{R}}(T,p,\overline{x}) = K_{\mathrm{c,mix}}\left[\lambda_{\mathrm{r,rf1}}^{\mathrm{R}} + \frac{\kappa_{\mathrm{mix}} - \kappa_{\mathrm{rf1}}}{\kappa_{\mathrm{rf2}} - \kappa_{\mathrm{rf1}}}\left(\lambda_{\mathrm{r,rf2}}^{\mathrm{R}} - \lambda_{\mathrm{r,rf1}}^{\mathrm{R}}\right)\right] \tag{3.114}$$

$$\kappa_{\mathrm{mix}} = \sum_{i=1}^{N} x_i\,\kappa_i . \tag{3.115}$$

Here the reduced residual contribution to the thermal conductivities of the reference fluids are obtained with the pseudo-critical values $K_{\mathrm{c,rf}i}$:

$$\lambda_{\mathrm{r,rf}i}^{\mathrm{R}} = \frac{\lambda_{\mathrm{rf}i}^{\mathrm{R}}(T_{\mathrm{rf}i},\rho_{\mathrm{m,rf}i})}{K_{\mathrm{c,rf}i}} \tag{3.116}$$

$$K_{\mathrm{c,rf}i} = \frac{R^{5/6}\,p_{\mathrm{c,rf}i}^{2/3}}{M_{\mathrm{rf}i}^{1/2}\,N_{\mathrm{A}}^{1/3}\,T_{\mathrm{c,rf}i}^{1/6}} . \tag{3.117}$$

Finally, the thermal conductivity of the mixture results according to Eq. (3.109).

Remarks concerning the implementation of the model on humid air:

In principle, the components of the binary mixture considered could be used as reference fluids. If the transport properties of humid air at low mole fractions of water are calculated, comparably large values result for $T_{\mathrm{rf}i}$ and $p_{\mathrm{rf}i}$ following from $T_{\mathrm{r,mix}}$ and $p_{\mathrm{r,mix}}$ which are mainly determined by the large contributions of the small critical constants of dry air. The water transport property correlations are not valid for such large values of $T_{\mathrm{H_2O}}$ and $p_{\mathrm{H_2O}}$. Consequently, water cannot be chosen as one of the reference fluids. Finally, dry air and argon were selected as reference fluids. Of course, an accurate equation of state [30] and reliable correlations for the viscosity and thermal conductivity [1] are available for argon over wide ranges of temperature and pressure. Furthermore, the scaling parameters can be deduced either from values of the saturated liquid (as proposed by Scalabrin *et al.*) or from data of the saturated vapour.

4 Comparison on Calculated Transport Properties of Dry and Humid Air

4.1 Experimental Data Measured for Dry Air in the Project

Viscosity data of dry air were measured by the working group from Ruhr-Universität Bochum [6] using a rotating-cylinder viscometer combined with a single-sinker densimeter. The measurements were performed between room temperature and 500 K up to a maximum pressure of 17 MPa. In Figure 4.1 the experimental data are compared with the correlation of Lemmon and Jacobsen [1]. The differences do not exceed ± 2% in the complete density range, with predominantly higher values resulting from the correlation. At low densities the differences are less than ± 0.5%. This demonstrates that on the one hand the experimental equipment at Ruhr-Universität Bochum should be suitable for the density and viscosity measurements planned in the project and that on the other hand the correlation of Lemmon and Jacobsen can be used to calculate the viscosity of dry air needed in the different prediction models.

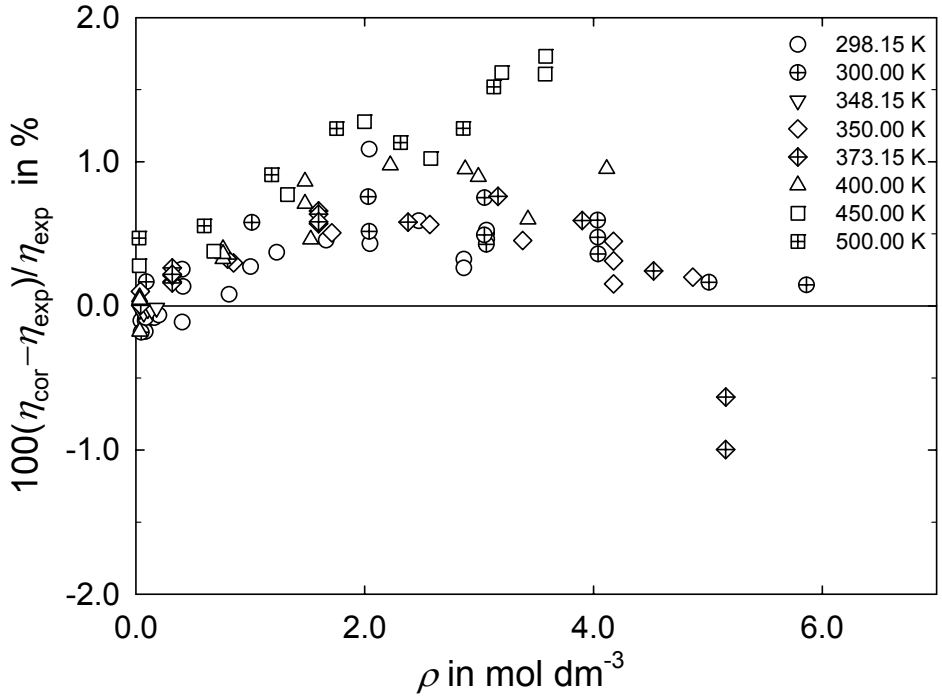

Figure 4.1: Differences between the values of the correlation of Lemmon and Jacobsen [1] and the experimental data from Ruhr-Universität Bochum [6] for the viscosity of dry air.

The working group from the Universidade de Lisboa [7] measured the thermal conductivity of dry air using a transient hot-wire technique in the temperature range between 316 K and 436 K and at pressures up to 10 MPa. Figure 4.2 illustrates the comparison between the experimental data and the values calculated with the correlation of Lemmon and Jacobsen [1]. Nearly all predicted values are higher than the experimental data with a tendency to smaller differences with increasing density. The reason for this trend is that the transient hot-wire technique is characterised by larger uncertainties at low densities. In addition, the

differences increase with temperature. Nevertheless, the transient hot-wire method is appropriate to be used for the measurements on humid air, too.

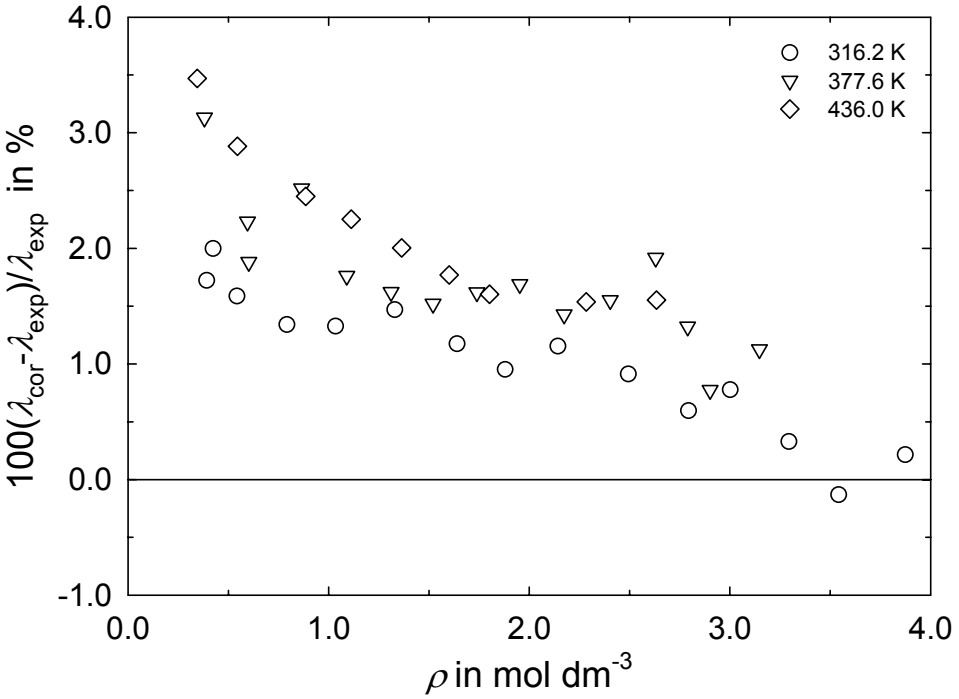

Figure 4.2: Differences between the values of the correlation of Lemmon and Jacobsen [1] and the experimental data from the Universidade de Lisboa [7] for the thermal conductivity of dry air.

4.2 Comparison for Humid Air

4.2.1 Comparison with Experimental Data from the Literature

As already mentioned, only two data sets for the viscosity and one data set for the thermal conductivity of humid air have been found in the literature. These experimental data were used as basis for a comparison of the different prediction models.
Results on the viscosity of humid air at atmospheric pressure and for a maximum water content of 12 mole percent were reported by Hochrainer und Munczak [3] who used a capillary viscometer between 285 K and 323 K. In Figure 4.3 the experimental data of Hochrainer and Munczak are compared with values predicted with the LibHuAir program package (LHA), the Vesovic-Wakeham procedure (VW), and the three-parameter corresponding states model of Scalabrin *et al.* (3PCS).

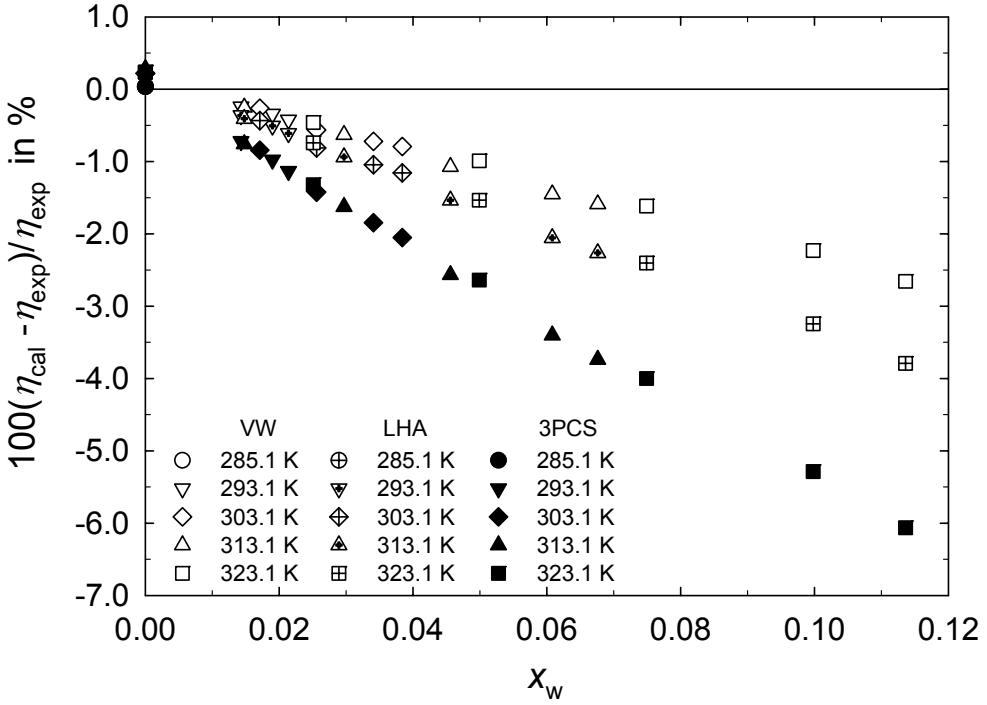

Figure 4.3: Deviations of the predicted values for the viscosity of humid air from the experimental data of Hochrainer and Munczak [3] at atmospheric pressure and at different temperatures. VW – Vesovic-Wakeham model; LHA – LibHuAir; 3PCS – model of Scalabrin *et al.*, scaling with saturated liquid data.

The figure makes evident that the composition dependence of the viscosity of humid air is not described by any of the procedures in these rather restricted ranges of pressure and composition. All models show the same tendency in the deviations with the largest ones (-6%) in the case of the 3PCS model, whereas the Vesovic-Wakeham procedure is characterised by the least differences (less than -3%).

Kestin and Whitelaw [2] measured the viscosity of humid air with an oscillating-disk viscometer between 298 K and 523 K for mole fractions of water up to nearly 0.8. Although the measurements were performed up to 7 atm, the authors corrected the data to a common pressure of 1 atm.
The comparison with the values predicted with the LibHuAir program package in Figure 4.4 shows deviations of -8% at medium values of x_w and of +6% at the highest mole fraction. The values resulting from the Vesovic-Wakeham procedure deviate from the experimental data of Kestin and Whitelaw in a similar manner with differences which are less than -6% at mole fractions $x_w < 0.5$ and increase up to +9% at $x_w = 0.8$. The 3PCS model provides values resulting in very large deviations (-13 to -14%) at medium mole fractions ($x_w = 0.4$-0.5) and still negative deviations at the highest values of x_w. Figure 4.4 makes evident that the prediction procedure of Vesovic and Wakeham leads to comparably good values up to $x_w \approx 0.5$. However, such high mole fractions are not of importance for the AA-CAES project.

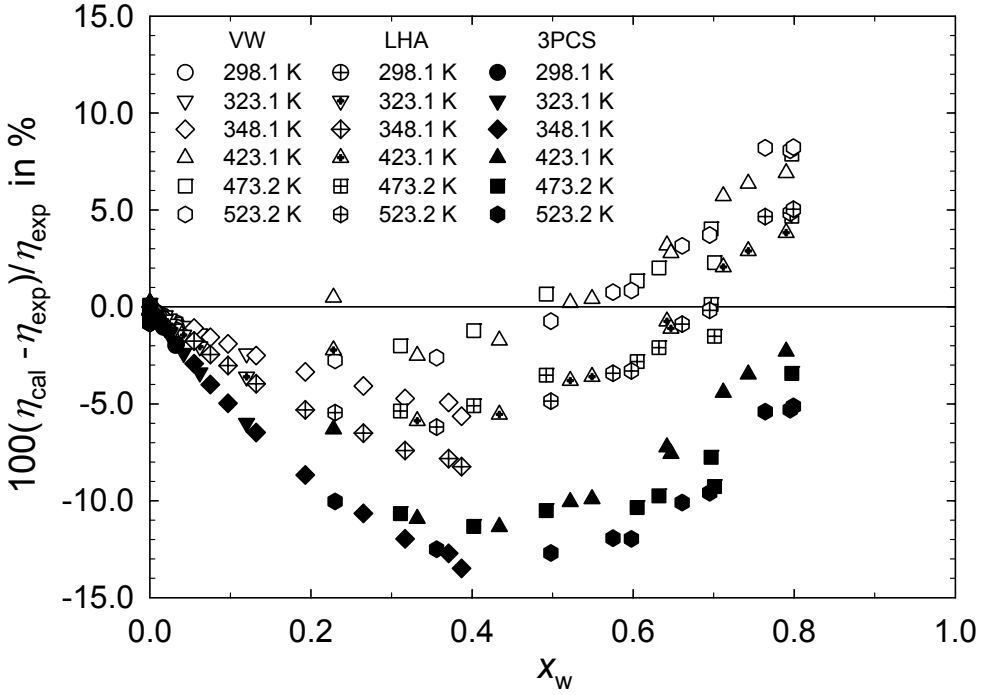

Figure 4.4: Deviations of the predicted values for the viscosity of humid air from the experimental data of Kestin and Whitelaw [2] at atmospheric pressure and at different temperatures. VW – Vesovic-Wakeham model; LHA – LibHuAir; 3PCS – model of Scalabrin *et al.*, scaling with saturated liquid data.

To clarify the ability of the Vesovic-Wakeham procedure to represent the composition dependence of the viscosity at least at mole fractions up to $x_w \approx 0.5$ and at low pressures in an appropriate manner, the experimental data of Kestin and Whitelaw and the different predicted values are directly plotted in Figure 4.5 and Figure 4.6 for two temperatures. Values for pure water vapour calculated with the IAPWS formulation [8] are added to complete the range of mole fractions. The figures illustrate that the LibHuAir program package corresponds to a linear interpolation between the pseudo-pure and pure components dry air and water, whereas the 3PCS model is not able to reproduce the viscosity of pure water and consequently that of humid air. The values predicted with the Vesovic-Wakeham procedure underestimate the experimental data of Kestin and Whitelaw at compositions with $x_w < 0.5$ and overestimate them at higher mole fractions, as demonstrated by the third-order polynomials fitted to the predicted values and to the experimental data.

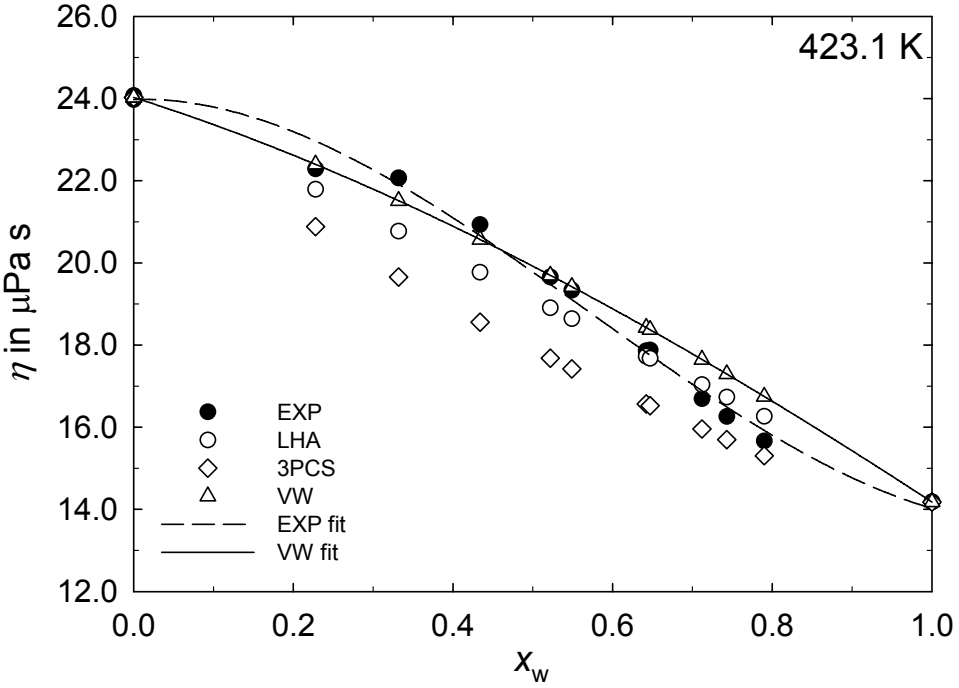

Figure 4.5: Comparison of the data of Kestin and Whitelaw [2] at atmospheric pressure with values for the viscosity of humid air at 423.1 K using the different prediction models. Curves correspond to a third-order polynomial fit to experimental data and to values predicted with the VW model; value for pure water from IAPWS formulation [8].

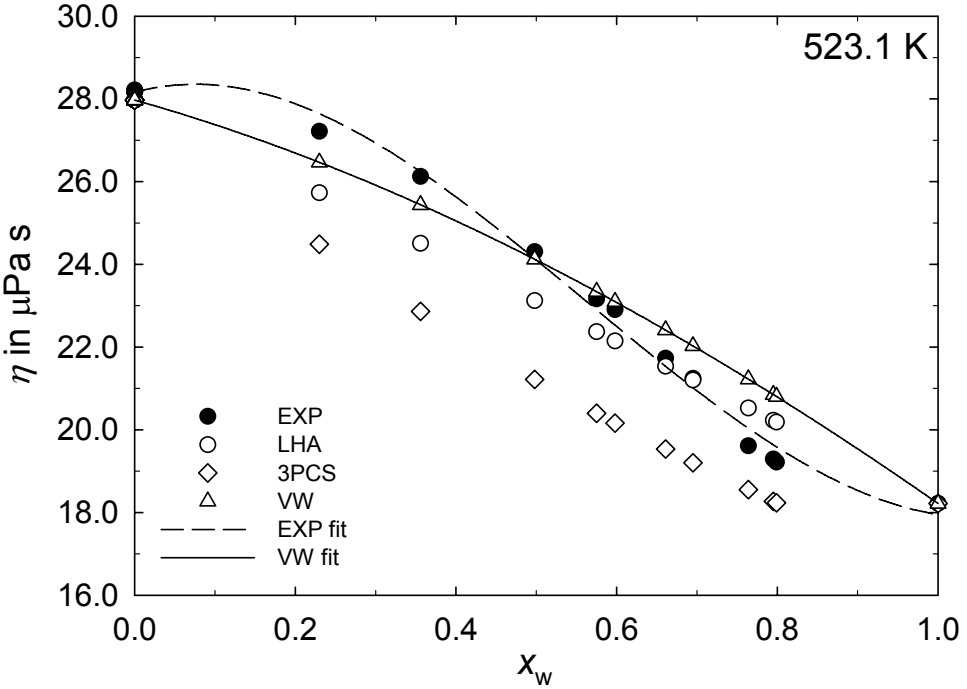

Figure 4.6: Comparison of the data of Kestin and Whitelaw [2] at atmospheric pressure with values for the viscosity of humid air at 523.1 K using the different prediction models. Curves correspond to a third-order polynomial fit to experimental data and to values predicted with the VW model; value for pure water from IAPWS formulation [8].

The Vesovic-Wakeham model is the only procedure in which one or more parameters $\left(\eta_{ij}^{0}, A_{ij}^{*}, B_{ij}^{*}\right)$ could be adjusted within the scope of a fit of the calculated values to the

experimental data. For that purpose the available low-density viscosity data at different mixture compositions could be used.

Grüß and Schmick [4] used the coaxial-cylinder method to measure the thermal conductivity of humid air at 353 K and at atmospheric pressure for several mole fractions of water. In this connection note that the values for the fractions in % H_2O given by those authors in their table 3 correspond to mole fractions.
The differences between the experimental data of Grüß and Schmick and the values predicted with the different models are given in Figure 4.7. With respect to the Vesovic-Wakeham procedure it is to be noted that four variants are included in the comparison following from the discussion in Section 3.2.3. This concerns the alternative mixing rule and the consideration of the dimerisation reaction. The experimental value of dry air differs by about + 5% from the correlation by Lemmon and Jacobsen [1] and proves a large experimental uncertainty of these data which has to be taken into account in the comparison with the different models. If it is supposed that the experimental data of Grüß and Schmick represent the composition dependence of the thermal conductivity still to some extent, the figure leads to the conclusion that the four variants of the Vesovic-Wakeham model approach rather reasonably the experimental data.

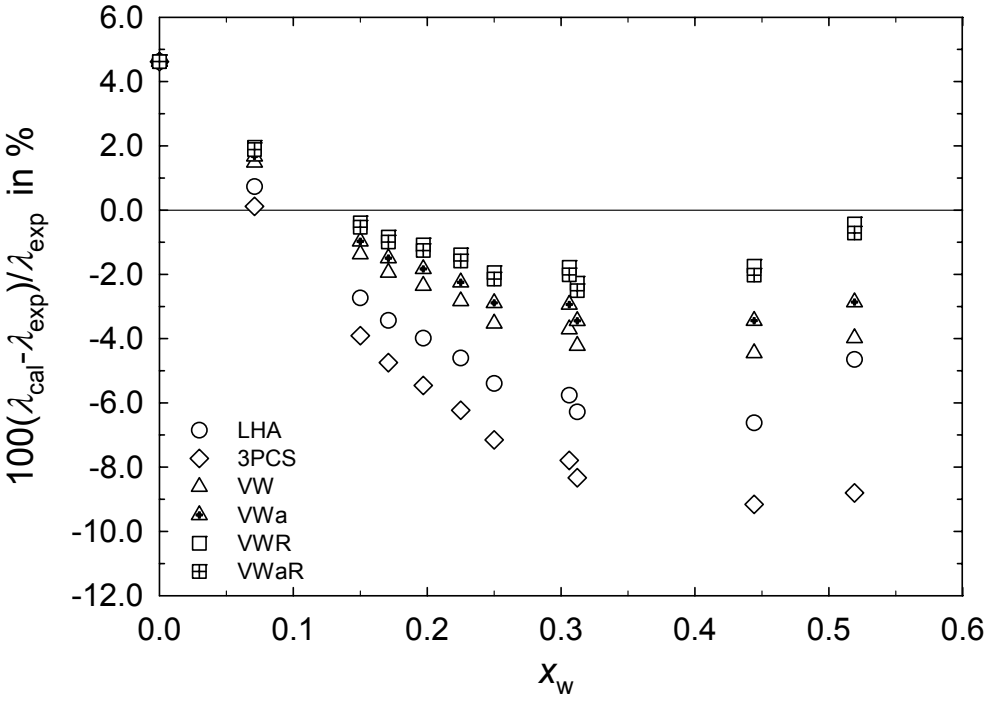

Figure 4.7: Deviations of the predicted values for the thermal conductivity of humid air from the experimental data by Grüß and Schmick [4] at atmospheric pressure and at 353.1 K. LHA – LibHuAir; 3PCS – model of Scalabrin *et al.*, scaling with saturated liquid values; VW – Vesovic-Wakeham model, a – alternative mixing rule, R – considering dimerisation reaction.

In analogy to the viscosity, the experimental data of Grüß and Schmick and values predicted with the different models are directly compared in Figure 4.8. The thermal conductivity value of pure water, calculated with the IAPWS formulation [9] for the density of the saturated vapour obtained from the IAPWS-95 formulation [12] at 353.1 K, was added so that third-order polynomial fits to the experimental data as well as to the

values predicted with the usual Vesovic-Wakeham procedure could again be performed. The curve resulting for the VW model is characterised by a weak curvature and is somewhat closer to the experimental data. Hence an improvement of the predicted values should be possible by adjusting one or more parameters of the VW model. Remarkably, the 3PCS model by Scalabrin *et al.* is not able to approach the values expected for medium and higher mole fractions of water, whereas the LHA program package interpolates practically between the values of dry air and of water vapour.

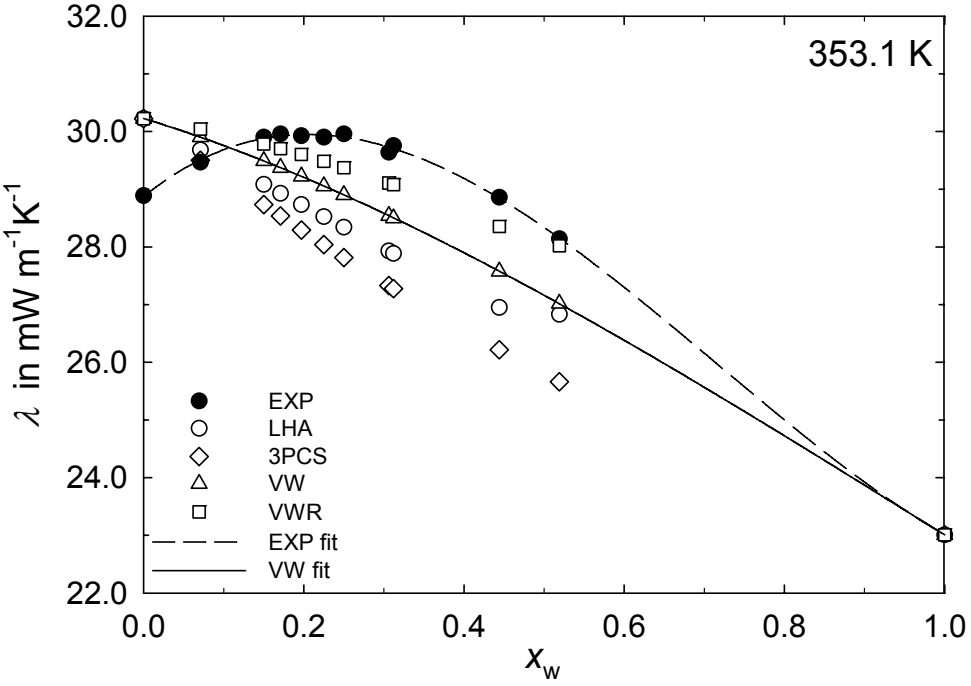

Figure 4.8: Comparison of experimental data of Grüß and Schmick [4] at atmospheric pressure with values for the thermal conductivity of humid air at 353.1 K using the different prediction models. Curves correspond to a third-order polynomial fit to experimental data and to values predicted with the VW model; value for pure water from IAPWS formulation [9]. R – considering dimerisation reaction.

4.2.2 Comparison with Experimental Data Measured in the Project

The working group from Ruhr-Universität Bochum [6] performed measurements on humid air at small mole fractions x_w between 300 K and 500 K up to a maximum pressure of 15 MPa using their combined viscometer-densimeter. The measuring program consisted of two parts each at two different mole fractions: part 1 at $x_w = 0.012$ and 0.030, part 2 at $x_w = 0.010$ and 0.030. In Figure 4.9 to Figure 4.12 results of these measurements at two temperatures (400 K and 450 K) are directly compared with values predicted with the different models. The reason for this is to have a closer look at the dependence of the viscosity on pressure and density, respectively. The pressure dependence of the viscosity of dry air calculated with the correlation of Lemmon and Jacobsen [1] is additionally plotted in each figure.

Figure 4.9 and Figure 4.10 presenting the results for the very low mole fractions at 400 K show that the viscosity of humid air at rather low pressures corresponds approximately to

that of dry air. This behaviour is in agreement with the findings for the composition dependence of viscosity derived from the measurements of Kestin and Whitelaw [2] as well as of Hochrainer and Munczak [3]. But the dependence on pressure is smaller than that of dry air considering the experimental results from the Ruhr-Universität Bochum. The results for the somewhat higher mole fraction at 400 K and 450 K illustrated in Figure 4.11 and Figure 4.12 lead to completely other conclusions. On the one hand, at the lowest pressures the experimental viscosity data of humid air are smaller by 2% than the results for dry air. This is in contradiction with the results at the lower mole fractions and with the composition dependence of the viscosity for humid air reported in the literature. Hence it could possibly be supposed that the measurements at Ruhr-Universität Bochum are influenced by any error. On the other hand, the pressure dependence of the viscosity resulting from these measurements agrees practically with that of dry air. It is hardly to expect that this pressure dependence varies strongly due to such a small change in the mole fraction x_w from 0.01 to 0.03. Therefore, we believe that the pressure dependence as well as the density dependence of the viscosity in the case of humid air will essentially agree with that of dry air.

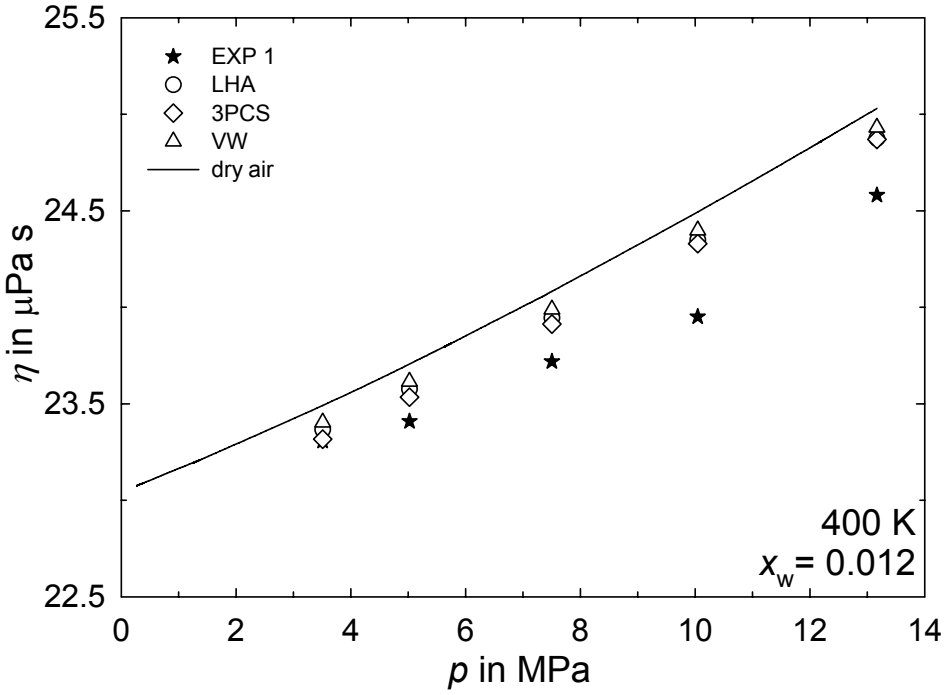

Figure 4.9: Comparison of experimental data from the Ruhr-Universität Bochum [6] with viscosity values predicted with different models for humid air with x_w = 0.012 at 400 K. Curve corresponds to values obtained for dry air with the correlation of Lemmon and Jacobsen [1].

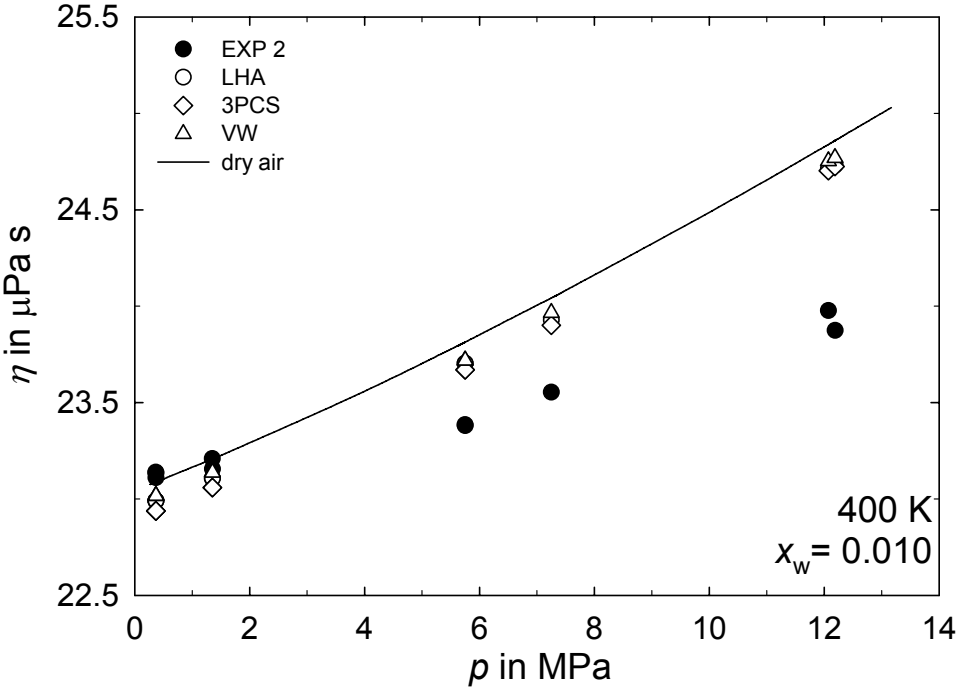

Figure 4.10: Comparison of experimental data from the Ruhr-Universität Bochum [6] with viscosity values predicted with different models for humid air with x_w = 0.010 at 400 K. Curve corresponds to values obtained for dry air with the correlation of Lemmon and Jacobsen [1].

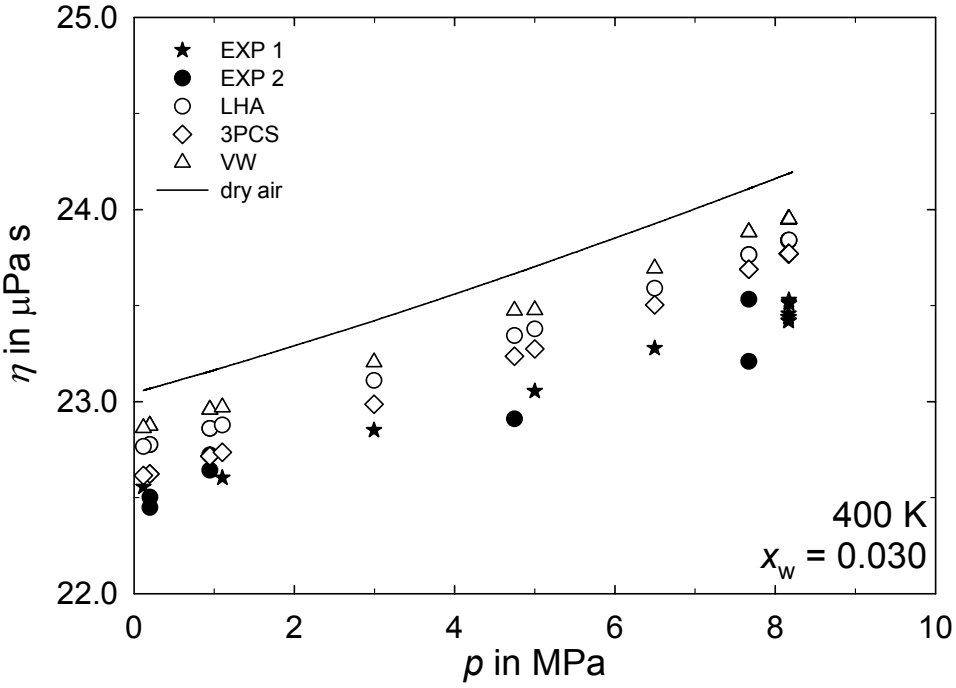

Figure 4.11: Comparison of experimental data from the Ruhr-Universität Bochum [6] with viscosity values predicted with different models for humid air with x_w = 0.030 at 400 K. Curve corresponds to values obtained for dry air with the correlation of Lemmon and Jacobsen [1].

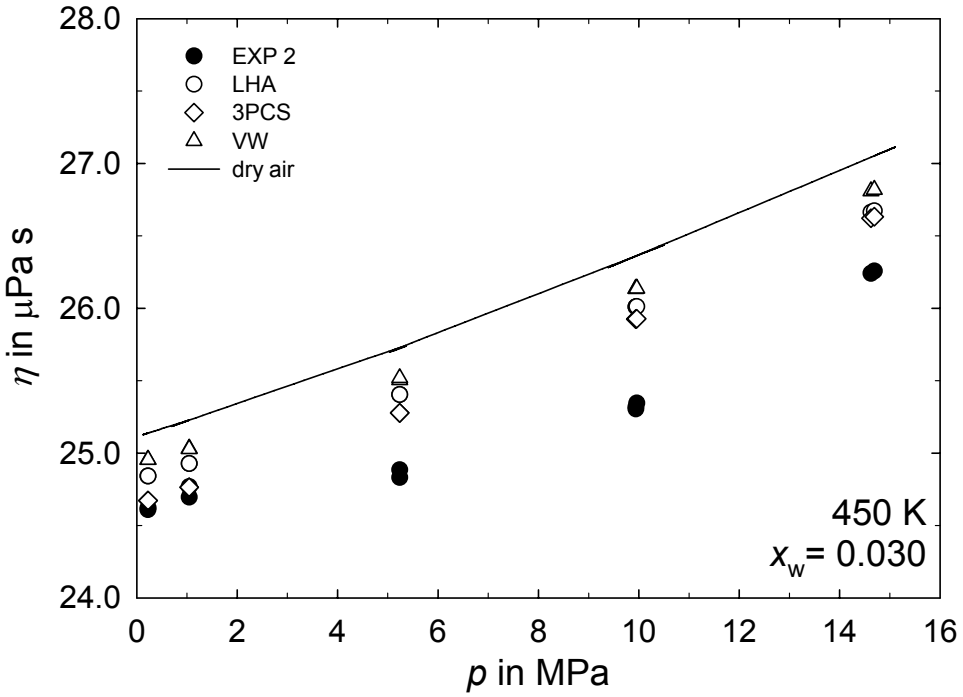

Figure 4.12: Comparison of experimental data from the Ruhr-Universität Bochum [6] with viscosity values predicted with different models for humid air with x_w = 0.030 at 450 K. Curve corresponds to values obtained for dry air with the correlation of Lemmon and Jacobsen [1].

Figure 4.9 to Figure 4.12 demonstrate that the pressure dependence of the viscosity values of humid air predicted with all three models considered is approximately in agreement with that of dry air. In addition, the values calculated with the VW model are higher than the values predicted with the other models. In accordance with the weak composition dependence in the range of small mole fractions x_w and at low pressures, it is to be expected that the viscosity values of dry air and those predicted for humid air with the VW model differ only a little, even in the larger pressure range considered.

4.2.3 Comparison of Predicted Values for the Different Models

In spite of the shortage of experimental data from which the pressure dependence or density dependence of humid air for both transport properties can be derived, the discussion should be continued, at least on the basis of the different prediction models. For that purpose, values of both transport properties were calculated and are compared for two mole fractions (x_w = 0.05 and x_w = 0.15) at two temperatures each (473.15 K and 673.15 K) in Figure 4.13 to Figure 4.20. The pressure range was limited to 20 MPa or to a partial pressure of water lower than the saturated vapour pressure at the subcritical temperature (up to 10 MPa at 473.15 K and at x_w = 0.15).

Figure 4.13 to Figure 4.16 demonstrate that the pressure dependence of the viscosity values of humid air predicted with all three models does not differ strongly. In addition, this pressure dependence is in rather good agreement with that of dry air. Taking also into account the results for the pressure dependence of the viscosity derived from the measurements at Ruhr-Universität Bochum [6] for the mole fraction x_w = 0.03 at 400 K

and 450 K (see Figure 4.11 and Figure 4.12), it can be concluded that the pressure dependence does not largely depend on the mole fraction when x_w is limited up to 0.15 or possibly 0.20. The differences between the viscosity values of humid air calculated with the different procedures are mainly determined by the viscosity at low pressure according to the composition dependence discussed in Section 4.2.1 using the experimental data of Kestin and Whitelaw [2] as well as of Hochrainer and Munczak [3]. As already stated the Vesovic-Wakeham procedure represents somewhat better the composition dependence at low pressures. Since this model possesses additionally adjustable parameters, it seems to be the most promising one in the complete ranges of temperature, pressure, and composition.

The data situation concerning the pressure dependence is even worse in the case of the thermal conductivity. There are neither data in the literature nor data resulting from measurements carried out in the project up to now. Therefore, the values calculated with the different prediction models are difficult to judge. At 473 K the 3PCS model of Scalabrin *et al.* provides, apart from the low pressure region, the highest values accompanied by the largest pressure dependence as shown in Figure 4.17 and Figure 4.18. On the contrary, the LibHuAir program package and the Vesovic-Wakeham procedure lead to distinctly smaller values, somewhat more or less smaller than those of dry air and connected with a small pressure dependence similar to that of dry air. On the other hand, the Vesovic-Wakeham model predicts the highest values with a very distinct pressure dependence at 673 K (above the critical temperature) for both mole fractions, as demonstrated in Figure 4.19 and Figure 4.20. At this temperature the other models yield smaller values with a reduced pressure dependence in the order 3PCS model and LibHuAir program package. The last model gives values in close agreement with those of dry air. All these findings cannot be explained without reliable experimental results, at least in a restricted range of temperature, pressure, and composition.

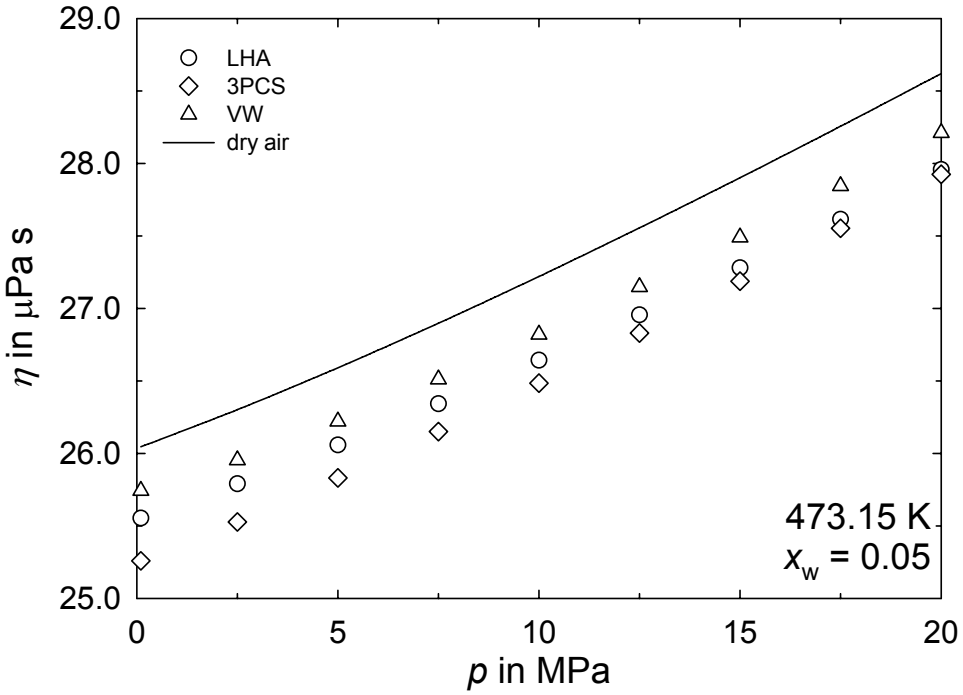

Figure 4.13: Comparison of the pressure dependence of viscosity values predicted with different models for humid air with $x_w = 0.05$ at 473.15 K. Curve corresponds to values calculated for dry air with the correlation of Lemmon and Jacobsen [1].

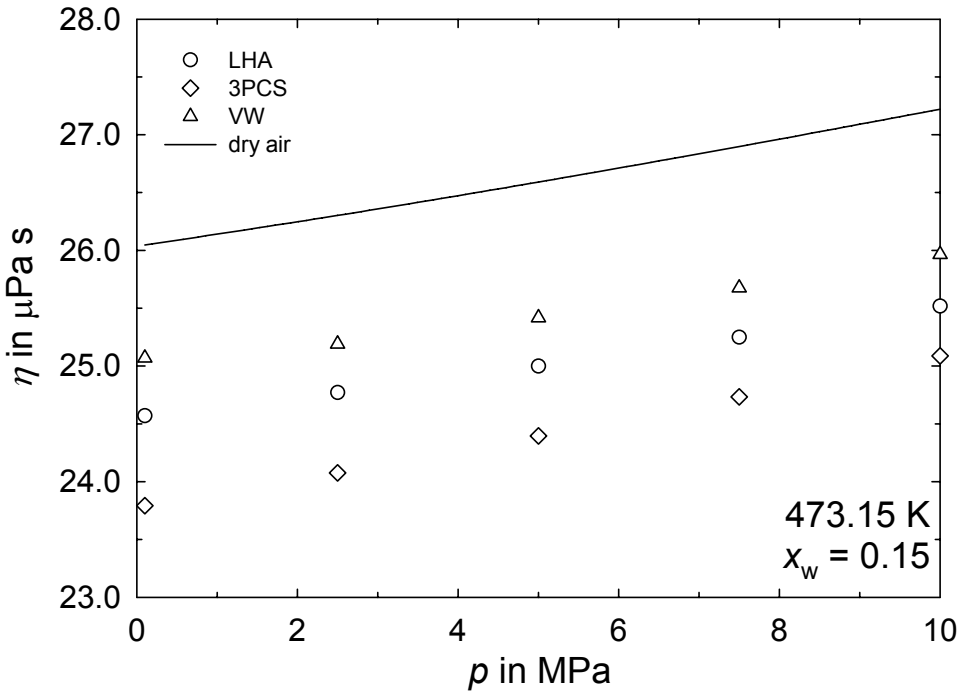

Figure 4.14: Comparison of the pressure dependence of viscosity values predicted with different models for humid air with $x_w = 0.15$ at 473.15 K. Curve corresponds to values calculated for dry air with the correlation of Lemmon and Jacobsen [1].

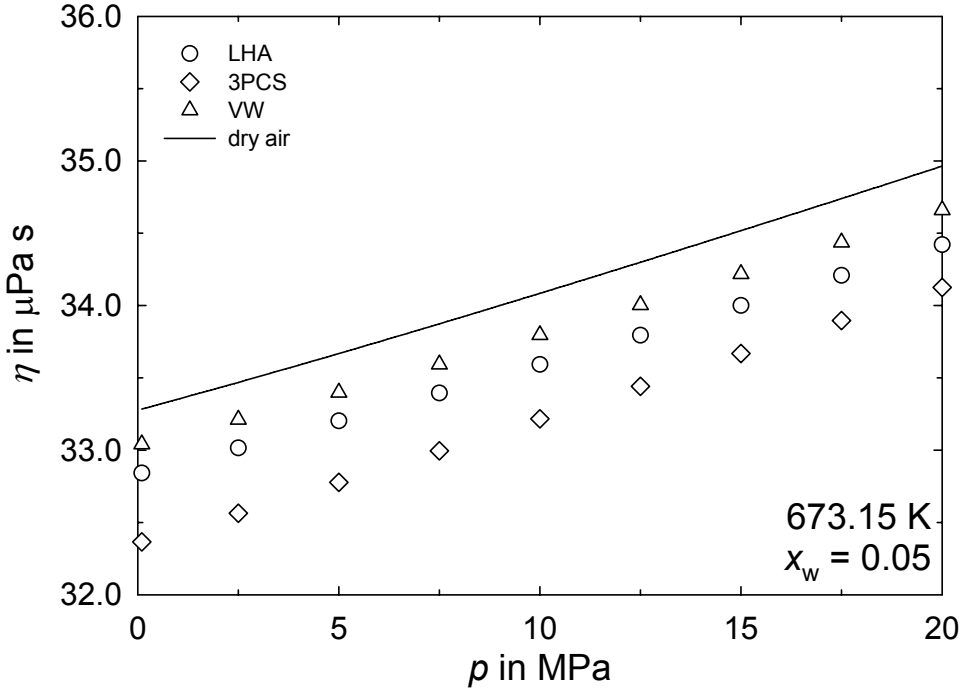

Figure 4.15: Comparison of the pressure dependence of viscosity values predicted with different models for humid air with $x_w = 0.05$ at 673.15 K. Curve corresponds to values calculated for dry air with the correlation of Lemmon and Jacobsen [1].

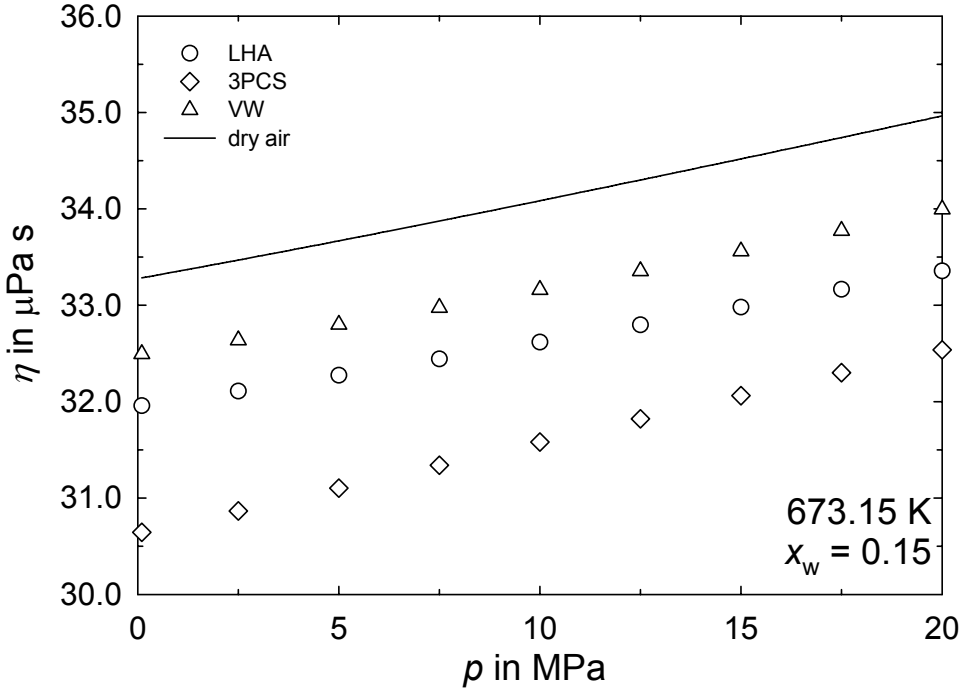

Figure 4.16: Comparison of the pressure dependence of viscosity values predicted with different models for humid air with $x_w = 0.15$ at 673.15 K. Curve corresponds to values calculated for dry air with the correlation of Lemmon and Jacobsen [1].

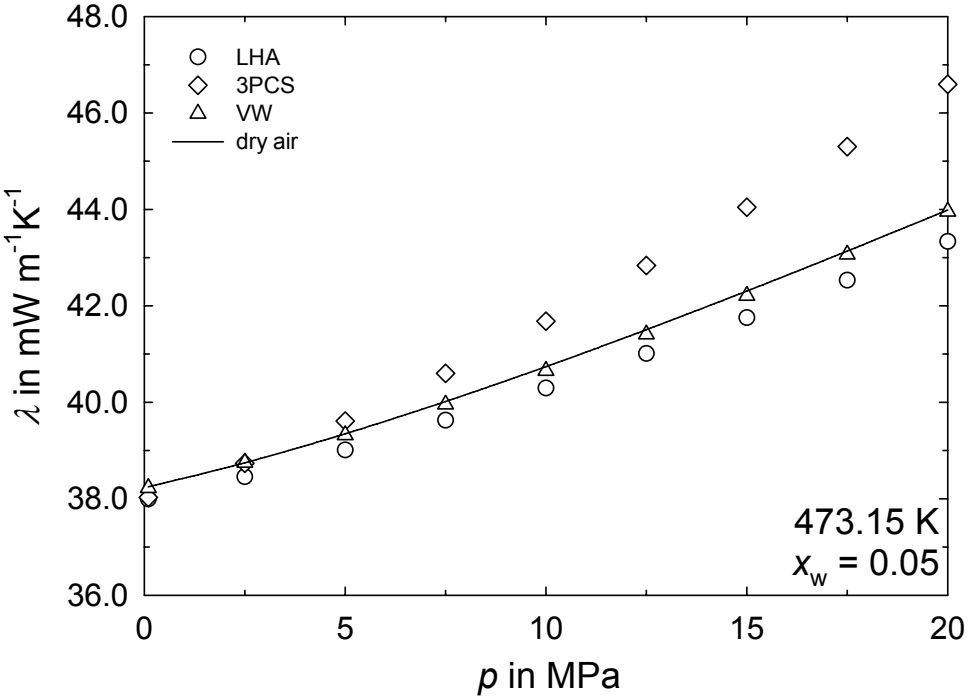

Figure 4.17: Comparison of the pressure dependence of thermal conductivity values predicted with different models for humid air with x_w = 0.05 at 473.15 K. Curve corresponds to values obtained for dry air with the correlation of Lemmon and Jacobsen [1].

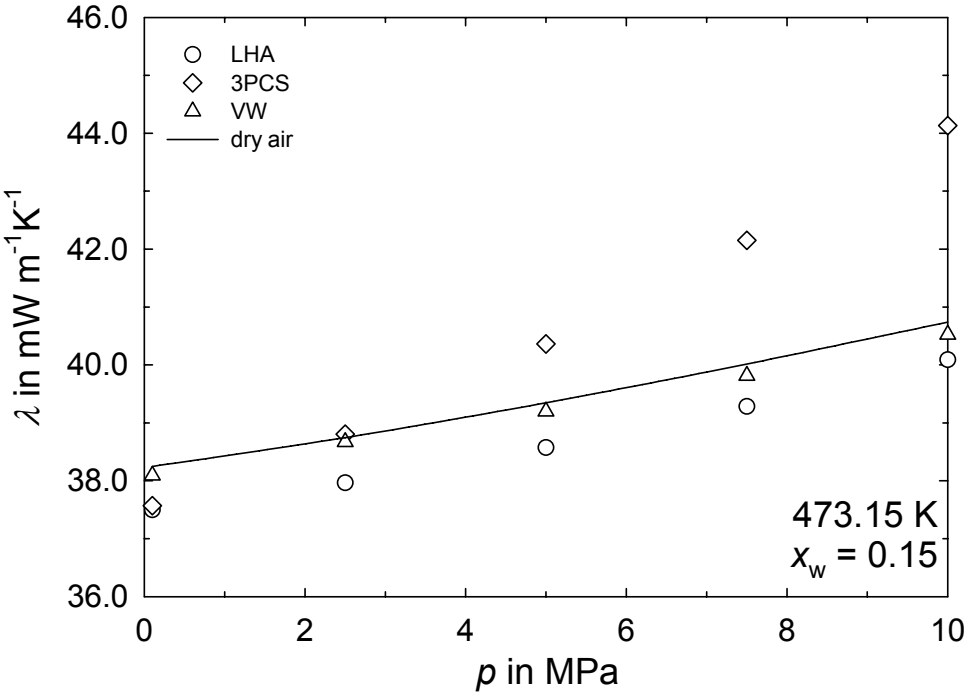

Figure 4.18: Comparison of the pressure dependence of thermal conductivity values predicted with different models for humid air with x_w = 0.15 at 473.15 K. Curve corresponds to values obtained for dry air with the correlation of Lemmon and Jacobsen [1].

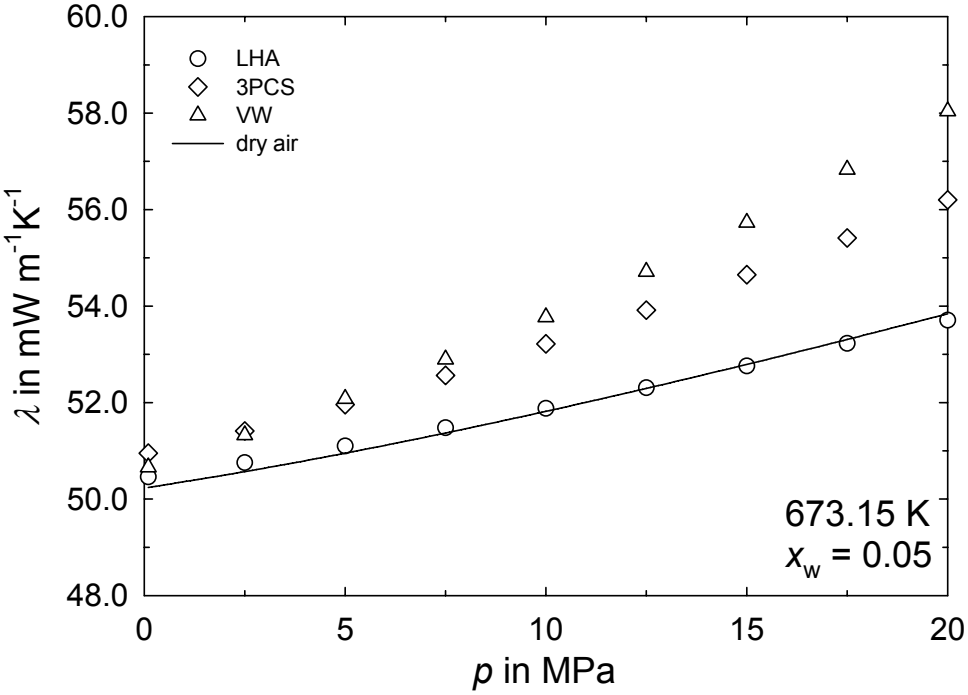

Figure 4.19: Comparison of the pressure dependence of thermal conductivity values predicted with different models for humid air with x_w = 0.05 at 673.15 K. Curve corresponds to values obtained for dry air with the correlation of Lemmon and Jacobsen [1].

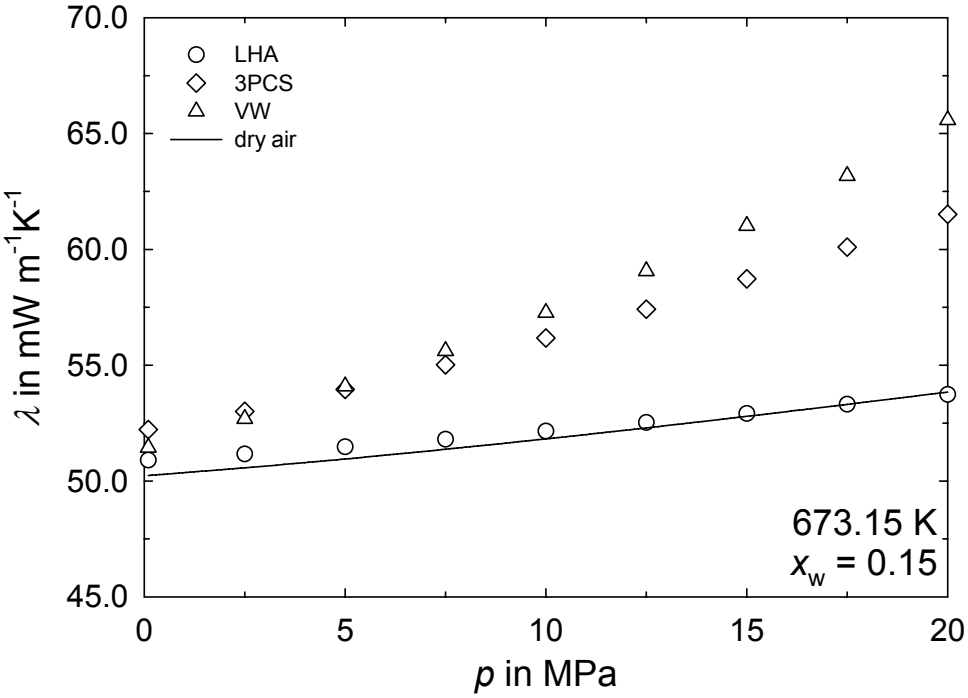

Figure 4.20: Comparison of the pressure dependence of thermal conductivity values predicted with different models for humid air with x_w = 0.15 at 673.15 K. Curve corresponds to values obtained for dry air with the correlation of Lemmon and Jacobsen [1].

4.3 Conclusions from the Evaluation of the Prediction Models

The evaluation of transport property models, which could be used for the prediction of the viscosity and thermal conductivity of humid air in large ranges of temperature and pressure as well as over a large composition range, is hampered due to the shortage of reliable measurements available in the literature. The data situation could not decisively be improved by the experimenters of work package 4 so that the evaluation of predicted values is extremely difficult.

A first analysis of four different models recommended in the literature for the prediction of the transport properties of gaseous mixtures showed that it is reasonable to consider dry air as a pseudo-pure component. Furthermore, a suitable model should be able to reproduce the properties of the pure and pseudo-pure components at least and should, consequently, include the correlations of the transport properties of dry air [1] and water [8], [9]. For these reasons, the multiparameter correlation of Chung *et al.* [14], [15] was excluded from the further evaluation. A prediction method proposed by co-workers of work package 4 [16] deals with humid air as an ideal mixture of real fluids. This procedure does approximately interpolate between the transport properties of the pure and pseudo-pure components. A more theoretically founded model recommended by Vesovic and Wakeham [17], [18] was applied in a totally predictive way using results from an extended corresponding states principle. But if experimental data of humid air were available, the results could be improved by adjusting one or more parameters of the model. In addition, a three-parameter corresponding states model of Scalabrin *et al.* [19], [20], requiring transport equations of two reference fluids as well as some values under saturation conditions for the reference fluids and for the components of the mixture, has been tested. It was not possible within the scope of this model to use both air and water as reference fluids, but only air, so that argon was chosen to be the second reference fluid. An overview on the considered prediction models for the transport properties of humid air including the required input quantities is given in Table 4.1.

The comparison of the different prediction models with experimental data from the literature concerning the composition dependence of the transport properties could only be performed in the low-pressure region due to the restricted data. It was found that the composition dependence of both transport properties of humid air is not adequately predicted by any of the procedures. All three models show the same tendency in the deviations. But the Vesovic-Wakeham procedure leads to comparably good values at mole fractions up to $x_{\mathrm{W}} \approx 0.5$, whereas higher mole fractions are probably not of importance for the project. Furthermore, the three-parameter corresponding states model is not able to reproduce the transport properties of pure water and consequently those of humid air.

Table 4.1: Prediction models for the transport properties of mixtures including input quantities.

Prediction model	Input quantities	Additional input
Multiparameter correlation of Chung *et al.*	T, $\rho_{\mathrm{m,mix}}$, $\overline{x}$	Critical constants $T_{\mathrm{c},i}$ and $V_{\mathrm{mc},i}$, acentric factor ω_i, dipole moment μ_i, hydrogen-bonding correction κ_i.
Program Package LibHuAir	T, p, $\overline{x}$	Equations of state and transport property correlations of the components: $\rho_i(T, p_i)$, $\eta_i(T, \rho_i)$, $\lambda_i(T, \rho_i)$.
Model of Vesovic and Wakeham	T, $\rho_{\mathrm{m,mix}}$, $\overline{x}$	Transport property correlations of the components: $\eta_i^0(T)$, $\eta_i(T, \rho_{\mathrm{m}})$, $\lambda_i^0(T)$, $\lambda_i(T, \rho_{\mathrm{m}})$; Mixture quantities from corresponding states model.
Three-parameter corresponding states model of Scalabrin *et al.*	T, p, $\overline{x}$	Critical constants $T_{\mathrm{c},i}$ and $p_{\mathrm{c},i}$; some saturated liquid data of the components and of the reference fluids at the same reduced temperature; equations of state and transport property correlations for the reference fluids $\rho_{\mathrm{m,rf}i}(T, p)$, $\eta_{\mathrm{rf}i}(T, \rho_{\mathrm{m}})$, $\lambda_{\mathrm{rf}i}(T, \rho_{\mathrm{m}})$; dilute-gas thermal conductivities of the components and of the reference fluids $\lambda_i^0(T)$, $\lambda_{\mathrm{rf}i}^0(T)$.

The results of viscosity measurements on humid air at comparably small mole fractions of water obtained at Ruhr-Universität Bochum [6] are characterised by some inconsistencies possibly caused by an error. Nevertheless, it could be assumed that both the absolute values and the pressure dependence of the viscosity of dry and humid air for small mole fractions of water do not differ very much. A comparison of values calculated with the different prediction models in larger ranges of temperature, pressure, and composition shows that the pressure dependence of the viscosity values of humid air agrees approximately with that of dry air. The differences between the calculated viscosity values of humid air are mainly determined by the viscosity at low pressure due to the composition dependence.

In the case of the thermal conductivity the differences of the values predicted with the various models are not only caused by the different composition dependence at low pressure but also by the unlike pressure dependence, so that the situation is more complicated than that for the viscosity. Unfortunately, the findings cannot be explained without reliable experimental results which should be available at least in a restricted range of temperature, pressure, and composition.

The Vesovic-Wakeham procedure seems to be the most promising one in the complete ranges of temperature, pressure, and composition required in the project. It represents

somewhat better the composition dependence of both transport properties at low pressures and should be improved by adjusting one or more parameters within the scope of a fit of the calculated values to the experimental data. Conclusions concerning the pressure dependence are hampered by the shortage of experimental data. Nevertheless, in the case of the viscosity the pressure dependence seems to be represented in an adequate manner.

5 Recommended Model for Transport Properties

An improved modification of the Vesovic-Wakeham procedure is recommended for the prediction of the transport properties of humid air. The method proposed by Vesovic and Wakeham [17], [18] to predict the transport properties of a dense fluid mixture is based on a rigid-sphere model. The real behaviour of the fluids is taken into account by the contact value of the pseudo-radial distribution function derived from the transport property correlations of the pure components. In the case of humid air, dry air is considered to be a pseudo-pure component so that the formulations for the viscosity and thermal conductivity reported by Lemmon and Jacobsen [1] can be applied. They are given in Section 5.1. In addition, the formulations for the viscosity and thermal conductivity of water and steam [8], [9] provided by the International Association for the Properties of Water and Steam (IAPWS) are needed and summarized in Section 5.2. The general scheme of the Vesovic-Wakeham procedure described in Sections 5.3.1 and 5.3.2 requires as input quantities the temperature, the molar density of the mixture and its composition, whereas experimental transport property data of the mixture are not necessary for the calculation. It is to be noted that Vesovic and Wakeham treated the transport properties in a way that the contributions resulting from the enhancement near to the critical point are excluded. Additional information concerning the implementation of the procedure for mixtures of dry air and water is included in Section 5.3.3. The improvement of the Vesovic-Wakeham procedure by adjusting the length scaling parameter needed for the interaction viscosity in the limit of zero density is presented in Section 5.3.4.

Furthermore, the recommended model makes possible calculation of the transport properties of humid air under the conditions of liquid fog and of ice fog. Liquid fog is treated as an ideal mixture of saturated humid air and of water droplets for the viscosity as well as for the thermal conductivity. In the case of ice fog, an approximation is used to determine the dynamic viscosity, because its value does not exist in the solid state of water. The calculation for the thermal conductivity treats ice fog as an ideal mixture of saturated humid air and of ice crystals.

5.1 Dry Air

5.1.1 Viscosity

The viscosity of dry air treated as pseudo-pure fluid is expressed according to Lemmon and Jacobsen [1] with the following equation in which no contribution considering the critical enhancement is included:

$$\eta = \eta^0(T) + \eta^{\mathrm{R}}(\tau, \delta)\,. \tag{5.1}$$

The dilute-gas viscosity (in $\mu\mathrm{Pa\,s}$) follows from:

$$\eta^0(T) = \frac{0.0266958\sqrt{MT}}{\sigma^2 \Omega^{(2,2)*}(T^*)}\,. \tag{5.2}$$

The reduced collision integral $\Omega^{(2,2)*}$ for viscosity and thermal conductivity is given as

$$\Omega^{(2,2)*}(T^*) = \exp\left\{\sum_{i=0}^{4} b_i \left[\ln\left(T^*\right)\right]^i\right\} \tag{5.3}$$

with

$$T^* = k_B T / \varepsilon \,. \tag{5.4}$$

Parameters needed for calculating the viscosity and thermal conductivity of dry air are given in Table 5.1.

Table 5.1: Parameters of the viscosity and thermal conductivity equations for dry air.

Parameter	Air
T_c / K	132.6312
ρ_{mc} / mol dm^{-3}	10.4477
p_c / MPa	3.78502
M / g mol^{-1}	28.9586
ε/k_B / K	103.3
σ / nm	0.360
ξ_0 / nm	0.11
Γ	0.055
q_D / nm	0.31
T_{ref} / K	265.262

The residual fluid contribution to the viscosity follows from

$$\eta^R(\tau,\delta) = \sum_{i=1}^{n} N_i \tau^{t_i} \delta^{d_i} \exp\left(-\gamma_i \delta^{l_i}\right) \tag{5.5}$$

with

$$\tau = T_c / T \;\text{ and }\; \delta = \rho / \rho_c \,. \tag{5.6}$$

All coefficients and exponents needed in Eq. (5.3) and in Eq. (5.5) are summarized in Table 5.2. The parameter γ_i equals zero, if l_i is zero, and is unity, if l_i is not zero.

Table 5.2: Coefficients and exponents of the dilute-gas viscosity equation [Eq. (5.3)] and of the residual-fluid viscosity equation [Eq. (5.5)] for dry air taken from Lemmon and Jacobsen [1].

i	b_i	i	N_i	t_i	d_i	l_i
			Air			
0	0.431	1	10.72	0.2	1	0
1	–0.4623	2	1.122	0.05	4	0
2	0.08406	3	0.002019	2.4	9	0
3	0.005341	4	–8.876	0.6	1	1
4	–0.00331	5	–0.02916	3.6	8	1

5.1.2 Thermal Conductivity

The thermal conductivity of dry air is expressed according to the correlation of Lemmon and Jacobsen [1] as:

$$\lambda = \lambda^0(T) + \lambda^{\mathrm{R}}(\tau,\delta) + \lambda^{\mathrm{C}}(\tau,\delta)\,. \tag{5.7}$$

The dilute-gas term of the thermal conductivity (in $\mathrm{mW\,m^{-1}\,K^{-1}}$) reads:

$$\lambda^0 = N_1\left[\frac{\eta^0(T)}{1\ \mu\mathrm{Pa\ s}}\right] + N_2\tau^{t_2} + N_3\tau^{t_3}\,, \tag{5.8}$$

whereas the residual contribution to the thermal conductivity is given as:

$$\lambda^{\mathrm{R}} = \sum_{i=4}^{n} N_i\tau^{t_i}\delta^{d_i}\exp\left(-\gamma_i\delta^{l_i}\right). \tag{5.9}$$

The coefficients and exponents needed in the last two equations are summarized in Table 5.3. As already mentioned above, the value of the parameter γ_i depends on the values of the exponent l_i and equals either zero or unity.

Table 5.3: Coefficients and exponents of the dilute-gas thermal conductivity [Eq. (5.8)] and of the residual-fluid thermal conductivity equations [Eq. (5.9)] for dry air taken from Lemmon and Jacobsen [1].

i	N_i	t_i	d_i	l_i
		Air		
1	1.308			
2	1.405	–1.1		
3	–1.036	–0.3		
4	8.743	0.1	1	0
5	14.76	0.0	2	0
6	–16.62	0.5	3	2
7	3.793	2.7	7	2
8	–6.142	0.3	7	2
9	–0.3778	1.3	11	2

The contribution to the thermal conductivity of the fluid due to the enhancement in the critical region is calculated by means of a model developed by Olchowy and Sengers [10].

$$\lambda^{\mathrm{C}} = \rho c_p \frac{k_{\mathrm{B}} R_0 T}{6\pi\xi\eta(T,\rho)}\left(\tilde{\Omega} - \tilde{\Omega}_0\right), \tag{5.10}$$

where

$$\tilde{\Omega} = \frac{2}{\pi}\left[\left(\frac{c_p - c_V}{c_p}\right)\tan^{-1}\left(\xi/q_{\mathrm{D}}\right) + \frac{c_V}{c_p}\left(\xi/q_{\mathrm{D}}\right)\right], \tag{5.11}$$

$$\tilde{\Omega}_0 = \frac{2}{\pi}\left\{1-\exp\left[\frac{-1}{\left(\xi/q_\mathrm{D}\right)^{-1}+\frac{1}{3}\left(\xi/q_\mathrm{D}\right)^2\left(\rho_\mathrm{c}/\rho\right)^2}\right]\right\}, \tag{5.12}$$

$$\xi = \xi_0\left[\frac{\tilde{\chi}(T,\rho)-\tilde{\chi}(T_\mathrm{ref},\rho)\frac{T_\mathrm{ref}}{T}}{\Gamma}\right]^{\nu/\gamma}, \tag{5.13}$$

$$\tilde{\chi}(T,\rho) = \frac{p_\mathrm{c}\rho}{\rho_\mathrm{c}^2}\left(\frac{\partial\rho}{\partial p}\right)_T. \tag{5.14}$$

In these equations, R_0, ν, and γ are theoretically based constants with values of $R_0 = 1.01$, $\nu = 0.63$, and $\gamma = 1.2415$, whereas the fluid-specific terms q_D, ξ_0, and Γ derived from a fit to experimental data in the critical region are given in Table 5.1. The specific isobaric and isochoric heat capacities, c_p and c_V, as well as the first derivative of mass density with respect to pressure are available from the equation of state given by Lemmon *et al.* [11]. The reference temperature T_ref (see Table 5.1) was chosen to be twice the critical temperature T_c. At temperatures higher than T_ref the bracket term in Eq. (5.13) becomes negative and the critical enhancement should be set zero.

5.2 Water and Steam

5.2.1 Viscosity

The viscosity of ordinary water substance is given for general and scientific use according to the IAPWS formulation [8] as:

$$\eta_\mathrm{r} = \eta_\mathrm{r}^0(T_\mathrm{r})\,\eta_\mathrm{r}^1(T_\mathrm{r},\rho_\mathrm{r})\,\eta_\mathrm{r}^2(T_\mathrm{r},\rho_\mathrm{r}) \tag{5.15}$$

The reference values to perform the reduction are given in Table 5.4.

Table 5.4: Reference constants and relationships to reduce viscosities and thermal conductivities for water and steam.

Reference constants	Reduced quantities	
$T^* = 647.226$ K	$T_\mathrm{r} = T/T^*$	(5.16)
$\rho^* = 317.763$ kg m^{-3}	$\rho_\mathrm{r} = \rho/\rho^*$	(5.17)
$p^* = 22.115$ MPa	$p_\mathrm{r} = p/p^*$	(5.18)
$\eta^* = 55.071$ μPa s	$\eta_\mathrm{r} = \eta/\eta^*$	(5.19)
$\lambda^* = 0.4945$ W m^{-1} K^{-1}	$\lambda_\mathrm{r} = \lambda/\lambda^*$	(5.20)

The reduced viscosity coefficient in the dilute-gas limit follows from:

$$\eta_{\mathrm{r}}^{0}(T_{\mathrm{r}}) = \frac{\sqrt{T_{\mathrm{r}}}}{\sum_{i=0}^{3} \frac{h_i}{T_{\mathrm{r}}^{i}}}, \tag{5.21}$$

with the coefficients h_i given in Table 5.5.

The term $\eta_{\mathrm{r}}^{1}(T_{\mathrm{r}}, \rho_{\mathrm{r}})$ is related to but not identical with the residual contribution of viscosity and reads as

$$\eta_{\mathrm{r}}^{1}(T_{\mathrm{r}}, \rho_{\mathrm{r}}) = \exp\left[\rho_{\mathrm{r}} \sum_{i=0}^{5} \sum_{j=0}^{6} h_{ij} \left(\frac{1}{T_{\mathrm{r}}} - 1 \right)^{i} \left(\rho_{\mathrm{r}} - 1 \right)^{j} \right] \tag{5.22}$$

with the coefficients h_{ij} also summarized in Table 5.5. All h_{ij} values with combinations of the indices i and j not given in this table are equal zero.

Table 5.5: Coefficients h_i for $\eta_{\mathrm{r}}^{0}(T_{\mathrm{r}})$ [Eq. (5.21)] and h_{ij} for $\eta_{\mathrm{r}}^{1}(T_{\mathrm{r}}, \rho_{\mathrm{r}})$ [Eq. (5.22)].

i	h_i	i	j	h_{ij}	i	j	h_{ij}
0	1.000000	0	0	0.5132047	2	2	–1.263184
1	0.978197	1	0	0.3205656	0	3	0.1778064
2	0.579829	4	0	–0.7782567	1	3	0.4605040
3	–0.202354	5	0	0.1885447	2	3	0.2340379
		0	1	0.2151778	3	3	–0.4924179
		1	1	0.7317883	0	4	–0.04176610
		2	1	1.241044	3	4	0.1600435
		3	1	1.476783	1	5	–0.01578386
		0	2	–0.2818107	3	6	–0.003629481
		1	2	–1.070786			

The term $\eta_{\mathrm{r}}^{2}(T_{\mathrm{r}}, \rho_{\mathrm{r}})$ of Eq. (5.15) accounting for the enhancement of the viscosity in the vicinity of the critical point has only to be considered in a limited range of temperature and density by

$$\eta_{\mathrm{r}}^{2}(T_{\mathrm{r}}, \rho_{\mathrm{r}}) = 0.922\, \tilde{\chi}^{0.0263} \qquad \text{if} \quad \tilde{\chi} \geq 21.93 \tag{5.23}$$

$$\eta_{\mathrm{r}}^{2}(T_{\mathrm{r}}, \rho_{\mathrm{r}}) = 1 \qquad \text{if} \quad \tilde{\chi} < 21.93\ . \tag{5.24}$$

The values for $\tilde{\chi}$ result from the equation of state according to the definition:

$$\tilde{\chi} = \rho_{\mathrm{r}} \left(\frac{\partial \rho_{\mathrm{r}}}{\partial p_{\mathrm{r}}} \right)_{T_{\mathrm{r}}}\ . \tag{5.25}$$

$\eta_r^2(T_r, \rho_r)$ can be chosen in ranges located outside the critical region to be equal unity to allow simplified calculations, what means to avoid the determination of $\tilde{\chi}$ for points beyond that region. The thermodynamically stable areas with $\eta_r^2 > 1$ are situated within:

$$0.996 \le T_r \le 1.01 \tag{5.26}$$

$$0.71 \le \rho_r \le 1.36 \ . \tag{5.27}$$

5.2.2 Thermal Conductivity

The equation for the thermal conductivity provided by the IAPWS [9] differs slightly from that for the viscosity due to the larger influence of the critical enhancement and reads in reduced form as follows:

$$\lambda_r = \lambda_r^0(T_r)\,\lambda_r^1(T_r, \rho_r) + \lambda_r^2(T_r, \rho_r)\,. \tag{5.28}$$

The thermal conductivity in the dilute-gas limit is written as

$$\lambda_r^0(T_r) = \frac{\sqrt{T_r}}{\sum_{i=0}^{3} \frac{l_i}{T_r^i}} \tag{5.29}$$

with the coefficients l_i given in Table 5.6.

The term $\lambda_r^1(T_r, \rho_r)$ is given similarly to the corresponding term in the viscosity equation:

$$\lambda_r^1(T_r, \rho_r) = \exp\left[\rho_r \sum_{i=0}^{4} \sum_{j=0}^{5} l_{ij} \left(\frac{1}{T_r} - 1 \right)^i \left(\rho_r - 1 \right)^j \right]. \tag{5.30}$$

The coefficients required in Eq. (5.30) are also listed in Table 5.6, whereas all values of l_{ij} not given are equal zero.

The additive term $\lambda_r^2(T_r, \rho_r)$ of Eq. (5.28) represents the contribution resulting for the enhancement of thermal conductivity in the vicinity of the critical point and is defined as:

$$\lambda_r^2(T_r, \rho_r) = \frac{0.0013848}{\eta_r^0(T_r)\,\eta_r^1(T_r, \rho_r)} \left(\frac{T_r}{\rho_r} \right)^2 \left(\frac{\partial p_r}{\partial T_r} \right)_{\rho_r}^2 \tilde{\chi}^{0.4678}\, \rho_r^{1/2} \cdot \exp\left[-18.66 \left(T_r - 1 \right)^2 - \left(\rho_r - 1 \right)^4 \right] \ . \tag{5.31}$$

Here the contributions $\eta_r^0(T_r)$ and $\eta_r^1(T_r, \rho_r)$ follow from the viscosity equations described above including the definition of the quantity $\tilde{\chi}$.

Table 5.6: Coefficients l_i for $\lambda_r^0(T_r)$ [Eq. (5.29)] and l_{ij} for $\lambda_r^1(T_r,\rho_r)$ [Eq. (5.30)].

i	l_i	i	j	l_{ij}	i	j	l_{ij}
0	1.000000	0	0	1.3293046	2	2	4.9874687
1	6.978267	1	0	1.7018363	3	2	4.3786606
2	2.599096	2	0	5.2246158	0	3	0.018660751
3	–0.998254	3	0	8.7127675	1	3	−0.76736002
		4	0	−1.8525999	2	3	−0.27297694
		0	1	−0.40452437	3	3	−0.91783782
		1	1	−2.2156845	0	4	−0.12961068
		2	1	−10.124111	1	4	0.37283344
		3	1	−9.5000611	2	4	−0.43083393
		4	1	0.93404690	0	5	0.044809953
		0	2	0.24409490	1	5	−0.11203160
		1	2	1.6511057	2	5	0.13333849

5.3 Improved Vesovic-Wakeham Model for Unsaturated and Saturated Humid Air

5.3.1 Viscosity

The viscosity of a dense fluid mixture containing N components is given for the molar density ρ_m and a composition characterised by the mole fractions x_i as:

$$\eta_{mix}(T,\rho_m,\bar{x}) = -\begin{vmatrix} H_{11} & \cdots & H_{1N} & Y_1 \\ \vdots & & \vdots & \vdots \\ H_{N1} & \cdots & H_{NN} & Y_N \\ Y_1 & \cdots & Y_N & 0 \end{vmatrix} \Bigg/ \begin{vmatrix} H_{11} & \cdots & H_{1N} \\ \vdots & & \vdots \\ H_{N1} & \cdots & H_{NN} \end{vmatrix} + \kappa_{mix} \tag{5.32}$$

$$Y_i = x_i\left(1+\sum_{j=1}^{N}\frac{m_j}{m_i+m_j}x_j\alpha_{ij}\bar{\chi}_{ij}\rho_m\right) \tag{5.33}$$

$$H_{ii} = \frac{x_i^2\bar{\chi}_{ii}}{\eta_i^0} + \sum_{\substack{j=1\\ j\neq i}}^{N}\frac{x_ix_j\bar{\chi}_{ij}}{2A_{ij}^*\eta_{ij}^0}\frac{m_im_j}{\left(m_i+m_j\right)^2}\left(\frac{20}{3}+\frac{4m_j}{m_i}A_{ij}^*\right) \tag{5.34}$$

$$H_{ij} = -\frac{x_ix_j\bar{\chi}_{ij}}{2A_{ij}^*\eta_{ij}^0}\frac{m_im_j}{\left(m_i+m_j\right)^2}\left(\frac{20}{3}-4A_{ij}^*\right) \quad (i \neq j) \tag{5.35}$$

$$\kappa_{mix} = \frac{16}{5\pi}\ \frac{15}{16}\rho_m^2\sum_{i=1}^{N}\sum_{j=1}^{N}x_ix_j\bar{\chi}_{ij}\alpha_{ij}^2\eta_{ij}^0\ . \tag{5.36}$$

The contact values of the pseudo-radial distribution function $\bar{\chi}_i$ follow from the viscosity of the pure component η_i after subtracting the critical enhancement η_i^{C}:

$$\bar{\chi}_i(T,\rho_{\mathrm{m}}) = \frac{\beta_\eta\left(\eta_i - \rho_{\mathrm{m}}\alpha_{ii}\eta_i^0\right)}{2\rho_{\mathrm{m}}^2\alpha_{ii}^2\eta_i^0} \pm \beta_\eta\left[\left(\frac{\eta_i - \rho_{\mathrm{m}}\alpha_{ii}\eta_i^0}{2\rho_{\mathrm{m}}^2\alpha_{ii}^2\eta_i^0}\right)^2 - \frac{1}{\beta_\eta\rho_{\mathrm{m}}^2\alpha_{ii}^2}\right]^{1/2}. \tag{5.37}$$

These values have to be unity in the limit of zero density so that the negative root is used first and the positive one is applied at densities higher than a so-called switch-over molar density ρ_{m}^*. This quantity is iteratively determined by a comparison of the derivative of the viscosity with respect to density with the ratio of viscosity to molar density:

$$\left[\frac{\partial\eta_i(T,\rho_{\mathrm{m}})}{\partial\rho_{\mathrm{m}}}\right]_T = \frac{\eta_i(T,\rho_{\mathrm{m}})}{\rho_{\mathrm{m}}^*}. \tag{5.38}$$

The parameter α_{ii} is derived using the value ρ_{m}^*:

$$\frac{\eta_i(T,\rho_{\mathrm{m}}^*)}{\rho_{\mathrm{m}}^*\alpha_{ii}\eta_i^0} = 1 + \frac{2}{\sqrt{\beta_\eta}} \tag{5.39}$$

with

$$\frac{1}{\beta_\eta} = \frac{1}{4} + \left(\frac{16}{5\pi}\right)\frac{15}{16}.$$

The quantities characterising the interaction between unlike molecules of species i and j are obtained from the following mixing rules:

$$\alpha_{ij} = \frac{1}{8}\left(\alpha_{ii}^{1/3} + \alpha_{jj}^{1/3}\right)^3 \tag{5.40}$$

$$\bar{\chi}_{ij} = 1 + \frac{2}{5}\sum_{k=1}^{N} x_k\left(\bar{\chi}_k - 1\right) + \frac{\frac{6}{5}\left(\bar{\chi}_i - 1\right)^{1/3}\left(\bar{\chi}_j - 1\right)^{1/3}\sum_{k=1}^{N} x_k\left(\bar{\chi}_k - 1\right)^{2/3}}{\left(\bar{\chi}_i - 1\right)^{1/3} + \left(\bar{\chi}_j - 1\right)^{1/3}}. \tag{5.41}$$

5.3.2 Thermal Conductivity

The thermal conductivity of a dense fluid mixture consists of a translational (mon - monatomic) and an internal (int) contribution:

$$\lambda_{\mathrm{mix}}(T,\rho_{\mathrm{m}}) = \lambda_{\mathrm{mix}}(\mathrm{mon})(T,\rho_{\mathrm{m}}) + \lambda_{\mathrm{mix}}(\mathrm{int})(T,\rho_{\mathrm{m}}). \tag{5.42}$$

The translational contribution is given similar to the formulae for the viscosity:

$$\lambda_{\mathrm{mix}}(\mathrm{mon})(T,\rho_{\mathrm{m}}) = -\begin{vmatrix} L_{11} & \cdots & L_{1N} & Y_1 \\ \vdots & & \vdots & \vdots \\ L_{N1} & \cdots & L_{NN} & Y_N \\ Y_1 & \cdots & Y_N & 0 \end{vmatrix} \Bigg/ \begin{vmatrix} L_{11} & \vdots & L_{1N} \\ \vdots & & \vdots \\ L_{N1} & \cdots & L_{NN} \end{vmatrix} + \kappa_{\mathrm{mix}} \tag{5.43}$$

$$Y_i = x_i \left[1 + \sum_{j=1}^{N} \frac{2 m_i m_j}{\left(m_i + m_j \right)^2} x_j \gamma_{ij} \overline{\chi}_{ij} \rho_{\mathrm{m}} \right] \tag{5.44}$$

$$\begin{aligned} L_{ii} = {} & \frac{x_i^2 \overline{\chi}_{ii}}{\lambda_i^0(\mathrm{mon})} \\ & + \sum_{\substack{j=1 \\ j \neq i}}^{N} \left[\frac{x_i x_j \overline{\chi}_{ij}}{2 A_{ij}^* \lambda_{ij}^0(\mathrm{mon}) \left(m_i + m_j \right)^2} \left(\frac{15}{2} m_i^2 + \frac{25}{4} m_j^2 - 3 m_j^2 B_{ij}^* + 4 m_i m_j A_{ij}^* \right) \right] \end{aligned} \tag{5.45}$$

$$L_{ij} = -\frac{x_i x_j \overline{\chi}_{ij}}{2 A_{ij}^* \lambda_{ij}^0(\mathrm{mon})} \frac{m_i m_j}{\left(m_i + m_j \right)^2} \left(\frac{55}{4} - 3 B_{ij}^* - 4 A_{ij}^* \right) \quad (i \neq j) \tag{5.46}$$

$$\kappa_{\mathrm{mix}} = \frac{16}{5\pi} \frac{10}{9} \rho_{\mathrm{m}}^2 \sum_{i=1}^{N} \sum_{j=1}^{N} \frac{m_i m_j}{\left(m_i + m_j \right)^2} x_i x_j \overline{\chi}_{ij} \gamma_{ij}^2 \lambda_{ij}^0(\mathrm{mon}) \,. \tag{5.47}$$

The translational contributions of the thermal conductivity in the limit of zero density $\lambda_i^0(\mathrm{mon})$ and $\lambda_{ij}^0(\mathrm{mon})$ are derived from the corresponding values of the viscosity in the same limit:

$$\lambda_i^0(\mathrm{mon}) = \frac{5}{2} \left[\frac{c_{V\mathrm{m}}^{\mathrm{o}}(\mathrm{mon})}{M_i} \right] \eta_i^0 \,. \tag{5.48}$$

The internal contribution to the thermal conductivity reads as:

$$\lambda_{\mathrm{mix}}(\mathrm{int})(T,\rho_{\mathrm{m}}) = \sum_{i=1}^{N} \left[\frac{\lambda_i^0 - \lambda_i^0(\mathrm{mon})}{\overline{\chi}_{ii}} \right] \left[1 + \sum_{\substack{j=1 \\ j \neq i}}^{N} \frac{x_j \lambda_i^0(\mathrm{mon}) \overline{\chi}_{ij} A_{ii}^*}{x_i \lambda_{ij}^0(\mathrm{mon}) \overline{\chi}_{ii} A_{ij}^*} \right]^{-1} \,. \tag{5.49}$$

The contact value of the pseudo-radial distribution function $\overline{\chi}_i$ follows from the thermal conductivity of the pure component λ_i after subtracting the critical enhancement λ_i^{C}:

$$\bar{\chi}_i(T,\rho_\mathrm{m}) = \frac{\beta_\lambda\left[\lambda_i - \rho_\mathrm{m}\gamma_{ii}\lambda_i^0(\mathrm{mon})\right]}{2\rho_\mathrm{m}^2\gamma_{ii}^2\lambda_i^0(\mathrm{mon})} \pm \beta_\lambda\left\{\left[\frac{\lambda_i - \rho_\mathrm{m}\gamma_{ii}\lambda_i^0(\mathrm{mon})}{2\rho_\mathrm{m}^2\gamma_{ii}^2\lambda_i^0(\mathrm{mon})}\right]^2 - \frac{\lambda_i^0}{\beta_\lambda\rho_\mathrm{m}^2\gamma_{ii}^2\lambda_i^0(\mathrm{mon})}\right\}^{1/2} \tag{5.50}$$

The switch-over molar density ρ_m^* and the parameter γ_{ii} are derived from:

$$\left[\frac{\partial\lambda_i(T,\rho_\mathrm{m})}{\partial\rho_\mathrm{m}}\right]_T = \frac{\lambda_i(T,\rho_\mathrm{m})}{\rho_\mathrm{m}^*} \tag{5.51}$$

$$\frac{\lambda_i(T,\rho_\mathrm{m}^*)}{\rho_\mathrm{m}^*\gamma_{ii}\lambda_i^0(\mathrm{mon})} = 1 + \frac{2}{\sqrt{\beta_\lambda}}\left[\frac{\lambda_i^0}{\lambda_i^0(\mathrm{mon})}\right]^{1/2} \tag{5.52}$$

with $\frac{1}{\beta_\lambda} = \frac{1}{4} + \left(\frac{16}{5\pi}\right)\frac{5}{18}$.

The analogous mixing rules as formulated for the prediction of the viscosity are applied to determine the mixture quantities $\bar{\chi}_{ij}$ and γ_{ij}.

5.3.3 Implementation of the Vesovic-Wakeham Model for the Prediction of the Transport Properties of Humid Air

Treatment of the critical enhancement

In principle, the contributions of the critical enhancement have to be subtracted from the total values of the viscosity and of the thermal conductivity for the pure fluid *i*:

$$\eta_i(T,\rho_\mathrm{m}) = \eta_{i,\mathrm{total}}(T,\rho_\mathrm{m}) - \eta_i^\mathrm{C}(T,\rho_\mathrm{m}) \tag{5.53}$$

$$\lambda_i(T,\rho_\mathrm{m}) = \lambda_{i,\mathrm{total}}(T,\rho_\mathrm{m}) - \lambda_i^\mathrm{C}(T,\rho_\mathrm{m}) \tag{5.54}$$

But this has to be performed for water only, because these contributions are negligible for dry air under the conditions of interest, even in the case of the thermal conductivity. Although the critical enhancement of the viscosity is comparably small, apart from a very close region near to the critical point (see IAPWS formulations [8], [9]), this contribution was also subtracted for the viscosity in order to avoid numerical problems in determining the contact values of the pseudo-radial distribution function. This is particularly of importance at the reference temperature concerning the hypothetical fluid (see next point).

For the final calculation of the thermal conductivity for humid air, the contribution due to the critical enhancement of water has again to be added according to the partial density $\rho_\mathrm{m,w}$:

$$\lambda_\mathrm{mix,total}(T,\rho_\mathrm{m}) = \lambda_\mathrm{mix}(T,\rho_\mathrm{m}) + \lambda_\mathrm{w}^\mathrm{C}(T,\rho_\mathrm{m,w}). \tag{5.55}$$

But in the case of the viscosity the critical enhancement has not been considered due to its minor contribution following from the proportion of water in humid air.

Transport properties of water as a hypothetical fluid

The transport properties of the pure components are needed at the same temperature and density as the mixture and additionally for the complete temperature range up to high densities in order to determine the switch-over molar density ρ_{m}^{*}, the mean free-path shortening parameters α_{ii} and γ_{ii}, and particularly the contact value of the pseudo-radial distribution function $\overline{\chi}_i$. Since water can be a liquid under the conditions of interest, it has to be treated as a hypothetical fluid that has the same properties as the real component in the single-phase region, but does not undergo a phase separation.

The following equations have to be applied to calculate the transport properties of a hypothetical fluid at temperatures below the critical temperature ($T < T_{\mathrm{c}}$) and at densities higher than the saturated vapour molar density ($\rho_{\mathrm{m}} > \rho_{\mathrm{ms}}$):

$$\eta_i(T,\rho_{\mathrm{m}}) = \eta_i(T,\rho_{\mathrm{ms}}) + \left[\eta_i(T_{\mathrm{ref}},\rho_{\mathrm{m}}) - \eta_i(T_{\mathrm{ref}},\rho_{\mathrm{ms}})\right] \tag{5.56}$$

$$\lambda_i(T,\rho_{\mathrm{m}}) = \lambda_i(T,\rho_{\mathrm{ms}}) + \left[\lambda_i(T_{\mathrm{ref}},\rho_{\mathrm{m}}) - \lambda_i(T_{\mathrm{ref}},\rho_{\mathrm{ms}})\right] \tag{5.57}$$

In our investigation the reference temperature was chosen to be T_{ref} = 650 K marginally higher than the critical temperature of water. In all other ranges of temperature and density the transport properties of water are calculated according to the IAPWS formulations [8], [9].

Quantities characterising the interaction between the unlike molecules

The interaction viscosity in the limit of zero density is determined based on an extended corresponding states principle [27] using a universal correlation with a functional S_{η}^{*} derived from the HFD potentials of the rare gases [28]. First, individual scaling factors σ_{ii} and ε_{ii} were calculated from zero-density viscosity values of the correlation by Lemmon and Jacobsen [1] for dry air and experimentally based zero-density viscosity values for water vapour [31]. For that purpose the equations formulated below were used for pure gases in an analogous manner. The scaling factors for water and dry air resulting from that analysis are given as:

Water:	σ_{ii}	=	0.26949 nm	$\varepsilon_{ii}/k_{\mathrm{B}}$	=	768.47 K
Dry air:	σ_{jj}	=	0.36175 nm	$\varepsilon_{jj}/k_{\mathrm{B}}$	=	99.33 K

Then the scaling parameters for the unlike interactions were derived with the help of common mixing rules from the individual parameters of the pure components:

$$\sigma_{ij} = \frac{1}{2}\left(\sigma_{ii} + \sigma_{jj}\right) \tag{5.58}$$

$$\varepsilon_{ij} = \left(\varepsilon_{ii}\varepsilon_{jj}\right)^{1/2} . \tag{5.59}$$

The unlike scaling parameters have the following values:

Humid air: σ_{ij} = 0.31562 nm $\varepsilon_{ij}/k_{\mathrm{B}}$ = 276.28 K.

Finally, the interaction viscosity in the limit of zero density results from:

$$\eta_{ij}^{0}(T) = \frac{0.021357\left(\dfrac{2M_i M_j}{M_i + M_j}T\right)^{1/2}}{\sigma_{ij}^{2} S_{\eta}^{*}(T_{ij}^{*})} \tag{5.60}$$

with

$$\ln S_{\eta}^{*}(T_{ij}^{*}) = \sum_{k=0}^{4} a_k \left[\ln\left(T_{ij}^{*}\right)\right]^{k} \tag{5.61}$$

and

$$T_{ij}^{*} = \frac{k_{\mathrm{B}}\,T}{\varepsilon_{ij}} . \tag{5.62}$$

The universal constants a_k of the functional S_{η}^{*} are given in the range $1.2 < T^{*} < 10$ according to Bich *et al.* [28]:

$a_0 =$ 0.2218816, $a_1 =$ –0.5079322, $a_2 =$ 0.1285776,

$a_3 =$ –0.008328165, $a_4 =$ –0.002713173.

The quantities A_{ij}^{*} and B_{ij}^{*} characterising the relationships between different collision integrals are taken to be 1.10 in the whole range of temperature.

Furthermore, in the case of the thermal conductivity unreasonable values for the interaction quantities $\overline{\chi}_{ij}$, $\overline{\chi}_{ii}$, and $\overline{\chi}_{jj}$ can occur for high mole fractions of water, if the common mixing rule is applied. This would also lead to inadequate results for the thermal conductivity of the mixture and can be avoided by using the following simpler alternative mixing rules for the interaction quantities:

$$\overline{\chi}_{ii} = \overline{\chi}_{i} \quad , \quad \overline{\chi}_{jj} = \overline{\chi}_{j} \quad , \quad \overline{\chi}_{ij} = \left(\overline{\chi}_{i}\overline{\chi}_{j}\right)^{1/2} .$$

According to experience gained in the project the common mixing rule can be applied for mole fractions up to $x_{\mathrm{w}} \approx 0.5$.

5.3.4 Improvement of the Vesovic-Wakeham Model by Using Experimental Data

As already stated in Section 4.3, the ability of the Vesovic-Wakeham model in predicting the transport properties of humid air can be improved by taking into consideration experimental data available in restricted ranges of temperature, pressure, and composition. Figure 4.3 to Figure 4.8, concerning the comparison of viscosity and thermal conductivity data for humid air at different temperatures and at atmospheric

pressure with values predicted using the Vesovic-Wakeham model, demonstrated that the differences are dependent on the composition of the mixtures. This is certainly caused by the fact that the interactions between the molecules of dry air and water do not correspond to spherically symmetric interaction potentials and that the theorem of corresponding states is inappropriate to represent the interaction viscosity in the limit of zero density η_{ij}^{0} of such mixtures. In fact, the kinetic theory for molecules with intermolecular potential energy hypersurfaces is very complicated and has to take into account the internal degrees of freedom. Therefore, it seemed to be reasonable to consider the interaction viscosity as dependent on the mole fraction x_{w}. This composition dependence was introduced into the interaction viscosity in that way that the length scaling factor σ_{ij} was considered to be dependent on the composition of the mixture. For that purpose, the experimental data for the viscosity of humid air of Kestin and Whitelaw [2] as well as of Hochrainer and Munczak [3] at atmospheric pressure and at different temperatures have been used to adjust the coefficients b_k in the following equation:

$$\sigma_{ij}^{\mathrm{adj}}(x_{\mathrm{w}}) = \sigma_{ij}\left[1 + x_1 x_2 \sum_{k=1}^{n} b_k (x_1 - x_2)^k\right] \tag{5.63}$$

The coefficients b_k were derived as: $b_0 = 0.34831934$, $b_1 = 0.23343484$, $b_2 = 1.5288226$. The differences between the experimental viscosity data and the values calculated with the usual Vesovic-Wakeham model as well as by means of the procedure with the adjusted scaling factor $\sigma_{ij}^{\mathrm{adj}}$ are illustrated in Figure 5.1 and Figure 5.2.

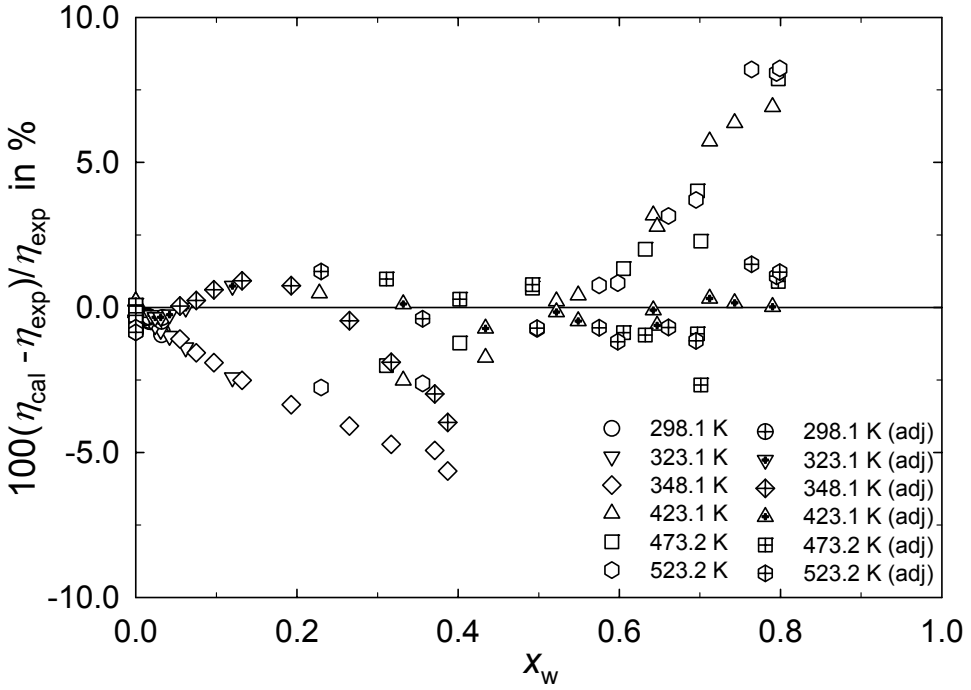

Figure 5.1: Deviations of the values calculated with the Vesovic-Wakeham model from the experimental data of Kestin and Whitelaw [2] for the viscosity of humid air at atmospheric pressure and at different temperatures. Open symbols – usual VW model, crossed symbols – VW model with adjusted scaling parameter.

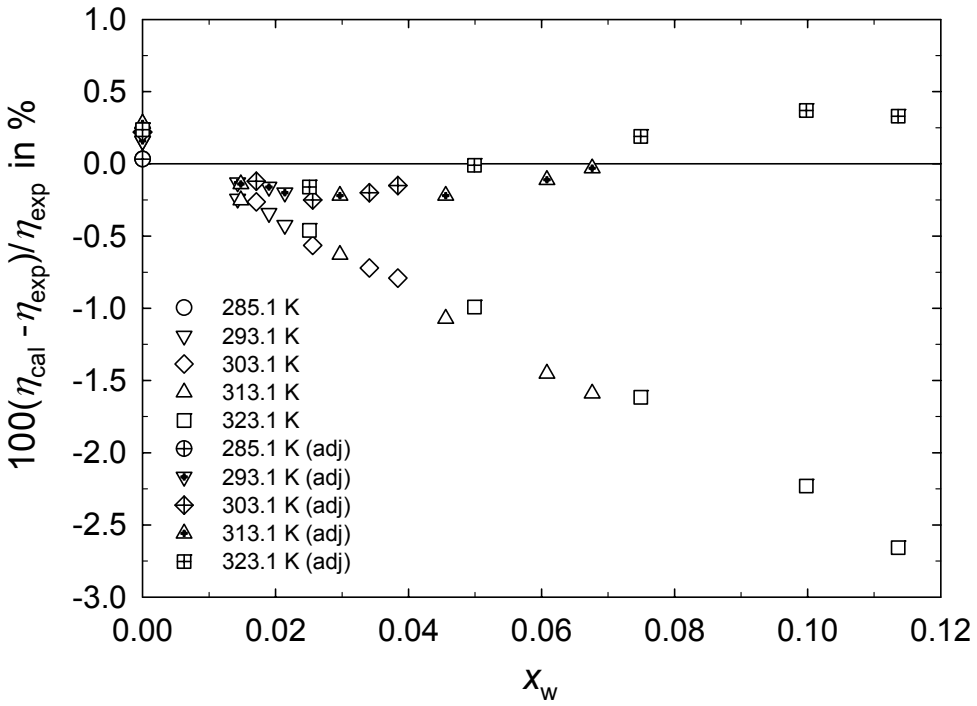

Figure 5.2: Deviations of the values calculated with the Vesovic-Wakeham model from the experimental data of Hochrainer and Munczak [3] for the viscosity of humid air at atmospheric pressure and at different temperatures. Open symbols – usual VW model, crossed symbols – VW model with adjusted scaling parameter.

The experimental data of Kestin and Whitelaw [2] shown in Figure 5.1 are described for all mole fractions within ± 2% using the procedure with the adjusted scaling factor apart from two values at 348.1 K at medium mole fractions and another value at 473.2 K at about $x_w \approx 0.7$. It is to be mentioned that an experimental outlier at 423.1 K was excluded from the fit. Figure 5.2 elucidates the improvement in the representation of the experimental data of Hochrainer and Munczak [3] by means of the variant of the VW model with the adjusted length scaling parameter σ_{ij}^{adj}.

The distinctly improved ability of the Vesovic-Wakeham procedure with the adjusted scaling parameter, to describe adequately the composition dependence of the viscosity of humid air at atmospheric pressure, is also demonstrated for the experimental data of Kestin and Whitelaw at 523.2 K in Figure 5.3. The value for pure water vapour calculated with the IAPWS formulation [8] is added to complete the range of mole fractions. The figure in which the values calculated with the different prediction models are compared makes evident that the Vesovic-Wakeham procedure with the adjusted scaling parameter is the only one which can represent the curvature of the composition dependence of the viscosity at low pressures.

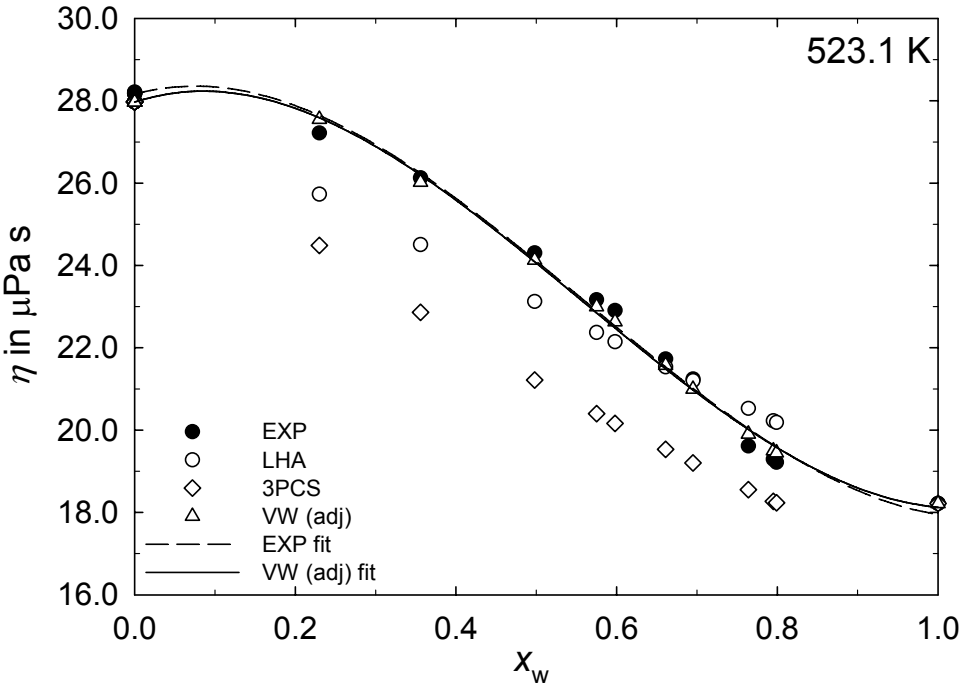

Figure 5.3: Comparison of experimental data (EXP) of Kestin and Whitelaw [2] at 523.1 K and at atmospheric pressure with values for the viscosity of humid air using the different prediction models (LHA – LibHuAir; 3PCS – three-parameter corresponding states model; VW – Vesovic-Wakeham procedure). Curves correspond to a third-order polynomial fit to experimental data and to values predicted by means of the VW model with the adjusted scaling parameter; value for pure water from IAPWS formulation [8].

Analogously to the viscosity, the experimental thermal conductivity data of Grüß and Schmick [4] and values predicted by means of the VW model with the adjusted scaling parameter as well as with the other models are directly compared in Figure 5.4. It has to be pointed out that, in addition to the original Vesovic-Wakeham procedure (VW), a variant was used in which the dimerisation reaction in water vapour has been considered (VWR). The thermal conductivity value of pure water calculated with the IAPWS formulation [9] for the density of the saturated vapour obtained from the IAPWS-95 formulation [12] at 353.1 K was added. This enables to perform, in the complete range of mole fractions, third-order polynomial fits to the experimental data as well as to the values predicted using the VW model with the adjusted scaling parameter. The curve resulting for the VW model is characterised by a curvature and a maximum similar to those of the experimental data. None of the other models leads to values with approximately the same behaviour. This can be established, even if it is taken into account that the experimental data have a large uncertainty which is obvious by the difference of nearly 5% compared with the nowadays accepted value for dry air resulting from the correlation of Lemmon and Jacobsen [1].

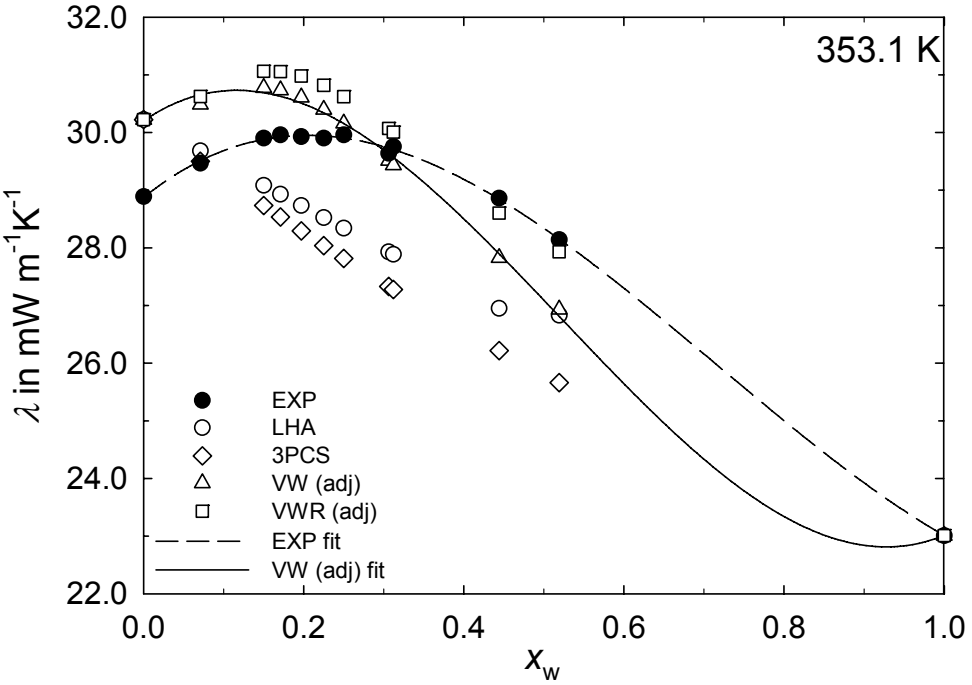

Figure 5.4: Comparison of experimental data (EXP) of Grüß and Schmick [4] at 353.1 K and at atmospheric pressure with values for the thermal conductivity of humid air using the different prediction models (LHA – LibHuAir; 3PCS – three-parameter corresponding states model; VW – Vesovic-Wakeham procedure; VWR – Vesovic-Wakeham procedure considering additionally the dimerisation reaction; adj – adjusted scaling parameter). Curves correspond to a third-order polynomial fit to experimental data and to values predicted by means of the VW model with the adjusted scaling parameter; value for pure water from IAPWS formulation [9].

To achieve a reliable judgement of the Vesovic-Wakeham procedure further experimental data for both transport properties are needed, in particular for the thermal conductivity over a large composition range at low as well as at high pressures.

5.4 Application to Liquid Fog and Ice Fog

5.4.1 Liquid Fog

Liquid fog is treated as an ideal mixture of saturated humid air and of water droplets in the calculation of its transport properties. As an assumption, the water droplets are considered to be equally distributed in the total volume or volume flow.
The transport properties are given for liquid fog ($\xi_{\mathrm{w}} > \xi_{\mathrm{s,w}}$ and $273.16 \le T < 647.096\,\mathrm{K}$) as:

Dynamic viscosity η

$$\eta = \eta_{\mathrm{s,w}} \left(\gamma_{\mathrm{a}} + \gamma_{\mathrm{w,vap}} \right) + \eta_{\mathrm{w,liq}} \gamma_{\mathrm{w,liq}} \tag{5.64}$$

with

$\eta_{\mathrm{s,w}} = f\left(T, \rho_{\mathrm{ms,w}}, x_{\mathrm{w}}\right)$ dynamic viscosity of the saturated composition obtained from Section 5.3

where

$\rho_{\mathrm{ms,w}} = \dfrac{M}{\dfrac{1}{v_{\mathrm{a}}\left(p_{\mathrm{a}},T\right)} + \dfrac{1}{v_{\mathrm{w,vap}}}}$ molar mixture density at saturation composition

$M = x_{\mathrm{a}} M_{\mathrm{a}} + x_{\mathrm{w}} M_{\mathrm{w}}$ molar mass of the mixture in $\mathrm{kg\,kmol^{-1}}$, and

$x_{\mathrm{a}} = 1 - x_{\mathrm{w}}$ mole fraction of air,

$x_{\mathrm{w}} = \dfrac{W}{\left(\dfrac{M_{\mathrm{w}}}{M_{\mathrm{a}}} + W\right)}$ mole fraction of water in the mixture with units $\mathrm{mol\,mol^{-1}}$,

W humidity ratio of the mixture with units $\mathrm{kg_w\,kg_a^{-1}}$.

$M_{\mathrm{a}} = 28.9586\,\dfrac{\mathrm{kg}}{\mathrm{kmol}}$ molar mass of air obtained from Lemmon *et al.* [11],

$M_{\mathrm{w}} = 18.015268\,\dfrac{\mathrm{kg}}{\mathrm{kmol}}$ molar mass of water obtained from IAPWS-95 [12], [13],

$v_{\mathrm{a}}\left(p_{\mathrm{a}},T\right)$ specific volume of air at partial pressure of air and temperature obtained from Lemmon *et al.*,

$v_{\mathrm{w,vap}} = f\left(p_{\mathrm{s,w}},T\right)$ specific volume of water vapour obtained from IAPWS-95.

$p_{\mathrm{s,w}} = f\left(p,T\right)$ partial pressure of water vapour of the saturated composition obtained from Nelson and Sauer [32], [33],

$\eta_{\mathrm{w,liq}} = f\left(T, v_{\mathrm{w,liq}}\right)$ dynamic viscosity of liquid water obtained from IAPWS-85 [8],

and

$v_{\mathrm{w,liq}} = f\left(p,T\right)$ specific volume of liquid water obtained from IAPWS-95,

$\gamma_{\mathrm{a}} = \xi_{\mathrm{a}}\,\dfrac{v_{\mathrm{a}}\left(p,T\right)}{v}$ volume fraction of air

where

$\xi_{\mathrm{a}} = 1 - \xi_{\mathrm{s,w}} - \xi_{\mathrm{w,liq}}$ mass fraction of air

$\xi_{\mathrm{s,w}} = \dfrac{W_{\mathrm{s}}}{1+W}$ mass fraction of saturated water vapour

W_s humidity ratio of the saturated composition calculated from the following equation $W_s = \frac{R_a}{R_w}\frac{p_{s,w}}{p - p_{s,w}}$,

Dry air

$R_a = \frac{R}{M_a}$ specific gas constant of air,

$R = 8.314510 \frac{\text{kJ}}{\text{kmol K}}$ molar gas constant obtained from Lemmon *et al.*,

Water and steam

$R_w = 0.46151805 \frac{\text{kJ}}{\text{kg K}}$ specific gas constant of water obtained from IAPWS-95,

$\xi_{w,liq} = \xi_w - \xi_{s,w}$ mass fraction of the liquid water in the fog

ξ_w mass fraction of water in the mixture,

$v_a(p,T)$ specific volume of air at mixture pressure and temperature obtained from Lemmon *et al.*,

$v = \frac{v_{s,w}(1+W_s) + v_{w,liq}(W - W_s)}{1+W}$ specific volume of fog

where

$v_{s,w} = \frac{1}{\rho_{ms,w} M}$ specific volume of the saturated composition

$v_{w,liq} = f(p,T)$ specific volume of liquid water obtained from IAPWS-95,

$\gamma_{w,vap} = 1 - \gamma_a - \gamma_{w,liq}$ volume fraction of water vapour,

$\gamma_{w,liq} = \xi_{w,liq}\frac{v_{w,liq}}{v}$ volume fraction of liquid water

with

$\xi_{w,liq} = \xi_w - \xi_{s,w}$ mass fraction of liquid water in the fog.

Thermal Conductivity λ

$$\lambda = \lambda_{s,w}\left(\gamma_a + \gamma_{w,vap}\right) + \lambda_{w,liq}\gamma_{w,liq} \tag{5.65}$$

with

$\lambda_{s,w} = \lambda\left(T, \rho_{ms,w}, x_w\right)$ thermal conductivity of the mixture obtained from Section 5.3

where

$\rho_{ms,w} = \dfrac{M}{\dfrac{1}{v_a\left(p_a, T\right)} + \dfrac{1}{v_{w,vap}}}$ molar mixture density at saturation composition

$M = x_a M_a + x_w M_w$ molar mass of the mixture in $\mathrm{kg\,kmol^{-1}}$,

and

$x_a = 1 - x_w$ mole fraction of air,

$x_w = \dfrac{W}{\left(\dfrac{M_w}{M_a} + W\right)}$ mole fraction of water in the mixture with units $\mathrm{mol\,mol^{-1}}$,

W humidity ratio of the mixture with units $\mathrm{kg_w\,kg_a^{-1}}$.

$M_a = 28.9586\,\dfrac{\mathrm{kg}}{\mathrm{kmol}}$ molar mass of air obtained from Lemmon *et al.* [11],

$M_w = 18.015268\,\dfrac{\mathrm{kg}}{\mathrm{kmol}}$ molar mass of water obtained from IAPWS-95 [12], [13],

$v_a\left(p_a, T\right)$ specific volume of air at partial pressure of air and temperature obtained from Lemmon *et al.*,

$v_{w,vap} = f\left(p_{s,w}, T\right)$ specific volume of water vapour obtained from IAPWS-95.

$p_{s,w} = f(p, T)$ partial pressure of water vapour of the saturated composition obtained from Nelson and Sauer [32], [33],

$\lambda_{w,liq} = f\left(T, v_{w,liq}\right)$ thermal conductivity of liquid water obtained from IAPWS-85 [9],

and

$v_{w,liq} = f\left(p, T\right)$ specific volume of liquid water obtained from IAPWS-95,

$\gamma_a = \xi_a \dfrac{v_a\left(p, T\right)}{v}$ volume fraction of air

where

$\xi_a = 1 - \xi_{s,w} - \xi_{w,liq}$ mass fraction of air

$\xi_{s,w} = \frac{W_s}{1+W}$ mass fraction of saturated water vapour

W_s humidity ratio of the saturated composition calculated from the following equation $W_s = \frac{R_a}{R_w}\frac{p_{s,w}}{p - p_{s,w}}$,

Dry air

$R_a = \frac{R}{M_a}$ specific gas constant of air,

$R = 8.314510 \frac{\text{kJ}}{\text{kmol K}}$ molar gas constant obtained from Lemmon *et al.*,

Water and steam

$R_w = 0.46151805 \frac{\text{kJ}}{\text{kg K}}$ specific gas constant of water obtained from IAPWS-95,

$\xi_{w,liq} = \xi_w - \xi_{s,w}$ mass fraction of the liquid water in the fog

ξ_w mass fraction of water in the mixture,

$v_a(p,T)$ specific volume of air at mixture pressure and temperature obtained from Lemmon *et al.*,

$v = \frac{v_{s,w}(1+W_s) + v_{w,liq}(W - W_s)}{1+W}$ specific volume of fog

where

$v_{s,w} = \frac{1}{\rho_{ms,w} M}$ specific volume of the saturated composition

$v_{w,liq} = f(p,T)$ specific volume of liquid water obtained from IAPWS-95,

$\gamma_{w,vap} = 1 - \gamma_a - \gamma_{w,liq}$ volume fraction of water vapour,

$\gamma_{w,liq} = \xi_{w,liq} \frac{v_{w,liq}}{v}$ volume fraction of liquid water

with

$\xi_{w,liq} = \xi_w - \xi_{s,w}$ mass fraction of liquid water in the fog.

5.4.2 Ice Fog

Note that the new model for calculating the transport properties of humid air has a limited temperature range starting from 273.16 K. Due to the fact that the dynamic viscosity of water in the solid state does not exist, an approximation is needed to determine the dynamic viscosity in the case of ice fog. The approximation consists in that the viscosity of the saturated composition is calculated using the equation from Brandt [34]. In the case of the thermal conductivity, ice fog is treated as an ideal mixture of saturated humid air, again calculated by means of the equation of Brandt, and of ice crystals. As an assumption, the ice crystals are considered to be equally distributed in the total volume or volume flow. Furthermore, a constant value for the thermal conductivity of the ice crystals is used [35].
The transport properties are given for ice fog ($\xi_\mathrm{w} > \xi_\mathrm{s,w}$ and $243.15 < \mathrm{T} \le 273.16\ \mathrm{K}$)[14] as:

Dynamic viscosity η

$$\eta = \eta_\mathrm{a}\gamma_\mathrm{a} + \eta_\mathrm{w,vap}\gamma_\mathrm{w,vap} \tag{5.66}$$

with

$\eta_\mathrm{a} = f\left(T, \tilde{v}_\mathrm{a}\right)$ dynamic viscosity of dry air obtained from Lemmon and Jacobsen [1],

$\eta_\mathrm{w,vap} = f\left(T\right)$ dynamic viscosity of water vapour of the saturated composition obtained from Brandt [34] for temperatures below freezing,

$\gamma_\mathrm{a} = \xi_\mathrm{a}\dfrac{v_\mathrm{a}\left(p,T\right)}{v_\mathrm{s,w}}$ volume fraction of air

where

$\xi_\mathrm{a} = 1 - \xi_\mathrm{s,w}$ mass fraction of air

$\xi_\mathrm{s,w} = \dfrac{W_\mathrm{s}}{1+W}$ mass fraction of saturated water vapour

W_s humidity ratio of the saturated composition calculated from the following equation

$$W_\mathrm{s} = \frac{R_\mathrm{a}}{R_\mathrm{w}}\frac{p_\mathrm{s,w}}{p - p_\mathrm{s,w}},$$

$p_\mathrm{s,w} = f(p,T)$ partial pressure of water vapour of the saturated composition obtained from Nelson and Sauer [32], [33],

Dry air

[14] For simplifying the use of the library, the ice fog was assigned to temperatures below the triple-point temperature 273.16 K of water.

$R_a = \frac{R}{M_a}$ specific gas constant of air,

$R = 8.314510 \frac{\text{kJ}}{\text{kmol K}}$ molar gas constant obtained from Lemmon *et al.* [11]

$M_a = 28.9586 \frac{\text{kg}}{\text{kmol}}$ molar mass of air obtained from Lemmon *et al.*

Water and steam

$R_w = 0.46151805 \frac{\text{kJ}}{\text{kg K}}$ specific gas constant of water obtained from IAPWS-95 [12], [13].

W humidity ratio of the mixture with units $\text{kg}_{\text{water}}\,\text{kg}_{\text{air}}^{-1}$.

$v_a(p,T)$ specific volume of air at mixture pressure and temperature obtained from Lemmon *et al.*,

$v_{s,w} = \frac{1}{\frac{1}{v_a(p_a,T)} + \frac{1}{v_{w,vap}}}$ specific volume of the saturation composition,

$v_a(p_a,T)$ specific volume of air at partial pressure of air and temperature obtained from Lemmon *et al.*,

$v_{w,vap} = f(p_{s,w},T)$ specific volume of water vapour obtained from IAPWS-95,

$\gamma_{w,vap} = 1 - \gamma_a$ volume fraction of water vapour in the mixture.

Thermal conductivity λ

$$\lambda = \lambda_a \gamma_a + \lambda_{w,vap} \gamma_{w,vap} + \lambda_{w,ice} \gamma_{w,ice} \tag{5.67}$$

with

$\lambda_a = f(T, \rho_{m,a})$ thermal conductivity of dry air obtained from Lemmon and Jacobsen [1],

$\lambda_{w,vap} = f(T)$ thermal conductivity of water vapour of the saturated composition obtained from Brandt [34] for temperatures below freezing,

$\lambda_{w,ice} = 2.21 \frac{\text{W}}{\text{m K}}$ thermal conductivity of ice obtained from Kretzschmar [35],

$\gamma_a = \xi_a \frac{v_a(p,T)}{v}$ volume fraction of air

where

$\xi_a = 1 - \xi_{s,w} - \xi_{w,ice}$ mass fraction of air

$\xi_{s,w} = \frac{W_s}{1+W}$ mass fraction of saturated water vapour

W_s humidity ratio of the saturated composition calculated from the following equation

$$W_s = \frac{R_a}{R_w}\frac{p_{s,w}}{p - p_{s,w}},$$

$p_{s,w} = f(p,T)$ partial pressure of water vapour of the saturated composition obtained from Nelson and Sauer [32], [33],

Dry air

$R_a = \frac{R}{M_a}$ specific gas constant of air,

$R = 8.314510 \frac{\text{kJ}}{\text{kmol K}}$ molar gas constant obtained from Lemmon *et al.* [11]

Water and steam

$R_w = 0.46151805 \frac{\text{kJ}}{\text{kg K}}$ specific gas constant of water obtained from IAPWS-95 [12], [13].

W humidity ratio of the mixture with units $\text{kg}_w\,\text{kg}_a^{-1}$.

$\xi_{w,ice} = \xi_w - \xi_{s,w}$ mass fraction of ice in the fog

ξ_w mass fraction of water in the mixture,

$v_a(p,T)$ specific volume of air obtained from Lemmon *et al.*,

$v = \frac{v_{s,w}(1+W_s) + v_{w,ice}(W - W_s)}{1+W}$ specific volume of fog

where

$v_{s,w} = \frac{1}{\frac{1}{v_a(p_a,T)} + \frac{1}{v_{w,vap}}}$ specific volume of the saturation composition

$v_{\mathrm{a}}\left(p_{\mathrm{a}}, T\right)$ specific volume of air at partial pressure of air and temperature obtained from Lemmon *et al.*,

$v_{\mathrm{w,vap}} = f\left(p_{\mathrm{s,w}}, T\right)$ specific volume of water vapour from IAPWS-95,

$\gamma_{\mathrm{w,vap}} = 1 - \gamma_{\mathrm{a}} - \gamma_{\mathrm{w,ice}}$ volume fraction of water vapour,

$\gamma_{\mathrm{w,ice}} = \xi_{\mathrm{w,ice}} \dfrac{v_{\mathrm{w,ice}}}{v}$ volume fraction of ice

with

$\xi_{\mathrm{w,ice}} = \xi_{\mathrm{w}} - \xi_{\mathrm{s,w}}$ mass fraction of ice in the fog.

6 Conclusions

The analysis of the different prediction models for the transport properties of humid air was hampered due to the lack of experimental data, especially in the case of the thermal conductivity. Nevertheless, the analysis showed that dry air should be treated as a pseudo-pure component. Furthermore, a suitable model should include the most reliable correlations available in the literature for the transport properties for the pure and pseudo-pure components water and dry air in large ranges of temperature and density or pressure and should be able to reproduce their properties at least. In addition, values for the viscosity and thermal conductivity at high temperatures and pressures calculated with four different prediction models were compared.

As a result of the comparison, one procedure is recommended for the calculation and prediction of the transport properties for humid air. It traces back to a theoretically-based model of Vesovic and Wakeham which was modified in this project. In principle, the Vesovic-Wakeham model is based on a formalism for the transport properties of a mixture of hard spheres, but it takes into consideration the behaviour of the real fluids in a suitable manner. The general scheme of this model and the specific features to be considered in its implementation for mixtures containing water were given in detail.

Although the model of Vesovic and Wakeham describes best the transport properties of humid air in a predictive manner, it was distinctly improved by the adjustment of one parameter using a very limited number of experimental viscosity data available at low densities. More accurate statements about the ability of this procedure to describe particularly the pressure dependence of humid air are not possible without new experimental data in extended ranges of temperature, pressure, and composition.

7 References

[1] Lemmon, E. W.; Jacobsen, R. T.: Viscosity and Thermal Conductivity Equations for Nitrogen, Oxygen, Argon, and Air. *Int. J. Thermophys.* **25**, 21-69 (2004).

[2] Kestin, J.; Whitelaw, J. H.: The Viscosity of Dry and Humid Air. *Int. J. Heat Mass Transfer* **7**, 1245-1255 (1964).

[3] Hochrainer, D.; Munczak, F.: Viscosity Measurements on Air of Different Humidity and Temperature. *Sitzungsber., Österr. Akad. Wiss., Abt. II* **175**, 539-550 (1966) (in German).

[4] Grüß, H.; Schmick, H.: On the Thermal Conductivity of Gaseous Mixtures. *Wiss. Veröffentl. Siemens-Konzern* **7**, 202-224 (1928) (in German).

[5] Assael, M. J.; Polimatidou, S.; Vesovic, V.; Wakeham, W. A.: Viscosity of Gaseous Binary Mixtures Containing Water Vapour. *High Temp.-High Press.* **29**, 519-524 (1997).

[6] Wöll, O.: Measurements on Dynamic Viscosity and Density of Dry and Humid Air and Further Development of a Combined Viscosity Density Measuring System. Dissertation, Ruhr-Universität Bochum, Faculty of Mechanical Engineering, Bochum (2005) (in German).

[7] Nieto de Castro, C.: Private communication (2005).

[8] IAPWS. Revised Release on the IAPS Formulation 1985 for the Viscosity of Ordinary Water Substance. 2003; available from the IAPWS Executive Secretary, Dr. R. B. Dooley, Structural Integrity Associates, Inc., Oakville, Ontario L6J 7L7, Canada, www.iapws.org.

[9] IAPWS. Revised Release on the IAPS Formulation 1985 for the Thermal Conductivity of Ordinary Water Substance. 1998; available from the IAPWS Executive Secretary, Dr. R. B. Dooley, Structural Integrity Associates, Inc., Oakville, Ontario L6J 7L7, Canada, www.iapws.org.

[10] Olchowy, G. A.; Sengers, J. V.: A Simplified Representation for the Thermal Conductivity of Fluids in the Critical Region. *Int. J. Thermophys.* **10**, 417-426 (1989).

[11] Lemmon, E. W.; Jacobsen, R. T.; Penoncello, S. G.; Friend, D. G.: Thermodynamic Properties of Air and Mixtures of Nitrogen, Argon, and Oxygen from 60 to 2000 K at Pressure to 2000 MPa. *J. Phys. Chem. Ref. Data* **29**, 331-385 (2000).

[12] Wagner, W.; Pruß, A.: The IAPWS Formulation 1995 for the Thermodynamic Properties of Ordinary Water Substance for General and Scientific Use. *J. Phys. Chem. Ref. Data* **31**, 387-535 (2002).

[13] IAPWS. Release on the IAPWS Formulation 1995 for the Thermodynamic Properties of Ordinary Water Substance for General and Scientific Use. 1995; available from the IAPWS Executive Secretary, Dr. R. B. Dooley, Structural Integrity Associates, Inc., Oakville, Ontario L6J 7L7, Canada, www.iapws.org.

[14] Chung, T.-H.; Lee, L. L.; Starling, K. E.: Applications of Kinetic Gas Theories and Multiparameter Correlation for Prediction of Dilute Gas Viscosity and Thermal Conductivity. *Ind. Eng. Chem. Fundam.* **23**, 8-13 (1984).

[15] Chung, T.-H.; Ajlan, M.; Lee, L. L.; Starling, K. E.: Generalized Multiparameter Correlation for Nonpolar and Polar Fluid Transport Properties. *Ind. Eng. Chem. Res*. **27**, 671-679 (1988).

[16] Kretzschmar, H.-J.; Stöcker, I.; Jähne, I.; Knobloch, K.; Hellriegel, T.; Kleemann, L.; Seibt, D.: Property Library LibHuAir for Humid Air Calculated as Ideal Mixture of Real Fluids and Add-In FluidEXL for MS Excel. Zittau/Goerlitz University of Applied Sciences, Department of Technical Thermodynamics, Zittau (2001-2005), available from http://thermodynamics-zittau.de.

[17] Vesovic, V.; Wakeham, W. A.: Prediction of the Viscosity of Fluid Mixtures Over Wide Ranges of Temperature and Pressure. *Chem. Eng. Sci.* **44**, 2181-2189 (1989).

[18] Vesovic, V.; Wakeham, W. A.: Prediction of the Thermal Conductivity of Fluid Mixtures Over Wide Ranges of Temperature and Pressure. *High Temp.-High Press.* **23**, 179-190 (1991).

[19] Scalabrin, G.; Cristofoli, G.; Grigiante, M.: Modeling Alkane and Haloalkane Mixture Viscosities in a Three-Parameter Corresponding States Format. *Int. J. Thermophys.* **26**, 429-452 (2005).

[20] Scalabrin, G.; Piazza, L.; Grigiante, M.; Baruzzo, M.: Thermal Conductivity Modeling of Refrigerant Mixtures in a Three-Parameter Corresponding States Format. *Int. J. Thermophys.* **26**, 399-412 (2005).

[21] IAPWS Release on the IAPWS Industrial Formulation 1997 for the Thermodynamic Properties of Water and Steam. 1997; available from the IAPWS Executive Secretary, Dr. R. B. Dooley, Structural Integrity Associates, Inc., Oakville, Ontario L6J 7L7, Canada, www.iapws.org.

[22] Butler, J. N.; Brokaw, R. S.: Thermal Conductivity of Gas Mixtures in Chemical Equilibrium. *J. Chem. Phys.* **26**, 1636-1643 (1957).

[23] Brokaw, R. S.: Thermal Conductivity of Gas Mixtures in Chemical Equilibrium. II. *J. Chem. Phys.* **32**, 1005-1006 (1960).

[24] Curtiss, L. A.; Frurip, D. J.; Blander, M.: Studies of Molecular Association in H_2O and D_2O Vapors by Measurement of Thermal Conductivity. *J. Chem. Phys.* **71**, 2703-2711 (1979).

[25] Xantheas, S. S.: Ab Initio Studies of Cyclic Water Clusters $(H_2O)_n$, n = 1-6. III. Comparison of Density Functional with MP2 Results. *J. Chem. Phys.* **102**, 4505-4517 (1995).

[26] Glazunov, A. I.; Sabirzyanov, A. N.: Thermodynamic Functions of Water Dimer. *Zh. Fiz. Khim.* **72**, 2171-2175 (1998) (in Russian).

[27] Maitland, G. C.; Rigby, M.; Smith, E. B.; Wakeham, W. A.: *Intermolecular Forces: Their Origin and Determination.* Clarendon Press, Oxford, 1987.

[28] Bich, E.; Millat, J.; Vogel, E.: Interatomic Interactions in Noble Gases and Extended Corresponding States Principle. *Wiss. Z. W.-Pieck-Univ. Rostock* **36** (N8), 5-12 (1987) (in German).

[29] Mason, E. A.; Saxena, S. A.: Approximate Formula for the Thermal Conductivity of Gas Mixtures. *Phys. Fluids* **1**, 361-369 (1958).

[30] Tegeler, C.; Span, R.; Wagner, W.: A New Equation of State for Argon Covering the Fluid Region for Temperatures From the Melting Line to 700 K at Pressures up to 1000 MPa. *J. Phys. Chem. Ref. Data* **28**, 779-850 (1999).

[31] Teske, V.; Vogel, E.; Bich, E.: Viscosity Measurements on Water Vapor and Their Evaluation. *J. Chem. Eng. Data* **50**, 2082-2087 (2005).

[32] Nelson, H. F.; Sauer, H. J.: Formulation of High-Temperature Properties of Humid Air. *HVAC&R Research* **8**, 311-334 (2002).

[33] Gatley, D. P.: *Understanding Psychrometrics,* 2nd ed., ASHRAE, Atlanta (2005).

[34] Brandt, F.: *Wärmeübertragung in Dampferzeugern und Wärmetauschern.* FDBR-Fachbuchreihe, Bd. 2, Vulkan, Essen (1985).

[35] Kretzschmar, H.-J.: Stoffwertsammlung Technische Thermodynamik, Wärme- und Stoffübertragung, Zittau/Goerlitz University of Applied Sciences, Department of Technical Thermodynamics, Zittau (2003), available from http://thermodynamics-zittau.de.

Part C

Property Library LibAirWa

for Humid Air

1 Property Functions

The recommended models described in Chapters 5 of Part A and B, respectively, have been made available in the property **Lib**rary for the mixture humid air called LibAirWa (**Air-Wa**ter). This property library contains the model ideal mixture of the real fluids dry air and water for calculating the thermal and caloric properties of humid air (Section 5.3 of Part A), prepared by Zittau/Goerlitz University of Applied Sciences. For calculating the saturated composition of humid air, the model of Nelson and Sauer (Section 5.4 of Part A) is used. In addition, the library LibAirWa includes the equations for the transport properties of Vesovic and Wakeham improved by the University of Rostock (Part B).
Table 1.1 comprises the property functions available by the library LibAirWa. The input variables for the calculation of all thermophysical properties are pressure, temperature, and mass fraction of water. Furthermore, the backward functions of the given variables (p,h), (h,s), and (p,s) which are required in process modelling can be calculated.
The functions are valid for:

- unsaturated humid air
- saturated humid air
- liquid fog at $\xi_w > \xi_{s,w}$ and $T \geq 273.16$ K
- ice fog at $\xi_w > \xi_{s,w}$ and $T < 273.16$ K[15]

In the case of liquid fog and ice fog, humid air is treated as an ideal mixture of saturated humid air and of water droplets or ice crystals, respectively. As an assumption, water droplets or ice crystals are considered to be equally distributed in the total volume or volume flow.

Table 1.1: Property functions of the library LibAirWa in alphabetical order.

Functional Dependence	**Property or Function**
$a = f(p,T,\xi_w)$	Thermal diffusivity
$c_p = f(h,s,\xi_w)$	Backward function: specific isobaric heat capacity from specific enthalpy and specific entropy
$c_p = f(p,h,\xi_w)$	Backward function: specific isobaric heat capacity from pressure and specific enthalpy
$c_p = f(p,s,\xi_w)$	Backward function: specific isobaric heat capacity from pressure and specific entropy
$c_p = f(p,T,\xi_w)$	Specific isobaric heat capacity
$c_p = f(T,s,\xi_w)$	Backward function: specific isobaric heat capacity from temperature and specific entropy
$c_v = f(p,T,\xi_w)$	Specific isochoric heat capacity
$\eta = f(p,T,\xi_w)$	Dynamic viscosity

[15] For simplifying the use of the library, the ice fog was assigned to temperatures below the triple-point temperature 273.16 K of water.

Functional Dependence	Property or Function
$h = \mathrm{f}(p, s, \xi_\mathrm{w})$	Backward function: specific enthalpy from pressure and specific entropy
$h = \mathrm{f}(p, T, \xi_\mathrm{w})$	Specific enthalpy
$h = \mathrm{f}(T, s, \xi_\mathrm{w})$	Backward function: specific enthalpy from temperature and specific entropy
$\kappa = \mathrm{f}(p, s, \xi_\mathrm{w})$	Backward function: isentropic exponent from pressure and specific entropy
$\kappa = \mathrm{f}(p, T, \xi_\mathrm{w})$	Isentropic exponent
$\lambda = \mathrm{f}(p, T, \xi_\mathrm{w})$	Thermal conductivity
$\nu = \mathrm{f}(p, T, \xi_\mathrm{w})$	Kinematic viscosity
$p = \mathrm{f}(h, s, \xi_\mathrm{w})$	Backward function: pressure from specific enthalpy and specific entropy
$p = \mathrm{f}(T, s, \xi_\mathrm{w})$	Backward function: pressure from temperature and specific entropy
$p_\mathrm{d} = \mathrm{f}(p, T, \xi_\mathrm{w})$	Partial pressure of steam
$p_\mathrm{dsatt} = \mathrm{f}(p, T)$	Saturation pressure of water
$\varphi = \mathrm{f}(p, T, \xi_\mathrm{w})$	Relative humidity
$p_\mathrm{l} = \mathrm{f}(p, T, \xi_\mathrm{w})$	Partial pressure of air
$\mathrm{Pr} = \mathrm{f}(p, T, \xi_\mathrm{w})$	PRANDTL-number
$\psi_\mathrm{l} = \mathrm{f}(\xi_\mathrm{w})$	Mole fraction of air
$\psi_\mathrm{w} = \mathrm{f}(\xi_\mathrm{w})$	Mole fraction of water
Region = $\mathrm{f}(h, s, \xi_\mathrm{w})$	Region from specific enthalpy and specific entropy
Region = $\mathrm{f}(p, h, \xi_\mathrm{w})$	Region from pressure and specific enthalpy
Region = $\mathrm{f}(p, s, \xi_\mathrm{w})$	Region from pressure and specific entropy
Region = $\mathrm{f}(p, T, \xi_\mathrm{w})$	Region from pressure and temperature
Region = $\mathrm{f}(T, s, \xi_\mathrm{w})$	Region from temperature and specific entropy
$\rho = \mathrm{f}(p, T, \xi_\mathrm{w})$	Density
$s = \mathrm{f}(p, h, \xi_\mathrm{w})$	Backward function: specific entropy from pressure and specific enthalpy
$s = \mathrm{f}(p, T, \xi_\mathrm{w})$	Specific entropy
$\sigma = \mathrm{f}(T)$	Surface tension of water
$T = \mathrm{f}(h, s, \xi_\mathrm{w})$	Backward function: temperature from specific enthalpy and specific entropy
$T = \mathrm{f}(p, h, \xi_\mathrm{w})$	Backward function: temperature from pressure and specific enthalpy
$T = \mathrm{f}(p, s, \xi_\mathrm{w})$	Backward function: temperature from pressure and specific entropy
$T_\mathrm{f} = \mathrm{f}(p, T, \xi_\mathrm{w})$	Wet bulb temperature
$T_\tau = \mathrm{f}(p, \xi_\mathrm{w})$	Dew point temperature

Functional Dependence	Property or Function
$u = \mathrm{f}(p, T, \xi_\mathrm{w})$	Specific internal energy
$v = \mathrm{f}(h, s, \xi_\mathrm{w})$	Backward function: specific volume from specific enthalpy and specific entropy
$v = \mathrm{f}(p, h, \xi_\mathrm{w})$	Backward function: specific volume from pressure and specific enthalpy
$v = \mathrm{f}(p, s, \xi_\mathrm{w})$	Backward function: specific volume from pressure and specific entropy
$v = \mathrm{f}(p, T, \xi_\mathrm{w})$	Specific volume
$v = \mathrm{f}(T, s, \xi_\mathrm{w})$	Backward function: specific volume from temperature and specific entropy
$w = \mathrm{f}(p, T, \xi_\mathrm{w})$	Isentropic speed of sound
$\xi_\mathrm{w} = \mathrm{f}(p, T, p_\mathrm{d})$	Mass fraction of water from partial pressure of steam
$\xi_\mathrm{w} = \mathrm{f}(p, T, \varphi)$	Mass fraction of water from temperature and relative humidity
$\xi_\mathrm{w} = \mathrm{f}(p, T_\tau)$	Mass fraction of water from dew point temperature
$\xi_\mathrm{w} = \mathrm{f}(p, T, T_\mathrm{f})$	Mass fraction of steam from temperature und wet bulb temperature
$\xi_\mathrm{wf} = \mathrm{f}(p, T, \xi_\mathrm{w})$	Mass fraction of water
$\xi_\mathrm{wsatt} = \mathrm{f}(p, T)$	Mass fraction of steam from saturated air
$x_\mathrm{w} = \mathrm{f}(\xi_\mathrm{w})$	Humidity ratio from mass fraction of water

The functions can be calculated for unsaturated and saturated humid air as well as for liquid fog ($\xi_\mathrm{w} > \xi_\mathrm{s,w}$ and $T \geq 273.16$ K) and ice fog ($\xi_\mathrm{w} > \xi_\mathrm{s,w}$ and $T < 273.16$ K). In the latter cases humid air is treated as an ideal mixture of saturated humid air and of water droplets and ice crystals, respectively.

2 Range of Validity

The property library LibAirWa can be used in the following ranges of temperature and pressure:

T = 243.15 K … 2000 K and p = 611.2 Pa … 100 MPa,

with the limitation that the partial pressure of steam is restricted to 16 MPa.

Some functions have closer limits with respect to their calculated values. The ranges of validity of these functions are listed in Table 2.1:

Table 2.1: Property functions with a more restricted range of validity.

Functional Dependence	Property	Range of Validity
$p_{\mathrm{dsatt}} = \mathrm{f}(p,T)$	Saturation pressure of water	$243.15\ \mathrm{K} \le T \le 647.096\ \mathrm{K}$, $0.0006112\ \mathrm{MPa} \le p \le 100\ \mathrm{MPa}$
$\varphi = \mathrm{f}(p,T,\xi_{\mathrm{w}})$	Relative humidity	$243.15\ \mathrm{K} \le T \le 647.096\ \mathrm{K}$, $0.0006112\ \mathrm{MPa} \le p \le 100\ \mathrm{MPa}$, $0\ \mathrm{kg/kg} \le \xi_{\mathrm{w}} \le \xi_{\mathrm{wsatt}}(p,T)$
$\sigma = \mathrm{f}(T)$	Surface tension of water	$273.15\ \mathrm{K} \le T \le 647.096\ \mathrm{K}$
$T_\tau = \mathrm{f}(p,\xi_{\mathrm{w}})$	Dew point temperature	$0.0006112\ \mathrm{MPa} \le p \le 100\ \mathrm{MPa}$, $\xi_{\mathrm{wsatt}}(p,243.15\,\mathrm{K}) \le \xi_{\mathrm{w}}$
$\xi_{\mathrm{w}} = \mathrm{f}(p,T,p_{\mathrm{d}})$	Mass fraction of water from partial pressure of steam	$243.15\,\mathrm{K} \le T \le 2000\ \mathrm{K}$, $0.0006112\ \mathrm{MPa} \le p \le 100\ \mathrm{MPa}$, $0.0006112\ \mathrm{MPa} \le p_{\mathrm{d}} \le p_{\mathrm{dsatt}}(p,T)$ for $T \le 647.096\ \mathrm{K}$ and $p_{\mathrm{d}} \le 100\ \mathrm{MPa}$ for $T > 647.096\ \mathrm{K}$
$\xi_{\mathrm{w}} = \mathrm{f}(p,T,\varphi)$	Mass fraction of water from relative humidity	$273.15\ \mathrm{K} \le T \le 647.096\ \mathrm{K}$, $0.0006112\ \mathrm{MPa} \le p \le 100\ \mathrm{MPa}$, $0\% \le \phi \le 100\%$
$\xi_{\mathrm{w}} = \mathrm{f}(p,T_\tau)$	Mass fraction of water from dew point temperature	$243.15\ \mathrm{K} \le T \le T_{\mathrm{s}}(p,p_{\mathrm{d}})$, $0.0006112\ \mathrm{MPa} \le p \le 100\ \mathrm{MPa}$
$\xi_{\mathrm{w}} = \mathrm{f}(p,T,T_{\mathrm{f}})$	Mass fraction of steam from wet bulb temperature	$243.15\ \mathrm{K} \le T \le 647.096\ \mathrm{K}$, $243.15\ \mathrm{K} \le T_{\mathrm{f}} \le T_{\mathrm{s}}(p,p_{\mathrm{d}})$, $0.0006112\ \mathrm{MPa} \le p \le 100\ \mathrm{MPa}$
$\xi_{\mathrm{wf}} = \mathrm{f}(p,T,\xi_{\mathrm{w}})$	Mass fraction of water	$T_\tau(p,\xi_{\mathrm{w}}) \le T \le T_{\mathrm{s}}(p,p_{\mathrm{d}})$, $0.0006112\ \mathrm{MPa} \le p \le 100\ \mathrm{MPa}$, $\xi_{\mathrm{wsatt}}(p,243.15\ \mathrm{K}) \le \xi_{\mathrm{w}}$
$\xi_{\mathrm{wsatt}} = \mathrm{f}(p,T)$	Mass fraction of steam of saturated humid air	$243.15K \le T \le T_{\mathrm{s}}(p,p_{\mathrm{d}})$, $0.0006112\ \mathrm{MPa} \le p \le 100\ \mathrm{MPa}$

3 Application in Excel® and Mathcad®

For convenient use of the property library LibAirWa in Excel® and Mathcad® the Add-In FluidEXL and the Add-On FluidMAT are available. A detailed description is given in [2] and [3].

4 References

[1] Zunft, S.; Tamme, R.; Nowi, A.; Jakiel, C.: Adiabatic Compressed Air Storage Power Plants. *Energiewirtschaftliche Tagesfragen* **55**, 254-258 (2005) (in German).

[2] Kretzschmar, H.-J.; Vogel, E.; Herrmann, S.; Stoecker, I.; Teske, V.: Property Library for Humid Air Calculated as an Ideal Mixture of Real Fluids LibAirWa, and Add-In FluidEXL for MS Excel. Zittau/Goerlitz University of Applied Sciences, Department of Technical Thermodynamics, University of Rostock, Physical Chemistry Group, Zittau, Rostock (2006), available from http://thermodynamics-zittau.de or www.chemie.uni-rostock.de/pci.

[3] Kretzschmar, H.-J.; Vogel, E.; Herrmann, S.; Stoecker, I.; Teske, V.: Property Library for Humid Air Calculated as an Ideal Mixture of Real Fluids LibAirWa, and Add-On FluidMAT for Mathcad. Zittau/Goerlitz University of Applied Sciences, Department of Technical Thermodynamics, University of Rostock, Physical Chemistry Group, Zittau, Rostock (2006), available from http://thermodynamics-zittau.de or www.chemie.uni-rostock.de/pci.

Part D

Property Database for Thermodynamic and Transport Properties

1 Structure and Contents of the Database

The aim of the database was to collect all relevant data and information which are necessary to investigate the behaviour of humid air. The database developed comprises information on thermodynamic and transport properties of humid air, dry air, humid gases, and humid combustion gases. Data were taken from the literature and also new measured data were included. The database contains currently 225 sources including thermodynamic and transport properties. A more detailed description of the structure and the contents of the database is given in [1]. The authors thankfully acknowledge the support of E. Lemmon [2] (NIST, Boulder CO, USA) and J. Yan [3] (KTH, Stockholm, Sweden).

The contents of the database are managed by the Excel® Database Table. Figure 1.1 demonstrates the structure of the database.

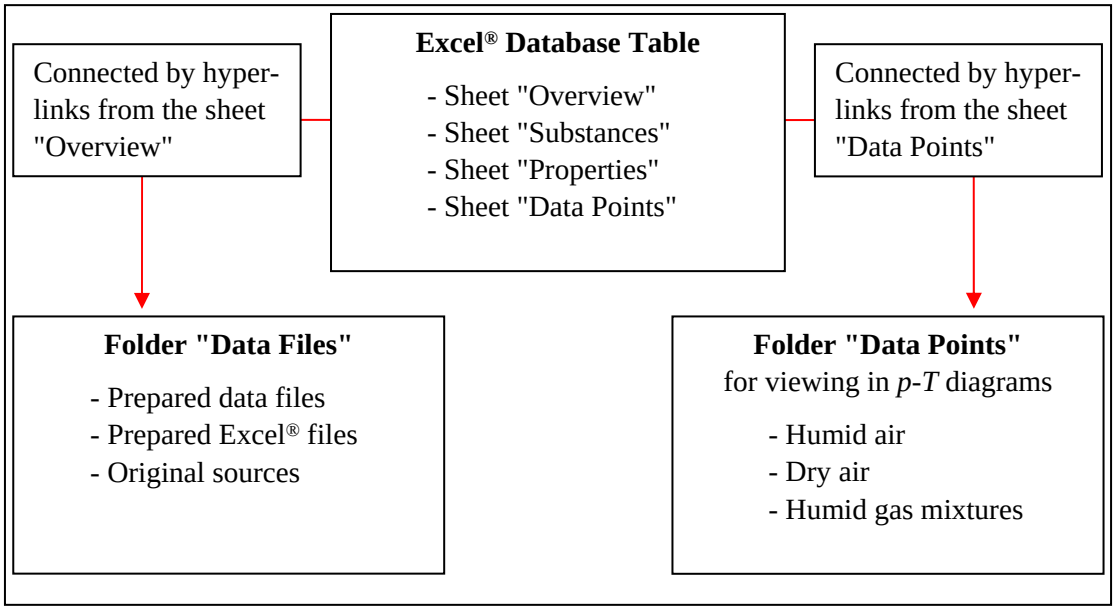

Figure 1.1: Structure of the database.

The sheet "Overview" is the starting point for using the database. This sheet covers all information of the collected sources and the hyperlinks to all files of the database. Figure 1.2 illustrates the first part of the sheet "Overview".

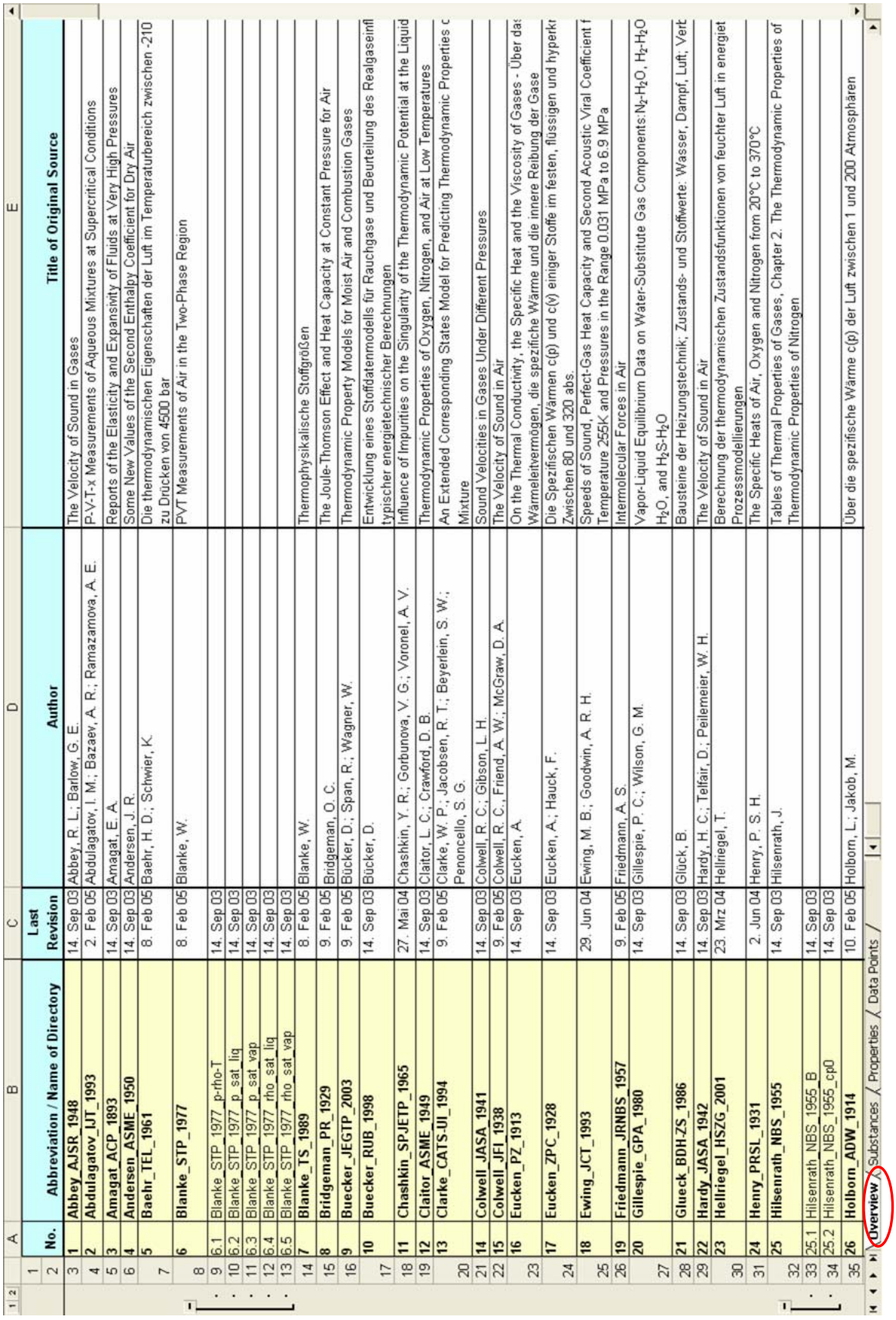

No.	Abbreviation / Name of Directory	Last Revision	Author	Title of Original Source
1	Abbey_AJSR_1948	14. Sep 03	Abbey, R. L.; Barlow, G. E.	The Velocity of Sound in Gases
2	Abdulagatov_IJT_1993	2. Feb 05	Abdulagatov, I. M.; Bazaev, A. R.; Ramazanova, A. E.	P-V-T-x Measurements of Aqueous Mixtures at Supercritical Conditions
3	Amagat_ACP_1893	14. Sep 03	Amagat, E. A.	Reports of the Elasticity and Expansivity of Fluids at Very High Pressures
4	Andersen_ASME_1950	14. Sep 03	Andersen, J. R.	Some New Values of the Second Enthalpy Coefficient for Dry Air
5	Baehr_TEL_1961	8. Feb 05	Baehr, H. D.; Schwier, K.	Die thermodynamischen Eigenschaften der Luft im Temperaturbereich zwischen -210 zu Drücken von 4500 bar
6	Blanke_STP_1977	8. Feb 05	Blanke, W.	PVT Measurements of Air in the Two-Phase Region
6.1	Blanke_STP_1977_p-rho-T	14. Sep 03		
6.2	Blanke_STP_1977_p_sat_liq	14. Sep 03		
6.3	Blanke_STP_1977_p_sat_vap	14. Sep 03		
6.4	Blanke_STP_1977_rho_sat_liq	14. Sep 03		
6.5	Blanke_STP_1977_rho_sat_vap	14. Sep 03		
7	Blanke_TS_1989	8. Feb 05	Blanke, W.	Thermophysikalische Stoffgrößen
8	Bridgeman_PR_1929	9. Feb 05	Bridgeman, O. C.	The Joule-Thomson Effect and Heat Capacity at Constant Pressure for Air
9	Buecker_JEGTP_2003	9. Feb 05	Bücker, D.; Span, R.; Wagner, W.	Thermodynamic Property Models for Moist Air and Combustion Gases
10	Buecker_RUB_1998	14. Sep 03	Bücker, D.	Entwicklung eines Stoffdatenmodells für Rauchgase und Beurteilung des Realgaseinfl typischer energietechnischer Berechnungen
11	Chashkin_SPJETP_1965	27. Mai 04	Chashkin, Y. R.; Gorbunova, V. G.; Voronel, A. V.	Influence of Impurities on the Singularity of the Thermodynamic Potential at the Liquid
12	Claitor_ASME_1949	14. Sep 03	Claitor, L. C.; Crawford, D. B.	Thermodynamic Properties of Oxygen, Nitrogen, and Air at Low Temperatures
13	Clarke_CATS-UI_1994	9. Feb 05	Clarke, W. P.; Jacobsen, R. T.; Beyerlein, S. W.; Penoncello, S. G.	An Extended Corresponding States Model for Predicting Thermodynamic Properties c Mixture
14	Colwell_JASA_1941	14. Sep 03	Colwell, R. C.; Gibson, L. H.	Sound Velocities in Gases Under Different Pressures
15	Colwell_JFI_1938	9. Feb 05	Colwell, R. C.; Friend, A. W.; McGraw, D. A.	The Velocity of Sound in Air
16	Eucken_PZ_1913	14. Sep 03	Eucken, A.	On the Thermal Conductivity, the Specific Heat and the Viscosity of Gases - Über das Wärmeleitvermögen, die spezifiche Wärme und die innere Reibung der Gase
17	Eucken_ZPC_1928	14. Sep 03	Eucken, A.; Hauck, F.	Die Spezifischen Wärmen c(p) und c(v) einiger Stoffe im festen, flüssigen und hyperkr Zwischen 80 und 320 abs.
18	Ewing_JCT_1993	29. Jun 04	Ewing, M. B.; Goodwin, A. R. H.	Speeds of Sound, Perfect-Gas Heat Capacity and Second Acoustic Viral Coefficient f Temperature 255K and Pressures in the Range 0.031 MPa to 6.9 MPa
19	Friedmann_JRNBS_1957	9. Feb 05	Friedmann, A. S.	Intermolecular Forces in Air
20	Gillespie_GPA_1980	14. Sep 03	Gillespie, P. C.; Wilson, G. M.	Vapor-Liquid Equilibrium Data on Water-Substitute Gas Components: N_2-H_2O, H_2-H_2O H_2O, and H_2S-H_2O
21	Glueck_BDH-ZS_1986	14. Sep 03	Glück, B.	Bausteine der Heizungstechnik; Zustands- und Stoffwerte: Wasser, Dampf, Luft, Verb
22	Hardy_JASA_1942	14. Sep 03	Hardy, H. C.; Telfair, D.; Pellemeier, W. H.	The Velocity of Sound in Air
23	Hellriegel_HSZG_2001	23. Mrz 04	Hellriegel, T.	Berechnung der thermodynamischen Zustandsfunktionen von feuchter Luft in energiet Prozessmodellierungen
24	Henry_PRSL_1931	2. Jun 04	Henry, P. S. H.	The Specific Heats of Air, Oxygen and Nitrogen from 20°C to 370°C
25	Hilsenrath_NBS_1955	14. Sep 03	Hilsenrath, J.	Tables of Thermal Properties of Gases, Chapter 2. The Thermodynamic Properties of Thermodynamic Properties of Nitrogen
25.1	Hilsenrath_NBS_1955_B	14. Sep 03		
25.2	Hilsenrath_NBS_1955_cp0	14. Sep 03		
26	Holborn_ADW_1914	10. Feb 05	Holborn, L.; Jakob, M.	Über die spezifische Wärme c(p) der Luft zwischen 1 und 200 Atmosphären

Overview | Substances | Properties | Data Points

Figure 1.2: Sheet "Overview" of the database.

Each literature source is listed in one row and the respective information is given in different columns. If data for several properties are reported in one source, they are listed in different rows and grouped subsequently. The sheet "Overview" contains information about:

- Bibliographical information: author, title, and name of journal/proceeding/monograph
- Data type: experimental, calculated, algorithms, tables, graphics, or software
- Substances: humid air, dry air, and components of mixtures
- Properties: thermodynamic, transport, and others
- Range of temperature, pressure, and density
- Prepared data files in ASCII format
- Prepared data files in Excel® format

For the experimental data, ASCII and Excel® files were prepared and connected with the Excel® sheet by hyperlinks. These prepared files can be used on request at http://thermodynamics-zittau.de.

The sheet "Substances" comprises the fluids included in the database.

The sheet "Properties" explains the symbols, abbreviations, and units of the considered properties.

The sheet "Data Points" contains links to pressure-temperature diagrams (*p*-*T* diagrams) in the folder "Data_Points", covering all experimental data points available in the database. The sheet gives an overview about the properties for which experimental data are available for dry air, humid air, and relevant mixtures. For example, *p*-*T* diagrams for dry air, humid air, and nitrogen-water mixtures are shown in Part A, Figure 2.1 to Figure 2.8.

The folder "Data_Files" contains all prepared data files, prepared Excel® files, and original source files.

2 Access to the Database

The property database for humid air is located on the server connected with internet via an IP-Address. The access to the server is possible by Secure FTP (SFTP). The data are transferred encoded. The server can be accessed by using programs which support SFTP, e.g., SSH Secure Shell (www.ssh.com), or WinSCP (winscp.vse.cz).

A comprehensive User's Guide was prepared to facilitate an easy use of the database. It describes the access to the server and the structure of the property database. The User's Guide can be obtained at http://thermodynamics-zittau.de.

3 References

[1] Buttig, D.: Determination of the Thermodynamic Properties for Humid Air for the Calculation of Advanced Compressed Air Storage Systems. Diploma Thesis, Zittau/Goerlitz University of Applied Sciences, Faculty of Mechanical Engineering, Zittau (2003) (in German).

[2] Lemmon, E.: Database for Dry Air. National Institute of Standards and Technology, Physical and Chemical Properties Division, Boulder, personal communication, (2002).

[3] Yan, J.: Database for Humid Air and Humid Gases. University of Stockholm, internal communication within the AA-CAES project (2004).